

WA School of Mines: Minerals, Energy and Chemical Engineering

**Optimisation of Mono-Ethylene Glycol Regeneration Chemistry and
Corrosion Inhibition Strategies**

Adam Daniel Soames

**This thesis is presented for the degree of
Doctor of Philosophy
of
Curtin University**

February 2020

DECLARATION OF ACADEMIC INTEGRITY

To the best of my knowledge and belief this thesis contains no material previously published by any other person except where due acknowledgment has been made.

This thesis contains no material of which has been accepted for the award of any other degree or diploma in any university.

Signature: _____ (Adam Daniel Soames)

Date: 6/2/2020

COPYRIGHT

I warrant that I have obtained, where necessary, permission from copyright owners to use any third-party copyright material reproduced in the thesis, or to use any of my own published work (e.g. journal articles) in which the copyright is held by another party (e.g. publisher, co-author).

Signature: _____ (Adam Daniel Soames)

Date: 6/2/2020

ACKNOWLEDGEMENTS

I would like to acknowledge the support of my supervisors including Ahmed Barifcani, Rolf Gubner, Mobin Salasi and Stefan Iglauer during my PhD research.

Finally, I acknowledge the contribution of the Australian Government Research Training Program Scholarship in supporting my PhD research.

LIST OF PUBLICATIONS

Primary Author:

Paper One. Removal of Organic Acids during Mono-Ethylene Glycol Distillation and Reclamation to Minimise Long-Term Accumulation

Soames, A., A. Barifcani, and R. Gubner, *Removal of Organic Acids during Mono-Ethylene Glycol Distillation and Reclamation to Minimise Long-Term Accumulation*. Industrial & Engineering Chemistry Research, 2019. **58**(16): p. 6730-6739.

Paper Two. Operation of a MEG Pilot Regeneration System for Organic Acid and Alkalinity Removal during MDEA to FFCI Switchover

Soames, A., E. Odeigah, A. Al Helal, S. Zaboon, S. Iglauer, A. Barifcani, and R. Gubner, *Operation of a MEG Pilot Regeneration System for Organic Acid and Alkalinity Removal During MDEA to FFCI Switchover*. Journal of Petroleum Science and Engineering, 2018. **169**: p. 1-14.

Paper Three. Corrosion of Carbon Steel during High Temperature Regeneration of Mono-Ethylene Glycol in the Presence of Methyldiethanolamine

Soames, A., M. Salasi, A. Barifcani, and R. Gubner, *Corrosion of Carbon Steel during High Temperature Regeneration of Mono-Ethylene Glycol in the Presence of Methyldiethanolamine*. Industrial & Engineering Chemistry Research, 2019. **58**(32): p. 14814-14822.

Paper Four. Effect of Wettability on Particle Settlement Behaviour within Mono-Ethylene Glycol Regeneration Pre-Treatment Systems

Soames, A., S. Al-Anssari, S. Iglauer, A. Barifcani, and R. Gubner, *Effect of wettability on particle settlement behavior within Mono-Ethylene Glycol regeneration pre-treatment systems*. Journal of Petroleum Science and Engineering, 2019. **179**: p. 831-840.

Paper Five. Acid Dissociation Constant (pK_a) of Common MEG Regeneration Organic Acids and Methyldiethanolamine at Varying MEG Concentration, Temperature and Ionic Strength

Soames, A., S. Iglauer, A. Barifcani, and R. Gubner, *Acid Dissociation Constant (pK_a) of Common Monoethylene Glycol (MEG) Regeneration Organic Acids and Methyldiethanolamine at Varying MEG Concentration, Temperature, and Ionic Strength*. Journal of Chemical & Engineering Data, 2018. **63**(8): p. 2904-2913.

Paper Six. Experimental Vapour–Liquid Equilibrium Data for Binary Mixtures of Methyldiethanolamine in Water and Ethylene Glycol under Vacuum

Soames, A., A. Al Helal, S. Iglauer, A. Barifcani, and R. Gubner, *Experimental Vapour–Liquid Equilibrium Data for Binary Mixtures of Methyldiethanolamine in Water and Ethylene Glycol under Vacuum*. Journal of Chemical & Engineering Data, 2018. **63**(5): p. 1752-1760.

Co-Author:

Paper One. Recovery of Mono-Ethylene Glycol Distillation and the Impact of Dissolved Salts Simulating Field Data

Zaboon, S., A. Soames, V. Ghodkay, R. Gubner, and A. Barifcani, *Recovery of Mono-Ethylene Glycol by Distillation and the Impact of Dissolved Salts Evaluated Through Simulation of Field Data*. Journal of Natural Gas Science and Engineering, 2017. **44**: p. 214-232.

Paper Two. Measurement of mono ethylene glycol volume fraction at varying ionic strengths and temperatures

Al Helal, A., A. Soames, R. Gubner, S. Iglauer, and A. Barifcani, *Measurement of Mono Ethylene Glycol Volume Fraction at Varying Ionic Strengths and Temperatures*. Journal of Natural Gas Science and Engineering, 2018. **54**: p. 320-327.

Paper Three. Influence of Magnetic Fields on Calcium Carbonate Scaling in Aqueous Solutions at 150°C and 1 Bar

Al Helal, A., A. Soames, R. Gubner, S. Iglauer, and A. Barifcani, *Influence of magnetic fields on calcium carbonate scaling in aqueous solutions at 150°C and 1bar*. Journal of Colloid and Interface Science, 2018. **509**: p. 472-484.

Paper Four. Performance of Erythorbic Acid as an Oxygen Scavenger in Thermally Aged Lean MEG

Al Helal, A., A. Soames, R. Gubner, S. Iglauer, and A. Barifcani, *Performance of Erythorbic Acid as an Oxygen Scavenger in Thermally Aged Lean MEG*. Journal of Petroleum Science and Engineering, 2018. **170**: p. 911-921.

Paper Five. The Influence of Magnetic Fields on Calcium Carbonate Scale Formation within Ethylene Glycol Solutions at Regeneration Conditions

Al Helal, A., A. Soames, S. Iglauer, R. Gubner, and A. Barifcani, *The influence of magnetic fields on calcium carbonate scale formation within monoethylene glycol solutions at regeneration conditions*. Journal of Petroleum Science and Engineering, 2019. **173**: p. 158-169.

Paper Six. Evaluating Chemical-Scale-Inhibitor Performance in External Magnetic Fields Using a Dynamic Scale Loop

Al Helal, A., A. Soames, S. Iglauer, R. Gubner, and A. Barifcani, *Evaluating chemical-scale-inhibitor performance in external magnetic fields using a dynamic scale loop*. Journal of Petroleum Science and Engineering, 2019. **179**: p. 1063-1077.

Conference Papers

Paper One. Effect of Organic Acids upon Sulphite Oxygen Scavenger Performance within Mono-Ethylene Glycol Injection Systems – **Primary Author**

Paper Two. Effect of Pre-Treatment Process on Scale Formation in the Reboiler Section of a Mono-Ethylene Glycol Regeneration Plant – **Co-Author**

ABSTRACT

The formation of natural gas hydrates represents a significant risk to the continuous and safe operation of multi-phase wet natural gas transportation pipelines. Due to the continued expansion of hydrocarbon production operations to increasingly remote sub-sea locations, the high pressure, low temperature conditions typically found within these fields and long-distance pipelines exacerbates the risk of hydrate formation. Mono-Ethylene Glycol (MEG) injection has been widely applied to prevent the formation of natural gas hydrates through its injection into pipelines to lower hydrate formation temperatures. Due to the ability to effectively regenerate and re-use MEG post hydrate inhibition, MEG injection provides a cost-effective method to prevent hydrate formation compared to other thermodynamic hydrate inhibitors including methanol and alternate polymer based kinetic hydrate inhibitors. Furthermore, various natural gas pipeline corrosion inhibition strategies including pH stabilisation and/or the injection of film forming corrosion inhibitors (FFCI) can be applied through the MEG injection systems.

However, due to the relatively new adaptation of MEG for hydrate inhibition compared to other methods, low industry experience (particularly in Australia) and unexpected effects of MEG on process chemistry, various operational issues often arise during the MEG regeneration process. In particular, MEG as a solvent can have significant impacts on production chemical performance, chemical and physical behaviour of process contaminants (organic acids and salts) and process measurement capabilities and accuracy. Furthermore, it is often the case that significant operational issues arise following the commissioning and initial start-up of MEG regeneration systems that are not considered during the initial design phase. This body of work ultimately aims to optimise various aspects of the MEG regeneration process including process chemistry, corrosion inhibition strategies as well as developing solutions to operational problems identified through consultation with industrial operators of MEG systems.

One such issue involves the long-term accumulation of organic acids, including acetic, within MEG regeneration loops owing to either suboptimal removal conditions, namely unsuitable pH levels and/or a lack of vacuum reclamation systems for organic salt removal. Excessive levels of organic acids represents a potential problem for MEG regeneration systems and associated natural gas pipelines due to their potential effect on production chemical performance and aggravation of both general and top-of-the-line corrosion. To alleviate this risk, the removal efficiency of acetic acid was studied over a wide range of operational conditions (pH levels and salinities) to model the removal during MEG regeneration and vacuum reclamation. Overall, the results highlight the conditions necessary during regeneration and reclamation, coupled with predicted pH changes generated during the distillation process required to prevent organic acid accumulation within closed loop MEG systems.

A novel approach to providing continuous, long-term and cost effective corrosion inhibition for natural gas fields that contain high gas phase carbon dioxide (CO₂) has also been proposed.

In such systems, the long-term injection of FFCIs for corrosion control is often cost prohibitive and the use of traditional salt based pH stabilisers (e.g. hydroxides) may be unsuitable if the dosage rate required to provide sufficient corrosion control is beyond the salt's solubility limit in MEG. As such a new corrosion mitigation strategy has been evaluated that utilises long-term operation under pH stabilisation using methyldiethanolamine (MDEA) coupled with the transition to FFCIs following formation water breakthrough. As part of this study, the feasibility of transitioning from MDEA pH stabilisation to FFCIs was investigated and the optimal operating conditions required to achieve such a goal determined. Through the usage of MDEA pH stabilisation, long-term and cost effective corrosion mitigation for high CO₂ partial pressure natural gas systems can be achieved. Furthermore, the transition to FFCIs post formation water breakthrough can extend production capabilities of formation water producing wells where operation under pH stabilisation would otherwise be detrimental due to scaling.

However, it is important to consider the potential unintended side effects associated with performing a novel operational methodology such as the one proposed prior to being applied to industrial systems. To provide further insight, a study was undertaken to evaluate the corrosion potential of lean MEG solutions under simulated MDEA pH stabilisation at varying pH levels and temperatures representative of a MEG regeneration system. It was found that under specific operational conditions, namely low to moderate pH and high temperature, the presence of MDEA poses a significant corrosion risk to components manufactured from carbon steel with those within the MEG regeneration system particularly susceptible. As such, if a corrosion inhibition switch-over from MDEA to FFCI is to be performed, the corrosion risk to carbon steel components of the regeneration column and associated heating systems must be considered with selection of alternate materials such as stainless steel made during the design phase.

Finally, two studies were conducted looking at operational issues that were identified through industry consultation including poor oxygen scavenger performance and particle settlement problems within MEG systems. Sulphite based oxygen scavengers are widely used in various industrial operations to prevent oxygen based corrosion and were found to, in the presented work, be detrimentally impacted by their interaction with organic acids. Therefore, their application to MEG systems where organic acids are widely experienced is problematic, and as such, several operational recommendations are presented to alleviate the risk of poor field performance. Conversely, the settlement behaviour of solid particles entering into a MEG regeneration system was found to be drastically impacted by their exposure to natural surfactants in the condensate phase of the up-stream pipeline rendering them oil-wet. Said exposure can ultimately lead to poor settlement and excessive down-stream filtration requirements and hence operational costs, but however, could be successfully alleviated through the use of cationic surfactants to modify particle surface properties. These works have direct application to most industry MEG systems due to the common nature of the problems and can provide significant operational cost savings if implemented.

CONTENTS

DECLARATION OF ACADEMIC INTEGRITY	i
COPYRIGHT.....	ii
ACKNOWLEDGEMENTS.....	iii
LIST OF PUBLICATIONS.....	iv
ABSTRACT.....	vi
1.0 INTRODUCTION.....	1
1.1 Overview.....	1
1.2 Objectives	3
1.3 Hypotheses and Overall Significance of Research	2
1.4 Thesis Structure	3
2.0 LITERATURE REVIEW.....	6
2.1 Hydrate Formation in Natural Gas Pipelines	6
2.1.1 Risk of Hydrate Formations and Implications on Flow Assurance	6
2.1.2 Hydrate Formation Conditions and Mechanisms.....	7
2.2 Inhibition of Hydrate Formation.....	8
2.2.1 Thermodynamic Hydrate Inhibitors	8
2.3 Regeneration of Mono-Ethylene Glycol	9
2.3.1 Distillation.....	9
2.3.1 Conventional Recovery Operation (No Reclamation)	10
2.3.2 Full Stream Vacuum Reclamation Operation	10
2.3.3 Slip-Stream Vacuum Reclamation Operation	11
2.3.3.1 Rich MEG Pre-Treatment	12
2.4 Salts, Scaling and Organic Acids within MEG Regeneration Systems.....	13
2.4.1 Monovalent Salts	13
2.4.2 Divalent Cations and Scaling Within MEG Regeneration Systems and Natural Gas Pipelines.....	13
2.4.2.1 MEG Regeneration Systems.....	14
2.4.2.2 Natural Gas Pipelines and Scale Inhibition	15
2.4.3 Organic Acids	16
2.5 Corrosion and Corrosion Prevention in Natural Gas Pipelines and MEG Regeneration Systems.....	17
2.5.1 Types of Corrosion.....	17
2.5.1.1 General Corrosion	17
2.5.1.2 Uniform Corrosion	18

2.5.1.3	Pitting Corrosion	18
2.5.1.4	Crevice Corrosion	19
2.5.2	Corrosion in Natural Gas Pipelines	19
2.5.2.1	Factors Influencing Natural Gas Pipeline Corrosion	21
2.5.2.1.1	Gas Phase Composition	21
2.5.2.1.2	Liquid Phase pH.....	21
2.5.2.1.3	Temperature	21
2.5.2.2	Top of Line Corrosion	21
2.5.3	Corrosion in MEG Regeneration Systems.....	22
2.5.4	Corrosion Mitigation Methods	23
2.5.4.1	pH Stabilisation	23
2.5.4.2	Film Forming Corrosion Inhibitors	24
2.5.4.3	Corrosion Mitigation Strategy Switchover	25
2.5.4.4	Oxygen Scavengers	26
2.6	Chemical and Physical Behaviour in MEG Systems	27
2.6.1	Uncertainty and Operational Issues Faced in Industry.....	27
2.6.2	Vapour-Liquid Equilibrium (VLE).....	28
2.6.2.1	Modelling of VLE Systems	28
2.6.3	Particle Settlement within MEG Regeneration Systems	31
2.6.3.1	Physical Factors Influencing Particle Settlement	31
2.6.3.1.1	Particle Physical Properties.....	31
2.6.3.1.2	Liquid Phase Properties	32
2.6.3.2	Chemical Factors Influencing Particle Settlement	32
2.6.3.2.1	Particle Wettability	32
2.6.3.2.2	Particle-Particle Attraction and Zeta Potential	33
2.6.3.2.3	Behaviour of Hydrophobic Particles in Liquid Suspensions	34
2.6.3.3	Particle Wettability in MEG Systems and Factors Affecting Wettability	35
2.6.3.3.1	Measurement of Wettability	35
2.6.3.3.2	Liquid Surface Tension	36
2.6.3.3.3	Particle Shape, Size and Surface Roughness.....	37
2.6.3.3.4	Surface Heterogeneity	37
2.6.3.3.5	Presence of Metal Cations / Salinity	38
2.6.3.3.6	Application of Surfactants for Particle Surface Modification	38
2.6.4	Acid Dissociation Behaviour of Chemical Species	39
3.0	EXPERIMENTAL EQUIPMENT, METHODOLOGIES AND MEASUREMENT TECHNIQUES	42
3.1	Mono-Ethylene Glycol Regeneration Pilot Plant	42

3.1.1	MEG Regeneration Unit (Distillation)	42
3.1.2	Feed Blender, Rich MEG Pre-Treatment Unit and Three Phase Separator	43
3.1.3	Vacuum Reclamation Unit	45
3.1.4	System Control	46
3.1.5	Process Instrumentation	46
3.1.5.1	pH Measurement	46
3.1.5.2	Dissolved Oxygen Measurement	46
3.1.5.3	Control of Gas Compositions and Flow Rates	46
3.1.5.4	Liquid Stream Flow Rates	46
3.2	Experimental Measurement and Analysis	47
3.2.1	Ion Chromatography	47
3.2.2	High Performance Liquid Chromatography	47
3.2.3	Determination of Alkalinity by Titration	48
3.2.3.1	Alkalinity Titration Procedure	48
3.2.4	Measurement of MEG Concentration	50
4.0	REMOVAL OF ORGANIC ACIDS DURING MONO-ETHYLENE GLYCOL DISTILLATION AND RECLAMATION TO MINIMISE LONG-TERM ACCUMULATION	51
4.1	Introduction	51
4.2	Experimental Methodology	53
4.2.1	Chemicals	53
4.2.2	Experimental Apparatus and Procedure	53
4.2.2.1	Regeneration Process	53
4.2.2.2	Reclamation Process	54
4.3	Results and Discussion	56
4.3.1	Speciation of Acetic Acid in MEG Solutions at Varying Temperature and Salinity	56
4.3.2	pH Change Induced During MEG Distillation	56
4.3.3	Removal Efficiency of Acetic Acid during MEG Distillation	59
4.3.4	Removal Efficiency of Acetic Acid during MEG Reclamation	60
4.3.4.1	Generation of Organic Acids during Reclamation through Thermal Degradation	60
4.3.5	Modelling of Plant Wide Acetic Acid Removal	62
4.4	Conclusion	65
5.0	OPERATION OF A MEG PILOT REGENERATION SYSTEM FOR SIMULTANEOUS ORGANIC ACID AND ALKALINITY REMOVAL DURING MDEA TO FFCI SWITCHOVER	67
5.1	Introduction	67
5.2	Organic Acids within MEG Regeneration Systems	68

5.3	Operational Scenario	69
5.3.1	Comparison of Operational Methodologies	70
5.3.2	Behaviour of Organic Acids and MDEA during MEG Regeneration and Reclamation	71
5.4	Process Design and Configuration	74
5.5	Chemicals and Feed Stream Compositions	76
5.6	Operating Procedure	77
5.7	Operating Results and Discussion.....	78
5.7.1	pH Change during MEG Regeneration Process.....	78
5.7.2	Removal of MDEA and Alkalinity: Comparison between Operational Methods.....	81
5.7.3	Removal of Organic Acids through the MEG Regeneration and Reclamation System (Modified Procedure)	84
5.7.4	Accumulation of Sodium within MEG Regeneration Loop	87
5.8	Conclusion	88
6.0	CORROSION OF CARBON STEEL DURING HIGH TEMPERATURE REGENERATION OF MONO-ETHYLENE GLYCOL IN THE PRESENCE OF METHYLDIETHANOLAMINE.....	89
6.1	Introduction	89
6.2	Experimental Methodology	92
6.2.1	Materials, Chemicals and Solution Preparation	92
6.2.2	Experimental Procedure	93
6.2.2.1	Experimental Apparatus and Test Conditions.....	93
6.2.2.2	Corrosion Measurement	94
6.2.2.3	pH Measurement	95
6.3	Results and Discussion.....	95
6.3.1	Speciation of MDEA at Varying Temperature.....	95
6.3.2	Effect of MDEA on Corrosion at Regeneration Temperature (140°C).....	96
6.3.3	Effect of Temperature and Initial Lean Glycol pH _{25°C} on Corrosion	96
6.3.4	Pilot Scale Distillation Corrosion Testing	98
6.3.5	Process Fouling Concerns due to Corrosion	98
6.3.6	Application of Corrosion Inhibitors during High Temperature Regeneration	100
6.4	Conclusion	102
7.0	EFFECT OF WETTABILITY ON PARTICLE SETTLEMENT BEHAVIOUR WITHIN MONO-ETHYLENE GLYCOL REGENERATION PRE-TREATMENT SYSTEMS	104
7.1	Introduction	104
7.2	Wettability of Solid Particles	105
7.2.1	Wettability in Oil and Gas Reservoirs and Pipelines.....	106
7.3	Chemicals and Particle Modification Procedure	107

7.4	Results and Discussion.....	108
7.4.1	Behaviour of Particles at MEG-Vapour and MEG-Condensate Interface	108
7.4.2	Settlement of Particles within Rich Glycol Systems	108
7.4.3	Selection of Suitable Surfactants through Zeta Potential Measurement.....	111
7.4.4	Application of Surfactants to Modify Particle Surface Properties.....	114
7.5	Conclusion	119
8.0	ACID DISSOCIATION CONSTANT (pK_a) OF COMMON MEG REGENERATION ORGANIC ACIDS AND METHYLDIETHANOLAMINE AT VARYING MEG CONCENTRATION, TEMPERATURE AND IONIC STRENGTH	121
8.1	Introduction	121
8.2	Experimental Methodology	122
8.2.1	Chemicals.....	122
8.2.2	Apparatus and Procedure.....	122
8.3	Determination of pK_a Values	125
8.4	Results and Discussion.....	126
8.4.1	Effect of MEG Concentration on pK_a	126
8.4.2	Effect of temperature on pK_a	126
8.4.3	Estimation of Thermodynamic Properties.....	132
8.4.4	Effect of Sodium Chloride Content and Ionic Strength on pK_a	134
8.4.5	pK_a Modelled as Function of MEG Concentration, Temperature and Ionic Strength (NaCl)	137
8.5	Conclusion	140
9.0	EXPERIMENTAL VAPOUR-LIQUID EQUILIBRIUM DATA FOR BINARY MIXTURES OF METHYLDIETHANOLAMINE IN WATER AND ETHYLENE GLYCOL UNDER VACUUM	141
9.1	Introduction	141
9.2	Experimental Methodology	142
9.2.1	Materials.....	142
9.2.2	Apparatus and Procedure.....	142
9.3	Results and Discussion.....	144
9.3.1	Correlation of VLE Data	146
9.3.1	Thermodynamic Consistency.....	148
9.3.2	Analysis of Model Accuracy	153
9.4	Conclusion	158
10.0	CONCLUSION: SUMMARY, RELEVANCE OF WORK TO INDUSTRY AND RECOMMENDATIONS FOR FUTURE WORKS.....	159
10.1	Optimisation of Organic Acid Removal to Prevent Long-Term Accumulation	160
10.2	Corrosion Inhibition Switchover from MDEA to FFCI	160

10.3	Potential Corrosion Issues arising from MDEA and MDEA-to-FFCI Switchover	161
10.4	Diagnosing Routine Settlement Problems in MEG Regeneration Systems	162
10.5	Generation of Chemical and Physical Data Relevant to Industrial MEG System Operation and Design	163
10.6	Optimisation of Sulphite Based Oxygen Scavenger Performance in MEG Systems	164
10.7	Relevance of Work to Industry	164
10.8	Recommendations for Future Work.....	165
REFERENCES		167
Appendix A: MEG Regeneration Flow-Scheme Utilising Pre-Treatment and Slip-Stream Reclamation		
		185
Appendix B: Curtin Corrosion Centre’s MEG Regeneration Pilot Plant		
		186
Appendix C: Supplementary Particle Wettability Results – Chapter Seven.....		
		187
Appendix D: Supplementary Acid Dissociation Experimental Data – Chapter Eight		
		191
Appendix E: Effect of Organic Acids upon Sulphite Oxygen Scavenger Performance within Mono-Ethylene Glycol Injection Systems		
		194
1.0	Introduction	194
2.0	Review of Sulphite Based Oxygen Scavengers	195
3.0	Experimental System and Methodology	197
3.1	Experimental Apparatus	197
3.2	Experimental Methodology	198
4.0	Experimental Results and Discussion	199
4.1	Effect of Organic Acids on Sulphite Oxygen Scavenger Performance	199
4.2	Effect of Salt Content (NaCl) on Sulphite Oxygen Scavenger Performance	201
5.0	Identification of Optimal Operating Window for Oxygen Removal at Varying Salt and Organic Acid Concentrations	204
6.0	Effect of Sulphite Oxygen Scavenger on Lean MEG pH	207
7.0	Conclusion	208
Appendix F: Published Journal Manuscripts		
		210
Appendix G: Written Statements from Co-authors of the Publications		
		216
Appendix H: Copyright Statements.....		
		223

LIST OF FIGURES

Figure 1-1. Thesis structure	5
Figure 2-1: Methane hydrate type sII (Janda [25]).....	6
Figure 2-2. Gas hydrate plug in pipeline (Makogon [26])	7
Figure 2-3. locations of gas hydrate formation in offshore systems (Giavarini and Hester [31])	7
Figure 2-4. Fields using MEG injection for hydrate inhibition (modified from Al Harooni [34]) ..	8
Figure 2-5. Full-Stream reclamation system	11
Figure 2-6. MEG regeneration unit tube bundle fouled by FeCO_3 (Latta [10])	15
Figure 2-7. Corrosion of carbon steel by hydrogen reduction.....	18
Figure 2-8. Internal corrosion of a natural gas pipeline (Popoola [98]).....	20
Figure 2-9. Pitting failure of a natural gas pipeline (Mansoori [82]).....	20
Figure 2-10. TLC mechanism due to water condensation (Yeaw [106])	22
Figure 2-11. T-XY Diagram of MEG-water binary system at 101.325 kPa.....	29
Figure 2-12. VLE Diagram MEG-water binary system at 101.325 kPa	29
Figure 2-13. Electrical double layer around a positively charged colloidal particle from Tadros [152]).....	33
Figure 2-14. Effect of pH on particle surface charge in water (Frimmel [158])	34
Figure 2-15. Wettability with respect to contact angle of liquid droplet (Yuan and Lee [142]).	36
Figure 2-16. Contact angle measurement by tilted plate method (Yuan and Lee [142])	36
Figure 2-17. Surface roughness effect on liquid particle – surface interaction. a) smooth surface b) rough surface with increased liquid-solid interfacial contact (Kumar and Prabhu [179])	37
Figure 2-18. Effect of temperature on the pK_a of MDEA in water ^[196]	41
Figure 2-19. Effect of temperature on the speciation of MDEA in water.....	41
Figure 3-1. Curtin Corrosion Centre MEG distillation system.....	43
Figure 3-2. Curtin Corrosion Centre MEG reclamation system	45
Figure 3-3. Forward titration to determine hydroxide, carbonate and total alkalinity.....	49
Figure 3-4. Backward titration to determine carboxylic alkalinity.....	49
Figure 4-1. Laboratory MEG regeneration system.....	55
Figure 4-2. Laboratory MEG vacuum reclamation system	55
Figure 4-3. Speciation of acetic acid as a function of pH (80% wt. MEG) at varying temperature. acetic acid pK_a at 125°C extrapolated from model of Soames [195] (Chapter 8 – Equation 8-12)	56
Figure 4-4. Effect of initial rich glycol (50 wt. %) $\text{pH}_{25^\circ\text{C}}$ and gas phase CO_2 concentration on final lean MEG (80 wt. %) $\text{pH}_{25^\circ\text{C}}$ using sodium hydroxide pH control	58
Figure 4-5. Effect of initial rich glycol (50 wt. %) $\text{pH}_{25^\circ\text{C}}$ and gas phase CO_2 concentration on final lean MEG (80 wt. %) $\text{pH}_{25^\circ\text{C}}$ using MDEA pH control.....	58
Figure 4-6. Removal efficiency of acetic acid during 80% wt. MEG distillation.....	59
Figure 4-7. Removal efficiency of acetic acid during 80% wt. MEG reclamation	61
Figure 4-8. MEG organic acid degradation products generated during reclamation	62
Figure 4-9. Comparison of modelled acetic acid removal rate during distillation and reclamation	63
Figure 4-10. Simulated acetic acid removal rate full reclamation	64
Figure 4-11. Simulated acetic acid removal rate with 20% partial reclamation.....	65
Figure 5-1. Industrial FFCI to MDEA switchover methodology	72
Figure 5-2. Alternative FFCI to MDEA switchover methodology	72
Figure 5-3. Speciation of acetic acid – acetate	73

Figure 5-4. MEG reclamation removal efficiency at 25°C, 80% wt. Lean MEG.....	74
Figure 5-5. pH levels during MEG regeneration (industry operational philosophy).....	79
Figure 5-6. pH levels during MEG regeneration (modified operational philosophy)	80
Figure 5-7. Ideal target pHs and current pH change during regeneration (industry operational philosophy)	80
Figure 5-8. Ideal target pHs and current pH change during regeneration (Modified Operational Philosophy)	81
Figure 5-9. Lean Glycol Tank MDEA and alkalinity measurements (industry operational philosophy)	82
Figure 5-10. Lean Glycol Tank MDEA and alkalinity measurements (modified operational philosophy)	82
Figure 5-11. Comparison of MEG regeneration alkalinity removal methods	83
Figure 5-12. Acetic acid content within rich and lean glycol tanks.....	85
Figure 5-13. Acetic acid content within reflux drum	85
Figure 5-14. Average percentage removal of acetic acid during distillation	86
Figure 5-15. Accumulation of sodium within the MEG regeneration loop (modified philosophy)	87
Figure 6-1. Experimental autoclave apparatus for corrosion testing	94
Figure 6-2 A) Effect of temperature on MDEA dissociation constant within 80% wt. MEG solution (Soames [195] – Chapter 8) and B) Speciation of MDEA in 80% wt. MEG at varying temperature.....	95
Figure 6-3. Effect of MDEA on corrosion at varying initial lean glycol pH _{25°C} and 140°C	96
Figure 6-4. Corrosion rate of carbon steel at varying pH _{25°C} and temperature	97
Figure 6-5. Comparison of corrosion measurement techniques at 140°C	97
Figure 6-6. Comparison of autoclave vs. distillation column corrosion measurements (140°C – LPR measurement).....	98
Figure 6-7. Corrosion of LPR probe during regeneration (pH _{25°C} = 7, 140°C).....	98
Figure 6-8. Potential impact of MDEA corrosion and excessive iron particles on MEG regeneration unit	99
Figure 6-9. Fe ²⁺ concentration after 3-days of corrosion (140°C).....	100
Figure 6-10. Final solution after 3-days of corrosion (pH _{25°C} = 7, 140°C)	100
Figure 6-11. Corrosion rates of carbon steel under high temperature conditions with FFCIs present (pH _{25°C} 7)	101
Figure 6-12. Corrosion inhibition efficiencies of FFCIs under high temperature conditions (pH _{25°C} 7).....	102
Figure 7-1. Curtin Corrosion Centre’s rich MEG pre-treatment and settlement systems	105
Figure 7-2. Particle size analysis of field rich MEG samples	107
Figure 7-3. Settlement of water/MEG-wetted FeCO ₃ (10-32 µm) in 50% wt. MEG solution ...	109
Figure 7-4. Settlement of oil-wetted FeCO ₃ (10-32 µm) in 50% wt. MEG solution	110
Figure 7-5. Settlement of water/MEG-wetted quartz (10-32 µm) in 50% wt. MEG solution...	111
Figure 7-6. Settlement of oil-wetted quartz (10-32 µm) in 50% wt. MEG solution.....	111
Figure 7-7. Zeta potential of quartz and FeCO ₃ within 50% wt. MEG solution	113
Figure 7-8. Effect of CTAB and SDS on particle Zeta potential (pH 9).....	113
Figure 7-9. Effect of CTAB on initially oil-wet 10-32 µm FeCO ₃ and quartz settlement.....	115
Figure 7-10. Effect of SDS on initially Oil-Wet 10-32 µm FeCO ₃ and quartz settlement	116
Figure 7-11. Effect of CTAB on FeCO ₃ particle size after oil-wetted to water/MEG-wetted transition.....	116

Figure 7-12. Effect of SDS on FeCO ₃ particle size after oil-wetted to water/MEG-wetted transition.....	117
Figure 7-13. Comparison of generic and commercially available surfactants (50 ppm) - FeCO ₃	118
Figure 7-14. Modification of FeCO ₃ surface properties by CTAB and SDS surfactants	119
Figure 8-1. Effect of temperature on pK _a of acetic and propanoic acid (aqueous solution)	124
Figure 8-2. Effect of temperature on pK _a of formic acid (aqueous solution)	124
Figure 8-3. Effect of temperature on pK _a of MDEA (aqueous solution)	125
Figure 8-4. Effect of MEG concentration on pK _a of organic acids (25°C).....	128
Figure 8-5. Effect of MEG concentration and temperature on pK _a of MDEA	128
Figure 8-6. Dielectric constant of varying MEG concentration solutions ^[289, 290]	129
Figure 8-7. Dielectric constant vs. organic acid pK _a (25°C)	129
Figure 8-8. Dielectric constant vs. MDEA pK _a	130
Figure 8-9. Effect of temperature on pK _a of organic acids (30% wt. MEG)	130
Figure 8-10. Effect of temperature on pK _a of organic acids (50% wt. MEG)	131
Figure 8-11. Effect of temperature on pK _a of organic acids (80% wt. MEG)	131
Figure 8-12. Effect of temperature on pK _a of MDEA in varying concentration MEG solution .	132
Figure 8-13. Effect of salinity (NaCl) on pK _a of MDEA in varying MEG concentration solution (25°C)	136
Figure 8-14. Effect of salinity (NaCl) on pK _a of acetic acid in varying MEG concentration solution (25°C)	136
Figure 8-15. Acetic acid pK _a within 80% wt. MEG as a function of ionic strength and temperature.....	138
Figure 8-16. MDEA pK _a within 80% wt. MEG as a function of ionic strength and temperature	139
Figure 8-17. Acetic acid pK _a within 80% (yellow), 50% (green), 30% (blue) wt. MEG as a function of ionic strength and temperature. Data points = measured pK _a (Appendix D Table D1), mesh plot = calculated pK _a (Equation (8-12))......	139
Figure 9-1. Experimental apparatus (Heidolph Hei-VAP Rotary Evaporator)	143
Figure 9-2. Refractive index vs. MDEA mole fraction calibration curve at 20°C, 101.325 kPa. A) Water-MDEA, B) MEG-MDEA.....	144
Figure 9-3. VLE data for water-MDEA at 40 kPa	149
Figure 9-4. VLE data for water-MDEA at 20 kPa	149
Figure 9-5. VLE data for water-MDEA at 10 kPa	150
Figure 9-6. VLE data for MEG-MDEA at 20 kPa	150
Figure 9-7. VLE data for MEG-MDEA at 10 kPa.....	151
Figure 9-8. VLE data for MEG-MDEA at 5 kPa.....	151
Figure 9-9. MEG-MDEA δT residual	152
Figure 9-10. MEG-MDEA $\delta \gamma_1$ residual.....	152
Figure 9-11. MEG-MDEA $\delta(\gamma_1/\gamma_2)$ residual.....	153
Figure 9-12. Comparison of experimental to modelled relative volatility for MEG-MDEA at 20 kPa.....	155
Figure 9-13. Comparison of experimental to modelled relative volatility for MEG-MDEA at 10 kPa.....	156
Figure 9-14. Comparison of experimental to modelled relative volatility for MEG-MDEA at 5 kPa.....	156
Figure 9-15. Percentage error in model K-values in comparison to experimental data for MEG-MDEA	157

Figure 9-16. Percentage error in model K-values in comparison to experimental data for Water-MDEA	157
Figure C-1. Behaviour of oil-wetted solid particles at MEG-air interface	187
Figure C-2. Oil-wetted quartz particle attraction at MEG-air interface	187
Figure C-3. Behaviour of solid particles at MEG-condensate interface	187
Figure C-4. Settlement of water/MEG-wetted FeCO ₃ (>63 μm) in 50% wt. MEG solution	188
Figure C-5. Comparison of water/MEG-wetted and oil-wetted quartz (>63 μm) in 50% wt. MEG solution	189
Figure E-1. Experimental apparatus.....	198
Figure E-2. Effect of acetic acid concentration on sulphite oxygen scavenger performance at pH 9	200
Figure E-3. Effect of acetic acid concentration on sulphite oxygen scavenger performance at pH 11	201
Figure E-4. Performance of sulphite oxygen scavenger at pH 11 within 50 g/L NaCl lean MEG	202
Figure E-5. Effect of salt content (NaCl) on oxygen removal performance at varying acetic acid concentration (pH 11)	203
Figure E-6. Effect of salt content (NaCl) on oxygen removal performance at varying acetic acid concentration (<200 ppb oxygen region) (pH 11).....	203
Figure E-7. Effect of acetic acid and NaCl on oxygen removal rate at pH 9 (0, 1 and 4 g/L NaCl)	205
Figure E-8. Effect of pH, salinity (NaCl) and acetic acid on oxygen scavenger performance ...	205
Figure E-9. Speciation of acetic acid in 85% MEG Solution ^[195] and effect on oxygen scavenger performance	206
Figure E-10. Effect of oxygen scavenger on lean MEG pH	207

LIST OF TABLES

Table 2-1. Chemical and physical properties of methanol and MEG (Akers [35])	9
Table 2-2. Comparison of three MEG regeneration operational methods ^[1, 8, 32]	12
Table 2-3. Dominant scale formation reactions in MEG and natural gas systems	14
Table 2-4. General corrosion electrochemical reactions	18
Table 2-5. NRTL activity coefficient model	31
Table 3-1. MEG distillation column design specifications	42
Table 3-2. MEG distillation column packing specifications.....	43
Table 3-3. Pre-treatment / three-phase separator specifications.....	44
Table 3-4. Cation ion chromatography specifications	47
Table 3-5. Anion ion chromatography specifications	47
Table 3-6. High performance liquid chromatography specifications.....	48
Table 4-1. Regressed model parameters and average model errors	63
Table 5-1. Feed stream compositions	76
Table 5-2. Sparging gas compositions.....	77
Table 6-1. Electrochemical corrosion reactions with MEG/Water/MDEA systems.....	92
Table 6-2. Chemical purity and structures.....	93
Table 6-3. FFCIs evaluated at high temperature regeneration conditions.....	101
Table 7-1. Generic and commercially available surfactants	117
Table 8-1. Chemical purity and structures.....	123
Table 8-2. Water pK _a comparison to literature ^a	123
Table 8-3. Effect of MEG concentration on measured organic acid pK _a (25°C) ^a	126
Table 8-4. Effect of temperature on measured organic acid pK _a in aqueous and varying MEG concentration solution ^a	127
Table 8-5. Effect of MEG concentration and temperature on measured MDEA pK _a ^a	127
Table 8-6. Comparison of MDEA thermodynamic quantities in aqueous solution (25°C) ^a	133
Table 8-7. Comparison of organic acid thermodynamic quantities in aqueous solution (25°C) ^a	133
Table 8-8. MDEA thermodynamic quantities in varying MEG concentration solutions (25°C) ^a	133
Table 8-9. Organic acid thermodynamic quantities in varying concentration MEG solution (25°C) ^a	134
Table 8-10. Effect of salinity (NaCl) on pK _a of acetic acid and MDEA in varying MEG concentration solution (25°C) ^a	135
Table 8-11. pK _a model coefficients and errors.....	138
Table 9-1. Chemicals, suppliers and purity	142
Table 9-2. Refractive indices (<i>n_D</i>), boiling points and critical properties ^a	142
Table 9-3. VLE data and calculated activity coefficients γ for Water-MDEA and MEG MDEA systems ^a	145
Table 9-4. Water vapour pressure and MEG Antoine parameters	146
Table 9-5. Activity coefficient models.....	146
Table 9-6. Molecule volume parameters <i>r</i> , area parameters <i>q</i> and <i>Z</i> parameter for the UNIQUAC Model	147
Table 9-7. Water-MDEA binary interaction parameters.....	147
Table 9-8. MEG-MDEA binary interaction parameters	148
Table 9-9. Herrington thermodynamic consistency test	148

Table 9-10. Water-MDEA RMS error for model fitting	154
Table 9-11. MDEA-MDEA RMS error for model fitting	155
Table C-1. Industrial rich MEG solution compositions.....	190
Table D-1. Effect of MEG concentration, temperature and ionic strength on acetic acid pK_a^a	191
Table D-2. Effect of MEG concentration, temperature and ionic strength on MDEA pK_a^a	192
Table E-1. Experimental matrix.....	199
Table E-2. Effect of NaCl on final lean MEG pH	204
Table E-3. Operating envelope for use of sulphite oxygen scavenger in lean MEG solutions..	209

1.0 INTRODUCTION

1.1 Overview

Within the last twenty years, numerous off-shore natural gas production systems in Northern Europe and Australia have adopted MEG for hydrate inhibition over traditional thermodynamic hydrate inhibitors (THI) including methanol [1-3]. The standard industrial philosophy regarding MEG for hydrate inhibition entails the separation of MEG from the desired hydrocarbon products alongside the water phase to facilitate its regeneration and ultimately its reuse to minimise long term operational costs [1,4-7]. The recent adaption of MEG combined with the differences in chemical behaviour in MEG solutions compared to aqueous systems, results in numerous uncertainties in regard to the industrial usage of MEG, particularly the regeneration process [5,8-11]. Due to the wide range of operational conditions (pH, temperature, salinity) and contaminants (organic acids, mineral salts, production chemicals) potentially present within MEG regeneration systems, the optimisation of process conditions and chemistry is extremely important to optimise the overall regeneration process and to prevent unforeseen operational issues occurring.

Although the removal of water from MEG is simple, various processes involved with the industrial regeneration of MEG are less understood with unforeseen operational issues often arising. Various chemical and physical processes are utilised to purify and treat the rich MEG returning from the natural gas pipeline. These processes include salt and particle removal systems to prevent long-term build up or scaling risks [9, 10], removal of excess water by distillation to produce 'lean MEG' [1, 12] and the injection of production chemicals including corrosion and scaling inhibitors to protect down-stream injection systems and the primary natural gas pipeline [2, 5, 12-14]. Any unforeseen behaviour of chemical species (contaminant or production chemical) or separation systems may have significant implications on overall process efficiency or long-term viability of the system.

In particular, the corrosion of metal systems within the MEG regeneration loop and associated natural gas transportation pipeline is a continuous operational issue facing industry [4,15]. Various techniques have been applied to inhibit the occurrence of corrosion within wet gas pipelines utilising MEG for hydrate inhibition including artificially increasing pH (pH stabilisation) [4, 16, 17], injection of chemical corrosion inhibitors [2, 4, 8] and dosage of oxygen scavengers to prevent oxygen based corrosion [8, 18, 19]. The optimisation of these corrosion inhibition techniques, including the transition between them when required, coupled with minimising the

accumulation of corrosive species can have significant implications on the continued and safe operation of the MEG regeneration system and associated natural gas pipelines. Through optimised corrosion mitigation strategies, significant safety and operational risks associated with the corrosion of production and sub-sea systems can be minimised and the overall life span of the system extended to improve long-term return on investment.

Detailed studies have been conducted of which form this thesis, analysing various aspects of the MEG regeneration and hydrate inhibition process. These topics include optimisation of separation processes, contaminant removal, process chemistry and production chemical performance and the evaluation of corrosion inhibition strategies associated with the MEG regeneration and natural gas systems. As part of this work, a MEG regeneration pilot plant operated by the Curtin Corrosion Centre has been utilised to facilitate MEG regeneration research. Furthermore, to facilitate insights generated using the pilot MEG system, various laboratory work has been conducted to improve the understanding of MEG chemistry including generation of novel experimental and chemical data. The overall goal of this body of work was to generate better knowledge of MEG regeneration operations, chemical and physical behaviour within MEG systems and to provide effective solutions to several operational problems currently being faced by industrial MEG system operators.

1.2 Hypotheses and Overall Significance of Research

It is hypothesised that through careful optimisation of various operational conditions in several areas of the MEG regeneration and reclamation processes, significant operational efficiency improvements and cost savings can be achieved by industrial MEG system operators. These can include improved removal of various contaminants from the MEG systems, reducing both their impact and removal costs, improved production chemical performance and their associated applications costs and reduced risks of various forms of corrosion. Overall, the improvements and research into MEG regeneration processes contained within this thesis can help reduce long-term operational costs and improve asset reliability of industrial MEG regeneration systems.

The significance of this research primarily relates to the optimisation of the overall MEG regeneration process and the resulting operational benefits and reduction in long-term operational costs that result. Furthermore, the identification of process inefficiencies, undesirable operating conditions (corrosion / poor production chemical performance) and optimised corrosion inhibition strategies, particularly those using MDEA, will improve the design and operation of future MEG regeneration systems. There is also a limited volume of peer-reviewed literature available on the industrial regeneration of MEG with the bulk of information

primarily limited to industry and non-peer reviewed conference papers. The research reported in this study significantly expands on the availability of information regarding the industrial regeneration of MEG.

1.3 Research Objectives

Through consultation with industry including major oil and gas producers, various uncertainties and issues associated with the industrial regeneration of MEG have been identified and researched as part of this study. On this basis, the overall objectives of this research are as follows:

1. Identify through consultation with industry partners various operational issues and uncertainties currently faced within major MEG regeneration systems in Western Australia and areas of potential process efficiency optimisation
 - a. Optimisation of process chemistry to minimise chemical dosage and hence reduce long-term operational costs
 - b. Study the behaviour of MDEA as a pH stabiliser within MEG systems
 - c. Optimisation of separation processes including MDEA from MEG/water or organic acids from MEG
 - d. Optimisation of production chemical performance in MEG systems
 - e. Identification of potentially undesirable process conditions (corrosion risks)
2. Modelling of MEG regeneration processes and chemistry to facilitate the above objectives and the identification of optimal operation conditions to achieve various operational goals

1.4 Thesis Structure

This thesis consists of eleven chapters including an introduction and literature review analysing the overall industrial MEG regeneration process, common issues faced within industry and the general physical and chemical behaviour relevant to MEG systems. Chapter three provides information regarding experimental process equipment and analytical techniques utilised in the development of this thesis. Chapters four to nine outline various experimental and theoretical studies conducted to optimise several aspects of the MEG regeneration process and associated corrosion inhibition strategies with particular focus on issues identified by industry, with additional details provided below. Figure 1-1 provides a framework for the structure of this thesis outlining the issues that have been identified in consultation with industry and how each individual chapter attempts to improve knowledge within these areas.

- **Chapter Four** studies the removal of organic acids, primarily acetic acid, from closed loop MEG regeneration systems under varying pH and salinity levels through distillation and vacuum reclamation. The overall objective was to optimise the long-

term removal of organic acids from MEG systems to minimise the associated corrosion risk to down-stream natural gas systems.

- **Chapter Five** analyses the potential switchover from pH stabilisation using MDEA to film forming corrosion inhibitors (FFCI) and recommendations to improve the overall efficiency of the process. To date, the switchover from MDEA to FFCIs has not yet been performed in industry with Chapter Five providing the first in-depth analysis of the process and identification of potential issues.
- **Chapter Six** attempts to identify potentially corrosive conditions resulting from the switchover from MDEA to FFCI due to the low pH / high temperature conditions experienced within the MEG regeneration unit.
- **Chapter Seven** identifies the potential effects of particle wettability on the settlement behaviour of solid particles including iron carbonate and quartz within MEG settlement systems based on issues faced within an industrial MEG regeneration system in Western Australia.
- **Chapter Eight** provides an in-depth analysis of how various process conditions including MEG concentration, temperature and ionic strength influence the acid dissociation behaviour of common organic acids found in MEG systems and MDEA. The experimental results and generated models allow the optimisation of process conditions required for the removal of the respective chemicals from MEG systems.
- **Chapter Nine** analyses the behaviour of MDEA within MEG and water systems under high temperature vacuum conditions to simulate the vacuum reclamation process. Greater knowledge of MDEA behaviour and design data such as vapour liquid equilibrium (VLE) data will allow improved design of vacuum reclamation systems for the removal of MDEA from closed loop MEG systems.
- **Chapter Ten** summaries the work conducted within this thesis and discusses the conclusions drawn from each individual study. Further discussion of how this work is relevant to industry and potential future work recommendations are also presented.
- **Appendix E** presents a conference paper analysing the behaviour of sulphite-based oxygen scavengers in the presence of various commonly encountered contaminants including organic acids and mineral salts with MEG systems. The study provides various recommendations to increase sulphite oxygen scavenger performance to minimise the risk of oxygen-based corrosion in MEG injection systems.

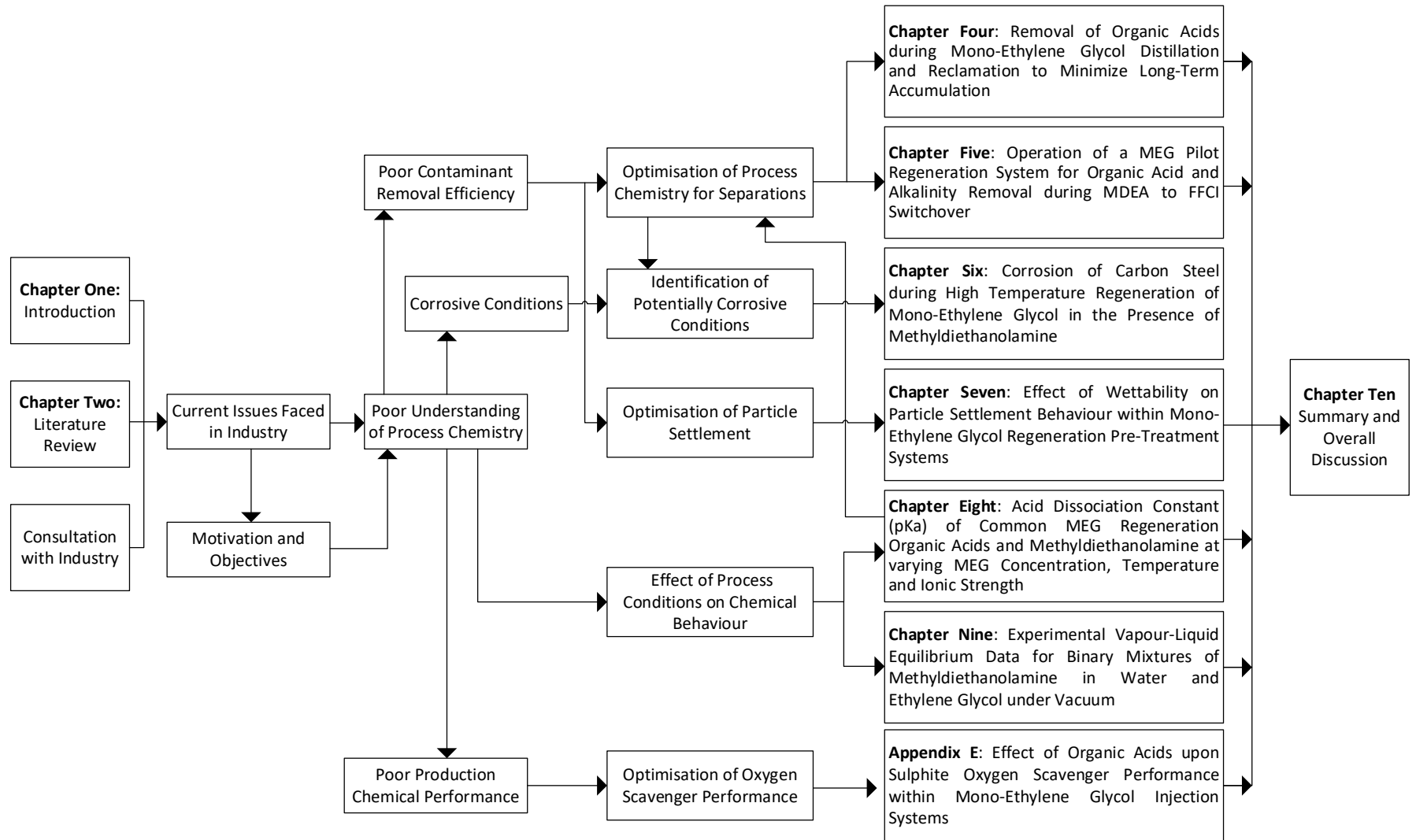


Figure 1-1. Thesis structure

2.0 LITERATURE REVIEW

2.1 Hydrate Formation in Natural Gas Pipelines

The formation of natural gas hydrates poses a significant threat to both the safe and continuous operation of natural gas transportation pipelines and is considered to be the most critical aspect of continued flow assurance ^[20, 21]. The formation of gas hydrates arises following the ‘entrapment’ of small gaseous molecules within a lattice of water forming an ice-like solid structure ^[20, 22-24] – (Figure 2-1). Methane, ethane, propane, butane, hydrogen sulphide, nitrogen and carbon dioxide represent the most well-known hydrate forming components ^[22, 23]. The presence of gas molecules within the water lattice increases the stability of the lattice structure allowing gas hydrates to exist at much higher temperatures than pure ice ^[21, 24].

2.1.1 Risk of Hydrate Formations and Implications on Flow Assurance

Gas hydrate formation within transportation lines can pose a significant risk to the continued economical and safe operation of flow-lines. The formation of gas hydrate blockages (Figure 2-2) within critical systems can halt production for several days to months depending on the severity, with the abandonment of a pipeline possible if hydrate removal is considered too costly or impractical ^[20-22]. The large amount of energy required to dissociate hydrate formations coupled with the poor heat transfer through the hydrate structure makes them difficult to remove ^[21]. Furthermore, the formation of hydrate slugs may ultimately damage flow systems including pipeline walls and downstream flow restrictions, valves or bends if repeated impacts occur ^[21, 23]. The blockage or damage of transportation lines also poses significant risk of environmental damage if rupture and release of hydrocarbons and process chemicals into the surrounding environment results.

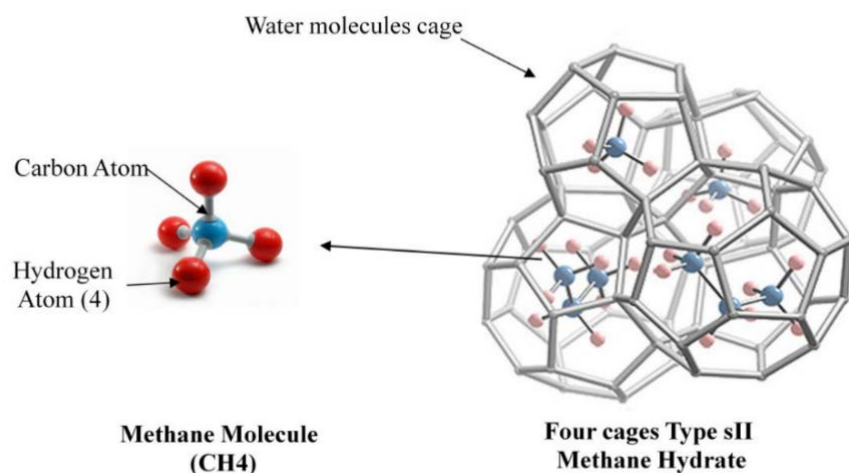


Figure 2-1: Methane hydrate type sII (Janda [25])



Figure 2-2. Gas hydrate plug in pipeline (Makogon [26])

2.1.2 Hydrate Formation Conditions and Mechanisms

The formation of hydrates within natural gas systems primarily occurs in two distinct structures; structure 1 hydrates form a body-centred cubic cell whereas structure 2 hydrates form a diamond lattice [22, 23, 27]. The combination of low temperatures and high pressure conditions are essential for the formation of gas hydrates to occur [20-24, 26, 28]. For natural gas systems, sub-sea pipelines exposed to low ambient water temperatures and high pressure originating from the well are particularly at risk of hydrate formation [21]. Furthermore, as natural gas production expands into deeper waters and more cold climates, the risk of hydrate formation poses a continually growing risk to flow assurance due to more favourable hydrate formation conditions [29, 30]. Figure 2-3 shows the locations within offshore natural gas extraction systems where hydrates are most likely to form, typically where pressure is greatest and following exposure to the cold sea environment.

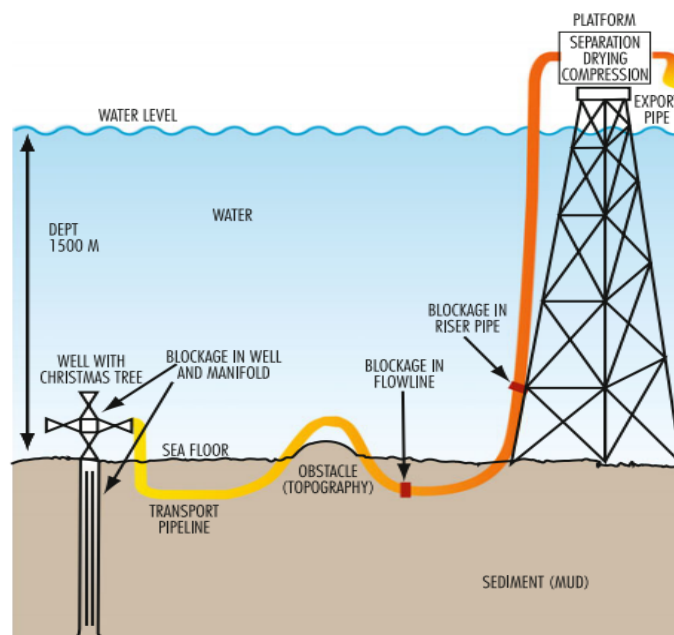


Figure 2-3. locations of gas hydrate formation in offshore systems (Giavarini and Hester [31])

2.2 Inhibition of Hydrate Formation

Due to the inherent risks of hydrates, numerous methods to prevent their formation have been developed. Modern hydrate inhibition methods can be categorised into three main techniques: (1) injection of thermodynamic hydrate inhibitors (methanol, ethanol, MEG), (2) injection of low-dosage hydrate inhibitors such as kinetic hydrate inhibitors of which modify hydrate nucleation and growth mechanics and (3) maintaining pipeline operating conditions (temperature and pressure) outside the hydrate formation zone ^[20, 23, 29]. Due to impracticalities often surrounding modifying pipeline temperature and pressure, the injection of thermodynamic and kinetic hydrate inhibitors is most commonly performed ^[20, 27, 32].

2.2.1 Thermodynamic Hydrate Inhibitors

Thermodynamic hydrate inhibitors (THI) operate by shifting the hydrate formation conditions outside of the operational zone of the pipeline towards lower temperature and higher pressure conditions ^[4, 27, 29, 32]. The current industry trend for newer natural gas developments is to use MEG as a hydrate inhibitor, replacing more traditional chemicals such as methanol due to variety of health, safety and environmental concerns ^[1, 4, 27, 32]. Figure 2-4 illustrates the locations of natural gas systems utilising MEG injection for hydrate inhibition around the world, within Australia specifically, several new developments have been recently commissioned. The hydrate inhibition effect of MEG occurs through its interaction with water through hydrogen bonding between water and the MEG hydroxyl functional group ^[30]. The resulting bond effectively reduces the hydrate stability temperature for a given pressure as the number of water hydrogen bond sites available for hydrate formation to occur are reduced ^[30, 33]. Table 2-1 compares the physical and chemical properties of methanol and MEG, the two most common THIs.

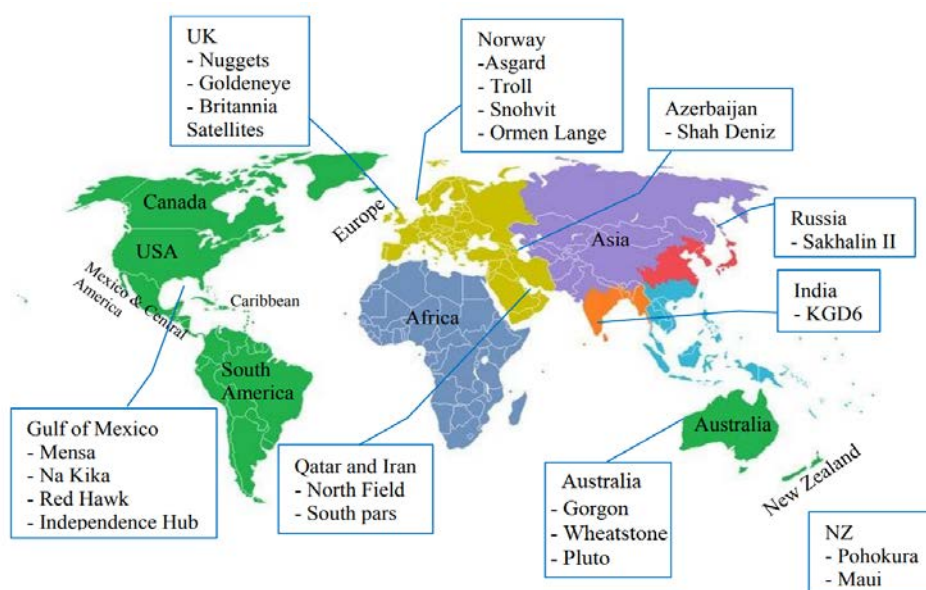


Figure 2-4. Fields using MEG injection for hydrate inhibition (modified from Al Harooni [34])

Table 2-1. Chemical and physical properties of methanol and MEG (Akers [35])

	Methanol	MEG
Family	Alcohol	Glycol
Chemical Formula	CH ₃ OH	C ₂ H ₄ (OH) ₂
Chemical Structure	$\begin{array}{c} \text{H} \\ \\ \text{H}-\text{C}-\text{O}-\text{H} \\ \\ \text{H} \end{array}$	$\begin{array}{c} \text{H} \quad \text{H} \\ \quad \\ \text{HO}-\text{C}-\text{C}-\text{OH} \\ \quad \\ \text{H} \quad \text{H} \end{array}$
Molecular Weight (g/mol)	32.04	68.068
Density (g/cm ³) at 20°C	0.7915	1.1135
Viscosity (cP) at 20°C	0.55	21
Freezing point (°C)	-97 (176 K)	-12.9 (260 K)
Boiling point (°C)	64.7 (337.8 K)	197.3 (470 K)
Flash point (°C)	11	111
Solubility in water	Fully miscible	Fully miscible

2.3 Regeneration of Mono-Ethylene Glycol

In order to minimise the operational costs associated with the injection of MEG for hydrate control, the MEG is separated alongside the water phase and regenerated through a series of chemical and physical processes to remove excess water, salts and production chemicals [1, 4-7]. The design of closed loop MEG systems are highly variable depending on expected fluid compositions and field requirements with only the distillation step being constant throughout. Depending on expected salt loads, industrial MEG regeneration systems may operate using no salt control systems, a pre-treatment stage for divalent cation removal, vacuum reclamation or a combination of both. Appendix A illustrates an industrial MEG regeneration flow-scheme utilising a combination of pre-treatment and slip-stream vacuum reclamation for salt control.

2.3.1 Distillation

The distillation step is the most crucial aspect of MEG regeneration process due to the need to remove excess water to facilitate continued hydrate inhibition. To produce a final lean MEG product suitable for reinjection at the well-head, excess water is separated from rich MEG (30-60 wt. % MEG) by distillation to regain a MEG concentration typically between 80-90% by weight [1, 7, 9, 12, 36]. To achieve the desired lean MEG concentration, the MEG regeneration unit (MRU) is typically operated between 120-140°C at atmospheric pressure [1, 37, 38]. Several operational issues are faced within the MRU including corrosion at low pH if manufactured of low corrosion resistant carbon steel, scaling at high temperature and pH conditions and fouling due to the presence of incompatible production chemicals [7, 9, 10].

2.3.1 Conventional Recovery Operation (No Reclamation)

The conventional regeneration of MEG post hydrate inhibition simply involves the removal of excess water via a single distillation column (or multiple in parallel) [1, 9, 32]. Of the most common MEG regeneration philosophies, the conventional method is the most simple, but however, comes with several drawbacks due the lack of salt handling systems. Dissolved salts and other process contaminants entering into the system will accumulate within the closed MEG loop leading to various long-term operational issues, potentially requiring total or partial replacement of the MEG inventory. As such, the conventional regeneration method is only applied to systems where the expected level of dissolved salts over the life time of the system is low, or formation water producing wells are expected to be shut-in [39].

2.3.2 Full Stream Vacuum Reclamation Operation

The reclamation of glycol solutions during the MEG regeneration process is an additional step that may be performed in order to control the levels of dissolved salts within closed loop MEG systems. The reclamation process entails the vaporisation of the MEG solution in order to force the precipitation of dissolved ionic species including organic and inorganic salts [1, 7, 8, 40]. The MEG solution is boiled under low pressure (≈ 100 mbar [7, 8, 32, 38, 40]) to minimise the operational temperature required (120 - 150°C [2, 7, 38, 40]) to vaporise the MEG/water phase in order to reduce heating requirements and to prevent thermal degradation of the MEG at excessive temperatures ($>150^\circ\text{C}$ [5, 7, 38, 41]). The vaporised MEG solution is then condensed and recovered whilst any remaining non-volatile salt components removed from the liquid phase through solid handling systems such as centrifuges.

MEG systems utilising reclamation may operate using either full-stream reclamation whereby the rich glycol stream is flashed under vacuum to totally remove dissolved salts or using a slip-stream mode post distillation to remove primarily monovalent ions from a fraction of the produced lean glycol [1, 2, 7, 8, 32, 42]. The type of reclamation process employed is determined by the expected salt production rate over the life-span of the asset with systems operating at high salt loads requiring full-stream reclamation [8, 9]. During full-stream reclamation, all salt species are removed from the MEG/water phase producing a salt free rich glycol that is then reconcentrated. The full-stream reclamation flow-scheme is illustrated by Figure 2-5. Typically, an initial separation stage is utilised prior to the reclamation system whereby the MEG is heated and depressurised within a three-phase separator to remove residual hydrocarbons from the MEG/water phase.

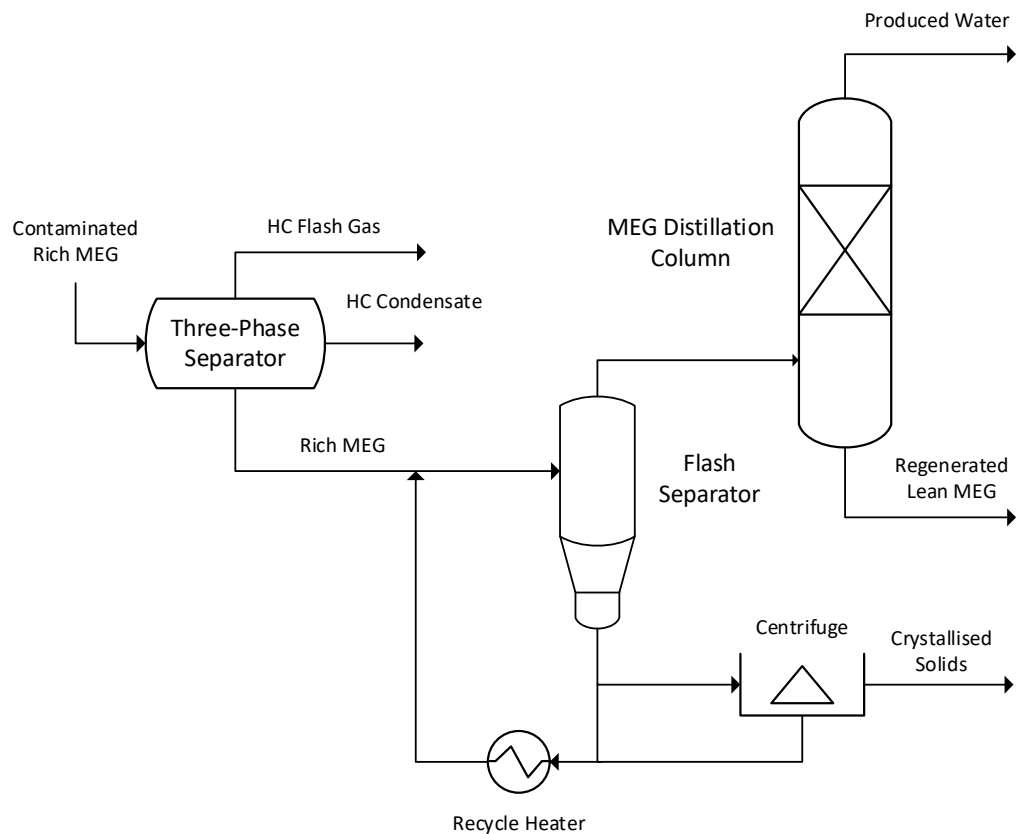


Figure 2-5. Full-Stream reclamation system

2.3.3 Slip-Stream Vacuum Reclamation Operation

In contrast, for fields with relatively low salt production rates, a lean glycol slip-stream reclamation system is often sufficient to control the salt content within the MEG loop ^[1, 8, 43] with such a flow scheme presented in Appendix A. For such systems, only a fraction of the produced lean glycol product from the regeneration unit is processed effectively reducing the total operational costs and capital expenditure requirements compared to full-stream reclamation ^[8]. The operational slip-stream rate is dictated by the expected salt load at maximum formation water production and the corresponding fraction required to maintain a constant tolerable level of dissolved salts within the MEG loop ^[8]. Furthermore, slip-stream reclamation systems are typically operated in conjunction with pre-treatment systems to remove divalent cations prior to the regeneration unit. Divalent cations such as calcium and iron are removed to prevent the formation of scale on high temperature heat exchanging equipment whilst monovalent cations such as sodium pass through and are removed during down-stream reclamation ^[9, 10, 12].

Table 2-2 compares the advantages and disadvantages of both reclamation operational methodologies and the conventional recovery method without reclamation facilities. Ultimately, for MEG systems operating past formation water breakthrough, the removal of

dissolved salts is essential to avoid mineral deposition and to ensure salt concentrations remain within operational limits. The optimisation of operational conditions during the vacuum reclamation process can provide significant improvement in the removal of organic based contaminants including organic acids and production chemicals such as corrosion inhibitors if desired.

Table 2-2. Comparison of three MEG regeneration operational methods ^[1, 8, 32]

Operating Model	Advantages	Disadvantages
Conventional Recovery	<ul style="list-style-type: none"> • Least expensive in terms of operational and capital cost • Simplest system to operate • No loss of salt based pH stabilisers 	<ul style="list-style-type: none"> • Unable to handle continuous formation water production. Non-volatile chemicals (organic acids) and salts will accumulate within closed loop • Risk of scaling in regeneration column due to salt build-up
Full-Stream Reclamation	<ul style="list-style-type: none"> • Total removal of non-volatile chemicals and dissolved salts • Can withstand full formation water production • Prevention of scaling downstream during regeneration 	<ul style="list-style-type: none"> • Highest operational and initial capital cost • Larger physical size of unit compared to slip-stream mode • Salt based pH stabilisers removed
Slip-Stream Reclamation	<ul style="list-style-type: none"> • Reduced cost compared to full stream reclamation • Lower operational and capital cost compared to full stream reclamation. Reduced throughput requires less heating and cooling and reduced system size • More flexible operation compared to full stream reclamation 	<ul style="list-style-type: none"> • Accumulation of salts and impurities within recycle loop may be problematic. Viscosity must be controlled • Cannot handle excessive salt loads within MEG loop • Pre-treatment required to prevent scaling within regeneration column

2.3.3.1 Rich MEG Pre-Treatment

Where slip-stream reclamation is utilised, the pre-treatment of rich MEG is performed to prevent the formation of scaling products downstream within the regeneration system that would otherwise significantly impact operational performance ^[9, 10, 12]. Section 2.4.2 outlines the most prevalent scaling products found within MEG regeneration systems and the operational concerns regarding their presence and the overall need for pre-treatment. The removal of predominantly divalent cationic species (calcium, iron and potentially magnesium) during the pre-treatment process is achieved by generating alkaline conditions that favour the formation and subsequent precipitation of divalent salts ^[10, 12]. The presence of dissolved carbon dioxide from the pipeline coupled with alkaline conditions (typically pH >8) allows the formation of

carbonate (Equation (2-1)) facilitating the formation of carbonate salts, namely calcium and iron carbonate (Equations (2-3) and (2-4)). The formation of hydroxyl salts may also occur at pHs greater than 10.2 allowing the removal of magnesium (Equation (2-5)). Solids precipitated during the pre-treatment process can be removed via either settlement within down-stream storage tanks or in-line filtration systems at sufficiently large particle sizes.

A variety of operational issues may be faced within industrial pre-treatment and associated settlement systems stemming from poor particle size, sub-optimal operating conditions, as well as the effect of production chemicals such as scale inhibitors and hydrocarbons on crystallisation mechanisms and particle behaviour ^[10, 12].

2.4 Salts, Scaling and Organic Acids within MEG Regeneration Systems

During the regeneration of MEG, various contaminants can be experienced within the regeneration system including mineral salts, both mono and divalent, organic acids and production chemicals including corrosion and scale inhibitors.

2.4.1 Monovalent Salts

The presence of monovalent ions within closed loop MEG regeneration systems primarily occurs in the form of sodium, potassium, chloride and bromide. Monovalent species may enter the system via two path ways including the dosage of production chemicals such as basic chemicals for pH control or following formation water breakthrough. The term formation water defines the liquid water naturally present within the pores of the reservoir rock formation ^[10]. The breakthrough of formation water refers to the commencement of extraction of said water from the reservoir and may not occur until several years into the production ^[10]. Dissolved sodium alone may account for as much as 90-95% of all dissolved cationic species within closed loop MEG systems with potassium accounting for the majority of the remainder ^[1, 7, 10]. In a similar manner, chloride and bromide ions are the primary anionic species found within MEG regeneration systems and may pose significant operational issues at high concentrations including contribution to general and pitting corrosion ^[44-46]. Due to the high levels of sodium and chloride ions typically found within closed loop MEG systems, sodium chloride is one of the primary salts produced within salt removal reclamation systems ^[7, 47].

2.4.2 Divalent Cations and Scaling Within MEG Regeneration Systems and Natural Gas Pipelines

The formation of mineral scaling is a continuous concern within MEG regeneration systems and natural gas pipelines due to the presence of divalent cation species and favourable scale formation conditions. Divalent cations including calcium, magnesium and barium may enter the

natural gas and MEG regeneration systems following the breakthrough of formation water as they are naturally present within the pores of the reservoir [7, 9, 10, 12, 48, 49]. The presence of dissolved iron instead arises from the corrosion of the carbon steel pipeline with between 10-100 ppm Fe²⁺ typically experienced at the pipeline outlet within the aqueous/MEG phase [48]. The primary scale formations experienced within MEG/natural gas systems and their respective formation reactions are outlined by Table 2-3. The primary risk of scale formation occurs within natural gas pipelines and MEG systems operating under pH stabilisation post formation water breakthrough where the pH is sufficiently high to form carbonate ions (pH > 8.2) [48, 50, 51]. The formation of scale within sub-sea injection systems and tie-ins can result in significant operational issues including blockages and restriction of flow [48, 50, 51].

Table 2-3. Dominant scale formation reactions in MEG and natural gas systems

Carbonate	$\text{CO}_2 + \text{H}_2\text{O} \leftrightarrow \text{H}_2\text{CO}_3 \leftrightarrow \text{HCO}_3^- + \text{H}^+ \leftrightarrow \text{CO}_3^{2-} + 2\text{H}^+$	(2-1)
	$\text{CO}_2 + \text{MDEA} \leftrightarrow \text{HCO}_3^- + \text{MDEAH}^+$	(2-2)
Calcium	$\text{Ca}^{2+} + \text{CO}_3^{2-} \leftrightarrow \text{CaCO}_3$	(2-3)
Iron	$\text{Fe}^{2+} + \text{CO}_3^{2-} \leftrightarrow \text{FeCO}_3$	(2-4)
Magnesium	$\text{Mg}^{2+} + \text{OH}^- \leftrightarrow \text{Mg}(\text{OH})_2$	(2-5)
Barium	$\text{Ba}^{2+} + \text{SO}_4^{2-} \leftrightarrow \text{BaSO}_4$	(2-6)

2.4.2.1 MEG Regeneration Systems

The primary risk of scaling within MEG regeneration system specifically arises within systems operating at high temperatures including the main MRU and heat exchanging equipment [9, 10, 12]. Operating at temperatures between 120-140°C to boil-off excess water [1, 7, 38], processing of rich MEG solutions containing divalent cations will result in significant scale formation within the reboiler due to the inverse solubility of carbonate salts with respect to temperature [7, 9, 10, 12, 49]. Excessive scale formation upon the reboiler bundle will ultimately reduce heat transfer efficiency of the reboiler increasing heating requirements or require frequent cleaning reducing operational uptime. Typically, the most frequently experienced scaling during MEG regeneration includes the formation of various calcium carbonate polymorphs including vaterite, aragonite and calcite [48-50, 52, 53], magnesium-based scales (hydroxide at high pH, dolomite in the presence of calcium) and iron-based scales including iron carbonate and sulphide following corrosion in the pipeline [7, 9, 10, 12, 49]. Figure 2-6 illustrates a MRU reboiler bundle fouled by predominantly FeCO₃ during industrial MEG regeneration resulting in reduced operational performance. In order to prevent scaling within MEG regeneration systems, either pre-treatment or full-stream reclamation is performed to remove scaling products from the system prior to entering the MRU.



Figure 2-6. MEG regeneration unit tube bundle fouled by FeCO_3 (Latta [10])

2.4.2.2 Natural Gas Pipelines and Scale Inhibition

To combat the risk of scale formation, scale inhibitors may be injected independently or in conjunction with pre-treatment to ensure scaling does not occur within subsea systems where scale formation would be costly and difficult to remove [53]. However, if the breakthrough of formation water and subsequent introduction of divalent cations is not correctly predicted and controlled through either scale inhibitors and/or pre-treatment, the lean MEG injected at elevated pH and alkalinity poses a significant scaling risk downstream of MEG injection points and the primary pipeline [1, 7, 48]. Potential temperature and pressure changes along the pipeline during transportation may shift the salt concentration into their respective super saturation regions resulting in scale formation [48]. Although the conditions for scale formation are present, the actual formation of scale is dependent upon the ability of scale nucleation to occur and induction time [48]. The work of Flaten and co-workers [48, 50, 52, 54, 55] has extensively covered the formation of scale in terms of formation mechanics, induction times and polymorphism of calcium carbonate within MEG systems.

Multiple mechanisms by which scale inhibitors influence or disrupt the formation of scale have been proposed including the inhibition of nucleation and the inhibition of crystal growth [56-62]. Nucleation inhibition refers to the process by which scale proto-crystals successfully form but are then redissolved through interaction with inhibitor molecules hence disrupting significant growth [56, 59, 60]. Conversely, some scale inhibitors may act by retarding the growth of the crystal following nucleation through adsorption or interaction with the active crystal growth sites hindering future crystal growth [56, 59, 60]. It is widely agreed upon that most commercially

available scale inhibitors varying from phosphonates to polymeric types, inhibit scale formation through a combination of both mechanisms ^[56]. However, the extent to which a scale inhibitor influences scale through either mechanisms is dependent on the type of scale being inhibited. Smaller phosphonate based inhibitors primarily operate through inhibition of crystal growth whilst polymeric based inhibitors such as carboxylic acids typically inhibit the nucleation process ^[56, 59].

2.4.3 Organic Acids

The presence of organic acids within natural gas pipelines and associated MEG regeneration systems can occur through several pathways. Primarily, free organic acids present within the reservoir will enter through the condensed water phase and ultimately transition into the MEG regeneration system alongside MEG and water during initial inlet separation from the gaseous and liquid hydrocarbons ^[7-9, 63]. The primary organic acids experienced during industrial natural gas processing and MEG regeneration include acetic, propanoic, butanoic and formic acids ^[7, 9, 63], with acetic acid accounting for an estimated 50-90% of total organic acid content ^[64]. Additionally, further organic acids may enter into the system during key points in a natural gas production systems lifespan including post formation water breakthrough or during back-production of well drilling/completion fluids following new well start-up ^[9, 63]. The thermal degradation of MEG during high temperature regeneration in the presence of oxygen may also provide an additional avenue in which organic acids are produced. MEG will undergo thermal oxidation at temperatures above 110°C with the primary products including glycolic, formic and acetic acids ^[1, 3, 5, 39, 63].

The introduction of organic acids into natural gas transportation pipelines and MEG systems can have several adverse operational effects including direct reduction of the pipeline's liquid phase pH. Ultimately, reduced pH within the liquid phase of a transportation pipeline can pose a corrosion risk through increased solubility of protective iron carbonate film formed during pH stabilisation requiring sufficient alkalinity within the injected lean MEG to neutralise incoming organic acids ^[65-68]. Organic acids have been directly linked to increased corrosion rates in carbon and mild steel piping in industrial natural gas and oilfield systems ^[69-72] and are capable of being reduced upon the surface of metals and hence contributing to electrochemical corrosion reactions ^[67, 68, 72]. Furthermore, in combination with carbon dioxide, organic acids may exacerbate the rate of Top-of-the-Line-Corrosion (TLC) ^[17, 63, 72-76]. As such, the presence of organic acids within natural gas transportation pipelines may pose significant operational issues in terms of corrosion. Although the introduction of organic acids into the system from the

reservoir cannot be prevented, the total system wide level of organic acids can be controlled through the MEG regeneration system via either distillation or reclamation. Optimisation of organic acid removal during MEG processing can therefore help to minimise the long-term corrosion risks associated with organic acids.

2.5 Corrosion and Corrosion Prevention in Natural Gas Pipelines and MEG Regeneration Systems

The corrosion of metals is one of the most consistent problems faced in almost every chemical processing industry, with the prevention of corrosion in the oil and gas industry particularly important. Various processing systems within the oil and gas industry are susceptible to corrosion including long distance transportation pipelines made of poor corrosion resistant carbon steel and high temperature/pressure systems where the risk of failure can have significant implications on safety and the environment. Within the oil and gas industry, the cost of corrosion has been estimated by the National Association of Corrosion Engineers (NACE) to be as high as \$1.372 billion owing to unscheduled plant shutdowns, equipment failure, maintenance and regulatory fines due to loss of containment and environmental damage^[77]. As such, the prevention or minimisation of corrosion can have significant implications on all industries in terms of reduced operational expenditure and improved process safety^[78-80].

2.5.1 Types of Corrosion

2.5.1.1 General Corrosion

The corrosion of metals occurs as part of an electrochemical reaction between the metal and its environment^[78-80]. Electrochemical reactions involve the transfer of electrons from one chemical species to another, with the metal surface acting as the anode during corrosion process providing electrons for a reduction reaction to occur^[80]. For systems comprised of steel, corrosion of the metal surface occurs through the anodic dissolution of iron and subsequent oxidation to Fe(III) given by Equations (2-7) and (2-8). For the corrosion process to occur, the metal surface must be in contact with a liquid phase containing dissolved chemical species to facilitate the corresponding cathodic reduction reaction. Within most liquid systems, the presence of hydrogen ions at low pH and dissolved oxygen are the primary reduction reactions as given by Equations (2-9), (2-10) and (2-11). In terms of general corrosion, dissolved oxygen is considered a stronger oxidant than the hydrogen reduction reaction and may occur at all pH levels^[81]. Figure 2-7, illustrates the corrosion of a carbon steel surface through the reduction of hydrogen ions by Equation (2-7) and (2-9).

Table 2-4. General corrosion electrochemical reactions

Oxidation (Anode):		
Iron	$\text{Fe} \rightarrow \text{Fe}^{2+} + 2\text{e}^{-}$	(2-7)
	$\text{Fe}^{2+} \rightarrow \text{Fe}^{3+} + \text{e}^{-}$	(2-8)
Reduction (Cathode):		
Hydrogen ions	$2\text{H}^{+} + 2\text{e}^{-} \rightarrow \text{H}_2$	(2-9)
Oxygen (low pH)	$\text{O}_2 + 4\text{H}^{+} + 4\text{e}^{-} \rightarrow 2\text{H}_2\text{O}$	(2-10)
Oxygen (high pH)	$\text{O}_2 + 2\text{H}_2\text{O} + 4\text{e}^{-} \rightarrow 4\text{OH}^{-}$	(2-11)

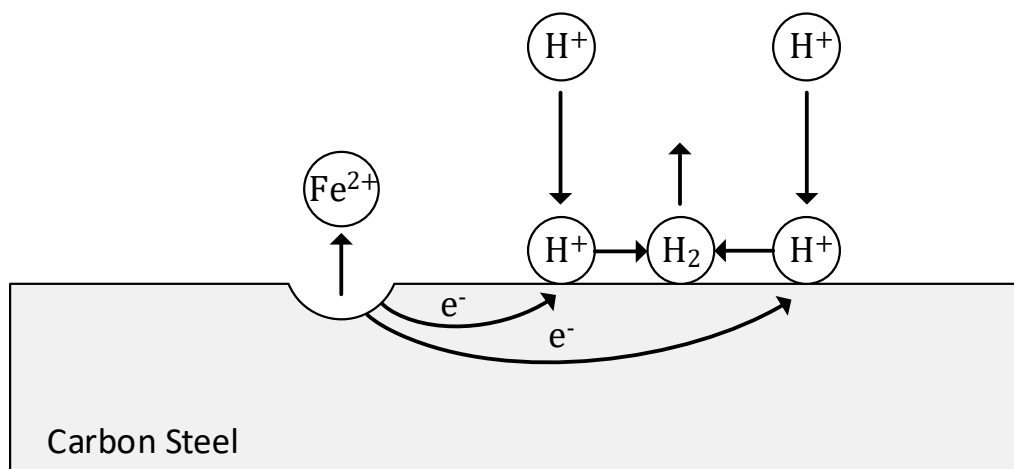


Figure 2-7. Corrosion of carbon steel by hydrogen reduction

2.5.1.2 Uniform Corrosion

Uniform corrosion is one of the most common types of corrosions of metal surfaces within aqueous environments where uniform contact between the corrosive medium and metal surface occurs [78-80]. Uniform corrosion involves an even attack across the surface of a metal and is considered one of the more mild forms of corrosion due to its ease in detection, reproducibility and prevention [80].

2.5.1.3 Pitting Corrosion

Pitting corrosion is a localised form of corrosion leading to the formation of cavities or 'pits' upon the surface of a metal [78-80]. Pitting corrosion is considered one of the most destructive types of corrosion due to the difficulty in detecting the formation of pits and problems in designing against pitting corrosion [80, 82, 83]. The formation of a deep, narrow pit can ultimately lead to the complete failure of an entire system with transportation pipelines particularly susceptible to failure [82, 83]. Several factors may contribute to the onset and propagation of pitting corrosion including [78-80, 82-84]:

-
- Localised damage to protective films formed on the surface of the metal such as during pH stabilisation of natural gas pipelines. Breakdown may occur through mechanical or chemical means with several factors influencing chemical breakdown:
 - Dissolving of protective films under acidic conditions, metal oxides and carbonates will dissolve at low pH.
 - Dissolved oxygen ^[84-86] and high chloride concentrations ^[80, 87] will destabilise protective films.
 - Poor application or selection of coatings.
 - Non-uniformities in the metal structure of the surface including non-metallic inclusions at the metal surface providing active sites for corrosion to occur.

2.5.1.4 Crevice Corrosion

Crevice corrosion is another form of localised corrosion of which occurs when stagnant microenvironments form within shielded areas including under washers, bolt heads, gaskets and potentially under scale and other surface formations ^[78-80]. Crevice corrosion is often initiated by a variation in oxygen concentration between the crevice corrosion site and the adjacent bulk fluid, often referred to as the differential-aeration mechanism. Oxygen present within the crevice corrosion site is consumed through reaction with the metal (Equation (2-10) and (2-11)) leading to a differential aeration cell due to restricted oxygen diffusion into the area. Due to the limited oxygen supply available, the cathodic oxygen-reduction reaction cannot be sustained within the crevice and reduction commences at the surface of the metal. The large cathodic surface area relative to the anodic corrosion site exacerbates the rate of corrosion due to the high current density ^[80]. Furthermore, within the crevice microenvironment, metal ions produced during corrosion tend to readily hydrolyse forming hydrogen ions and as a result, a highly acidic microenvironment conducive to corrosion.

2.5.2 Corrosion in Natural Gas Pipelines

Long distance natural gas and condensate pipelines are typically constructed from low corrosion resistant carbon steel due to the low cost of production ^[4, 88] and are susceptible to 'sweet' and 'sour' corrosion in the presence of acid gases and free water during transport and processing, refer to Figure 2-8 ^[4, 89, 90]. The primary gas phase contributors to corrosion in natural gas pipelines include CO₂ (sweet) and H₂S (sour) ^[4, 51, 81, 88, 91-94] with up to 60% of corrosion experienced in the oil and gas industry resulting from CO₂ based corrosion ^[88, 95]. The presence of these acidic gases in the gas phase will lead to their dissolution into the liquid phase resulting in the release of hydrogen ions and hence reduced liquid pH (refer to Equations (2-12) and (2-13)). The low corrosion resistance of carbon steel ultimately requires effective corrosion

mitigation strategies to maintain pipeline integrity over the life span of the asset. The presence of MEG itself has also been shown to impede CO₂ corrosion of carbon steels when used as a hydrate inhibitor through adsorption to the metal surface [4, 96, 97]. Furthermore, natural gas pipelines are susceptible to failure due to excessive pitting corrosion arising from dissolved oxygen in drilling fluids and the breakdown of protective films such as coatings, organic films (FFCI) or mineral deposits (pH stabilisation) [82, 83, 98]. Figure 2-9 illustrates the failure of a natural gas pipeline due to pitting corrosion.

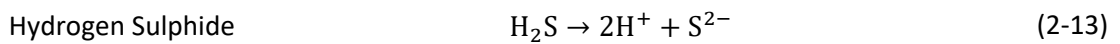
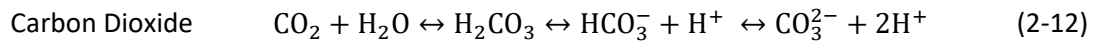


Figure 2-8. Internal corrosion of a natural gas pipeline (Popoola [98])



Figure 2-9. Pitting failure of a natural gas pipeline (Mansoori [82])

2.5.2.1 Factors Influencing Natural Gas Pipeline Corrosion

2.5.2.1.1 Gas Phase Composition

One of the primary factors driving the rate of corrosion in wet gas and condensate transportation pipelines is the composition of the gas phase [88]. The presence and partial pressure of acidic gases (CO_2 and H_2S) within the gas phase will ultimately dictate the acidity of the liquid phase and the rate of pipeline corrosion [4, 91, 93]. Many wet gas pipelines will experience sweet corrosion due to the presence of CO_2 , however, H_2S may not be present within all systems [88]. The additional presence of H_2S can increase that rate of CO_2 based corrosion acting as a promoter of the anodic dissolution of iron. However, one of the primary concerns regarding the presence of H_2S includes the potential for sulphide stress cracking corrosion to occur [99].

2.5.2.1.2 Liquid Phase pH

The liquid phase pH within a wet gas pipeline plays an important role in determining the rate and extensiveness of corrosion. Predominantly, the liquid phase pH is a measurement of hydrogen ion activity and hence an indirect measure of how corrosive a liquid will be [88]. Maintaining a high pH can have significant corrosion benefits to the operation of a pipeline including buffering against acidic gases, reduction in hydrogen availability for cathodic reduction and the promotion of protective scale formations [4, 88]. However, excessively high pH levels may contribute to stress cracking corrosion of steel [100] and undesirable scaling of process systems.

2.5.2.1.3 Temperature

The operating temperature of a pipeline can have numerous impacts on the rate of corrosion predominantly through its effects upon the formation of protective films (discussed in Section 2.5.3.1) including reaction kinetics, morphology and film stability [4, 88, 91, 94, 101]. At low temperatures ($<30^\circ\text{C}$), the solubility of FeCO_3 is high and the kinetics of formation low resulting in difficulties in the formation of protective FeCO_3 films [4, 51, 88]. With increasing temperature, the rate of formation of protective scale films increases reducing the overall corrosion rate in the presence of CO_2 [102-104]. Furthermore, with increasing temperature the thickness of the FeCO_3 protective film increases further providing corrosion prevention [101].

2.5.2.2 Top of Line Corrosion

The occurrence of Top of Line Corrosion (TLC) is a common issue facing the oil and gas industry, particularly within multi-phase wet gas and condensate pipelines [16, 63, 65, 72, 105]. Water within the gas phase of the pipeline tends to condense above the liquid phase level commonly referred to as the top of the line. Acidic gases such as carbon dioxide and hydrogen sulphide within the pipeline dissolve within the condensed water forming a highly corrosive low pH solution [63, 65, 72, 105] as illustrated by Figure 2-10. The occurrence of TLC is often difficult to control

as conventional corrosion inhibitors are restricted to the liquid phase of the pipeline and often cannot reach where TLC occurs [63, 65, 72, 105]. Furthermore, organic acids are often present within the produced gas and will condense alongside water further reducing pH and contributing to TLC [63, 72].

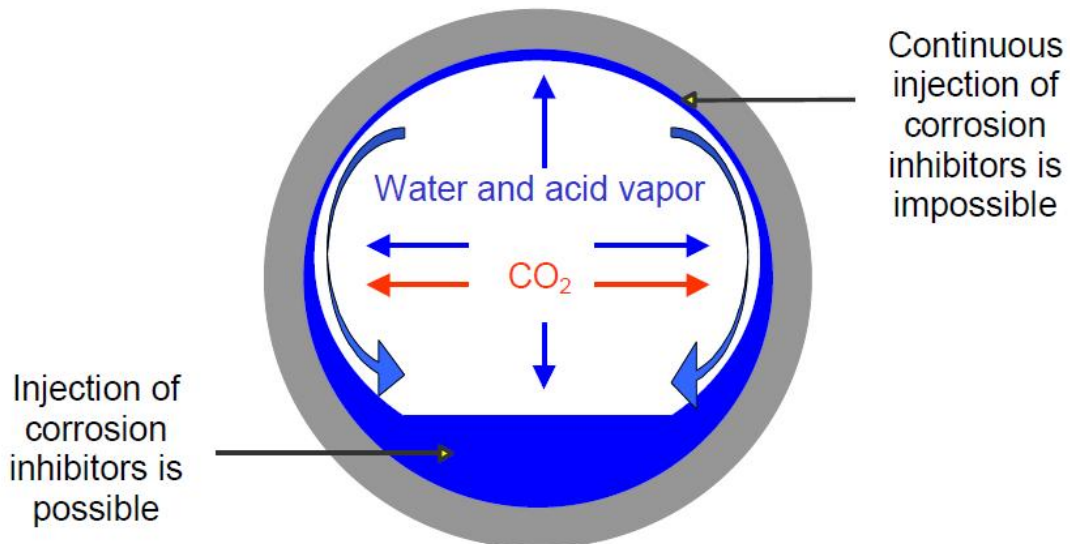


Figure 2-10. TLC mechanism due to water condensation (Yeaw [106])

TLC corrosion can be minimised by various techniques including internal cladding of pipelines with corrosion resistance alloys (CRA) and the use of thermal insulation to reduce the water condensation rate [63]. Volatile corrosion inhibitors have also been developed in attempts to control TLC through their condensation above the liquid line to form a protective film [63, 107, 108]. The presence of MEG has been demonstrated to influence the rate of TLC in wet gas pipelines through several factors including, differences in CO₂ solubility in the liquid phase compared to pure water [4, 72] and potential absorption of water from the gas phase reducing the rate of condensation [72]. Alternatively, wet gas pipelines operating under pH stabilisation typically experience TLC to a significantly less extent than those utilising FFCIs [8, 17]. A high pH within the liquid phase helps neutralise free organic acids preventing their evaporation and subsequent condensation at the top of the line [4, 16, 51, 72].

2.5.3 Corrosion in MEG Regeneration Systems

A wide range of operational conditions including temperature and pH may be utilised in MEG regeneration systems in order to remove water (distillation) and other process contaminants that potentially require low pH to facilitate their removal during vacuum reclamation. Additionally, due to the high partial pressure of CO₂ in the transportation pipeline, the pH of the incoming rich glycol is often highly acidic. As such, care must be taken during

industrial MEG regeneration to ensure that the operational conditions do not pose a corrosion risk to systems constructed of carbon steel including storage vessels and potentially the MRU reboiler [2, 9, 10]. The study of Gonzalez [109] found high corrosion rates of carbon steel in rich MEG solutions up to 95°C at pH 5. For rich glycol solutions at the higher temperatures tested, carbon steel showed corrosion rates of up to 0.45 mm/y and the occurrence of pitting. Furthermore, oxygen may be present within high concentrations within the rich and lean glycol solutions with oxygen contamination potentially occurring through various pathways including [8, 19, 84, 86].

- Impure blanketing gases for MEG storage vessels containing up to 3-5% oxygen
- Vacuum reclamation systems operating under vacuum may result in oxygen intrusion through poor seals
- Oxygen contaminated production chemicals injected into the MEG system

The presence of oxygen may facilitate corrosion through the reduction of oxygen upon the metal surface (Equation (2-10) and (2-11)). Palencsár [86] studied the corrosion of carbon steel MEG injection lines in the presence of oxygen contaminated lean MEG. The study concluded that the contribution of oxygen reduction on the overall corrosion of carbon steel between 5-65°C over a wide range of pHs was minimal. It was suggested that the bulk of oxygen was typically consumed by ferrous ions present within the solution before corrosion could occur. However, if insufficient consumption of oxygen occurs, the presence of oxygen may pose a risk to both the injection pipeline and sub-sea MEG injection systems made of corrosion resistant alloys (CRA). The presence of even minute concentrations of oxygen prior the reinjection has been shown to present a significant corrosion risk to the CRAs used in sub-sea systems [8, 81, 82, 84, 110-113]. Furthermore, oxygen may negatively influence the stability and corrosion mitigation properties of passivating iron carbonate films formed during pH stabilisation [81, 111]. To minimise the risk of corrosion via oxygen, it is common practice in industry to reduce the total dissolved oxygen content in the lean MEG to below 20 ppb prior to injection through either chemical oxygen scavengers or ultra-pure blanketing gasses [8, 83, 113, 114].

2.5.4 Corrosion Mitigation Methods

2.5.4.1 pH Stabilisation

pH stabilisation is a corrosion mitigation strategy utilised in carbon steel wet gas and condensate pipelines operating using MEG for hydrate inhibition to limit the rate of internal corrosion. The basis of pH stabilisation entails artificially increasing the liquid phase pH to reduce the availability of hydrogen ions for the cathodic corrosion reaction, whilst also promoting the formation of a protective FeCO_3 film on the surface of the pipeline [4, 15, 17, 51, 96]. The application

of pH stabilisation is primarily utilised in systems experiencing sweet corrosion due to the presence of CO₂ [9, 17, 51, 115]. Where H₂S is present within the reservoir, limited industrial usage of pH stabilisation for corrosion control has been reported, however, several studies indicate pH stabilisation may be suitable for sour gas systems [17, 115]. Corrosion control by pH stabilisation can be achieved through dosage of any basic chemical including salt-based hydroxides and carbonates as well as amine compounds such as methyldiethanolamine (MDEA). The selection of suitable pH stabiliser is dependent on several operational concerns including solubility in MEG, compatibility with other process chemicals and the behaviour during the regeneration and reclamation processes [4].

The lean glycol pH or alkalinity required to achieve sufficient corrosion control during pH stabilisation is primarily dependant on the partial pressure of CO₂ within the pipeline and the pipelines operating temperature [15, 17, 51]. Pipelines operating at lower temperatures require significantly more bicarbonate alkalinity to generate the protective FeCO₃ films due to the high solubility and reduced formation kinetics of FeCO₃ at low temperatures [17]. At temperatures below 20°C, Pojtanabuntoeng [4] suggested that corrosion control by pH stabilisation was limited to the neutralisation of acidic gases due to limited FeCO₃ precipitation.

The application of pH stabilisation has several operational limits including the high risk of scaling once formation water breakthrough occurs [9, 15, 17, 116]. Upon the onset of formation water production, the introduction of divalent cations including calcium, magnesium and barium pose a significant scale risk to sub-sea MEG injection systems and the primary pipeline at the high pHs and alkalinities (carbonate and hydroxide) maintained during pH stabilisation. As such, the application of pH stabilisation for corrosion control is limited to systems producing condensed water only. Likewise, during well clean-up operations the sudden back production of drilling and completion fluids may also pose a scaling risk [4].

Where moderate to high risk of formation water production is present, such systems may instead operate under partial pH stabilisation in conjunction with the injection of film forming corrosion inhibitors (FFCIs) to ensure adequate corrosion control [4, 17]. A chemical scale inhibitor may also be injected to minimise the risk associated with sudden formation water breakthrough [17, 32]. The dual combination of partial pH stabilisation and FFCIs provides good control of both general and local CO₂ corrosion and reduced TLC rates compared to pure FFCI usage [8, 17].

2.5.4.2 Film Forming Corrosion Inhibitors

Film forming corrosion inhibitors (FFCIs) are another corrosion mitigation strategy commonly used in carbon steel wet gas pipelines and can be utilised at the natural pH of the liquid phase [8-10, 14]. FFCIs provide corrosion protection through the formation of a thin film upon

the surface of the pipeline preventing direct contact with the corrosive liquid phase and pipeline wall. FFCIs typically consist of surfactant molecules that attach themselves to the pipeline surface through chemisorption or physisorption forming a hydrophobic surface that repels water. The film formed by FFCIs must be capable of withstanding high shear stress to prevent degradation of the protective film and hence loss of corrosion protection ^[2, 117]. The generally accepted limit for corrosion in pipelines using FFCIs is 0.1 mm/year ^[4, 14].

Several operational issues may be faced when utilising FFCIs for corrosion control including thermal degradation within MEG regeneration and reclamation systems at high temperature, and poor compatibility with other production chemicals ^[4, 8, 14]. The accumulation of FFCI degradation products may ultimately result in foaming, emulsion and fouling issues downstream over multiple regeneration cycles ^[2, 4, 8, 32]. Furthermore, localised corrosion including crevice and pitting corrosion may occur when utilising FFCIs if insufficient film formation occurs within difficult to reach areas ^[9, 10].

2.5.4.3 Corrosion Mitigation Strategy Switchover

The transition from one pH corrosion mitigation strategy, either pH stabilisation or FFCI injection, to the other method may be ideal under certain operational conditions ^[8-10, 14]. During the initial start-up of a MEG regeneration and natural gas pipeline and well clean-up operations, FFCIs are typically utilised for corrosion protection due to the scaling risk associated with sudden back production of drilling and completion fluids ^[4]. Once the scaling risk has subsided, the transition to pH stabilisation is ideal due to the better overall corrosion protection compared to FFCIs and can be achieved through removal of FFCIs within the vacuum reclamation system and simultaneous injection of basic pH stabilisers ^[8, 10].

Upon the onset of formation water production, the reverse switchover from pH stabilisation to FFCIs may instead be performed to minimise the risk of system wide scaling ^[8-10]. Under such an operational philosophy, pH stabilisation chemicals are gradually removed from the MEG loop through the vacuum reclamation system and a more neutral lean glycol pH maintained ^[8]. To provide adequate corrosion and scale control, FFCIs and scale inhibitors are injected into the lean glycol prior to being reinjected at the well-head ^[8-10]. Although scale inhibitors may be injected to control scale formation within systems operating under pH stabilisation, there are operational uncertainties regarding whether sufficient scale inhibition can be generated and the overall scale risk avoided under pH stabilisation conditions ^[8, 13, 14]. Lehmann [8] further suggests that the transition from pH stabilisation to FFCIs may be necessary once acetate levels in the lean MEG product exceeds 2 g/L due to associated TLC risks.

The conduction of a corrosion mitigation ‘switch-over’ from pH stabilisation using salt-based pH stabilisers including hydroxides can be achieved simply through the vacuum reclamation system and neutralisation of the lean glycol product to the target pH through hydrochloric acid (HCl) injection. In contrast, switchover from pH stabilisation using amines including MDEA is considerably more difficult and to date has not been performed. Due to the high MDEA content utilised to provide corrosion control, potentially up to 5% by volume in the lean glycol, the removal of MDEA represents a significant undertaking and may take several regeneration cycles to perform if slip-stream reclamation is utilised. Ultimately, the optimisation of MDEA removal from the closed loop MEG system during the switchover process can have considerably cost savings. The continued presence of MDEA in the MEG loop increases regeneration duty requirements^[1, 2] and will buffer against any targeted pH changes increasing the required dosage of acid and bases.

2.5.4.4 Oxygen Scavengers

There are two potential avenues in which oxygen-based corrosion can be avoided within MEG systems including the use of ultra-pure cryogenic nitrogen or chemical oxygen scavengers. However, the use of ultra-pure nitrogen may be impracticable in MEG regeneration systems where a cryogenic nitrogen generation system cannot be installed and operated due to potential CAPEX/OPEX considerations or space limitations if the regeneration system is located on an off-shore platform. In such cases, a chemical oxygen scavenger must instead be injected into the lean MEG product prior to reinjection at the well-head to provide oxygen control. Oxygen scavengers have been widely used in water systems including high temperature boilers and seawater injection systems for oxygen control, however, their application in MEG systems is often more complex and unpredictable^[8, 19, 113, 118]. One of the most widely used oxygen scavengers in water systems is sulphite due to its low cost, proven reaction kinetics and mechanism in water and chemical stability at high temperatures^[19, 119-123].

Extensive review of the oxygen scavenger performance of sulphite and a more recently developed organic acid based oxygen scavenger utilising erythorbic acid in MEG systems has been previously conducted^[8, 19, 113, 118]. The primary issues facing oxygen scavenger usage in MEG solutions include low temperatures in sub-sea pipelines reducing reaction kinetics and the negative interaction with process contaminants including salts and organic acids^[8, 19, 113]. Furthermore, various alcohols including MEG itself has been conclusively shown to inhibit the chain-reaction mechanism of oxygen scavengers including sulphite^[19]. As such, the optimisation of process conditions including pH are essential to maximise the performance of oxygen scavengers to reduce the risk of oxygen-based corrosion. However, previously conducted studies examining the performance of oxygen scavengers in MEG fail to conclusively measure

their performance over a wide range of contaminant concentrations and system conditions including pH leading to uncertainties in their usage. Conclusive measurement of oxygen scavenger performance under these conditions can therefore help to minimise the risk of oxygen-based corrosion in MEG systems.

2.6 Chemical and Physical Behaviour in MEG Systems

2.6.1 Uncertainty and Operational Issues Faced in Industry

Identifying how various production chemicals interact with each other and other process contaminants during operation is a primary concern in industry [8]. Unforeseen negative interactions between production chemicals can ultimately result in loss of efficacy leading to corrosion, scaling or other process concerns. Similarly, various production chemicals may cause operational issues including fouling, foaming or ultimately generate degradation products if exposed to high temperature conditions [4, 8-10]. For example, surfactant based corrosion inhibitors and demulsifying agents injected upstream may cause foaming within the high temperature MEG regeneration unit through reduce liquid phase surface tension [4, 8, 10, 51]. Foaming within the distillation column will ultimately result in entrainment and reduced separation efficiency [124, 125]. As such, identifying how various production chemicals interact and influence down-stream operations is extremely important to minimise process upsets.

Furthermore, difficulties in measuring various process parameters in MEG systems poses a significant risk to continued and optimal operation of industrial regeneration systems. For instance, Sandengen [11] outlined the uncertainty in pH measurements within MEG solutions. They concluded that with increasing MEG concentration, the inaccuracy of any pH measurement consequently increased and provided a calibration factor to correct for the effects of MEG content. Ultimately, pH is one of the most important operating parameters in MEG systems governing various processes including production chemical behaviour, corrosion and the potential removal of weak acid/base species from the MEG regeneration system. Any uncertainty associated with the measurement of pH will result in significant uncertainty associated with the aforementioned aspects of the MEG regeneration process. Furthermore, it is often difficult to measure important process parameters including dissolved oxygen content in remote locations including within sub-sea equipment where the presence of oxygen may pose a corrosion risk. The difficulty in such measurements requires certainty in the performance of production chemicals including oxygen scavengers over a wide range of conditions to prevent operational issues from arising.

The lack of rigorous design and experimental data regarding the behaviour of chemicals within MEG solutions can also have detrimental effects on the optimal design and operation of MEG regeneration systems. The generation of design data including vapour-liquid equilibrium

(VLE) behaviour under conditions relevant to MEG systems such as under vacuum (reclamation systems) can aid in the design of industrial separation systems designed for MEG processing. Likewise, better understanding regarding how the presence of MEG and other common contaminants in MEG systems influences chemical behaviour can help to optimise the overall MEG regeneration process. The presence of MEG often has significant implications for production chemical behaviour ^[2, 4, 8, 19, 126], behaviour of weak/acids and bases ^[127-130] and the settlement behaviour of solid particles ^[9, 10, 12].

2.6.2 Vapour-Liquid Equilibrium (VLE)

VLE is a fundamental concept describing the behaviour of gas and liquid phases within systems undergoing interfacial mass transfer and forms the basis of physical separation processes including distillation ^[124]. The concept of VLE describes the distribution of components within the liquid and gas phases within a system and can be used to define two component systems (binary) or systems composed of multiple components (refer to Figure 2-11). From a known liquid phase composition, the corresponding composition of the gas phase can be predicted, thus allowing the modelling of gas/liquid separation processes. The generation of experimental VLE data at untested temperatures and pressures can aid in the design of industrial separation equipment including distillation columns and potentially vacuum reclamation units.

VLE data can be used to describe isobaric (constant pressure) or isothermal (constant temperature) systems, with Figure 2-11 illustrating a T-xy diagram for an isobaric binary system of MEG and water at atmospheric pressure. A T-xy or P-xy diagram illustrates the known or estimated liquid and vapour fraction of a singular component in a binary system over a temperature or pressure range respectively. From T-xy or P-xy data, VLE diagrams can be constructed illustrating the distribution of a single component in a binary system between the liquid and vapour phase (Figure 2-12).

2.6.2.1 Modelling of VLE Systems

For the most basic ideal single component liquid-vapour systems, the distribution of the chemical species within the liquid and vapour phases can be described by Raoult's Law (Equation (2-14)). A species vapour pressure (P_i^*) at a given temperature can be calculated from the semi-empirical correlation given by the Antoine Equation (Equation (9-1)). For binary systems consisting of two ideal species, the distribution of each component can be calculated through Equation (2-15) by combining the individual component's Raoult's Law equations. However, most real-world systems are un-ideal and do not directly follow Raoult's law thus requiring correction parameters to accurately model such systems.

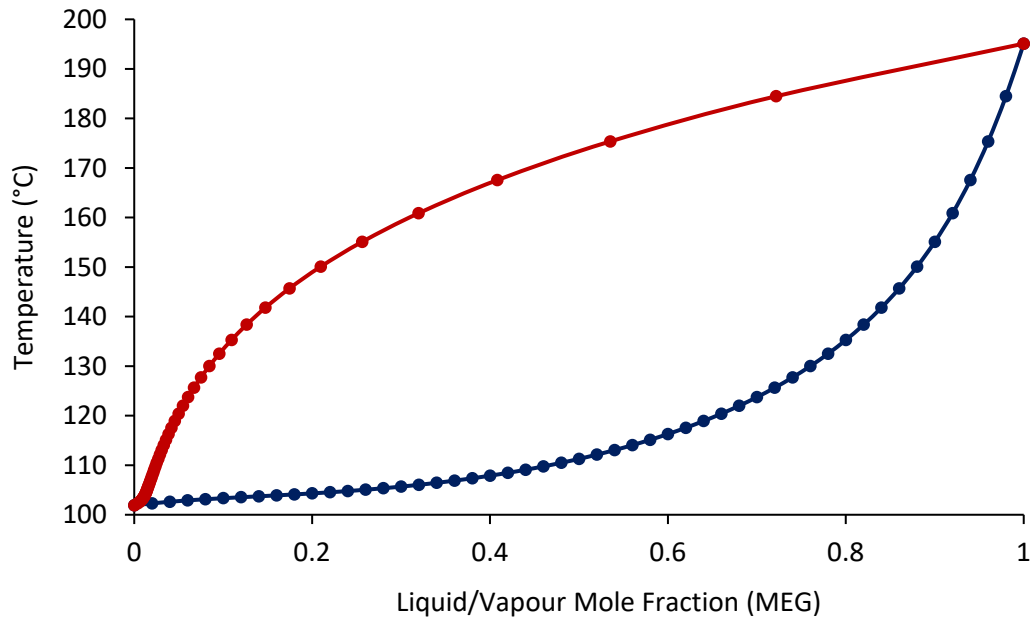


Figure 2-11. T-XY Diagram of MEG-water binary system at 101.325 kPa

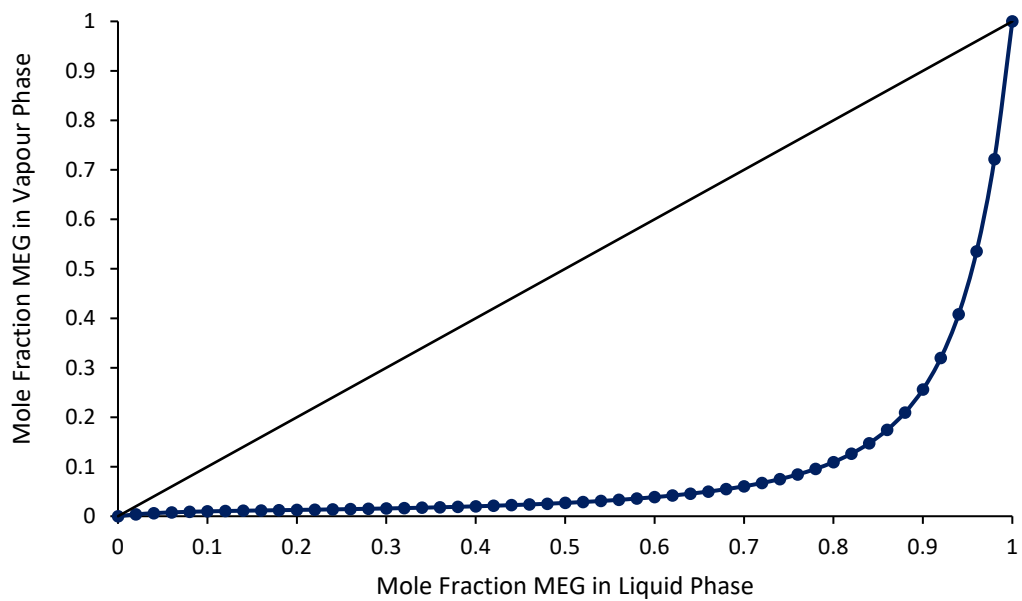


Figure 2-12. VLE Diagram MEG-water binary system at 101.325 kPa

$$y_i P = x_i P_i^* \quad (2-14)$$

$$P(y_i + y_j) = P_i^* x_i + P_j^* x_j \quad (2-15)$$

$$\log(P_i^*) = A - \frac{B}{T + C} \quad (2-16)$$

Where: P is the total system pressure, P_i^* the component 'i's vapour pressure and x_i , y_i the fraction of component 'i' in the liquid and vapour phase respectively.

To account for the un-ideal behaviour of gases and liquids, the two most commonly utilised correction parameters include activity coefficients and the fugacity coefficient. Activity coefficients are utilised to correct the un-ideal behaviour of the liquid phase resulting from an excess in Gibbs energy when compared to a corresponding ideal liquid. The required activity coefficient to correct for un-ideal behaviour can be estimated from Equations (2-17) and (2-18). In contrast, the fugacity coefficient corrects for the residual Gibbs energy of the un-ideal gas compared to that of a corresponding ideal gas and can be determined from Equations (2-19) and (2-20). From the activity and fugacity coefficients, the un-ideal behaviour of the liquid and gas phases can then be predicted using the extended Raoult's law equation given by Equation (2-21).

$$\ln(\gamma_i) = \frac{G_i^E}{RT} \quad (2-17)$$

$$G_i^E = G_{\text{real}} - G_{\text{ideal solution}} \quad (2-18)$$

$$\ln(\phi_i) = \frac{G_i^R}{RT} \quad (2-19)$$

$$G_i^R = G_{\text{real}} - G_{\text{ideal gas}} \quad (2-20)$$

$$y_i P \phi_i = x_i P_i^* \gamma_i \quad (2-21)$$

Where: The Gibbs energy, G of a chemical refers to the sum of its enthalpy (H) and entropy (S) at a given temperature ($G = H - TS$), R is the ideal gas constant, T the temperature of the system and ϕ_i the gas phase fugacity coefficient

However, the estimation of the excess or residual Gibbs energy of a liquid or gas respectively may not always be practical or possible. Various activity coefficient models have been proposed to facilitate the accurate modelling of the physical separation of chemical solutions without the need to determine the Gibbs energies of the system. The Non-Random Two Liquid (NRTL) model represents one of the most commonly used activity coefficient models for the calculation of phase equilibria with the NRTL model summarised in Table 2-5. To utilise the NRTL model, the binary parameters g_{ij} and g_{ji} must be regressed from experimental data. Furthermore, for most systems at atmospheric and vacuum pressure, the behaviour of the vapour phase is often considered ideal and the ϕ factor considered negligible^[131, 132]. However, for systems above a pressure of 10 bar, an equation of state (EOS) model is required to calculate the gas fugacity coefficient to allow accurate modelling of gas phase behaviour^[133].

Table 2-5. NRTL activity coefficient model

$$\ln\gamma_i = x_j \left[\frac{\tau_{ji}g_{ji}^2}{(x_i + x_jg_{ji})^2} + \frac{\tau_{ij}g_{ij}^2}{(x_j + x_i g_{ij})^2} \right]$$

$$\tau_{ij} = \frac{g_{ij} - g_{jj}}{RT} \quad \tau_{ji} = \frac{g_{ji} - g_{ii}}{RT}$$

$$g_{ij} = \exp(-\alpha_{ij}\tau_{ij}) \quad g_{ji} = \exp(-\alpha_{ji}\tau_{ji})$$

Where: α_{ij}, α_{ji} are non-randomness parameters from literature, τ_{ij}, τ_{ji} are dimensionless interaction parameters and g_{ij}, g_{ji} the NRTL binary parameters regressed from experimental data

2.6.3 Particle Settlement within MEG Regeneration Systems

The removal of divalent cationic species including calcium, iron and magnesium during the pre-treatment of rich glycol is an important aspect of the MEG regeneration process [9, 10, 12]. However, beyond simply the formation of divalent salts to facilitate cationic species removal, the formed salts must be removed from the bulk solution to complete the removal process. Removal of the solid particles can be achieved through either in-line filtration, particle settlement or a combination of both [10, 12]. Alongside mineral salt products formed during pre-treatment, corrosion products (iron carbonate and sulphide) formed within the pipeline and quartz from the reservoir may also enter the MEG regeneration system [9, 10]. The optimisation of particle settlement within MEG pre-treatment settlement systems can have significant operational implications through reduced filtration requirements and minimising any undesirable flow-through of particles into down-stream systems.

2.6.3.1 Physical Factors Influencing Particle Settlement

2.6.3.1.1 Particle Physical Properties

The primary particle physical properties that influence the settlement rate of solids particles include particle density, size, shape and concentration [134-137]. A particle will undergo settlement when its density exceeds that of the surrounding fluid with the settlement velocity of a singular particle under ideal conditions given by Stokes Law (Equation (2-22)). Within settlement systems where the concentration of the solid particles is high, Stokes Law fails to accurately predict settlement velocity due to particle-particle interactions including collisions, friction and particle-particle repulsion/attraction [136, 137]. Stokes Law is primarily applicable to particle settlement where the Reynolds number of the particle is low ($Re < 0.4$) [136, 137]. Furthermore, a particles shape may also influence particle settlement with irregularly shaped particles tending to settle slower compared to comparable spherical particles due to an increase in projected area exposed to frictional forces of the fluid [135, 136].

$$u = \frac{D^2 g}{18\eta} \Delta\rho \quad (2-22)$$

Where D = particle diameter, η = liquid viscosity $Pa \cdot s$, g = gravity m/s^2 and $\Delta\rho$ = density difference between solid particle and liquid phase kg/m^3

2.6.3.1.2 Liquid Phase Properties

In a similar manner to the particle, the density of the liquid phase is a primary factor influencing particle settlement as dictated by Stokes Law and equivalent settlement models [134, 136-138]. Other liquid phase factors influencing particle settlement include liquid viscosity (refer to Equation (2-22)), formation of independent water/polar and oil/non-polar phases and liquid convection currents. The combined presence of oil and water within a liquid system may influence particle settlement due to particle surface chemistry. Particles that are oil-wetted (discussed in proceeding section) have a strong tendency to adsorb to oil-water interfaces improving emulsion stability through reduced contact area between the two fluids [139, 140]. Likewise, most particles whether water-wet or oil-wet will have difficulties in transitioning through two distinct oil-water phases due to the high interfacial tension [141]. Liquid phase convection currents may also significantly influence particle settlement due to liquid phase flow against the direction of particle settlement. Convection currents can be generated by variations of liquid phase density and temperature (through effect on liquid density) due to uneven mixing, fluid composition and heating [134, 136-138], factors highly variable in large scale industrial systems including MEG settlement tanks.

2.6.3.2 Chemical Factors Influencing Particle Settlement

2.6.3.2.1 Particle Wettability

The 'wettability' of a solid surface is a measure of the surface's affinity to a liquid such as water, MEG, or oil with the degree of wettability is dictated by the liquids ability to spread on the solid surface [142]. In the presence of hydrocarbons and water, a particle may vary from strongly 'water-wet' to strongly 'oil-wet' with the degree of wettability providing a measure of a particles hydrophilicity or hydrophobicity [143, 144]. The wettability of a solid particle plays an important role in the particle agglomeration process necessary for settling to be achieved [145, 146]. The agglomeration of particles is facilitated by the formation of a '*liquid bridge*' between colliding particles [145, 147, 148] which is influenced by the particles wetted state [145, 146]. Furthermore, the wetted state of a particle may also influence its settlement behaviour. The process of film flotation is used to separate water-wet and oil-wet particles whereby particles are introduced at the water-air interface, as a result, the water-wet particles sink and oil-wet

particles float ^[149]. Particles are submerged into the wetting liquid only when the critical wetting surface tension of the particle is equal or greater than the surface tension of the liquid ^[141]. Diao and Fuerstenau [141] states that the floatation of particles is sensitive primarily to the hydrophobicity and heterogeneity of the particles with little impact due to particle size and density.

2.6.3.2.2 Particle-Particle Attraction and Zeta Potential

The stability of a dispersion of solid particles and ability to settle in liquid largely depends on particle-particle interactions that are primarily influenced by van der Waals, electrostatic and potentially steric forces ^[150, 151]. DLVO theory describes the interaction of particles by evaluating the balance between two opposing forces, electrostatic repulsion and van der Waals attraction. The net interaction between two particles is therefore the summation of the particle-particle repulsive and attractive forces. Van-der Waal attraction arises due polar interactions between molecules in the form of London Dispersion forces and Dipole-Dipole interactions. In contrast, electrostatic repulsion between similarly charged particles occurs between the electrical double layers surrounding the particles formed due to the particles surface charge ^[152-157] (refer to Figure 2-13). Particles with charged surfaces will attract counter-ions of which form a layer immediately adjacent to the particle surface as well as a second more diffuse layer of counter ions ^[157].

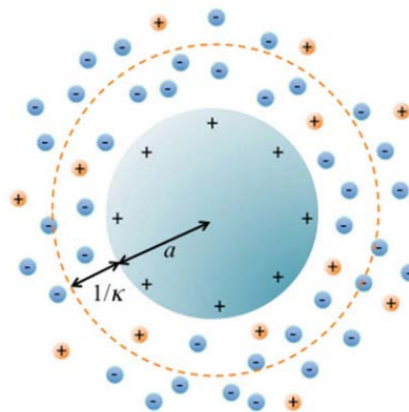


Figure 2-13. Electrical double layer around a positively charged colloidal particle from Tadros [152].

The formation of a surface charge upon a particle may arise due to defects in the structure of the crystal lattice and the interaction of the particle with electrolytes within the liquid ^[154, 158]. Solids with ionisable function groups (e.g. hydroxides) will also develop surface charges dependent on the degree of ionisation of the molecule ^[158]. Simultaneously, van der Waals attraction forces act upon particles in close proximity and must be greater than the electrostatic

repulsion due to the surface charge for agglomeration to occur^[153, 155]. Zeta potential represents a measure of the electrostatic charge repulsion/attraction between particles providing an analytical method to determine the stability of a particle suspension. At greater absolute zeta potentials, particles exert greater electrostatic repulsion between similarly charged particles prohibiting their agglomeration and settlement. Particles with low zeta potential will form large particle agglomerations and will have a stronger tendency to settle.

The presence of electrolytes strongly dictates the range of the double layer interaction between particles with increasing ionic strength reducing the overall electrostatic repulsion, indicated by reduced zeta potential^[155, 159-161]. In low ionic strength solutions where particles exhibit high surface potentials particle suspensions will tend to stabilise, in contrast, with greater ionic strength the particle suspension will lose stability and tend to flocculate and settle^[160-162]. Furthermore the surface charge of particles is also influenced by pH due to the change in hydronium and hydroxide concentrations as well as the degree of ionisation of molecules with ionisable function groups^[158] (refer to Figure 2-14). For silica particles, generation of a surface charge will occur due to the deprotonation of the surface hydroxyl sites followed by pH dependant dissociation forming discrete charged sites^[156]. As such, the surface of silica particles will tend to be positive at low pH and negatively charged at high pH. Similar behaviour is also observed for other particle species including calcite as depicted by Figure 2-14. The pH point of zero charge (pH_{pzc}) (also known as the isoelectric point) refers to the pH of the system whereby the surface charge of colloidal particles is zero^[158]. At this point, the particle will exhibit zero zeta potential indicating maximum agglomeration and hence settling potential.

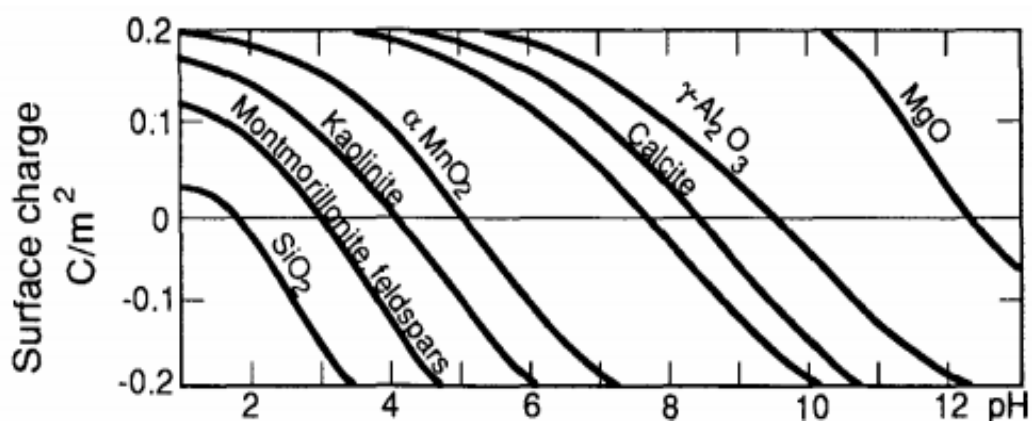


Figure 2-14. Effect of pH on particle surface charge in water (Frimmel [158])

2.6.3.2.3 Behaviour of Hydrophobic Particles in Liquid Suspensions

Non-polar substances such as hydrocarbons are insoluble within polar substances (such as water and MEG) due to the less stable nature of solute-solvent interactions compared to the

hydrogen bonds present among water-water and MEG-water molecules ^[156, 163]. However, the attraction between hydrophobic molecules (such as oil-wet particles) within water (and by extension MEG) is considered strong and a major source of particle agglomeration in other industries ^[156, 164-167]. Crist [167] evaluated the interaction behaviour of both hydrophilic and hydrophobic colloids within water. The results of the study indicated a strong interaction potential between hydrophobic particles at close distances within water leading to their aggregation. In contrast, the hydrophilic particles exhibited poorer interaction potential due to a repulsive energy barrier existing between the hydrophilic particles ^[167]. The greater aggregation of hydrophobic particles was attributed to the absence of an energy barrier between hydrophobic colloids and particle-particle interaction potential (van der Waal forces) over short distances. Ultimately, the strong tendency of hydrophobic particles in water and MEG solutions may facilitate greater settlement aiding in the removal of solid particles in the pre-treatment systems of MEG regeneration loops.

2.6.3.3 Particle Wettability in MEG Systems and Factors Affecting Wettability

Within MEG systems, the exposure to particles to condensate within the hydrocarbon transportation pipeline or organic compounds during pre-treatment may lead to the transition from water-wetted to oil-wetted. Polar organic compounds including long-chain fatty organic acids and potentially short-chain organic acids such as acetic, propanoic and butanoic may adsorb to the surface of positively charged particle surfaces including iron and calcium carbonate at low pH ^[143, 159, 168-170]. At low pH (<8-9 ^[171, 172]) the surface of carbonate salt particles becomes positively charged due to the presence of the divalent cation whereas at higher pH the increased concentration of CO_3^{-2} produces a negatively charged particle surface ^[171, 173]. The study by Thomas [172] suggests that medium to long chain fatty acids (octanoic, decanoic) show a strong affinity for the surface of calcite. However, the results of the study state that propionic acid did not show any significant adsorption onto the surface of calcite suggesting that short-chain acids such as acetate, butanoate and propanoate will not produce oil-wet surfaces. As such, the primary contribution to particle oil-wetting within MEG systems can be considered the exposure of particles such as iron corrosion products (carbonates, sulphides) and quartz (possibly present in the reservoir) to long chain fatty acids present within the hydrocarbon phase of the pipeline.

2.6.3.3.1 Measurement of Wettability

The measurement of contact angle is considered one of the primary analytical methods for quantifying the wettability of solid surfaces ^[143, 145, 174-176]. Typically, wettability is determined via contact angle measurements (θ) ^[177], which is a function of solid-fluid systems interfacial tension (Equation 2-23 – Young's equation). The degree of wettability is determined by the angle formed

by the intersection of the liquid-solid interface and the liquid-vapour interface where $\theta < 90^\circ$ indicates high wettability and $\theta > 90^\circ$ indicates poor wettability (refer to Figure 2-15) [142]. To characterise the wettability of a particle or surface, a substrate of the substance is prepared and the contact angle measured by various methods including the tilted plate contact angle method [159, 169, 174, 176]. The method involves tilting the substrate surface at an angle, introducing a droplet of the desired fluid and measured the advancing (θ_{\max}) and receding (θ_{\min}) contact angles [142, 159, 169, 176]. However, the validity of Young's equation (Equation (2-23)) and by extension the tilted plate contact angle method requires the solid surface to be smooth, flat, homogenous, inert, insoluble and non-porous [178, 179].

$$\cos\theta = \frac{\gamma_{(\text{Solid-Liquid})} - \gamma_{(\text{Solid-Air})}}{\gamma_{(\text{Liquid-Air})}} \quad (2-23)$$

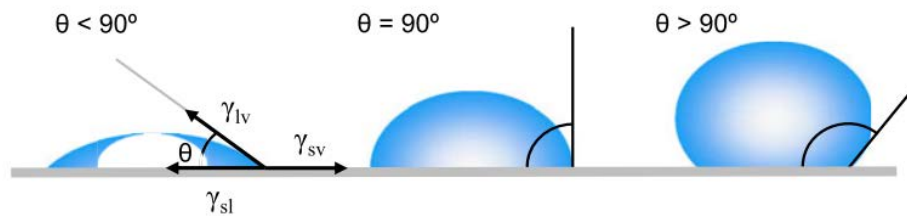


Figure 2-15. Wettability with respect to contact angle of liquid droplet (Yuan and Lee [142])

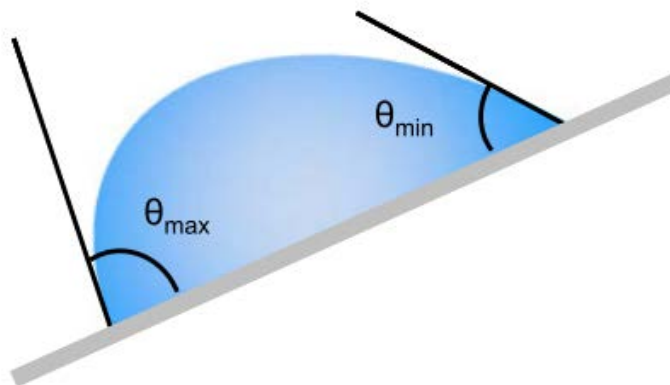


Figure 2-16. Contact angle measurement by tilted plate method (Yuan and Lee [142])

2.6.3.3.2 Liquid Surface Tension

The wettability of a solid surface is directly related to the surface tension of the surrounding liquid. A solid surface is more wettable when the liquid surface tension and the resulting liquid-solid contact angle is low [180]. The concept of critical surface tension provides a method to characterise a specific surface and by extension estimate its wettability [149, 180]. The critical surface tension corresponds to the surface tension at which a liquid completely wets a solid and

dictates at which liquid surface tension a particle will float or sink ^[149]. Furthermore, alcohol-water mixtures exhibit altered properties in comparison to pure water including reduced interfacial surface tension ^[181, 182]. Water-alcohol mixtures have also been shown to reduce the hydrophobic interaction of particles with increasing alcohol content by stabilising the structure of water around the hydrophobic surface ^[181]. As a result of reduced surface tension, the presence of ethanol has been demonstrated to reduce the contact angle of water (increased water-wetness) of initially partially hydrophobic surfaces ^[182].

2.6.3.3.3 Particle Shape, Size and Surface Roughness

The wetting behaviour of solid particles is influenced by the physical properties of the particle itself including surface roughness and particle size and shape ^[178, 179, 183]. For hydrophilic materials, increasing surface roughness results in a decrease in measured contact angle and hence more water-wet in the presence of water, whereas the opposite is true for hydrophobic particles ^[144, 178, 179, 184]. Figure 2-17 illustrates the influence of surface roughness on hydrophilic surface-particle interaction whereby the rougher surfaces provides a greater interfacial area for contact to occur ^[179]. Alternatively, for hydrophobic surfaces, the water bubble will attempt to distance itself from the crevices effectively limiting the total interfacial surface contact.

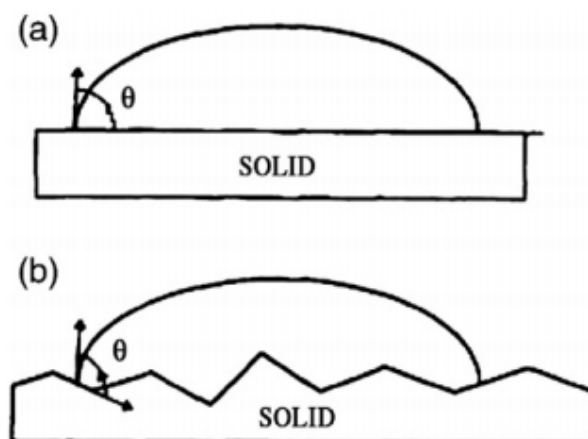


Figure 2-17. Surface roughness effect on liquid particle – surface interaction. a) smooth surface b) rough surface with increased liquid-solid interfacial contact (Kumar and Prabhu [179])

2.6.3.3.4 Surface Heterogeneity

Mixtures of solid particles typically exhibit significant heterogeneity due to differences in chemical compositions and crystal orientations ^[149]. Furthermore, individual surfaces may exhibit regions where the wettability of one area differs slightly from surrounding areas. Regions of chemical contamination also exhibit similar behaviour to chemical heterogeneities. For heterogeneous surfaces, the apparent contact angle (measured) is related to the Young's

contact angle (actual) by the Cassie Equation given by Equation (2-24).

$$\cos\theta_C = f_1\cos\theta_1 + f_2\cos\theta_2 \quad (2-24)$$

Where: f_1 and f_2 are the fractional areas of the surface for material 1 and 2

2.6.3.3.5 Presence of Metal Cations / Salinity

Within systems containing brine, oil and rocks, salinity can strongly influence the surface charge on the particles surface and liquid interface in turn affecting the particles wettability [185]. The presence of sodium, magnesium and sulphate ions within brine have been shown experimentally to reduce the oil-wetness of calcite surfaces in the presence of carboxylic anions [168, 170, 186, 187]. Rezaei Gomari and Hamouda [168] suggests that the adsorption of the dissolved ions onto the calcite surface (attraction to the negative double layer reduces the adsorption of carboxylics present in crude oil onto the calcite surface. Furthermore, Mg^{2+} exhibits a greater affinity for hydration than Ca^{2+} and as such the adsorption of Mg^{2+} onto the calcite surface may also lead to increased water-wetness [168].

The research of Qi [188] evaluated the wettability of quartz surfaces in the presence of asphaltenes present in crude oil. For quartz surfaces, the presence of magnesium and sulphate ions increased the oil-wettability of the surface by interacting with the negatively charged double layer surrounding the particle [188]. The resulting interaction between the metal cations and negative double layer reduced the magnitude of electrostatic repulsion facilitating greater adsorption of asphaltenes present in crude oil onto the quartz surface hence producing a hydrophobic surface [188]. Based on this, and the information presented in prior sections, the literature seems to suggest that factors that increase the water-wetness of calcite also increase the oil-wetness of quartz.

2.6.3.3.6 Application of Surfactants for Particle Surface Modification

The wetting preference of solid surfaces including calcium carbonate oil and gas reservoirs can be altered by interaction with surface-active agents such as emulsifiers and surfactants [176, 189, 190], with surfactants typically injected into reservoirs to reduce the oil/water interfacial tension and shift the wettability towards less oil-wet / more water-wet [190, 191]. The exposure of surfaces to surfactants/emulsifiers induces a change in the interfacial tension at the fluid/fluid and fluid/solids interface(s) by adsorption of the surfactant onto the particle surface [192, 193]. As a result, the wettability of the particle is altered dependent on the type of surfactant and the nature of rocks [156, 190, 191].

The interaction of surfactants is dependent on the surface charge of the particles, whether positive or negative. For example, a dissociated cationic surfactant ion is comprised of a

positively charged polar head and a neutral hydrocarbon tail. The positively charged head will be adsorbed to the surface of negatively charged particles due to electrostatic attraction with the particle surface displacing the counter ions present in the electrical double layer surrounding the particle [156]. As such, the neutral hydrocarbon tail will protrude from the particle into the bulk liquid producing an oil-wetted surface. However, if organic compounds such as carboxylics are initially present upon the particle surface, cationic surfactants will interact within the negatively charged carboxylics resulting in their desorption from the surface, and hence a more water-wet surface [194-196]. Alternatively, if crude oil components have been adsorbed onto the surface of a particle, anionic surfactants will form a monolayer on the surface through hydrophobic interactions [194, 197]. The resulting layer of adsorbed surfactants results in hydrophilic head groups covering the oil-wet particle producing a more water-wettable surface [190, 191].

2.6.4 Acid Dissociation Behaviour of Chemical Species

A chemical's acid or base dissociation constant (K_a , K_b) is a quantitative measure describing the extent an acid or base will dissociate within water or other solvents. Weak acids and bases will only partially dissociate, with the extent of dissociation calculable from the respective dissociation constants through Equations (2-25) and (2-26). A chemical's K_a and hence speciation behaviour can be influenced by a variety of factors including temperature, ionic strength and the dielectric constant (ϵ) of the solvent [130]. Organic solvents such as ethylene glycol typically result in an increase in acid/base dissociation constants compared to aqueous solutions [127-130].

$$K_a = \frac{[A^-][H^+]}{[HA]} \quad (2-25)$$

$$K_b = \frac{[BH^+][OH^-]}{[B]} \quad (2-26)$$

Where: A/B represent the undissociated acid or base and HA/BH⁺ represent the respective conjugate acid or base

The effect of temperature on acid dissociation behaviour is related to temperatures impact on the dissociation reaction's change in Gibbs free Energy given by Equations (2-27) in terms of standard state enthalpy change ΔH° (kJ. mol⁻¹) and entropy change ΔS° (kJ. mol⁻¹. K). The Gibbs free energy of a reaction can be related to the equilibrium constant, K_{eq} by Equation (2-28) to develop the van't Hoff equation given by Equation (2-29) of which can be used to estimate the effect of temperature on the equilibrium constant of a reaction [198]. For dissociation reactions which are endothermic, pK_a decreases within increasing temperature with the opposite occurring for exothermic reactions.

$$\Delta G^\circ = \Delta H^\circ - T\Delta S^\circ \quad (2-27)$$

$$\Delta G^\circ = -RT \ln K_{eq} \quad (2-28)$$

$$\ln K_{eq} = -\frac{\Delta H^\circ}{RT} + \frac{\Delta S^\circ}{R} \quad (2-29)$$

Due to the uncertainties associated with MEG chemistry, better understanding of how and to what extent various factors influence chemical speciation behaviour can have significant implications to the operation of MEG regeneration systems. In particular, the tendency to remove or retain weak acid/base chemical species including organic acids, amine-based pH stabilisers and other production chemicals during physical separation processes (distillation and reclamation) is dependent on the respective chemical's speciation behaviour. For long-term operation, it is ideal to minimise the loss of several process chemicals including pH stabilisers such as MDEA during the vacuum reclamation process to reduce re-dosage requirements and hence long-term operational costs [7, 8, 40, 199]. Alternatively, organic acids and MDEA post formation water breakthrough are undesirable and their removal from the closed loop MEG system beneficial [7]. As such, the accurate determination and modelling of acid dissociation constants under a wide range of conditions including MEG concentration, temperature and salinity will ultimately help to identify the critical pH levels required for either the optimal removal or retention of varying chemical species thus optimising the overall regeneration process.

For instance, Figure 2-18 illustrates the effect of temperature on the acid dissociation constant of MDEA within water as reported by Hamborg and Versteeg [200]. With increasing temperature, a lower pH is required to ensure MDEA is completely dissociated to its conjugate acid, MDEAH⁺ (Figure 2-19). Knowledge of such effects and accurate speciation data would therefore allow field operators to maximise the amount of MDEA removed during the vacuum reclamation process following the onset of formation water production. Similar improved speciation data can also help maximise the removal of organic acids during MEG regeneration separation processes. Furthermore, various process contaminants including organic acids may negatively interact with production chemicals including oxygen scavengers reducing their efficacy [19, 201, 202]. As such, improved speciation data of problematic chemicals such as organic acids tailored to the highly variable conditions within MEG regeneration systems may help to reduce negative interactions with production chemicals and resulting production issues.

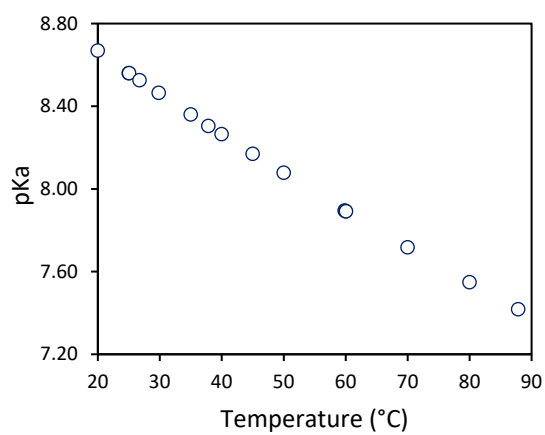


Figure 2-18. Effect of temperature on the pK_a of MDEA in water ^[200]

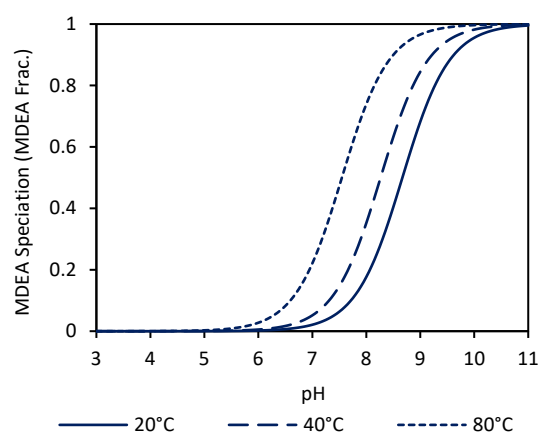


Figure 2-19. Effect of temperature on the speciation of MDEA in water

3.0 EXPERIMENTAL EQUIPMENT, METHODOLOGIES AND MEASUREMENT TECHNIQUES

This chapter outlines various experimental methodologies, description of process equipment, instrumentation and measurement methods common between all chapters within this thesis.

3.1 Mono-Ethylene Glycol Regeneration Pilot Plant

The pilot MEG regeneration plant utilised within several studies conducted as a part of this thesis is owned by the Curtin Corrosion Centre (CCC) to identify, study and solve potential issues facing industrial MEG regeneration systems. A flow-scheme outlining the various processes and equipment encompassing the system is presented in Appendix B.

3.1.1 MEG Regeneration Unit (Distillation)

The MRU is the primary process system utilised during the regeneration of MEG in order to achieve the desired final lean glycol purity necessary to facilitate continued hydrate inhibition. To simulate the MRU within the pilot plant, a glass distillation column constructed by De Dietrich Process Systems|QVF was utilised (Figure 3-1). The design and operational specifications of the distillation column are outlined by Table 3-1. The column was constructed using DuraPack borosilicate glass 3.3 structured packing developed by De Dietrich, with the packing selected for its high mass transfer efficiency. Table 3-2 outlines the specifications and dimensions of the structured packing.

Table 3-1. MEG distillation column design specifications

Feed Rate	Up to 6.5 kg/hr.
Feed Conditions	Temperature: 40-50°C, Pressure: 1.1 bara
Column Operating Pressure	(1) – (1.5) bar
Column Operating Temperature	(20) – (150)°C
Condenser Type	Total
Reflux Drum Capacity	5 Litres
Reboiler Type (Capacity)	Kettle type (8.5 Litres)
Reboiler Power requirements	5 kW
Column Diameter	DN 80 (76.2 mm)
Packing height	900 mm x 2 Sections
Packing material	Borosilicate glass 3.3 Structured Packing

Table 3-2. MEG distillation column packing specifications

Packing Surface Area	300.0 m ² /m ³
Packing Factor, F_p	195.3 m ² /m ³
Packing Void Fraction	0.824
Corrugation Base Width	1.8856 cm
Corrugation Side Dimension	1.3333 cm
Corrugation Height	0.94281 cm
Corrugation Angle	45°



Figure 3-1. Curtin Corrosion Centre MEG distillation system

3.1.2 Feed Blender, Rich MEG Pre-Treatment Unit and Three Phase Separator

The separation of hydrocarbons from the MEG/water phase is an important aspect of industrial natural gas processing in order to facilitate further refinement and production of the

desired natural gas and condensate products for sale. Initial separation of light gaseous hydrocarbons ranging from methane to propane is achieved within the slug-catcher and sent to the gas processing system. The liquid phase from the slug-catcher consisting of heavier hydrocarbons (condensate), water and MEG is then further separated within a three-phase separator. The condensate product is separated from the MEG solution due to inherent differences in density, however, the separation process is not perfect and condensate may enter into the MEG regeneration system. Within the MEG regeneration pilot plant, the feed blender simulates a slug catcher mixing MEG, water and hydrocarbons if present. Furthermore, the feed blender simulates the high partial pressure of carbon dioxide within natural gas pipelines saturating the MEG/water phase with CO₂ to replicate field conditions.

Following on from the feed blender, the rich glycol solution is fed into a pre-treatment vessel. The pilot plant pre-treatment system was designed for the dual purpose of the separation of hydrocarbon condensate from the rich MEG phase to simulate three-phase separation and the removal of divalent cations via pre-treatment. However, the studies conducted using the pilot plant within this thesis were conducted without hydrocarbon condensate present. As such, the system was utilised solely as a pre-treatment system for the removal of divalent cations prior to the regeneration process. Table 3-3 outlines the design specifications and typical operating conditions of the pilot plant pre-treatment system.

Table 3-3. Pre-treatment / three-phase separator specifications

Height	0.75 m
Diameter	0.45 m
Operating Temperature	80°C
Operating Pressure	1.3 bar

To facilitate the removal of divalent cations (typically calcium and iron) from the rich MEG solution, it is critical to control the pH and alkalinity of the liquid phase to allow formation and precipitation of divalent salt products. pH within the pre-treatment system was directly measured using a pH probe located within the recirculation loop of the system. Adjustment of pH was achieved through a Pro Minent dosing pump injecting 45% wt. sodium hydroxide into the recirculation loop of which is directly controlled via a PLC system (Section 3.1.4). To maintain sufficient carbonate alkalinity to form carbonate salts, carbon dioxide was continuously sparged into the liquid phase at a rate of 0.5 SLPM. The continuous sparging of carbon dioxide in conjunction with a consistent liquid phase pH above 8.2 allows the formation of carbonate ions and as a result, strong tendency to form carbonate salts.

3.1.3 Vacuum Reclamation Unit

Vacuum reclamation is an important aspect of the overall MEG regeneration process in order to control the level of dissolved salts within the closed loop MEG system. In order to simulate the reclamation process on a pilot plant scale, a Heidolph Hei-VAP Industrial vacuum rotary evaporation system was utilised (Figure 3-2). The system is capable of generated a vacuum as low as 5 kPa and a liquid phase temperature of $180^{\circ}\text{C} \pm 1^{\circ}\text{C}$ to allow boiling of the MEG/water phase. Salt rich lean glycol solution was fed into the reclamation system using the internal vacuum to generate liquid flow into the system. Once inside the liquid flask, the high temperature low pressure conditions evaporated the MEG/water solution facilitating the removal of any dissolved salts present.

The system was modified from its original batch design to allow continuous processing of lean MEG for salt removal. To allow continuous operation, the system was fitted with an external liquid level sensor upon the liquid phase collection flask of which was connected to a control system. Once a pre-defined liquid level was reached, the system would pump out the collect solution to be returned to the lean glycol storage tank.



Figure 3-2. Curtin Corrosion Centre MEG reclamation system

3.1.4 System Control

To facilitate long-term experimentation using the pilot plant, a programmable logic controller (PLC) system was utilised to control various operational processes. The PLC system procured from National Instruments allowed direct control of various process parameters within the pilot plant system. The primary parameters controlled during operation including reboiler temperature, stream flow rates and pH within various sections of the plant, particularly the rich and lean glycol tanks and within the pre-treatment system. To allow control of pH, the control system was connected to several Mettler Toledo M800 process measurement systems of which provided continuous measurement of pH and dissolved oxygen content with the locations illustrated in Appendix B.

3.1.5 Process Instrumentation

3.1.5.1 pH Measurement

Measurement of pH within the pilot regeneration plant was performed using Mettler Toledo InPro 4800(i) pH probes. InPro 4800(i) pH probes are capable of pH measurement between 0-14 pH ± 0.01 pH units from -5-80°C with automatic temperature compensation.

3.1.5.2 Dissolved Oxygen Measurement

Accurate measurement of dissolved oxygen concentration is an important process parameter due to the potential thermal degradation of MEG in the presence of oxygen during the regeneration process. Mettler Toledo InPro 6800 polarographic dissolved oxygen sensors were utilised for oxygen concentration determination. The InPro 6800 probes are capable of oxygen measurement from saturation to 6 ppb with an accuracy of $\pm 1\%$ up to 80°C.

3.1.5.3 Control of Gas Compositions and Flow Rates

Various gas compositions were utilised during pilot plant operation to simulate field and operational conditions. For example, within the feed blending system a CO₂/N₂ gas mixture was continuously sparged into the liquid phase to replicate the saturation of the rich MEG phase by CO₂ experienced within the hydrocarbon transportation pipeline. Likewise, nitrogen was continuously sparged into the storage vessels to drive out any dissolved oxygen to prevent thermal degradation during the regeneration process. To control the gas flow into the system, several Alicat mass flow controllers were utilised. Where mixtures of multiple gas were utilised, the pure gases were mixed using the gas mixing capabilities of the Alicat mass flow controllers to generate the required gas composition.

3.1.5.4 Liquid Stream Flow Rates

The mass flow rate of each liquid stream was measured by Promass A100 inline mass flow metres manufactured by Endress+Hauser with an accuracy of $\pm 0.1\%$. Flow rates were continuously monitored by the PLC and controlled via the respective variable speed pumps.

3.2 Experimental Measurement and Analysis

3.2.1 Ion Chromatography

Ion chromatography (IC) was utilised to measure the concentration of varying ionic species within MEG samples generated by pilot plant testing and laboratory scale experiments. The primary cationic species measured by IC including sodium, potassium, calcium, magnesium and dissociated MDEA (MDEAH^+). In contrast, anionic IC was performed in order to measure the concentration of various organic acids including acetic, butanoic, propanoic, glycolic and formic acids present either as part of simulated fluid compositions or generated by MEG thermal degradation. Table 3-4 and Table 3-5 outline the respective systems used to perform cation and anion ion chromatography. The system components and operational conditions were recommended by Thermo Fisher Scientific based on method development performed to measure dissolved salts components and organic acids within ethylene glycol matrices.

Table 3-4. Cation ion chromatography specifications

System	Dionex ICS-2100
Column	Dionex IonPac CS16, 2x250 mm
Conditions	0.36 ml/min flow rate, 30°C column temperature
Detector	Electrical Conductivity
Suppressor	Dionex CERS-500, 2 mm 32 ma
Eluent	Methanesulphonic acid, variable gradient

Table 3-5. Anion ion chromatography specifications

System	Dionex ICS-2100
Column	Dionex IonPac AS15, 2x250 mm
Conditions	0.30 ml/min flow rate, 30°C column temperature
Detector	Electrical Conductivity
Suppressor	Dionex ACRS 500, 2 mm with 25 mM H_2SO_4 regenerate
Eluent	Potassium Hydroxide, variable gradient

3.2.2 High Performance Reversed Phase Liquid Chromatography

In a similar manner, high performance liquid chromatography (HPLC) was utilised to perform chemical analysis of samples generated using the MEG pilot plant. The primary chemical species measured using HPLC was the FFCI utilised in Chapter 5 whilst studying the switchover between FFCIs to MDEA. HPLC was performed using the operational conditions and system components recommended by the FFCI supplier as outlined Table 3-6 and further discussed in the following section.

Table 3-6. High performance liquid chromatography specifications

System	Dionex Ultimate 3000
Column	Acclaim Surfactant HPLC, 5 μm 120 \AA 4.6x150 mm
Conditions	0.30 ml/min flow rate, 30°C column temperature
Detector	Ultraviolet – 240 nm Charged Aerosol Detector (CAD)
Eluent	50/50 DI water- acetonitrile

3.2.2.1 Selection of HPLC System Components and Operational Conditions

Column / Stationary Phase: In order to measure the concentration of the FFCI via either the UV or charged aerosol detectors, the FFCI was separated from the MEG using a dedicated surfactant HPLC column. The selected column utilises a silica-based stationary phase designed to facilitate surfactant separation via anion-exchange and dipole-dipole interactions. Unless separated, the MEG would otherwise interfere with the FFCI measurement by the UV and charged aerosol detectors due to the significantly higher concentration in each sample compared to the FFCI.

Detector: A combination of UV and a CAD was utilised to improve the reliability of FFCI determination and improve confidence in the reported result. UV detection at 240nm was used based on the reported functional group adsorption wavelengths provided by the FFCI supplier.

Eluent / Mobile Phase: A 50/50 DI water – acetonitrile eluent was used to ensure solubility of both polar and non-polar components due to the dual polarity nature of the FFCI surfactant molecule.

3.2.3 Determination of Alkalinity by pH Titration

Acid/base titrations were utilised as a chemical analytical technique to measure the alkalinity of samples generated during operation of the MEG pilot plant. The alkalinity of a sample is an important parameter for several MEG operations including pre-treatment and pH stabilisation corrosion control. Within MEG systems, the primary contributors to alkalinity are hydroxide, carbonate, carboxylic acids and MDEA if utilised as a pH stabiliser. Sample analysis by titration was performed using an automatic potentiometric Hanna HI902C titration system by pH measurement using 0.1 M HCl/NaOH as required. The following procedure was then utilised to estimate the molar concentration of each type of alkalinity present within a sample.

3.2.3.1 Alkalinity Titration Procedure

The total and individual alkalinities of the lean glycol was measured by a combination of forward titration using 0.1 M HCl and backward titration using 0.1 M NaOH with the individual alkalinities calculated using the inflection point method. The inflection point method is

illustrated by Figure 3-3 and Figure 3-4 for the forward and backward titrations respectively where no MDEA is present. As organic acids are typically present within the MEG samples, the total alkalinity calculated during the forward titration was inclusive of carboxylic alkalinity requiring the backward titration to estimate their contribution (refer to Equation (3-1)). To accurately estimate the concentration of carboxylics, following the forward titration the lean glycol sample was sparged with nitrogen for 15 minutes to drive out any dissolved CO₂. The concentration of each component was calculated from the volume at which the corresponding inflection point was determined. Where MDEA was present, a slightly modified procedure was utilised in which an additional inflection point associated with MDEA/MDEAH⁺ is measured on both the forward and reverse titrations.

$$A_T = [\text{HCO}_3^-] + 2[\text{CO}_3^{2-}] + [\text{OH}^-] + [\text{Carboxylics}] + [\text{MDEA}] \quad (3-1)$$

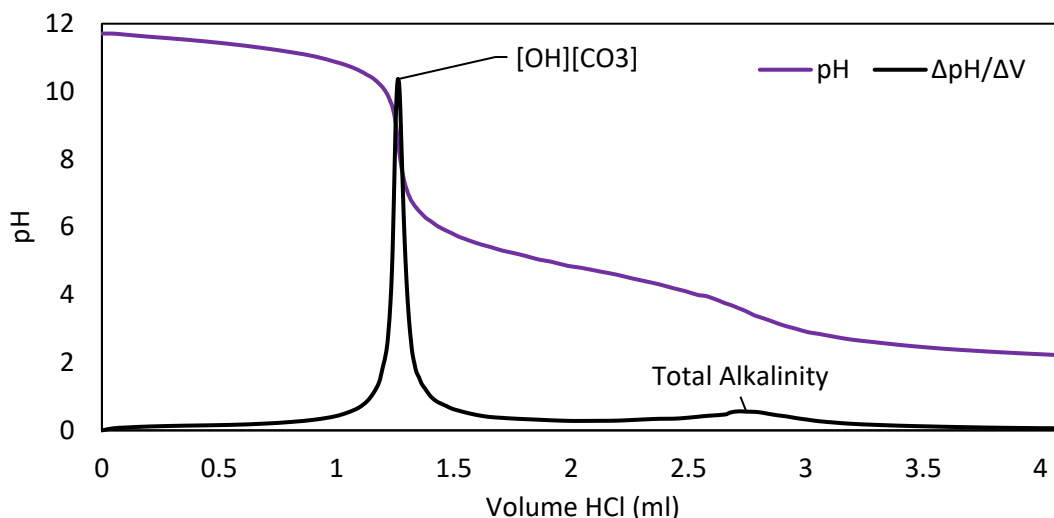


Figure 3-3. Forward titration to determine hydroxide, carbonate and total alkalinity

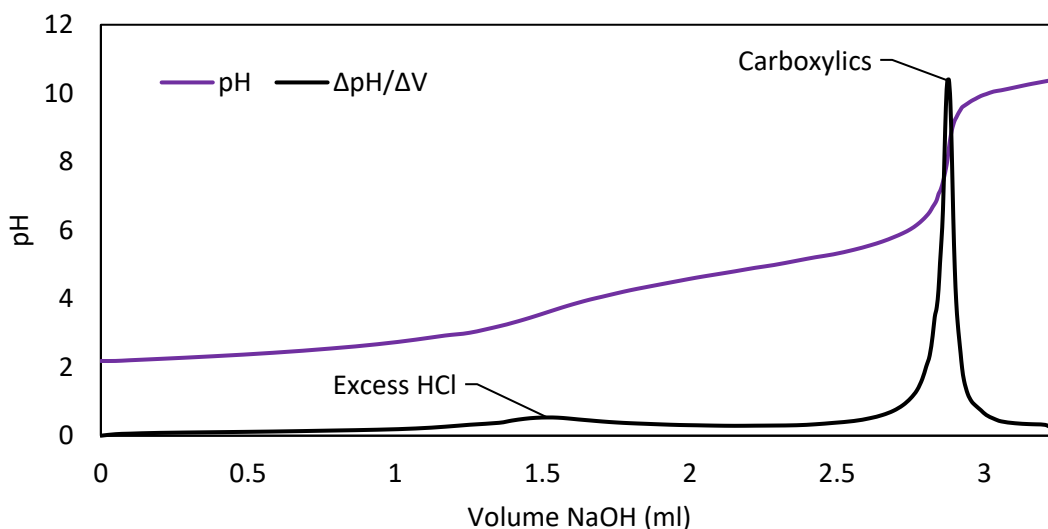


Figure 3-4. Backward titration to determine carboxylic alkalinity

3.2.4 Measurement of MEG Concentration

Verification of prepared solution MEG concentration during each experiment was performed using an ATAGO PAL-91S refractometer. The refractometer measures the MEG concentration within a 0-90% concentration range with an accuracy of $\pm 0.4\%$ (V/V) based upon the refractive index of the solution. Refractive index is a physiochemical property of a medium including liquid phases based on the ratio of the measured speed of light in a test medium compared to that in a vacuum. It can be used to estimate the ratio of chemical solvents based on the known refractive index of the pure chemicals.

4.0 REMOVAL OF ORGANIC ACIDS DURING MONO-ETHYLENE GLYCOL DISTILLATION AND RECLAMATION TO MINIMISE LONG-TERM ACCUMULATION

4.1 Introduction

Mono-ethylene glycol (MEG) has found widespread use as a thermodynamic hydrate inhibitor to prevent the formation of natural gas hydrates within offshore multiphase hydrocarbon transportation pipelines ^[1, 2, 4, 7, 9, 113]. In order to minimise the operational costs associated with MEG injection, post hydrate inhibition, the excess MEG is separated alongside the water phase to be regenerated and recycled for further use ^[1, 4-7]. The MEG regeneration process entails a series of chemical and physical steps to remove a wide range of contaminants including excess water, mineral salts and process chemicals ^[7, 9, 10, 40]. To produce a final lean MEG product suitable for reinjection at the wellhead, excess water is separated from rich MEG by distillation to regain a MEG concentration typically between 80-90% by weight ^[1, 7, 9, 12, 203]. To achieve the desired lean MEG concentration, the MEG regeneration unit (MRU) is typically operated between 120-140°C at atmospheric pressure ^[1, 37, 38].

Alongside other contaminants, organic acids such as acetic, propanoic, butanoic and formic may be present within the regeneration system originating from the condensed water phase or following formation water breakthrough ^[7, 9, 63]. Furthermore, the thermal degradation of MEG at high temperature in the presence of oxygen may also lead to the formation of organic acids including glycolic, acetic and formic acid ^[3, 5, 39, 63]. The presence of organic acids within industrial MEG regeneration systems can pose several operational issues including contributing to corrosion of downstream process equipment and pipe systems ^[7]. Organic acids have been found to increase the rate of corrosion of carbon and mild steel piping in natural gas and oil field systems through reduced system pH and direct reduction of the acid species ^[69-72]. In combination with carbon dioxide, acetic acid may also exacerbate the rate of Top-of-the-Line-Corrosion (TLC) ^[17, 63, 72-76]. Additionally, organic acids will directly reduce the pH of the liquid phase increasing the solubility of protective iron carbonate films, reducing corrosion protection and may also be directly reduced on the surface of metals enhancing the anodic reaction of the metal ^[67, 68, 72].

To minimise corrosion within natural gas pipelines two primary corrosion inhibition strategies can be utilised including pH stabilisation and injection of film forming corrosion inhibitors (FFCI) ^[4, 7, 9, 40, 70]. The basis of pH stabilisation entails artificially increasing system pH

to reduce the availability of hydrogen ions for the cathodic corrosion reaction, whilst also promoting the formation of a protective FeCO_3 film on the surface of the pipeline. The pH within pipelines is typically increased through addition of hydroxides, carbonates or amine based compounds including methyldiethanolamine (MDEA) [1, 4, 17, 40]. pH stabilisation as a corrosion mitigation strategy is most effective when carbon dioxide is the main source of corrosion and is limited to systems where formation water breakthrough has not occurred due to the scaling risk at high pH [9, 15, 17, 116]. Where scaling is a concern, FFCIs may instead be used due to their limited impact on system pH and hence scaling risk [2, 9, 15, 204].

The removal of excess ionic species including salt components from closed-loop MEG can be performed using vacuum reclamation systems. MEG systems utilising reclamation may operate under either full-stream reclamation whereby the rich glycol stream is flashed under vacuum to totally remove salts or using a slip-stream mode post distillation to remove primarily monovalent ions including sodium from a fraction of the produced lean glycol [1, 2, 7, 8, 32, 42]. The type of reclamation is dictated by the expected salt production rate with systems operating at high salt loads requiring full-stream reclamation. However, for systems with low salt production rates, a lean glycol slip-stream reclamation system is often sufficient to control the salt content within closed loop MEG systems [1, 8, 43].

In a similar manner, the removal of organic acids from the MEG regeneration loop is typically achieved via vacuum reclamation systems, however, removal through distillation may also occur [7]. If a high pH is maintained within the reboiler during the distillation process, organic acids will exist in their ionic form and tend to remain within the lean MEG product resulting in their accumulation within the MEG loop [7, 17, 116]. As such, to facilitate their removal during distillation, it is essential to maintain a low pH ($\text{pH} < 7$) within the reboiler to ensure the organic acids are present in their undissociated form and readily vaporised [7]. In contrast, vacuum reclamation may be utilised to remove organic acids through their reaction with monovalent salts including sodium to form non-volatile organic salts [7, 41]. The resulting salts will be subsequently captured within the vacuum reclamation system as the vaporisation of the MEG-water phase occurs, allowing their removal [7, 63]. As such, the removal of organic acid from the MEG loop by either process is primarily dependent on liquid phase pH.

The pH within closed loop MEG systems is influenced by several factors including the type of corrosion inhibition strategy used [4, 7, 51, 116], exposure to acidic gases such as CO_2 and H_2S , and a potential pre-treatment process used for divalent salt removal [5, 7, 12]. MEG systems operating under pH stabilisation maintain a high pH in the regenerated lean glycol and will naturally favour

removal of acetic acid during reclamation. In contrast, under FFCI corrosion control, a lower lean MEG pH can be expected to minimise the risk of scaling in subsea systems upon reinjection of the lean MEG [7,8]. Under both operational methods, the incoming rich glycol from the pipeline will be acidic due to the presence of acidic gases including CO₂ and H₂S within the well and subsequent gas phase of the pipeline. The acidic rich MEG will ultimately favour removal of organic acids during the distillation process if not otherwise controlled through the corrosion prevention methodology. If removal of divalent cationic species including calcium, magnesium and iron is required, pre-treatment prior to MRU may be performed through formation of divalent salt species at moderate to high pH (8-10 [7, 9, 12, 205]) resulting in alkaline rich MEG fed into the distillation system.

The study outlined in the subsequent chapter demonstrates the potential simultaneous removal of organic acids and MDEA during MDEA to FFCI corrosion inhibition switchover. By targeting a low pH (≈ 6) rich glycol feed to the MRU, sufficient levels of acetic acid were boiled over with the produced water to prevent accumulation whilst also achieving MDEA/alkalinity removal during downstream reclamation. Further to this study, the removal efficiency of acetic acid during MEG regeneration and reclamation has been investigated at varying pH and salinities to further optimise removal of organic acids during long term MEG regeneration. Based on the pH within key areas of the MEG regeneration process, coupled with estimated pH changes during distillation, the overall removal of acetic acid over an entire regeneration cycle has been estimated.

4.2 Experimental Methodology

4.2.1 Chemicals

MEG solutions were produced using MEG supplied by Chem Supply (CAS: 107-21-1) and deionised water with a resistivity of 18.2 M Ω .cm. Acetic acid was procured from Sigma Aldrich (CAS: 64-19-7) with a mass purity of $\geq 99\%$. To produce solutions of a given salt content, sodium chloride supplied by Chem Supply with a mass purity of $\geq 99\%$ was used. Where pH adjustment was performed, MDEA (CAS: 105-59-9, $\geq 99\%$ wt.), Hydrochloric acid (HCl) – CAS: 7647-01-0 and Sodium Hydroxide (NaOH) – CAS: 7647-01-0 from Sigma Aldrich was utilised.

4.2.2 Experimental Apparatus and Procedure

4.2.2.1 Regeneration Process

To measure the removal efficiency of acetic acid during atmospheric distillation of rich MEG to lean MEG, the experimental apparatus depicted by Figure 4-1 was utilised. A one litre glass cell was used to simulate the regeneration unit's reboiler with a 380 mm Aldrich Synder glass

distillation column from Sigma Aldrich used to replicate a distillation column. A heating mantle was used to heat the experimental solution with a temperature accuracy of $\pm 0.1^\circ\text{C}$. To analyse the removal efficiency of acetic acid during the regeneration process, 700 grams of 80% wt. lean glycol containing 1000 ppm acetic was filled into the reboiler cell. 420 grams of distilled water was added to the reflux chamber representing the amount of water removed during the transition from 50% wt. rich MEG [7, 38, 43] to a typical industry lean MEG concentration of 80% wt. [1, 7, 9, 12]. The distillation system was then operated with the condensed water phase continuously refluxed to the top stage of the distillation column until equilibrium concentration of acetic acid within the distillate product was reached. Testing was conducted over a pH range of 4-11 and salinities (NaCl) ranging from 0-5000 mg/L to analyse the removal of acetic acid over a wide range of potential field conditions.

To continuously monitor the transition of acetic acid into the produced distillate, a ThermoFisher Orion 8102BNU pH probe was submerged in the water reflux chamber. Post experiment, the concentration within the distillate was determined through ion chromatography using a Dionex ICS-2100 IC System. Furthermore, to prevent thermal degradation of the MEG solution at high temperature, ultra-pure nitrogen was continuously introduced into the reboiler and reflux chambers to minimise oxygen contamination. The prevention of thermal degradation is essential to prevent the formation of additional organic acid by-products and as a result, unwanted reduction in solution pH. To account for the inherent error associated with pH measurement in MEG solutions, the **empirical** correction factor described by Sandengen [11] given by Equations (4-1) and (4-2) was applied.

$$\Delta\text{pH}_{\text{MEG}} = 0.416w - 0.393w^2 + 0.606w^3 \quad (4-1)$$

where: w = weight fraction of MEG

$$\text{pH}_{\text{MEG}} = \text{pH}_{\text{Measured}} + \Delta\text{pH}_{\text{MEG}} \quad (4-2)$$

4.2.2.2 Reclamation Process

For the reclamation process, the apparatus depicted by Figure 4-2 was utilised in order to achieve complete vaporisation of initial MEG/water solution. A Heidolph vacuum pump connected to an Alicat vacuum pressure controller (± 1 mbar) was used to regulate the pressure within the reclamation chamber at a constant 100 mbar. A secondary Alicat mass flow controller with pressure measurement was utilised to verify the operating pressure within the chamber and to continuously introduce nitrogen into the system to minimise oxidative thermal degradation. Testing was again conducted from pH 4-11 and NaCl concentrations from 0-5000 mg/L.

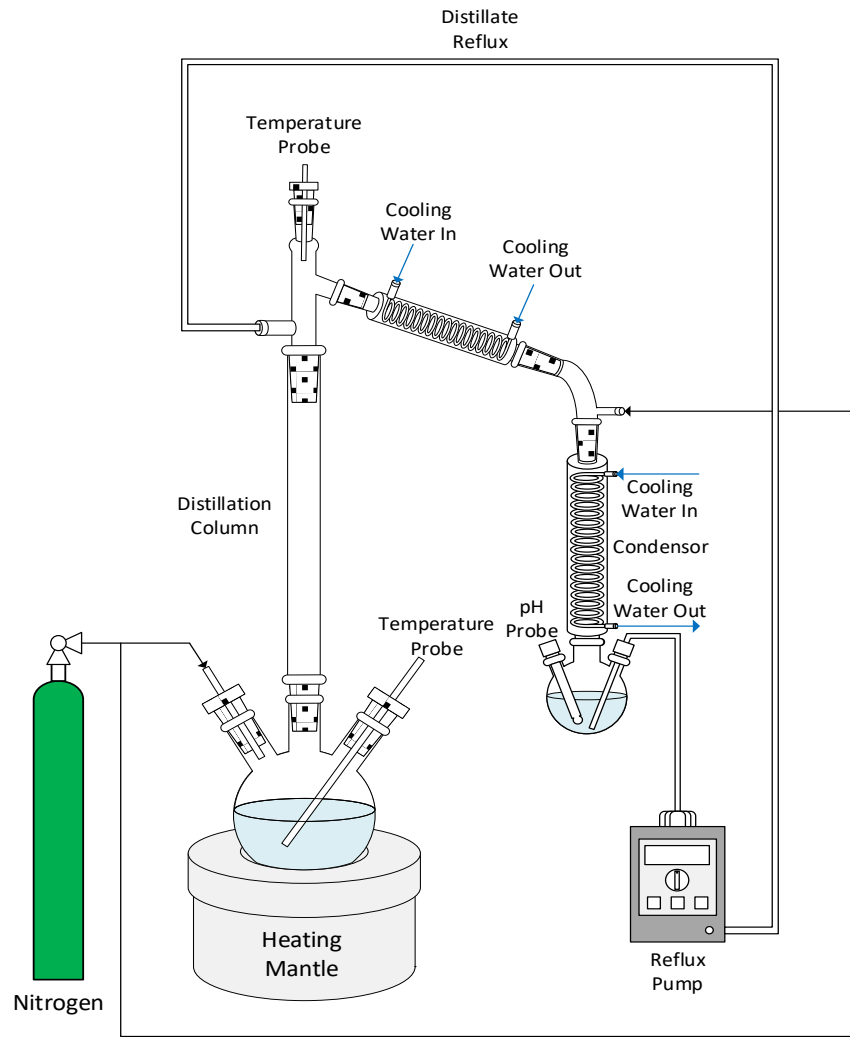


Figure 4-1. Laboratory MEG regeneration system

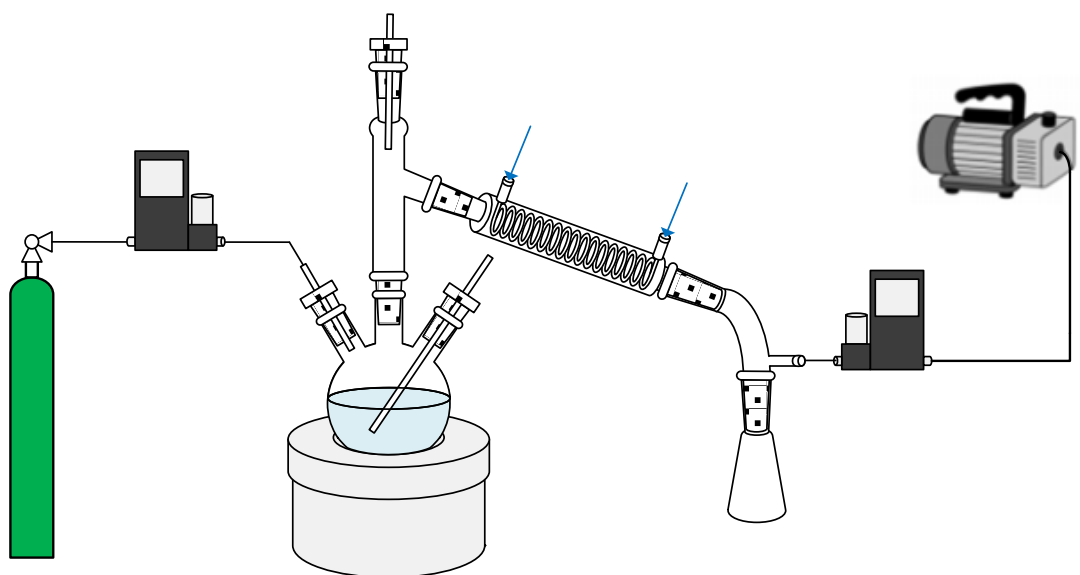


Figure 4-2. Laboratory MEG vacuum reclamation system

4.3 Results and Discussion

4.3.1 Speciation of Acetic Acid in MEG Solutions at Varying Temperature and Salinity

The speciation of acetic acid plays a vital role in determining its removal efficiency during separation processes [7]. Using the experimental model developed covered in Chapter 8 to estimate the dissociation constant (pK_a) of acetic acid at varying MEG concentration, temperatures and salinities, the theoretical maximum acetic acid available for removal can be calculated. Figure 4-3 illustrates the change in the speciation behaviour of acetic acid within 80% wt. MEG solution due to the effect of MEG concentration and temperature. In comparison to water, the pK_a of acetic acid within MEG solution is increased due to the change in dielectric constant of the solvent (ϵ) [127-130, 199]. Furthermore, the pK_a of acetic acid changes according to a parabolic function with respect to temperature [7, 199, 206, 207]. The resulting shift due to MEG concentration and temperature effectively increases the percentage of acetic acid present at higher pHs and subsequently the amount of acetic acid available to be vaporised during distillation [7]. A very small shift in pK_a can also be expected due to the presence of dissolved salts with the model presented Chapter 8 taking salinity into account.

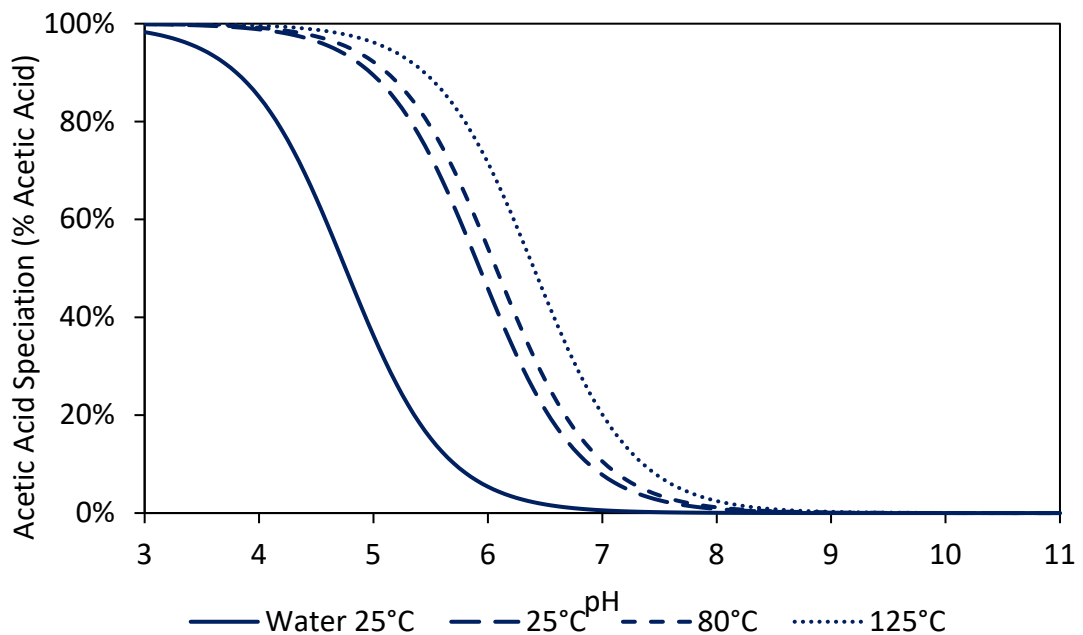


Figure 4-3. Speciation of acetic acid as a function of pH (80% wt. MEG) at varying temperature. acetic acid pK_a at 125°C extrapolated from model of Soames [199] (Chapter 8 – Equation 8-12)

4.3.2 pH Change Induced During MEG Distillation

Beyond the physical removal of water and subsequent reconcentration of rich MEG to lean, the MEG distillation process can have significant impact on system chemistry. In particular, the distillation of MEG can induce a substantial change in pH of the glycol stream through a combination of CO_2 boil off at high temperature and change in concentration of alkalinity due

to water removal ^[7]. The change in pH during the regeneration process is influenced by a combination of the initial concentration of dissolved CO₂ and pH of the rich glycol feed stream ^[7]. It is also important to consider how various pH stabilisers commonly used in industry such as hydroxides or amines including MDEA ^[4, 7, 8, 40, 199] induce different pH changes during the regeneration process. Overall, the change in pH occurring through the regeneration system can have a significant impact on the removal efficiency of acetic acid during the distillation and reclamation processes if operated downstream ^[7].

The effect of initial rich glycol pH, initial dissolved CO₂ concentration and type of pH stabiliser utilised was investigated to determine the corresponding pH change across the regeneration unit. Testing was conducted using a MEG concentration gradient of 50-80 wt. % representing a standard industry operation ^[7, 43] using either NaOH or MDEA to control the initial rich glycol pH. Testing utilising MDEA was performed using a base lean MEG MDEA concentration of 500mM (312.5 mM rich glycol) and the pH adjusted to the target initial rich glycol pH following CO₂ saturation using either HCl or NaOH as required to represent a standard industrial MDEA pH stabilisation scenario ^[7]. To allow comparison of initial and final pH values, all pH measurements were conducted at 25°C. The initial dissolved CO₂ concentration was varied by saturating the rich glycol solution at atmospheric pressure using varying gas phase CO₂/N₂ partial pressure ratios, followed by pH adjustment.

The pH change induced using hydroxide as the primary pH stabiliser is illustrated by Figure 4-4 showing a significant pH change occurring at initial when dissolved CO₂ is present for all initial pHs above six. In comparison, when no dissolved CO₂ is initially present and hydroxide is solely responsible for the pH change during distillation, only a minor pH change was found to occur. The results highlight the synergistic effect of CO₂ boil off and the concentration of hydroxide during the distillation process has on the pH change generated. In contrast, the pH change induced during distillation where MDEA was present was ultimately dependent on whether HCl or NaOH was used to supplement the pH control (Figure 4-5). For systems containing no dissolved CO₂ (unlikely during industrial operation) the change in pH occurring during distillation changed linearly with respect to the initial rich glycol pH. This also occurred for systems with the initial rich glycol pH adjusted using HCl after CO₂ saturation had occurred, a scenario possible during MDEA to FFCI switchover where pre-treatment prior to distillation is performed for divalent cation removal ^[7]. This operational methodology is discussed in Chapter 5 to facilitate simultaneous removal of acetic acid and MDEA from a closed loop MEG system. However, most significantly, upon the use of NaOH to supplement control of the initial rich glycol pH, the final lean glycol pH produced increased significantly in a similar manner to that generated using solely NaOH (Figure 4-4). This is likely for MEG systems operating under MDEA pH stabilisation where addition of NaOH is required following saturation of the

rich glycol with CO₂ within the natural gas transportation pipeline. The results again highlight that the most significant pH changed induced during MEG distillation occurs through the combination of hydroxide and carbon dioxide boil off.

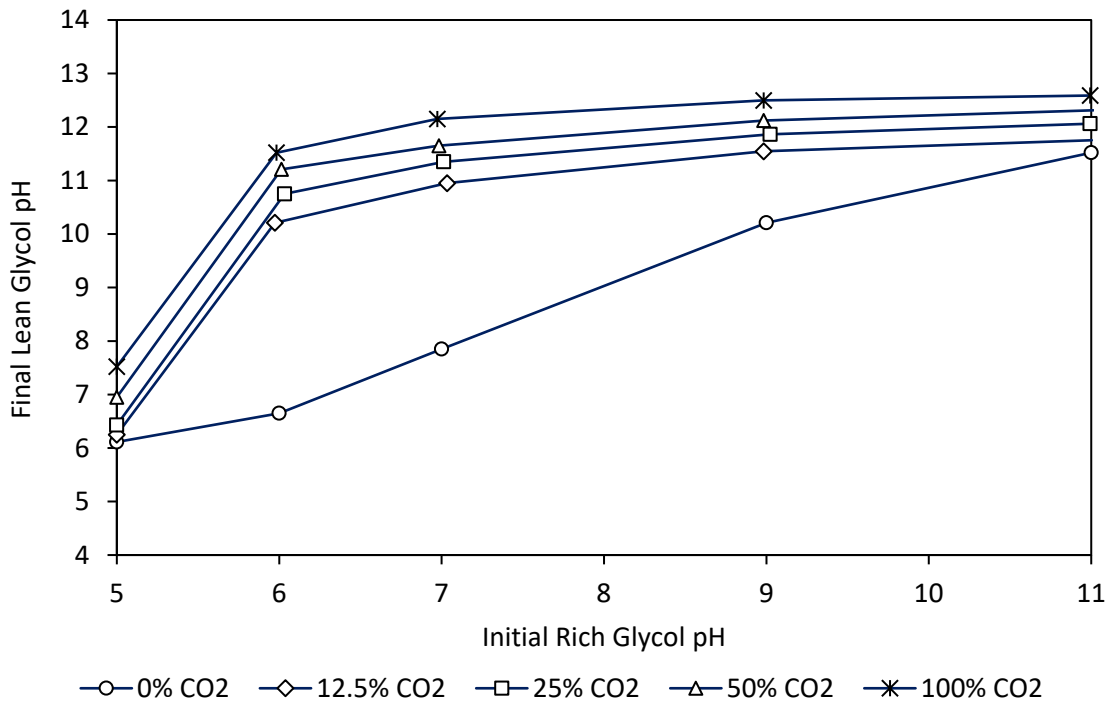


Figure 4-4. Effect of initial rich glycol (50 wt. %) pH_{25°C} and gas phase CO₂ concentration on final lean MEG (80 wt. %) pH_{25°C} using sodium hydroxide pH control

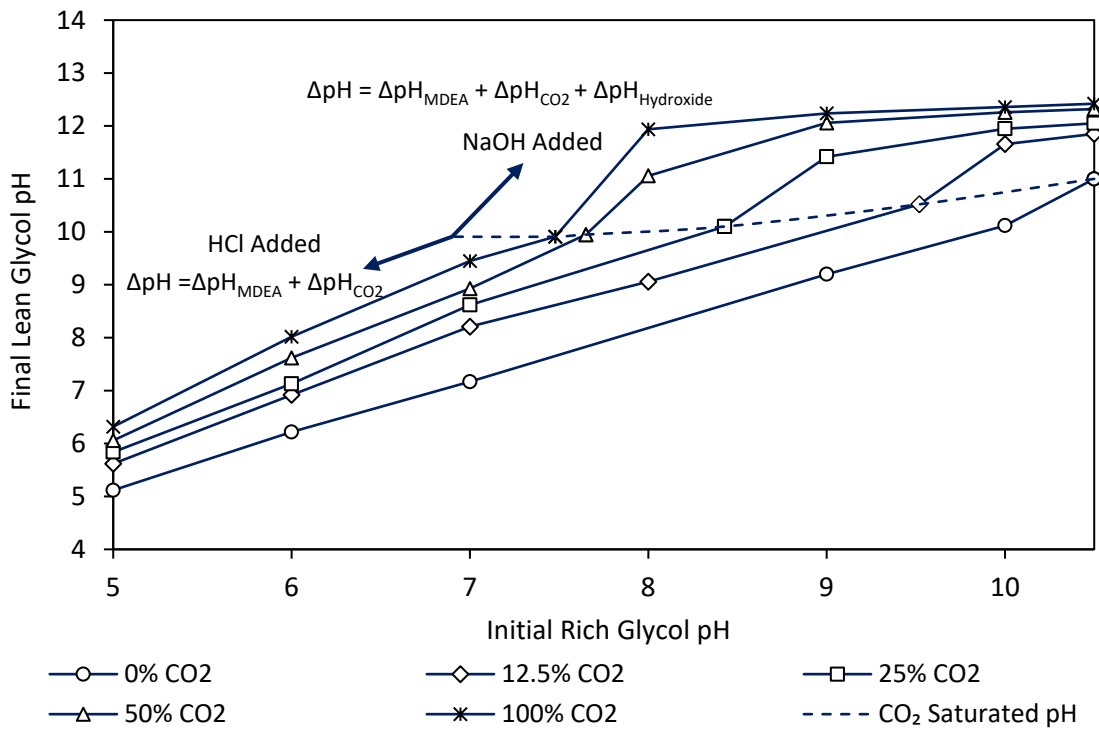


Figure 4-5. Effect of initial rich glycol (50 wt. %) pH_{25°C} and gas phase CO₂ concentration on final lean MEG (80 wt. %) pH_{25°C} using MDEA pH control

4.3.3 Removal Efficiency of Acetic Acid during MEG Distillation

The removal of organic acids including acetic through the distillation system may provide an alternative method to prevent their accumulation within closed loop MEG systems if a vacuum reclamation system is not utilised downstream or low pH is maintained during the reclamation process [7]. The removal efficiency of 1000 ppm (mg/L) acetic acid in 80% wt. MEG is illustrated by Figure 4-6 showing improved removal at lower pH levels in line with the acetic acid speciation behaviour. For comparison purposes, Aspen Plus® V8.4 was utilised to simulate the removal rate of acetic acid during MEG regeneration. The Electrolyte NRTL (ELECNRTL) property package was used to construct the simulation to allow modelling of acetic acid speciation, pH and interaction of acetate with other ionic species including sodium ions. The default Aspen Plus® ELECNRTL parameters including binary interaction, electrolyte pair and dissociation and salt reaction parameters were utilised. The simulated removal results were found to slightly overestimate the removal of acetic acid with the greatest absolute error occurring in the low pH region. Furthermore, the influence of salinity in the form of NaCl on the remove efficiency of acetic acid during the distillation process was found to be minimal over the entire pH range tested. With increasing salinity up to 5000 ppm (mg/L) NaCl, a small increase in acetic acid removal percentage was observed of which can be attributed to the minor effect of salinity on the acid dissociation of organic acids [199].

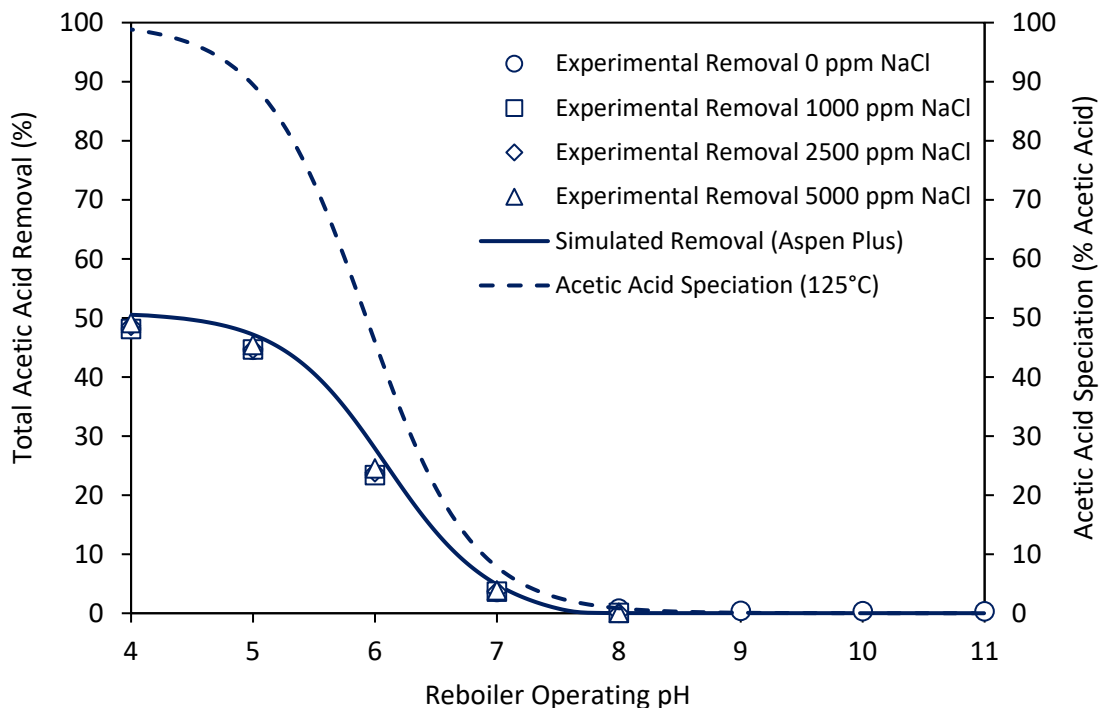
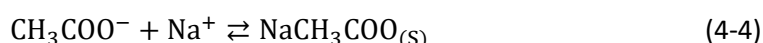
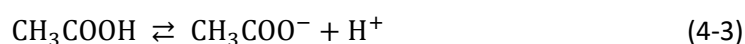


Figure 4-6. Removal efficiency of acetic acid during 80% wt. MEG distillation

4.3.4 Removal Efficiency of Acetic Acid during MEG Reclamation

MEG reclamation systems operate under low pressure conditions (≈ 100 mbar ^[7, 8, 32, 38, 40]) to minimise the operational temperature required to vaporise the MEG/water phase to reduce thermal degradation of the MEG (120 - 150°C ^[2, 7, 38, 40]). Vaporisation of the reclaimed solution results in separation from the non-volatile salt components facilitating their removal through solid handling systems. Organic acids present within the lean MEG in their conjugate base form prior to reclamation will also be separated upon reaction with cations including sodium through Equation (4-3) and (4-4) to form non-volatile organic salts ^[41, 208]. If no corresponding cationic species such as sodium are present, the formation of pure acetic acid crystals may occur ^[209]. In a similar manner to distillation, the removal efficiency of organic acids during reclamation is primarily influenced by the acids speciation behaviour (pK_a) and the lean glycol pH.



The removal efficiency of acetic acid during vacuum reclamation of 80% wt. lean glycol with 0, 2500 and 5000 ppm NaCl content is illustrated by Figure 4-7 with comparison to the simulated removal predicted by Aspen Plus[®] V8.4. Aspen Plus[®] V8.4 utilising the ELECCTRL with default parameters was again used for its ability to simulate salt formation and properties relevant to reclamation ^[43]. The experimental results were found to match that predicted by Aspen Plus[®] validating the simulation model. However, a small discrepancy in removal efficiency was observed at initial lean glycol pHs greater than nine within solutions containing no NaCl. The lower than simulated removal can be attributed to the formation of acidic degradation products, primarily glycolic and formic acids (Section 3.4.1), reducing the pH of the partially reclaimed solution. Ultimately, the reduction in pH during reclamation facilitated a minor carryover of acetic acid into the reclaimed MEG solution. The effect of pH reduction due to degradation product formation was found to be lower within solutions containing 2500 ppm and 5000 ppm NaCl likely as a result of the greater sodium content available for organic salt formation. A constant shift in the final reclaimed MEG solution pH was also measured when comparing corresponding points at varying salinity (0 and 5000 ppm illustrated in Figure 4-7). Furthermore, during each experiment, approximately 0.4-0.6% loss of MEG was experienced, a result in line with the simulation study of Son ^[43] and industry data reported by Trofimuk ^[42].

4.3.4.1 Generation of Organic Acids during Reclamation through Thermal Degradation

The work of Psarrou ^[38] and Rossiter ^[210] found formic and glycolic acid to be the dominant MEG degradation products formed during thermal degradation of MEG in the presence

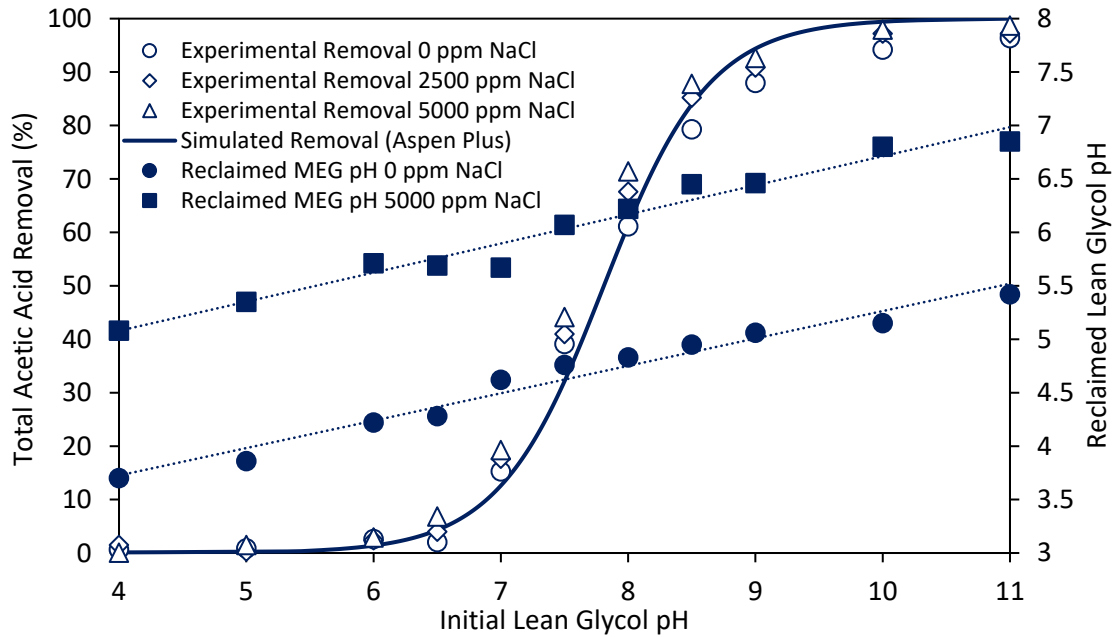
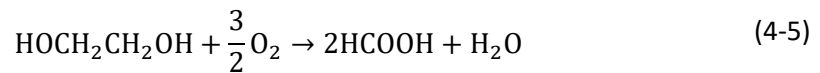


Figure 4-7. Removal efficiency of acetic acid during 80% wt. MEG reclamation

of oxygen (Equations (4-5) and (4-6) respectively). Conversely, the recent study by Odeigah [41] found significant production of acetic acid during MEG thermal degradation at high temperatures over prolonged periods (>60 hours). Organic acids formed through thermal degradation during reclamation will be subjected to removal as dictated by their speciation behaviour. Reclamation systems operating at low pH will ultimately generate greater concentrations of acidic degradation products in the reclaimed solution. Figure 4-8 illustrates the levels of glycolic and formic acid produced in the reclaimed lean glycol solution following the reclamation process used within this study. Although the initial lean glycol solution was sparged with nitrogen to sub 20 ppb oxygen content, and the apparatus continuously purged with ultra-pure nitrogen, significant levels of glycolic acid were produced likely as the result of minor oxygen intrusion under vacuum. As such, unless a high pH is maintained, significant accumulation of glycolic and formic acids through MEG degradation can be expected in the reclaimed lean MEG solution.

Furthermore, it can be suggested that the formation of acetic acid during the degradation process may account for the lower than simulated removal rates within the high pH regions (pH >9). Ultimately however, it was observed that minimal additional acetic acid was formed during the vacuum reclamation procedure through thermal degradation in this study. This suggests that the formation of acetic acid via MEG degradation primarily occurs after exposure to long term high temperatures as used by Odeigah [41]. This however may still influence industrial reclamation systems where dissolved oxygen concentrations may be higher or oxygen intrusion via vacuum leakage more severe, potentially leading to lower than expected acetic acid removal rates compared those reported in this study.



4.3.5 Modelling of Plant Wide Acetic Acid Removal

Through a combination of removal through the distillation and subsequent reclamation system (if present), it may be possible to optimise the removal of organic acids over the entire regeneration system. A low targeted rich glycol pH into the distillation column in combination with a high pH rise across the reboiler may ultimately further facilitate a high rate of acetic acid removal during down-stream reclamation. Control of the lean glycol pH entering into the reclamation system can either be achieved through control of the initial rich glycol pH and dissolved CO_2 concentration (Figure 4-4 and Figure 4-5) or through additional dosage of acids or bases following the regeneration process via in-line dosing points. To estimate the total plant wide acetic acid removal generated during distillation and reclamation or a combination of both, the experimental removal rates reported were fitted to the equations given by Equations (4-7) and (4-8) for distillation and reclamation respectively. The parameters A1/A2 and B1/B2 were regressed from the experimental data utilising the objective function given by Equation (4-10). The equation parameters and average error of the individually simulated results (distillation and reclamation) compared to experimental data are given in Table 4-1, with visual comparison of calculated and experimental data given in Figure 4-9. From the individual distillation and reclamation Equations (4-7 and 4-8), the total plant wide acetic acid removal can be estimated using Equation (4-9).

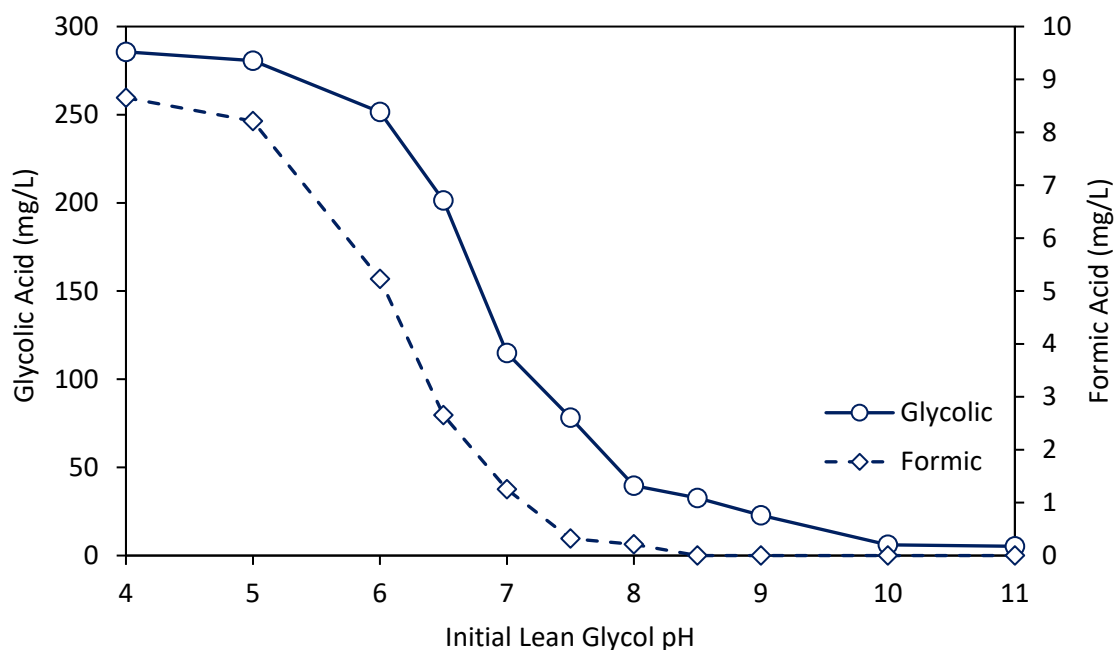


Figure 4-8. MEG organic acid degradation products generated during reclamation

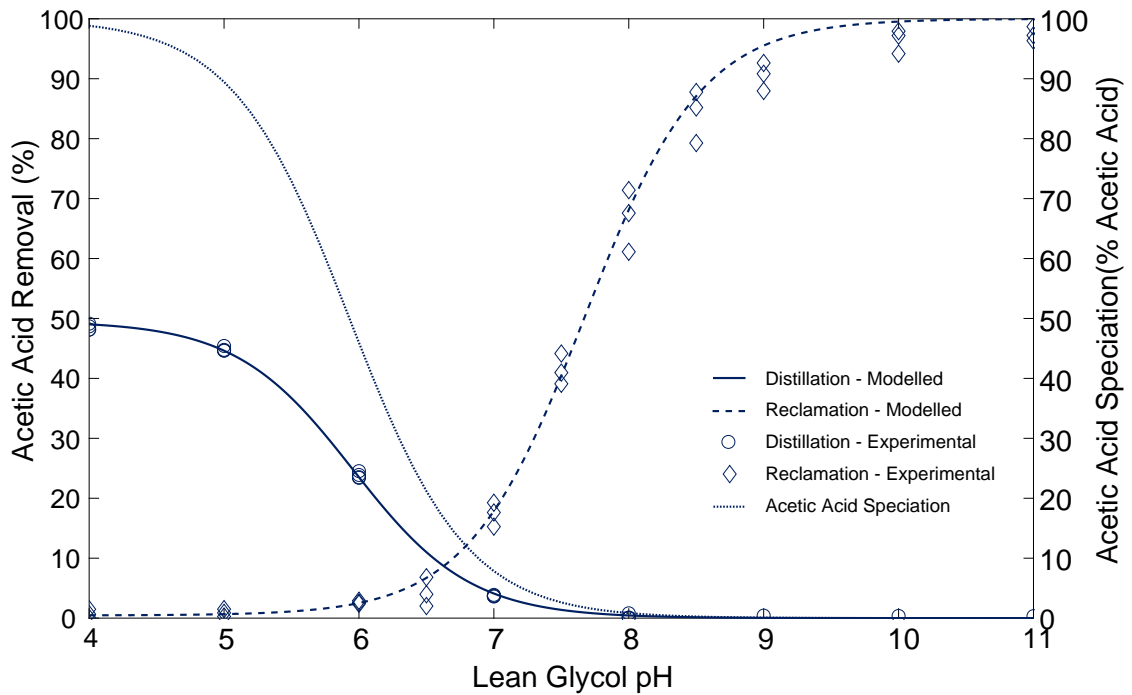


Figure 4-9. Comparison of modelled acetic acid removal rate during distillation and reclamation

$$\text{Distillation Removal, } R_D (\%) = B_1 - \frac{B_1 \times 10^{-A_1}}{10^{-\text{pH}_{\text{distillation}}} + 10^{-A_1}} \quad (4-7)$$

$$\text{Reclamation Removal, } R_R (\%) = F_R \times 100 - \left(B_2 - \frac{B_2 \times 10^{-A_2}}{10^{-\text{pH}_{\text{reclamation}}} + 10^{-A_2}} \right) \quad (4-8)$$

Where A and B are regressed parameters from experimental data and F_R is the slip-stream reclamation fraction

$$\text{Total Removal, } T_R (\%) = R_D + R_R \left(1 - \frac{R_D}{100} \right) \quad (4-9)$$

$$\text{OF} = \frac{\sum |y_{\text{exp}} - y_{\text{calc}}|}{n} \quad (4-10)$$

Table 4-1. Regressed model parameters and average model errors

Parameter	Distillation Removal (1)	Reclamation Removal (2)
A_1/A_2	5.916	7.707
B_1/B_2	50.268	99.552
Average Error (%)	0.38	2.6

The model given by Equation (4-9) was then used to identify the optimum rich glycol pH that in combination with a known pH rise across the reboiler (Figure 4-4 and Figure 4-5), are required to achieve the optimal conditions necessary to maximise plant wide acetic acid removal. Figure 4-10 illustrates the total acetic acid removed by distillation at an initial rich glycol

pH with incremental pH rises across the reboiler in combination with subsequent full-stream vacuum reclamation at the corresponding lean glycol pH. Systems with an initially low pH combined with low pH rise across the reboiler are ultimately constrained by the removal efficiency in the distillation system with minimal subsequent removal downstream in the reclamation system, reaching maximum acetic acid removal as per Figure 4-6. In contrast, systems generating a large pH increase across the reboiler, or utilising in-line dosage of bases into the reclaiming feed achieved significant removal of acetic acid primarily due to the reclamation stage (Figure 4-7). As such, it is evident that the maximum acetic acid removal is primarily generated through the reclamation system particularly for systems operating using a combination of low initial rich glycol pH and large pH rise across the regeneration system.

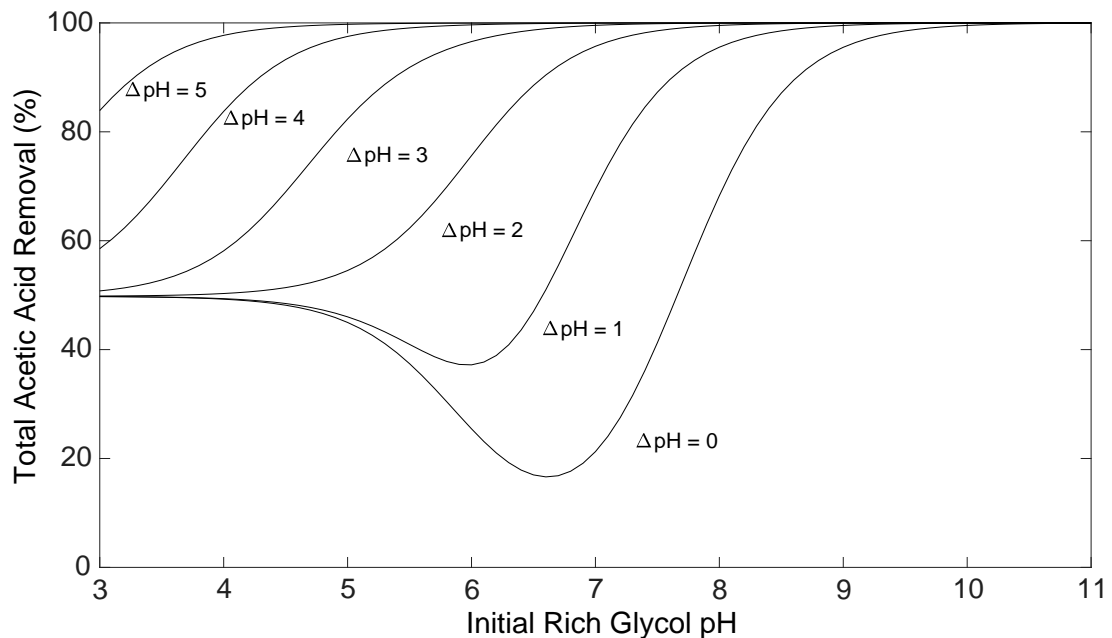


Figure 4-10. Simulated acetic acid removal rate full reclamation

However, it is important to consider that MEG systems utilising vacuum reclamation downstream of the regeneration unit typically operate using a slip-stream or partial reclamation mode to minimise operational costs and equipment size requirements [1, 7, 9]. Instead of full reclamation of the regenerated lean glycol product, only a fraction of the lean glycol is reclaimed with the fraction dependent on field requirements to maintain a specific level of salts within the closed-MEG loop. The study outlined in the preceding Section 5.0 utilised a slip-stream rate of 11% based on an Australian industrial MEG regeneration system processing up to 2500 m³ of MEG day. For the purposes of this study, a reclamation slip-stream rate of 20% was utilised to model the plant wide acetic acid removal rate illustrated by Figure 4-11. Due to the restricted reclamation rate, it is evident that the bulk of acetic acid removal is achieved when rich glycol

with pH levels below six is fed into the distillation system. Ultimately, if a low reclamation rate is utilised in combination with high lean glycol pH, accumulation of acetic acid within the MEG loop will occur. In the study discussed in Chapter 5.0, a lean MEG slip-stream rate of 11% was sufficient to prevent the accumulation of organic acids within a closed loop MEG system where the produced water contained approximately 200 mg/L total organic acid content.

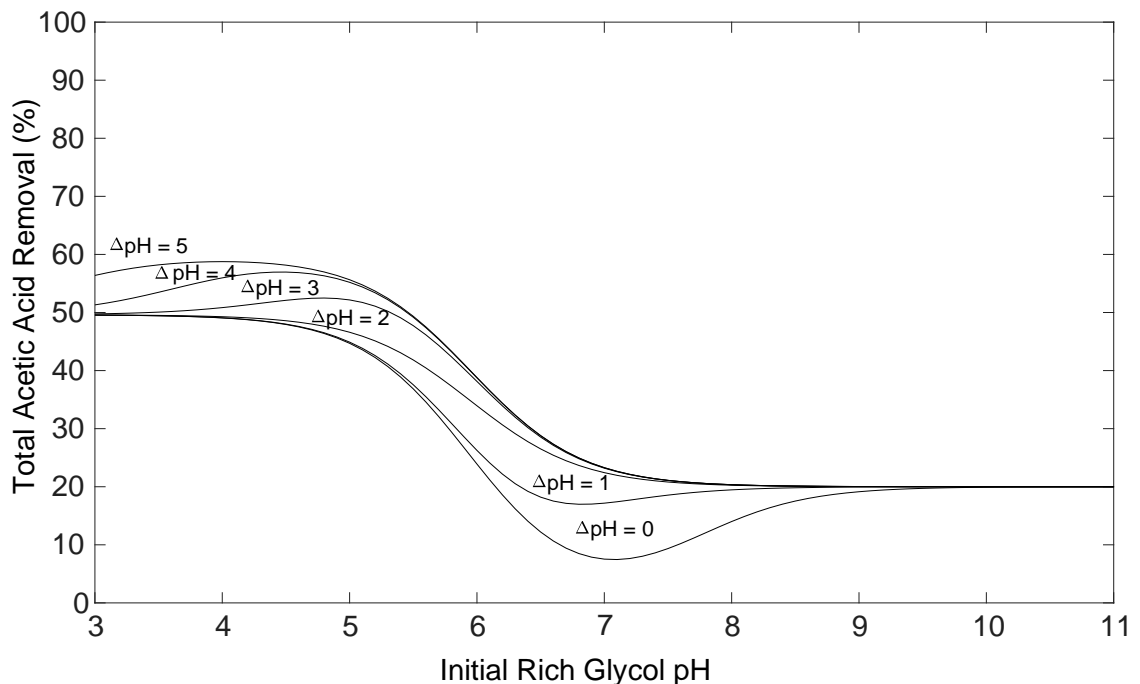


Figure 4-11. Simulated acetic acid removal rate with 20% partial reclamation

4.4 Conclusion

The level of organic acids within closed-loop MEG systems is often controlled via vacuum reclamation through the formation of non-volatile organic salt products allowing separation from the evaporated MEG/water phase. However, if a reclamation system is unavailable, or operated at low pH, organic acids will ultimately accumulate within the closed-loop MEG system. To maximise the removal of organic acids during long term operation, the removal efficiency of organic acid during a combination of distillation and reclamation has been studied in conjunction with measured pH changes during the MEG distillation process. The experimental results generated during distillation and reclamation were compared to models developed using Aspen Plus® simulation software with good agreement found. Using the experimentally reported data, two equations have been proposed to estimate the removal of acetic acid during distillation and reclamation individually with an average model error of 0.38% and 2.6% respectively. The individual distillation and reclamation models can be utilised to estimate the total plant wide acetic acid removal within closed loop MEG systems.

Overall, the results highlight the importance of both operational pH during the individual distillation and reclamation processes and the expected pH rise across the regeneration system in determining total organic acid removal from closed loop MEG systems. Although complete removal of acetic acid during reclamation is achieved for reclamation systems with a pH above nine, closed loop MEG systems are ultimately constrained by the operating slip-stream rate and may face acetic acid accumulation if the designed slip-stream rate is insufficient ^[7]. For such systems, it may be advantageous to operate with a low rich glycol pH feed into the distillation system, as per the recommendations made in Chapter 5.0, to allow simultaneous removal during the regeneration and reclamation processes given sufficient pH rise across the regeneration system. For MEG regeneration loops without reclamation facilities for salt handling, the removal of organic acids through the MRU may be the only option available to prevent long term accumulation besides costly replacement of MEG inventory. If left uncontrolled, accumulation of organic acids may lead to various operational issues including increased corrosion ^[17, 63, 72-76], TLC ^[17, 63, 72-76] and poor interaction with production chemicals such as oxygen scavengers ^[113, 118]. However, if organic acids are to be removed alongside the produced water in the regeneration system to maximise plant wide removal, the potential corrosion risk to overhead systems due to low pH must also be considered ^[10].

5.0 OPERATION OF A MEG PILOT REGENERATION SYSTEM FOR SIMULTANEOUS ORGANIC ACID AND ALKALINITY REMOVAL DURING MDEA TO FFCI SWITCHOVER

5.1 Introduction

The formation of natural gas hydrates in hydrocarbon transportation pipelines represents a major flow assurance concern with major implications upon safe and economical process operation. The inhibition of hydrate formation is of critical importance in maintaining process flow and the prevention of damage to process equipment and piping. The annual cost associated with preventing hydrate formation has been estimated to be greater than \$500 million through inhibition by methanol injection alone ^[211]. In many recent oil and gas developments, Mono-Ethylene Glycol (MEG) has seen increasing popularity replacing methanol as the thermodynamic hydrate inhibitor of choice ^[1, 4, 6]. The preference for MEG over methanol stems from its low volatility, toxicity and flammability, favourable thermodynamic behaviour and simple and proven technology requirements ^[2, 3].

Post hydrate inhibition, the recovery and reuse of MEG is essential due to the significant volume required to provide effective hydrate control, its high cost and its effects on downstream processes ^[4-6]. Following the three-phase separation from gaseous and liquid hydrocarbons, MEG is removed in combination with water and must be regenerated before it is recycled back to the wellhead for reinjection. The regeneration of MEG is typically performed by distillation to remove surplus water in order to regain a glycol purity between 80-90% by weight ^[9, 36].

Alongside hydrate inhibition, the prevention of corrosion in piping and processing systems is a critical aspect of hydrocarbon flow assurance. The majority of natural gas pipelines are manufactured from carbon steel and are susceptible to 'sweet' corrosion due to the presence of carbon dioxide and free water during transport and processing ^[4, 89, 90]. The annual global cost associated with corrosion has been estimated by Koch [212] at roughly US \$2.5 trillion with up to 60% of corrosion experienced in the oil and gas industry resulting from CO₂ based corrosion ^[95]. To combat corrosion in hydrocarbon pipelines two methods of corrosion control can be applied including the injection of film forming corrosion inhibitors (FFCI) and/or pH stabilisers ^[4, 9, 70]. The presence of MEG itself has also been shown to impede CO₂ corrosion of carbon steels ^[4, 96, 97].

Corrosion prevention through pH stabilisation can be achieved through the addition of salt based (hydroxide or carbonate salts) or amine-based compounds such as methyldiethanolamine (MDEA) ^[4, 17]. The basis of pH stabilisation is to promote the formation of an iron carbonate protective film in order to protect the surfaces exposed to corrosion ^[4, 16, 17, 72]. pH stabilisation is effective when carbon dioxide is the primary source of corrosion but less so when high levels of hydrogen sulphide are present ^[9]. The use of pH stabilisers to inhibit corrosion is limited to pipelines where little to no formation water is present and, in some cases, can be used in combination with FFCIs ^[9, 15, 17, 116]. Within systems with large quantities of formation water, pH stabilisation tends to promote the precipitation of divalent salts through reaction with alkalinity (carbonates, hydroxide) at elevated pH ^[2, 4, 9]. Where formation water is expected, the injection of film forming corrosion inhibitors is the preferred method of corrosion prevention due to its minimal impact on pH, lessening the potential for scale formation ^[2, 9, 15, 204]. Furthermore, pH stabilisers such as MDEA can result in the increased boiling point of lean MEG impacting upon the design and operation of the MEG regenerator and reclaimer systems ^[9].

Once formation water breakthrough occurs and the risk of scaling cannot be managed through alternative means including scale inhibitor injection, it may be beneficial to perform a corrosion strategy switch over from pH stabilisation to FFCIs to extend the life-span of the field ^[8, 9]. This process cannot be performed instantaneously, instead, once formation water is detected or anticipated, MDEA must be gradually removed from the system whilst FFCIs are introduced. The removal of MDEA may be accomplished through a vacuum reclamation system by converting MDEA to its salt form at low pH where it is not readily vaporised alongside the MEG solution ^[9]. The protonated form of MDEA, MDEAH⁺ can react within ionic species including chlorides, sulphates, sulphides and organic acid ions to form heat stable salts, a common occurrence in industrial CO₂ and H₂S capture systems using amines ^[213-217]. However, such low pH within the reclaimer may result in poor organic acid removal rates during reclamation leading to organic acid enrichment within the lean glycol. An increase in organic acids within the MEG regeneration loop may potentially lead to operational issues including corrosion of downstream process equipment and pipelines. The aim of this study is to investigate the feasibility of removing organic acids and MDEA simultaneously by careful adjustment of system pH at critical points to facilitate switch over from pH stabilisation using MDEA to FFCI.

5.2 Organic Acids within MEG Regeneration Systems

The presence of organic acids including acetic, propionic and butanoic acids within MEG regeneration systems may arise upon the breakthrough of formation water alongside mineral salts ^[9, 63]. The degradation of MEG if exposed to excessively high temperatures or oxidation

during the regeneration process can also lead to the production of organic acids including glycolic, acetic and formic acids [3, 5, 39, 63]. Furthermore, free organic acids may be present with the natural gas within the reservoir and may enter into the MEG regeneration system through the condensed water phase or formation water [63]. The presence of organic acids within carbon and mild steel piping has been shown to increase corrosion rates in natural gas and oilfield systems [69-72]. Top of the Line Corrosion (TLC) may also be experienced within carbon steel systems in the presence of carbon dioxide and acetic acid, with organic acids increasing the rate of TLC [17, 63, 72-76].

Organic acids present within the rich MEG can lead to reactions with the alkalinity contained within the MEG solution reducing the effective alkalinity within the system [8, 116]. Furthermore, organic acids will directly reduce the pH of the solution acting as a proton provider and may be directly reduced on the surface of metals enhancing the anodic reaction of the metal [67, 68, 72]. The presence of organic acids and the resulting low pH MEG will also pose a greater corrosion risk to carbon and mild steel piping through increased solubility of iron in the condensing water reducing its efficacy in forming a protective film [65-68]. This effect may be counteracted by use of pH stabilisation chemicals such as MDEA to raise the pH to safer levels and to promote the formation of protective corrosion films [72, 116]. Furthermore, the work conducted by Amri [73] suggests that the presence of acetic acid within the aqueous phase of gas condensate pipelines directly increases the potential for localised corrosion attacks in carbon steel pipelines.

During MEG regeneration by distillation where the water phase is boiled off, if a high pH is maintained in the reboiler, any organic acids present within the rich MEG will exist in their ionic form and accumulate within the regenerated lean MEG and will be recycled back to the wellhead [17, 116]. Therefore, if not otherwise removed, acetic acid will begin to build up within the MEG regeneration loop and excessive exposure will begin to occur within process pipelines enhancing the potential for corrosion. To ensure removal of organic acids during MEG regeneration, their removal can be performed through the reclamation system at elevated pH where organic acids will dissociate to their ions forming salts in the presence of monovalent cations [63]. The organic salts will subsequently be captured within the vacuum reclamation system whilst the lean MEG is evaporated and recovered to be reused.

5.3 Operational Scenario

The switch over from pH stabilisation (for example, using MDEA) to film forming corrosion

inhibitors may be required as part of the hydrocarbon pipeline corrosion inhibition strategy once formation water breakthrough has occurred. Upon the introduction of formation water, pH stabilisation will no longer be suitable due to its tendency to cause scaling issues as a result of the elevated pH [2, 4, 9]. Therefore, it may be necessary to 'switch over' from using a pH stabiliser to a more conventional corrosion inhibitor to limit scaling within the transportation pipelines to ensure flow can be maintained. To facilitate the switch over process, the MDEA must be removed from the MEG regeneration loop with removal through the reclamation system being a possible method [9, 15].

To achieve removal of MDEA within the reclamation system, MDEA must first be neutralised to its salt form to allow accumulation within the reclaimer [9, 40]. Through prior extensive testing conducted by the Curtin Corrosion Centre (CCC) involving removal of MDEA from lean MEG, a pH level below 8 has been identified as the pH range at which MDEA will begin to experience appreciable removal during reclamation. At a pH of approximately 8 and below, MDEA will be converted to its salt form allowing it to be removed along with any monovalent salt cations whilst MEG and water evaporate under vacuum [40]. However, if the pH into the reclaimer is too low, the tendency of organic acids to form salts will decrease leading to vaporisation within the reclaimer and carry over alongside the MEG and water. Thus, organic acid enrichment within the lean glycol may begin to occur. Therefore, significant removal of MDEA and organic acids can sometimes not be performed simultaneously within the reclaimer due to the opposing pH conditions required.

5.3.1 Comparison of Operational Methodologies

Two operational methods have been evaluated using a pilot MEG regeneration system at Curtin Corrosion Centre, the first being an industrial methodology and the second an alternative switch over strategy by the CCC. Experimental replication of the industrial methodology entails the injection of HCl in the lean glycol tank in order to target a lean glycol pH of 7. A target pH of 7 was selected to minimise the risk of scaling following the reinjection of the lean MEG at the well head following the breakthrough of formation water. Several questions arose during testing due to the rise in pH experienced across the reboiler as a result of CO₂ boil off and concentration of any alkalinity present within the lean MEG. The industrial switch over process is illustrated by Figure 5-1 with causes of pH change during a regeneration cycle identified. As formation water production had initiated, a pH of 8.2-8.3 within the pre-treatment vessel (MPV) was targeted to facilitate the removal of divalent cations (primarily calcium) through reaction with carbonate to

prevent scaling at higher temperature within the regeneration system.

An alternative switch over process developed by the CCC, involves the injection of HCl in-line into the rich glycol feed to the reboiler system. The pH of the rich glycol solution was not adjusted within the rich glycol tank its self to prevent redissolving of carbonate particles produced upstream during pre-treatment allowing them to settle within the tank. The proposed methodology was designed to minimise the pH change occurring across the reboiler by neutralising the additional alkalinity introduced during pre-treatment allowing improved MDEA removal within the reclamation system. Simultaneously, the removal of organic acids including acetic acid was theorised to occur at the target reboiler pH (pH 7) via the produced water product to a sufficient extent to prevent its accumulation within the regeneration loop. Under the industrial operational philosophy, removal of organic acids would otherwise occur in the reclaiming at high pH. Two primary goals were identified to improve the MDEA to FFCI switchover process including minimisation of total lean glycol alkalinity to below 5 mM as quickly as possible and the prevention of organic acid accumulation within the regeneration loop. Furthermore, targeting a lower pH within the reboiler reduces the risk of scaling within the regeneration system particularly on the surface of the reboiler bundle at high temperature.

5.3.2 Behaviour of Organic Acids and MDEA during MEG Regeneration and Reclamation

To facilitate the simultaneous removal of MDEA and organic acids within the MEG regeneration loop, it has been suggested that adjustment of the rich MEG feed pH prior to the reboiler may provide adequate removal of organic acids during distillation to prevent accumulation. Upon the introduction of acetic acid into the distillation system, the acetic acid will boil-off with the produced water and be removed within the reflux drum. However, the ability of acetic acid to be removed is highly dependent upon pH and the extent of dissociation of acetic acid to acetate. For removal of acetic acid to occur during distillation, it must remain in its un-dissociated form. If dissociation of acetic acid to acetate occurs, acetate will bond with free mineral ions including sodium to form low volatility salts that will remain within the lean MEG during distillation, a common occurrence in industry due to the high pH required upstream to remove divalent salts ^[2, 9]. Therefore, to achieve efficient removal of acetic acid during distillation, it is essential to maintain conditions that inhibit its dissociation to acetate namely low pH.

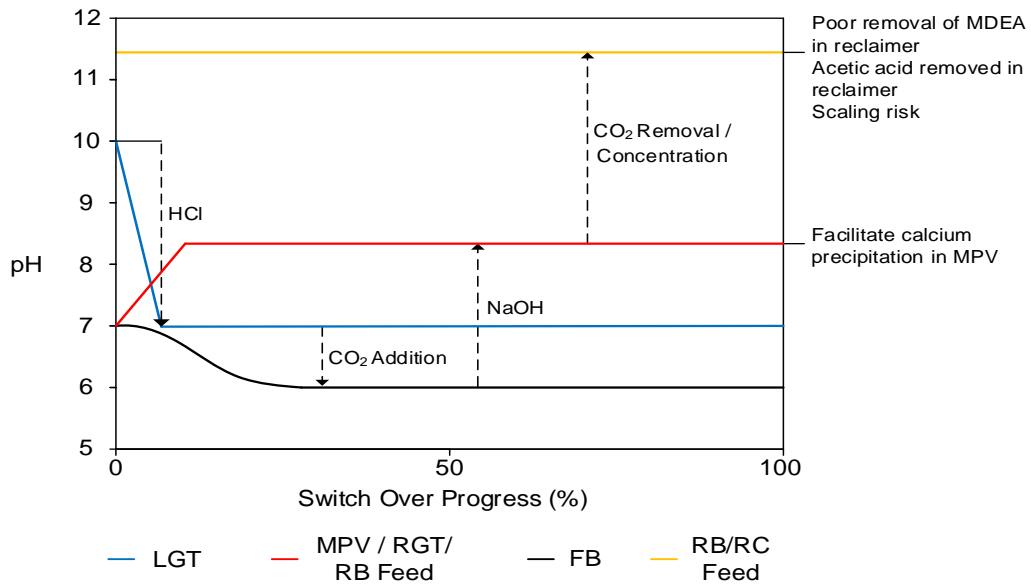


Figure 5-1. Industrial FFCI to MDEA switchover methodology

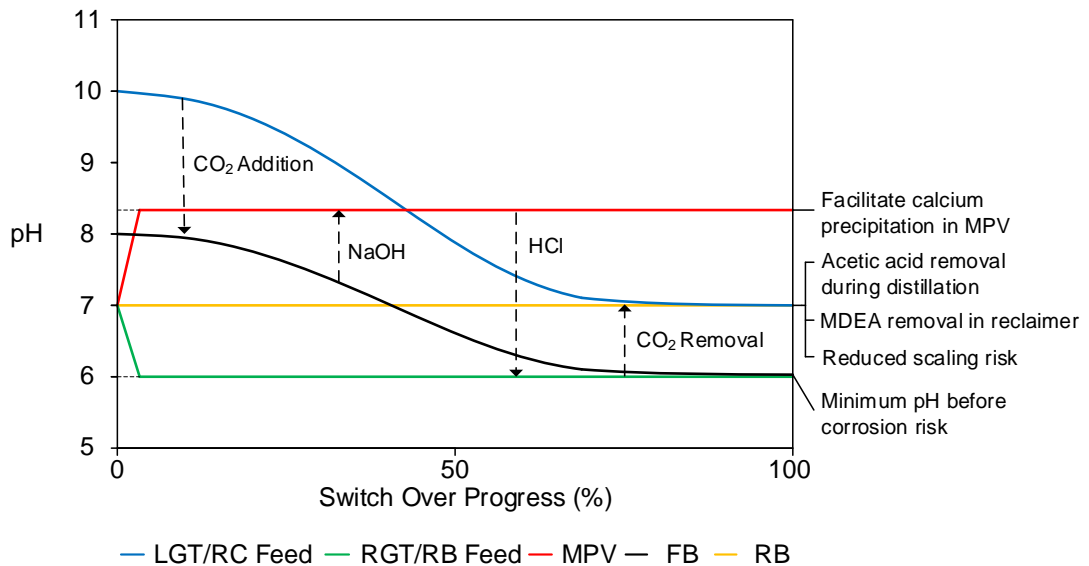
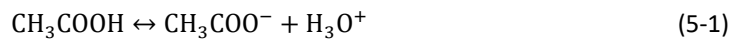


Figure 5-2. Alternative FFCI to MDEA switchover methodology

To obtain a better understanding of the behaviour of acetic acid during the MEG distillation process, the dissociation of acetic acid to acetate was modelled. Organic solvents such as ethylene glycol have been shown experimentally to influence the acid dissociation constant (pK_a) of various weak acids and bases typically increasing pK_a compared to aqueous solutions [127-129]. To estimate the dissociation of acetic acid to acetate within 80% wt. MEG solution at 130°C, the pK_a for acetic acid was determined experimentally by potentiometric titration. As evaporation of the MEG solution would occur at 130°C, multiple titrations were performed at varying temperatures (25-80°C) to generate a relationship between pK_a and temperature from which the pK_a of acetic acid at 130°C was extrapolated from. The resulting titration curves were then used to calculate the pK_a value of acetic acid at the respective temperature with determination of experimentally derived pK_a values discussed in Chapter 8.

However, the extent of acetic acid dissociation is dependent upon solution pH, with greater conversion of acetic acid to acetate occurring at higher pHs where it can be more readily neutralised [19, 119]. To calculate the percentage of acetic acid present, the acid dissociation equation represented by Equations (5-2) and (5-3) were used based upon the dissociation of acetic acid given by Equation (5-1). The percentage distribution of acetic acid and acetate can be then estimated through Equations (5-4), (5-5) and (5-6) where the concentration of the hydronium ion is calculated through pH. The overall percentage distribution of acetic acid with respect to pH is given by Figure 5-3 for varying MEG concentrations and temperatures based upon pK_a values estimated using the model proposed in Chapter 8.0. As such, it is clear that for appreciable removal of acetic acid to occur during distillation, a lower pH is required to ensure acetic acid is readily available to be removed.



$$K_A = 10^{-pK_A} = \frac{[\text{CH}_3\text{COO}^-][\text{H}_3\text{O}^+]}{[\text{CH}_3\text{COOH}]} \quad (5-2)$$

$$[\text{CH}_3\text{COOH}] = \frac{[\text{CH}_3\text{COO}^-][\text{H}_3\text{O}^+]}{K_A} \quad (5-3)$$

$$[\text{CH}_3\text{COOH}] + [\text{CH}_3\text{COO}^-] = \text{Total}[\text{HAc}] \quad (5-4)$$

$$\text{Total}[\text{HAc}] - [\text{CH}_3\text{COO}^-] = \frac{[\text{CH}_3\text{COO}^-][\text{H}_3\text{O}^+]}{K_A} \quad (5-5)$$

$$[\text{CH}_3\text{COO}^-] = \frac{\text{Total}[\text{HAc}] \cdot K_A}{[\text{H}_3\text{O}^+] + K_A} \quad (5-6)$$

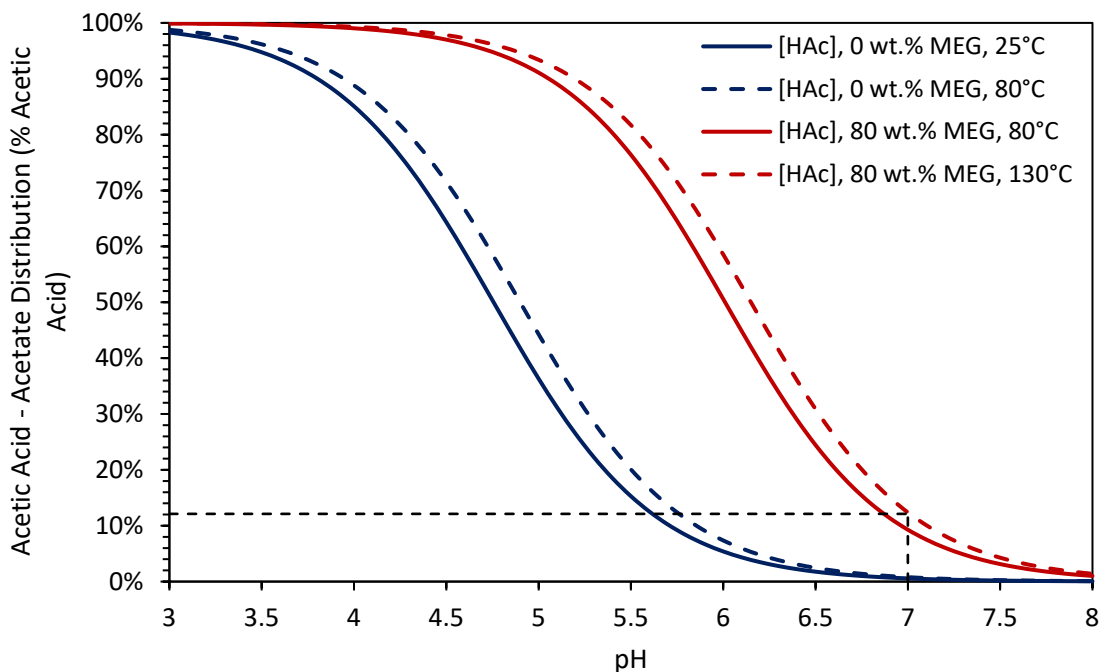


Figure 5-3. Speciation of acetic acid – acetate

Through prior testing conducted using the pilot MEG distillation system utilised within this study, a pH rise across the reboiler of approximately 1 pH unit can be expected during operation using the proposed alternative operational philosophy (refer to Figure 5-2). The rise in pH within the reboiler can be attributed to the removal of dissolved CO_2 . CO_2 is initially introduced into the rich MEG through sparging within the feed blender to simulate the presence of dissolved CO_2 originating from the well and is boiled off within the reboiler during operation when exposed to high temperature [9, 38]. Additional CO_2 is also introduced during the pre-treatment stage as a source of carbonate alkalinity to facilitate the removal of calcium. At the target reboiler feed pH of 5.8-6.0, the rise in pH over the reboiler will provide an estimated pH of 7.0, with approximately 12-15% of the total acetic acid within the MEG solution present in its undissociated form and potentially removed during distillation (Figure 5-3). Moreover, a lean MEG pH of 7 to the reclaimer will facilitate efficient removal of MDEA during the reclamation process as per Figure 5-4 due to the conversion of MDEA to its protonated form, MDEAH^+ at low pH. As a consequence of the lower reclaimer pH, a slight reduction in the removal of acetic acid will occur within the reclamation system in comparison to the industry procedure where a lean glycol above pH 11 is fed to the reclaimer.

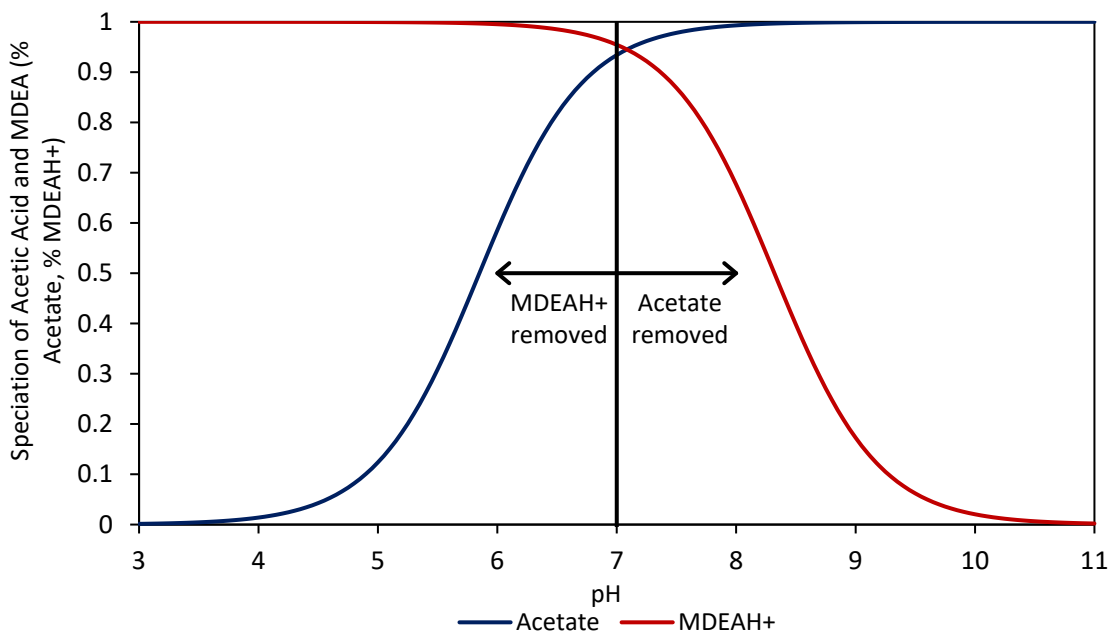


Figure 5-4. MEG reclamation removal efficiency at 25°C, 80% wt. Lean MEG

5.4 Process Design and Configuration

The MEG pilot plant utilised within this study was constructed by the Curtin Corrosion Centre to simulate the operation of an industrial MEG regeneration system. The operation of the pilot plant has been conducted to evaluate a number of different operating scenarios that

are likely to occur in the field. The regeneration system is comprised of a pre-treatment stage, a distillation system to remove excess water and a reclamation section to process and remove monovalent salts and other process chemicals from the lean MEG product as illustrated in Appendix B.

The pre-treatment section of the pilot plant includes a feed blender where brine is added as required and mixed with previously processed lean MEG to achieve the desired rich MEG composition. Following the blending process, the MEG solution undergoes pre-treatment to remove divalent cations from the solution within a multi-phase separation vessel. The pre-treated rich MEG is subsequently stored within the rich glycol where hydrochloric acid (HCl) was added to adjust the pH of the reboiler feed. A recirculation pump was added to the vessel to thoroughly blend the HCl into the rich MEG to achieve a more equal pH throughout the solution. From previous testing, it was found that if the HCl was added inline, the downstream inline pH probe would intermittently detect spikes of HCl leading to inaccurate pH measurement.

The main section of the distillation column is comprised of two individual sections; each one 900 mm in height with the sections connected and fitted with 80 mm DN (3") borosilicate glass structural packing, additional specifications of the distillation column are listed within Table 3-1 and Table 3-2. The rich MEG feed to the distillation column is introduced directly into the column's reboiler unit at temperature of between 40-50°C with mass flow rate measured by a Mass Flow Metre (MFM) and maintained by a programmable logic controller (PLC) at approximately 5.0 kg/hr. The distillation column operates using a 10-litre glass reboiler in combination with a 5 kW immersion heater. Throughout testing the reboiler unit was operated at 128°C ($\pm 1^\circ\text{C}$.) with operating temperature maintained during distillation by a PLC.

During distillation, lean MEG is extracted from the bottom of the column through the MEG pump with mass flow rate measured by a MFM. The lean MEG product is subsequently cooled through a plate heat exchanger operating using cooling water at 10°C and then store in the lean MEG tank. The regeneration system operates using a slip-stream reclamation methodology where a portion of the lean MEG product undergoes reclamation. Within this study, a slip stream rate of 11% was used to model the field operating conditions of a particular industrial facility. The reclamation process is performed to remove monovalent cations including sodium and potassium to prevent accumulation within the closed loop system. Under the operational scenario performed within this study, MDEA is also removed during the reclamation stage to simulate the switch over from MDEA to FFCI. The reclaimed lean MEG is then recycled back and mixed with remaining lean MEG within the lean glycol tank for further reuse as hydrate inhibitor.

To determine the composition of process streams within different sections of the MEG system including within the reboiler, reflux drum and storage tanks, sampling ports were installed to allow samples to be taken and tested at a later time using High-Performance Liquid Chromatography (HPLC) and Ion Chromatography (IC). HPLC was performed using a Thermo Scientific UltiMate 3000 LC/HPLC system whilst IC was performed using a Dionex ICS-2100 IC System. Inline pH measurements are also made continuously throughout operation at the points depicted in Appendix B using inline Mettler Toledo InPro 4800(i) pH probes connected to a Mettler Toledo M800 system to transmit data to the PLC. Other process measurements taken during operation include dissolved oxygen content and solution electrical conductivity using inline probes supplied by Mettler Toledo.

5.5 Chemicals and Feed Stream Compositions

The MEG used during operation of CCC's MEG regeneration pilot plant was supplied by Chem-Supply with a purity greater than 99.95% by weight. To produce the rich MEG and brine used within this study, distilled water with an electrical resistivity above 18 M Ω -cm was used. The brine and rich MEG compositions tested within this study were chosen to simulate the conditions of an industrial MEG regeneration facility. The compositions of the feed streams are outlined by Table 5-1 in terms of MEG and water mass fractions and the amounts of dissolved salt ions and organic acids in terms of parts per million by weight (ppmw). All metallic salts were supplied by Chem-Supply as metal chlorides and SO_4^{2-} and HCO_3^- as their respective sodium salts at a purity above 99% wt. Organic acids including acetic, propanoic, butanoic and pentanoic were sourced from Sigma Aldrich at a purity greater than 99% wt.

Additionally, the sparge gas compositions outlined by Table 5-2 were used to simulate the CO₂ of the well and as a source of carbonate alkalinity within the feed blender and pre-treatment vessel respectively. As the pilot MEG facility cannot operate under pressure in the feed blending unit, the partial pressure of carbon dioxide was limited to 1 bara. In a real pipeline, which operates at around 100 bara, the partial pressure of CO₂ will be much higher.

Table 5-1. Feed stream compositions

Stream Component	Brine	Rich MEG Reboiler Feed	Lean MEG Recycle
MEG (Mass Frac.)	-	0.440	0.800
Water (Mass Frac.)	0.99928	0.558	0.194

Table 5-1. Feed stream compositions continued

Stream Component	Stream Mass Compositions (ppmw)		
Na ⁺	266	994	1601
K ⁺	3.5	13	21
Ca ²⁺	3.4	4	5
Mg ²⁺	0.32	1.2	1.9
Fe ²⁺	0.033	0.12	0.20
Sr ²⁺	0.09	0.34	0.55
Ba ²⁺	0.64	2.4	3.9
Cl ⁻	118	440	709
HCO ₃ ⁻	1.1	4.0	6.4
SO ₄ ²⁻	193	721	1162
Acetic Acid	17	63	102
Propanoic Acid	4.1	15	24
Butanoic Acid	5.8	22	35
Pentanoic Acid	118	440	709
MDEA (mM)	0	319	580

Table 5-2. Sparging gas compositions

	Feed Blender	Pre-treatment Vessel
mol% CO ₂ at 1 bara	100%	76%
mol% N ₂ at 1 bara	0%	24%

5.6 Operating Procedure

Operation of the MEG regeneration pilot plant was initiated by pre-filling the lean glycol tank (LGT), rich glycol tank (RGT), feed blender and reboiler vessels with their respective MEG solutions. Furthermore, approximately two kilograms of distilled water was used to pre-fill the distillation column's reflux drum to provide liquid reflux upon the commencement of operation. Prior to the conduction of the experiment, each vessel was sparged with high purity nitrogen (purity >99.999 mol %) to achieve an oxygen content below 20 ppb. A low oxygen content (<20 ppb) is important to prevent degradation of MEG when exposed to high temperatures within the reboiler, and prevention of pitting corrosion of downstream process equipment including MEG injection lines [8, 114]. To commence operation, the distillation column was operated under total reflux conditions until the reboiler operating temperature was stabilised at 128°C and steady state conditions within the column reached. Once steady state operation of the column

had been achieved, the rich MEG feed was then introduced directly into the distillation column's reboiler and outlet valves opened.

For the industrial methodology, operation was commenced by neutralising the MDEA within the lean glycol tank by injection of HCl. To evaluate the system chemistry as lean glycol pH decreased to the target of pH seven, the lean glycol pH was decreased stepwise over multiple inventory turnovers (operational days). In contrast, for the proposed switch over procedure, during the first day of operation the pH within the RGT was adjusted from a starting pH of seven to six by continuous injection of HCl. Once sufficient neutralisation of the initial MDEA had occurred, the pH of the rich MEG feed to the column's reboiler was gradually decreased step-wise. In order to investigate the behaviour of organic acids during distillation, the pH was decreased in steps of 0.1 from a pH of six. Following each decrease of pH of the rich MEG feed, the pH was kept constant and operation allowed to proceed for one inventory turnover. To maintain a constant target pH within the rich and lean glycol tanks, HCl was added using a dosage pump controlled by a PLC system. The PLC system utilised a combination of feedback measurements from an inline pH probe located at the outlet of the pH adjustment vessel and a pH probe located within the vessel itself. The probes were connected to a Mettler Toledo M800 process measurement system to allow direct communication to the PLC.

Furthermore, to prevent accumulation of divalent salts such as calcium present in the brine from accumulating within the regeneration loop sodium hydroxide was dosed within the pre-treatment vessel (MPV). By maintaining a sufficiently high pH within the MPV (>8) the formation of carbonate alkalinity within the vessel allowed the precipitation of calcium carbonate facilitating its removal through settling downstream in the rich glycol tank. Conversely, monovalent salts such as sodium and potassium were partially removed via a vacuum reclamation unit operating at 100 mbara \pm 5 mbara and 120-130°C.

To determine whether separation of the organic acids from the MEG solution had occurred during distillation, samples were taken every three hours from various sampling ports located around the MEG distillation system. The samples were then analysed post operation using the ion chromatography system to determine the concentration of organic acid ionic species within each sample.

5.7 Operating Results and Discussion

5.7.1 pH Change during MEG Regeneration Process

The change in pH experienced within the LGT, RGT and reboiler under the industry and modified operational philosophies is illustrated by Figure 5-5 and Figure 5-6 respectively. Under the industry procedure, the pH within the LGT is gradually reduced over several regeneration

cycles to the target pH of 7. However, due to the addition of sodium hydroxide within the pre-treatment vessel to facilitate calcium removal and hence constant MPV pH, no variation in rich glycol pH and the produced lean glycol within the reboiler occurred. The removal of carbon dioxide and concentration of the hydroxide alkalinity within the produced lean glycol as excess water is removed ultimately produced a lean glycol feed to the reclamation system upwards of 11.2. The resulting high pH within the reclamation system will push the MDEA equilibrium from its dissociated MDEAH⁺ form to its more volatile form allowing it to be vaporised alongside the MEG solution inhibiting its removal.

In contrast, whilst targeting a pH of six within the rich glycol feed to the reboiler a pH of approximately 7-7.1 was maintained within the reboiler of the regeneration system. The addition of HCl into the rich glycol solution provided initial neutralisation of the excess carbonate and hydroxide alkalinity present within the rich glycol following pre-treatment. The resulting pH increase across the reboiler occurred due to the boiling off of dissolved carbon dioxide and organic acids suggesting that the addition of carbonate and hydroxide downstream and subsequent concentration is the primary cause of the high pH produced lean glycol experienced as per Figure 5-5. The produced lean MEG fed into the reclamation system at pH 7 would facilitate a greater conversion of MDEA to MDEAH⁺ allowing superior removal efficiency compared to the industrial procedure evaluated in this study. The effect of the regeneration process on the produced lean MEG is illustrated by Figure 5-7 and Figure 5-8 as the rich MEG from the pre-treatment vessel undergoes pH adjustment and distillation, ideal target pHs at the respective stages of the process have been included.

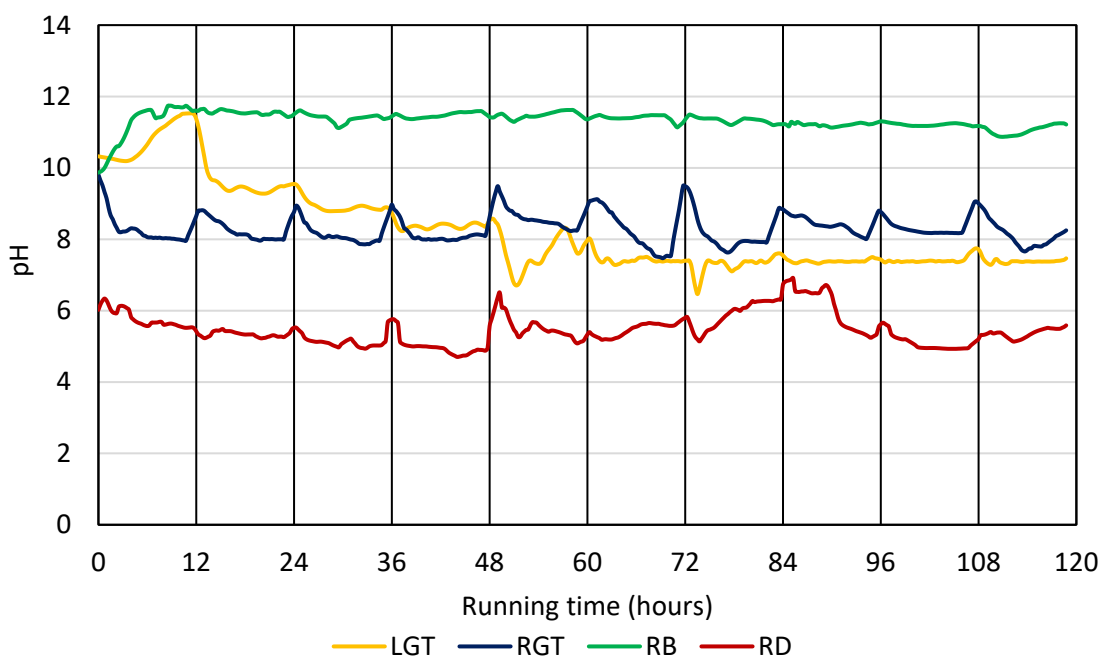


Figure 5-5. pH levels during MEG regeneration (industry operational philosophy)

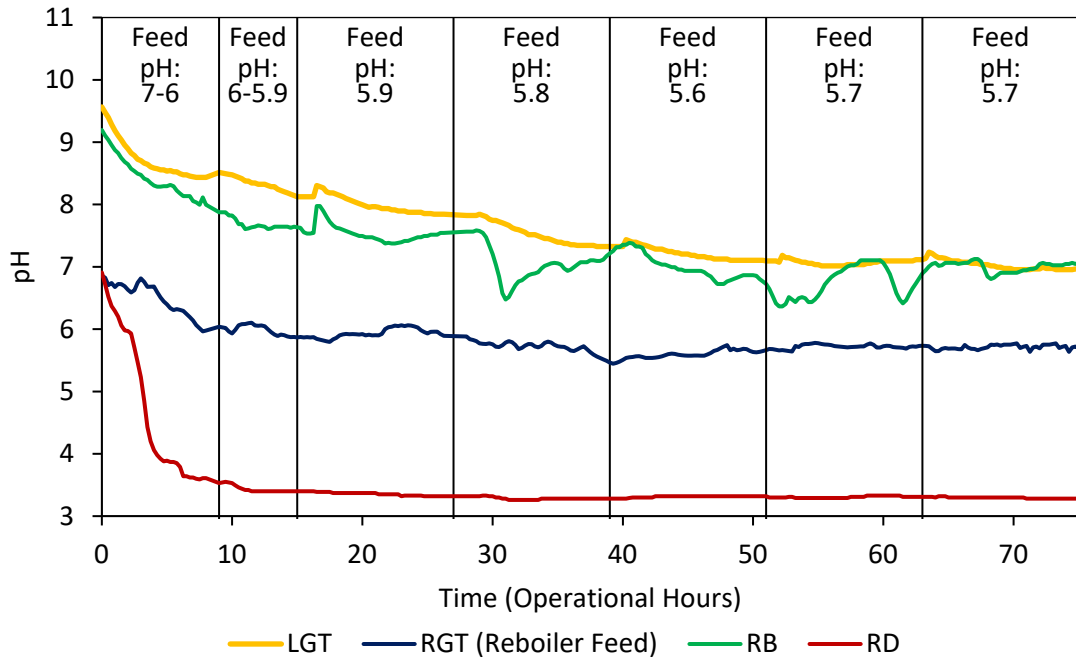


Figure 5-6. pH levels during MEG regeneration (modified operational philosophy)

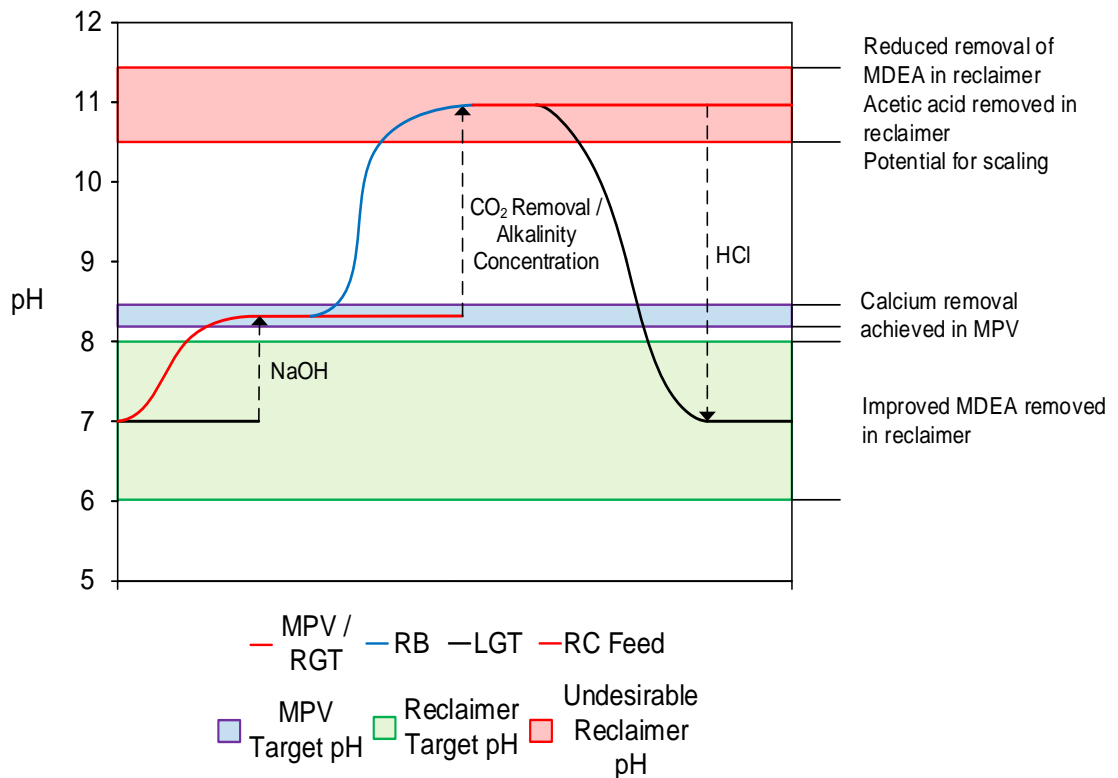


Figure 5-7. Ideal target pHs and current pH change during regeneration (industry operational philosophy)

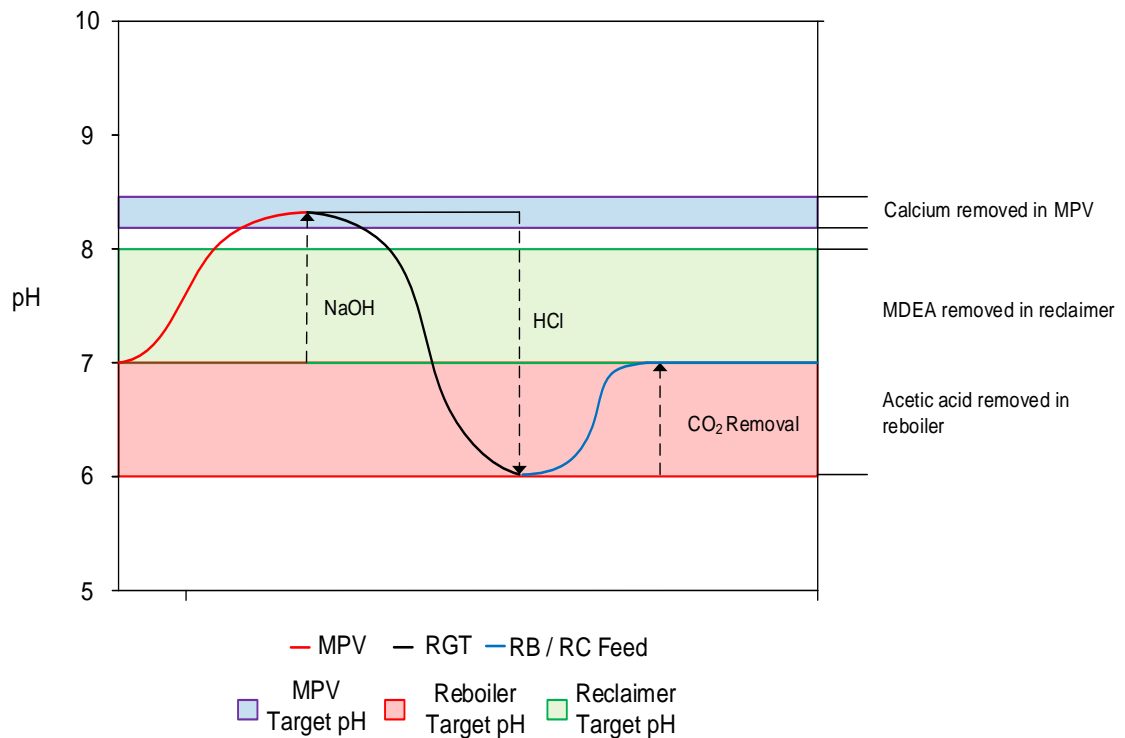


Figure 5-8. Ideal target pHs and current pH change during regeneration (Modified Operational Philosophy)

5.7.2 Removal of MDEA and Alkalinity: Comparison between Operational Methods

The removal of MDEA during the regeneration process was identified as a key criterion during operation to enable the switch over from pH stabilisation to FFCI. To assist with successful switch over to FFCI, the short-term operational goal was to reduce the total alkalinity within the lean glycol tank to below 5 mM to minimise the risk of scaling with complete removal of MDEA identified as a long-term target. The total alkalinity within the lean glycol tank represents the amount of un-dissociated MDEA remaining within the lean glycol product as well as carbonate and hydroxide alkalinity. The total alkalinity was determined through titration by 0.1 M HCl using a HI902 potentiometric automatic titration system. The total alkalinity measured over the entire operational period for the industrial and proposed switch over process are illustrated by Figure 5-9 and Figure 5-10 respectively. Furthermore, the respective figures illustrate the concentration of MDEA (MDEA and MDEAH⁺) measured via ion chromatography in three-hour intervals. The vertical gridlines drawn on Figure 5-9 and Figure 5-10 represent one successful completion of a regeneration cycle typically achieved after 10 hours of continuous operation.

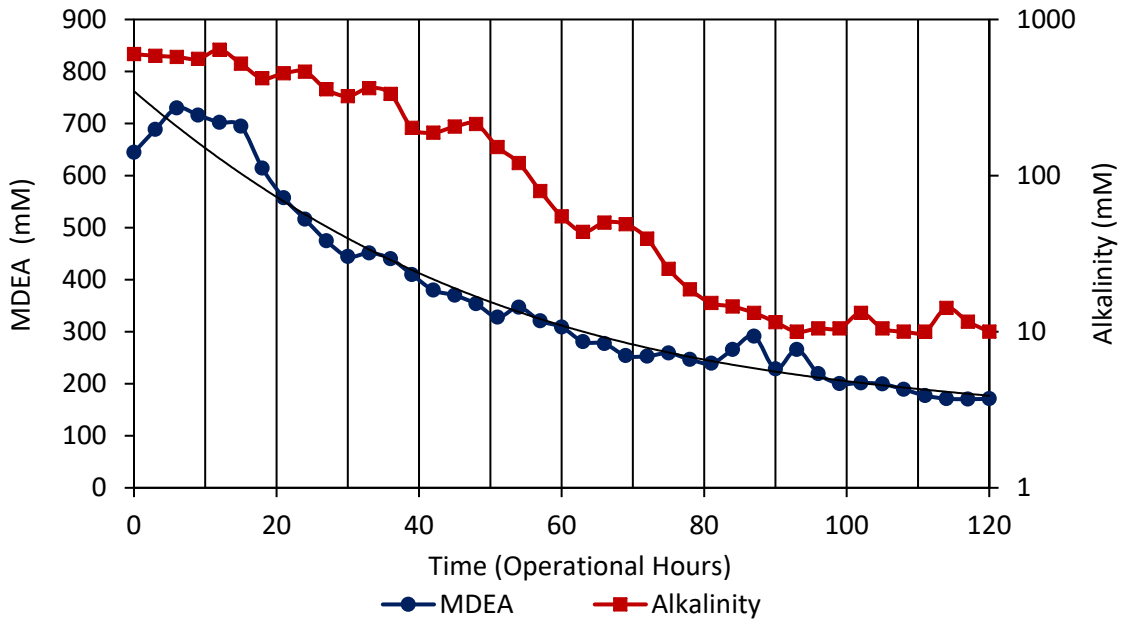


Figure 5-9. Lean Glycol Tank MDEA and alkalinity measurements (industry operational philosophy)

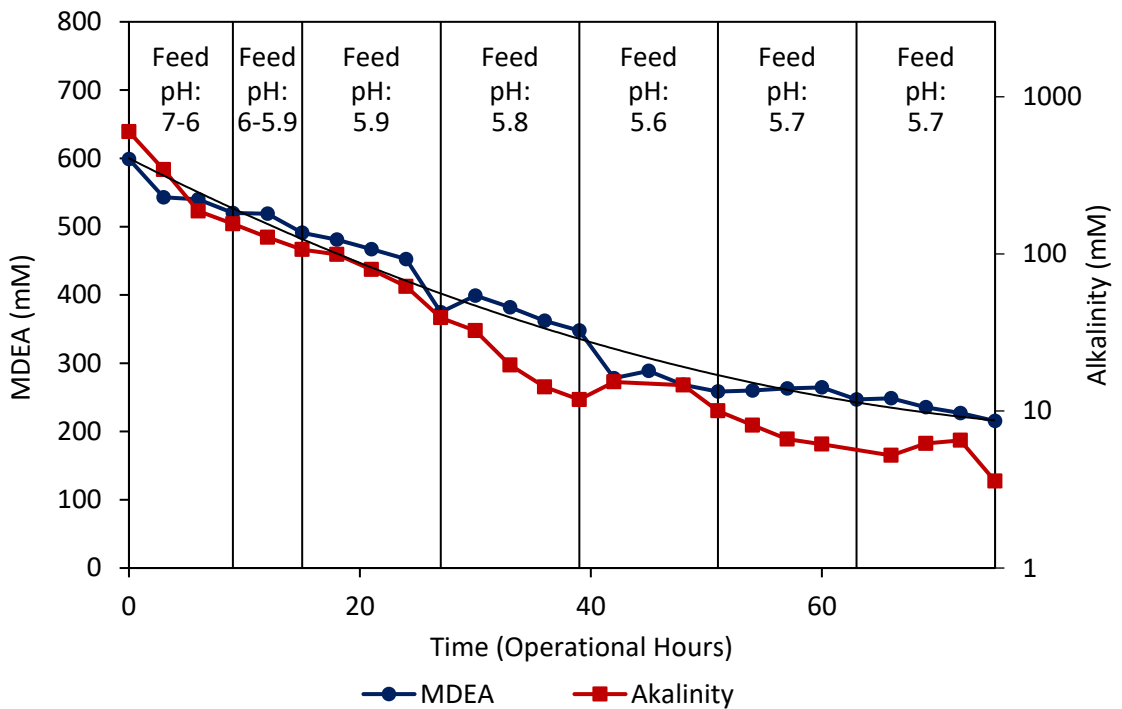


Figure 5-10. Lean Glycol Tank MDEA and alkalinity measurements (modified operational philosophy)

Complete removal of the total alkalinity within the lean glycol in this study was unable to be achieved under the industrial operational methodology plateauing at approximately 10 mM after 12 regeneration cycles. In comparison, whilst targeting a rich glycol pH of six, rapid removal of alkalinity was successfully achieved reaching below 10 mM total alkalinity approximately five regeneration cycles faster. Rapid reduction in alkalinity within the first two days of operation

was achieved as neutralisation of MDEA by hydrochloric acid occurs whilst targeting the desired rich glycol pH. Furthermore, the produced lean glycol at pH 7 reached below 5 mM total alkalinity successfully after six regeneration cycles, with a comparison of alkalinity removal under both methods given by Figure 5-11. As such, this study suggests that the short-term switch over from MDEA to FFCI can be significantly improved under the proposed operational methodology.

Furthermore, consistent removal of MDEA was achieved during the reclamation process under the modified procedure removing a total of 356 mM of MDEA over a period of seven days of operation as per Figure 5-9. The produced lean glycol at pH 7 (Figure 5-6) being fed into the reboiler facilitated the conversion of MDEA to MDEAH^+ (refer to Figure 5-4) allowing the formation of MDEA heat stable salts through reaction within anionic species including chloride, sulphate and organic acid ions ^[213-215]. The formation of heat stable salts therefore facilitated its removal within the reclamation system as the MEG solution evaporated under vacuum. In comparison, the removal of MDEA under the industry procedure occurred at a much slower rate reaching the same final MDEA concentration after an additional five regeneration cycles. Under both operational methodologies, the rate of MDEA removal was non-linear due to only a fraction (11% slip-stream) of the produced lean MEG undergoing reclamation, as such reduced MDEA removal is expected in proceeding cycles. Based on the operational results, it was estimated that under the current MDEA removal rates achieved under both operational methodologies, a total of approximately 25-30 regeneration cycles for the industry method and 10-11 cycles for the modified procedure would be required to achieve the desired final MDEA concentration within the MEG regeneration loop.

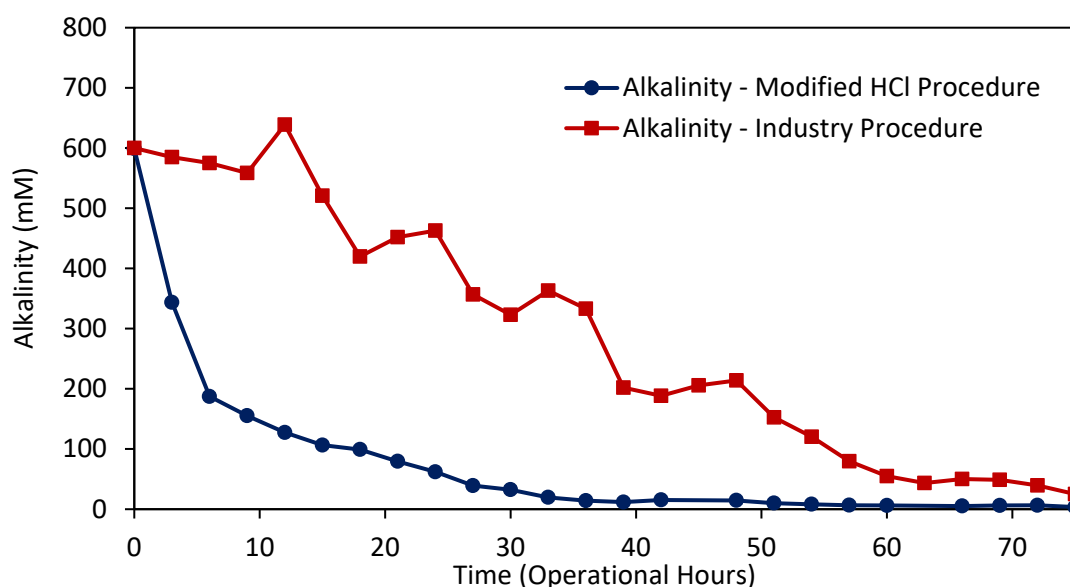


Figure 5-11. Comparison of MEG regeneration alkalinity removal methods

Due to the necessity to increase the pH of the rich MEG entering the regeneration system within the MPV to facilitate divalent salt removal, the continued presence of MDEA/alkalinity within the MEG loop will increase the amount of NaOH and HCl required to control the pH levels within the system and hence increase operational costs. It is therefore beneficial from an economic perspective to reduce the alkalinity and MDEA concentration within the regeneration loop as quickly as possible. Therefore, the modified HCl dosing procedure used in this study would reduce the total costs associated with NaOH and HCl dosage during the switchover process.

Furthermore, the continued presence of alkalinity in the form of carbonates and hydroxide can pose a scaling risk due their reaction with dissolved mineral salts [2, 218]. The formation of carbonates arises due to the presence of carbon dioxide from the well and can react with bases/pH stabilisers including MDEA to form bicarbonate and hence carbonate at higher pH [4, 9, 218, 219]. As such, the formation of mineral scales including CaCO_3 and $\text{Mg}(\text{OH})_2$ can pose operational issues if sudden formation water breakthrough occurs and the system is operating under high pH. Therefore, it is advantageous to remove alkalinity whether in the form of MDEA, hydroxide or carbonates as quickly as possible to minimise long term scaling. However, within this study the pH of the lean glycol was insufficient (<10.2) to produce hydroxide alkalinity with the primary non-MDEA alkalinity arising due to the presence of carbonate whilst above a pH of approximately 8.2-8.3.

5.7.3 Removal of Organic Acids through the MEG Regeneration and Reclamation System (Modified Procedure)

Under the experimental replication of the industrial operating procedure where the lean glycol was fed into the reclamation system at high pH (Figure 5-5), significant removal of organic acids in their ionic form would occur during reclamation (refer to Figure 5-4). However, due to the lower reclaimer feed pH produced during the modified operational procedure, reduced conversion of acetic acid to acetate can be expected. As such, it is important to maintain a careful balance of low reclaimer pH to facilitate MDEA removal whilst also either achieving sufficient removal of organic acids during distillation or in combination with partial removal during vacuum reclamation. A pH of 7 within the reboiler and hence feed to the reclaimer was selected as the ideal pH to achieve removal of both MDEA within the reclaimer and partial removal of acetic acid during both distillation and reclamation (Figure 5-4).

The concentration of acetic acid within the rich and lean glycol tanks of the pilot MEG regeneration system was monitored to evaluate the removal efficiency of acetic acid during distillation. Figure 5-12 illustrates the level of acetic acid (ppm) within the rich and lean glycol solutions over the 75-hour period of operation in 3-hour intervals under the modified

operational philosophy. The level of acetic acid within the MEG regeneration loop was found to remain stable over the entire operation within both vessels with an average acetic acid concentration of approximately 1040 and 1600 ppm for the rich and lean glycol tanks respectively. Furthermore, the accumulation of acetic acid over the 75 hours of operation within the reflux drum is illustrated within Figure 5-13 showing a gradually accumulation of acetic acid with time. The accumulation of acetic acid within the reflux drum resulted in a water distillate pH of approximately 3.3-3.5 (Figure 5-6), in comparison, under the industry procedure the water distillate pH stabilised between 5.5-6.0 (Figure 5-5).

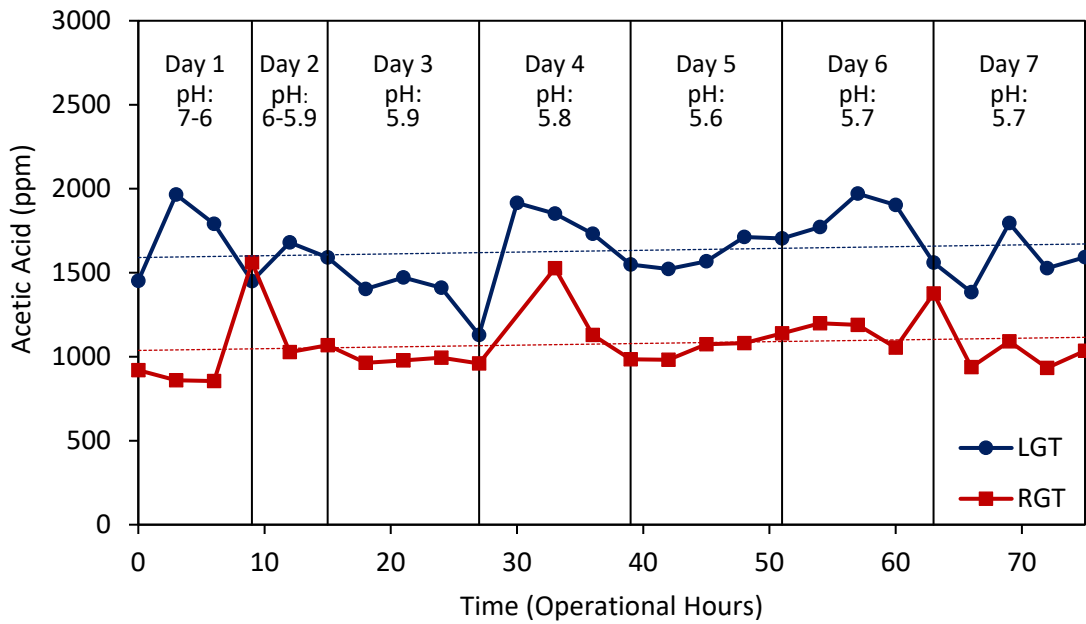


Figure 5-12. Acetic acid content within rich and lean glycol tanks

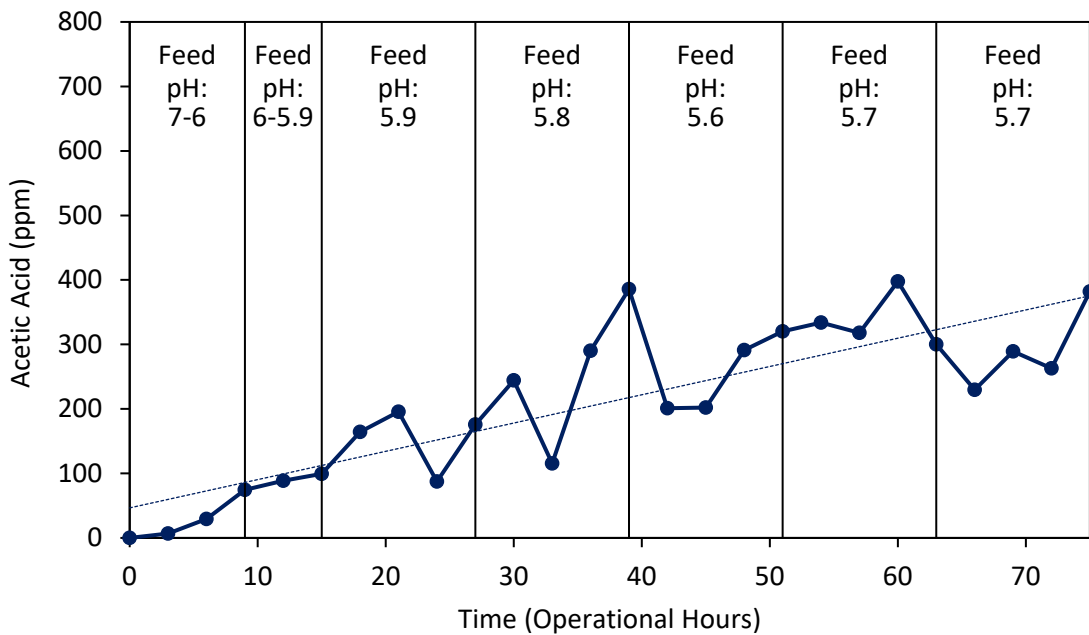


Figure 5-13. Acetic acid content within reflux drum

As such, it is evident that the organic acids entering into the MEG regeneration loop within the brine stream (refer to Table 5-1) were being sufficiently removed through the distillation column and reclamation system to prevent accumulation. As a result, the subsequent corrosion risks associated with organic acid accumulation within the MEG regeneration system [63, 69-73] has been reduced, whilst also achieving improved MDEA and alkalinity removal. Therefore, while complete removal of organic acids is not possible during the switch over from MDEA to FFCI under the proposed methodology, the accumulation of organic acids can be successfully prevented through control of the rich glycol pH to promote organic acid boil-off during the distillation process in combination with partial removal in the reclaimer.

From Figure 5-3, it was estimated that at a rich glycol feed pH to the reboiler of 5.8-6.0 and resulting pH 7 within the reboiler a 12-15% removal of acetic acid could be achieved during each cycle of the MEG regeneration loop. In comparison, during the experiment conducted, a maximum 10-12% removal of acetic acid was achieved within the distillation system over the final 3 days of operation as indicated by Figure 5-14. Overall, approximately 24-26% of the total incoming acetic acid present within the rich MEG was removed in comparison to the produced lean MEG. The remaining acetic acid removed following distillation occurred within the reclamation system (11% slip-stream). Improved organic acid removal may be achieved by targeting a lower rich glycol pH and hence lower pH within the reboiler and reclaimer to push the acetic acid – acetate equilibrium further. However, too low of a pH within the rich glycol tank may pose a corrosion risk to both the storage vessel and downstream carbon steel systems. The target rich glycol pH of 5.8-6.0 used within this study was identified as the minimum achievable pH to prevent corrosion of carbon steel components within the reboiler.

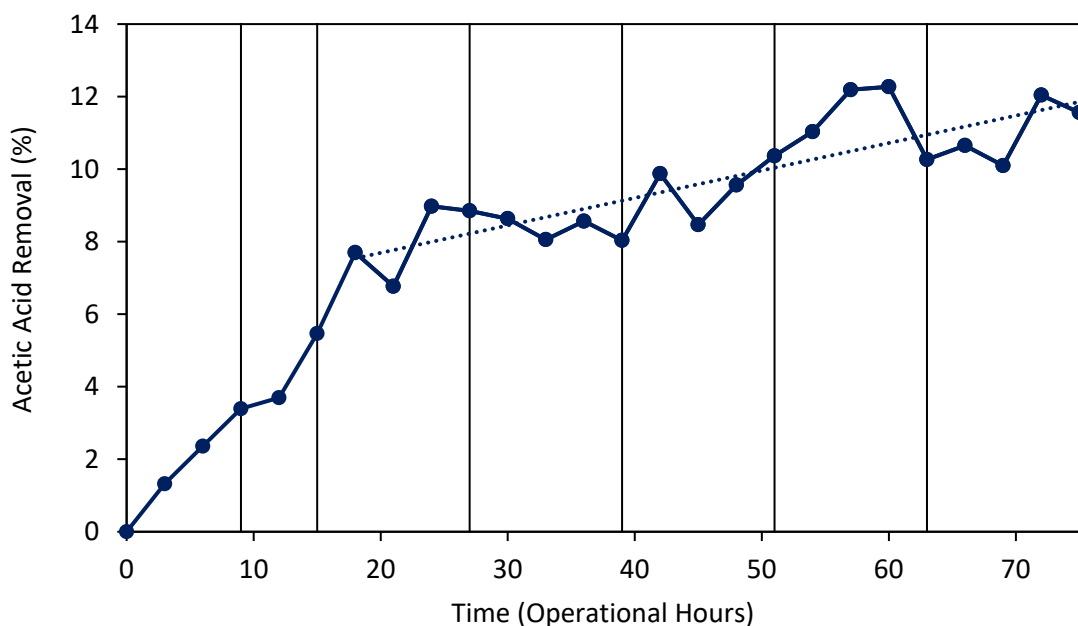


Figure 5-14. Average percentage removal of acetic acid during distillation

5.7.4 Accumulation of Sodium Ions within MEG Regeneration Loop

Under both operational methodologies, significant accumulation of sodium ions occurred within the MEG regeneration loop far greater than that introduced within the brine feed (Figure 5-15). The accumulation of sodium within the MEG regeneration loop occurs primarily due to the sodium hydroxide (NaOH) dosage requirement within the MEG pre-treatment vessel. To ensure sufficient removal of divalent salts including calcium occurs during pre-treatment, a sufficiently high pH was maintained to promote the formation of calcium carbonate that can be subsequently removed. The NaOH dosage requirement was exacerbated due to the low pH of the recycled MEG from the LGT following pH adjustment before the reboiler as well as the presence of protonated MDEA acting as a buffer. As such, it is further beneficial to remove the total alkalinity as quickly as possible to minimise the sodium hydroxide dosing requirement within the pre-treatment system

To ensure sufficient removal of sodium ions during the reclamation process, a greater reclamation slip stream rate would be required. The slip stream rate utilised within this study was fixed at 11% to simulate an industrial MEG regeneration system. However, if a greater reclamation slip-stream percentage was used, the increased reclamation rate would increase operational costs of the facility potentially making the operational scenario analysed within this study economically unfeasible. To determine whether or not an increased reclamation rate is feasible or if dumping and replacing of MEG within the regeneration loop is more favourable a full cost benefit analysis (CAPEX vs OPEX) between the reclaiming capacity and MEG loss is required to make this judgement.

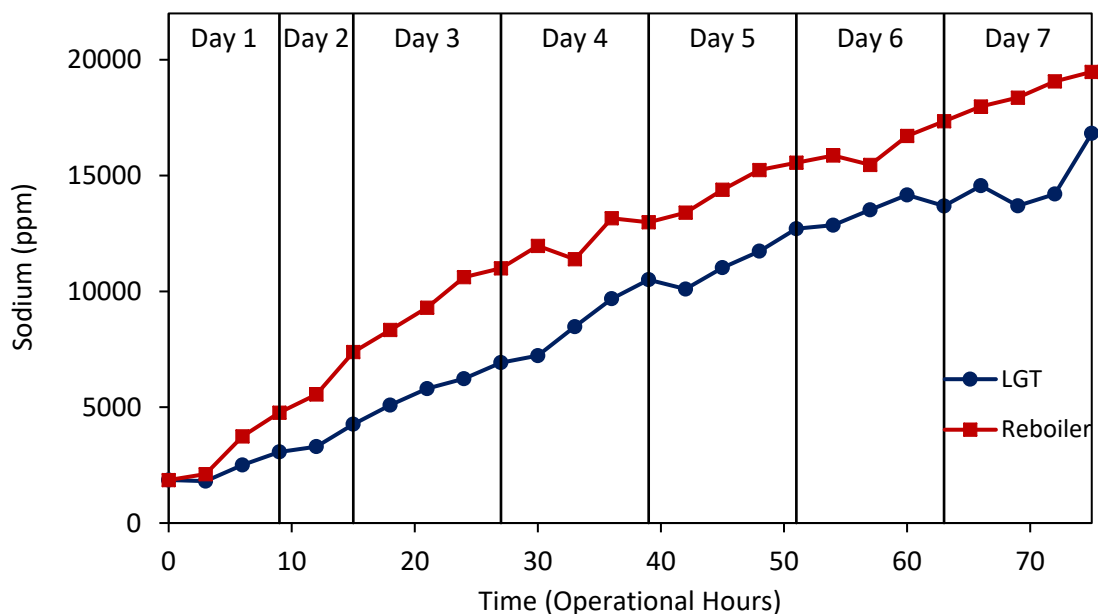


Figure 5-15. Accumulation of sodium within the MEG regeneration loop (modified philosophy)

5.8 Conclusion

A case study was performed to investigate the simultaneous removal of MDEA and hence lean glycol alkalinity alongside organic acids during the MEG regeneration process through adjustment of the pH of the rich glycol feed to the distillation system. Through the testing conducted, it was concluded that simultaneous removal of MDEA during reclamation can be achieved whilst preventing accumulation of organic acids within the MEG regeneration loop. A constant concentration of acetic acid was achieved within the lean glycol product whilst organic acids were introduced into the system through simulated brine by reducing the distillation feed pH to 5.8-6.0 to promote the removal of organic acids together with the water distillate. The prevention of organic acid accumulation within the MEG regeneration system during the switch over process will reduce the associated corrosion risk of excessive organic acid content [17, 63, 69, 70, 72, 73].

Furthermore, removal of MDEA was achieved within the reclamation system at pH 7 producing a lean glycol product of sufficiently low alkalinity to facilitate full switch over to FFCI corrosion inhibition after five regeneration cycles. It was observed that faster removal of alkalinity and MDEA was achieved in comparison to alternative testing conducted using the operational methodology of an external company where by the pH of the produced lean glycol was adjusted step-wise to pH seven by HCl. The proposed switch over process outlined in this study overall lead to reduced NaOH and HCl dosage requirements over the timeframe of the MDEA to FFCI switch over process through faster removal of the MDEA of which was acting as a buffer. The increased rate of MDEA and alkalinity removal can hence reduce the operational expenditure associated with the dosage of acids and bases during the corrosion inhibition switchover.

However, it was observed that an accumulation of sodium ions within the MEG regeneration loop occurred under both operational methodologies as a consequence of the divalent ion pre-treatment process. To achieve removal of divalent ions including calcium introduced through formation water, pH above 8 was required to facilitate their removal through reaction with carbonate. To achieve sufficient pH to facilitate divalent ion removal, sodium hydroxide was dosed within the pre-treatment system but consequently the removal of the additional sodium ions was unable to be achieved at the reclamation slip-stream rate used within this study (11%). A greater slip-stream rate could be used to remove a greater amount of sodium ions preventing its accumulation with the MEG regeneration loop however this was not investigated within this study.

6.0 CORROSION OF CARBON STEEL DURING HIGH TEMPERATURE REGENERATION OF MONO-ETHYLENE GLYCOL IN THE PRESENCE OF METHYLDIETHANOLAMINE

6.1 Introduction

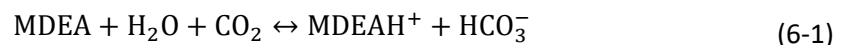
The formation of gas hydrates pose a major risk to the continuous and safe operation of wet gas/condensate pipelines. Gas hydrates form when water molecules surround gas molecules, such as methane, creating a solid material at the low temperatures and high pressures typically encountered in offshore hydrocarbon production flow lines [5, 220]. Under favourable formation conditions, hydrate blockages can occur rapidly, with hydrate plugs potentially taking days or weeks to remove whilst significantly impacting production capabilities and representing a major safety risk for the asset. The injection of Mono-Ethylene Glycol (MEG) is one of the preferred methods of preventing the formation of gas hydrates either during well restart and well testing operations, or in some instances, continuously during gas production [1, 5, 7, 32, 40]. MEG as a thermodynamic hydrate inhibitor (THI) achieves hydrate inhibition through shifting of the hydrate formation temperature below the pipeline operational temperature [1, 2, 4, 7, 9, 113].

In comparison to traditional THIs such as methanol, MEG can be effectively regenerated and reused over multiple regeneration cycles to significantly reducing long term operational costs [1, 4-7]. The regeneration of MEG involves a series of chemical and physical processes to remove excess water, production chemicals and contaminants including salts and organic acids [7, 9, 10, 40, 221]. The primary MEG regeneration process involves the distillation of 'rich MEG', typically between 30-60% wt. MEG, to achieve a final 'lean MEG' product above 80% wt. [1, 7, 9, 12]. To achieve sufficient MEG purity to facilitate reinjection, the MEG regeneration unit (MRU) is typically operated between 120-140°C at atmospheric pressure [1, 37, 38].

Alongside hydrate inhibition, mitigating corrosion is also an important aspect in maintaining continued flow assurance during hydrocarbon transportation and processing. Due to the widespread use of low corrosion resistant carbon steel for pipeline construction owing to its low cost relative to corrosion resistance alloys, the need for effective corrosion mitigation strategies is essential [4, 222]. The prevention of corrosion within carbon steel pipelines where CO₂ represents the primary corrosion risk [7, 17, 95, 223], is often achieved via one of two methods including pH stabilization or the injection of film forming corrosion inhibitors (FFCIs) [2, 4, 7, 9, 116]. Corrosion prevention via pH stabilization is achieved through the injection of basic chemicals including hydroxides, carbonates or amines to artificially increase the pipelines liquid phase pH

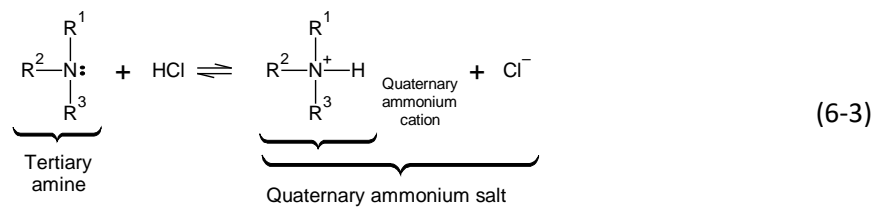
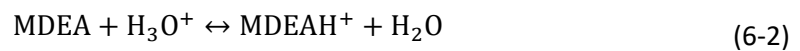
[1, 4, 17, 40]. Corrosion inhibition is achieved through a reduction in the availability of hydrogen ions (the primary corrosive species in CO₂ corrosion [4, 224, 225]) for the cathodic corrosion reaction whilst simultaneously promoting the formation of a protective iron carbonate film on the internal surface of the pipeline [4, 51, 116]. However, the use of pH stabilization is limited to systems where formation water breakthrough and the risk of scaling at high pH has not yet occurred [9, 17, 116]. Under such circumstances, FFCIs are instead used due to the limited impact on system pH [2, 9, 204]. For carbon steel pipelines where FFCIs are utilized, a corrosion rate below 0.1 mm/year is often targeted [4, 222].

Methyldiethanolamine (MDEA), a tertiary amine, has been used as a pH stabilizer to provide effective corrosion control of several large scale natural gas pipelines in Northern Europe and Western Australia [4, 7]. MDEA will react with dissolved carbon dioxide (CO₂) – Equation (6-1), and other corrosive acidic species including hydrogen sulphide and organic acids effectively neutralizing them as they enter the system. The use of MDEA over traditional salt based hydroxides or carbonates for pH stabilization has several advantages including thermal stability over multiple regeneration cycles, the ability to be reclaimed during vacuum reclamation minimizing continuous injection requirements and large buffer capacity [4, 7, 8, 40, 199]. The use of MDEA for pH stabilization however, is often only performed in natural gas systems where the expected CO₂ content in the gas phase will require dosage of salt based pH stabilizers beyond their solubility limits in MEG solutions potentially resulting in scale deposition [19]. Furthermore, the use of MDEA also has several drawbacks including increased MRU heating requirements [7, 9] and being less environmentally friendly compared to salt based pH stabilisers [4].



The introduction of divalent cations including calcium following formation water breakthrough represents a significant scaling risk at the high pH conditions under pH stabilization. If scaling cannot be managed through the injection of scale inhibitors or reallocation of production, it may be beneficial to gradually transition from MDEA pH stabilization to more scale friendly FFCIs to extend the life span of the field [7-9]. The removal of MDEA from the closed loop MEG system can be achieved by neutralizing MDEA to its protonated form MDEAH⁺ (Equation (6-2)) allowing its removal as a non-volatile quaternary ammonium salt from the vacuum reclamation system (Equation (6-3)) [7]. The continued presence of MDEA within the closed loop MEG system represents significant operational costs associated with increase MRU reboiler requirements and additional acid/base dosage due to MDEA's large

buffer capacity ^[7, 9]. As such, the rapid removal of MDEA from the MEG loop is desirable, with the study outlined in the previous chapter analysing the optimal operational conditions for removal of MDEA from a closed loop MEG system using slip-stream vacuum reclamation. Ultimately, it was found that maintaining a low pH (pH ≈ 6) rich MEG feed into the MRU was the optimal condition to remove MDEA during downstream vacuum reclamation whilst also minimizing the accumulation of organic acids within the loop. Furthermore, it may also be beneficial to operate the MRU at near neutral pH (pH = 6-7) to prevent the formation of carbonate scales, particularly FeCO₃, on the reboiler bundle which would otherwise reduce heat transfer efficiency and require frequent cleaning.



However, it is important to consider the potential corrosion effects of operating at moderate to low pH at high temperature in the presence of MDEA/MDEAH⁺ within the MRU. Various components within MRU reboiler systems may be constructed of carbon steel including the reboiler shell, piping systems and the reboiler bundle if corrosion is predicted to be minimal during the design phase. Components manufactured from carbon steel may be susceptible to corrosion under certain conditions, namely low pH. The study conducted by Pojtanabuntoeng [4] found low corrosion rates of carbon steel within 45.6% wt. MEG under simulated pH stabilization using MDEA at 10°C and pHs between 6.5-8.5. However, the effects of temperature can be considered a significant factor influencing corrosion, particularly due to its effect on the speciation of weak acid/base chemicals including MDEA ^[199, 200, 226-228]. Table 6-1 outlines the potential electrochemical reactions relevant to the corrosion of carbon steel in MRUs using MDEA ^[229, 230]. Protonated MDEA has been found to be a strong oxidizer and one of the primary contributors to the cathodic corrosion reaction in CO₂ capture systems utilizing MDEA ^[4, 229, 230]. Likewise, carbonic acid and bicarbonate may be present through the reaction of MDEA and dissolved CO₂ (Equation (6-1)) contributing to the corrosion of carbon steel ^[230]. In contrast, the oxidation of carbon steel by oxygen can be considered negligible within MRUs due to the low solubility of oxygen in MEG at high temperature ^[41, 231].

Table 6-1. Electrochemical corrosion reactions with MEG/Water/MDEA systems

Cathodic (Reduction) Reactions:		$E^0(V)$	
Hydronium	$2\text{H}_3\text{O}^+ + 2\text{e}^- \rightarrow 2\text{H}_2\text{O} + \text{H}_2$	0	(6-4)
Water	$2\text{H}_2\text{O} + 2\text{e}^- \rightarrow 2\text{OH}^- + \text{H}_2$	-0.83	(6-5)
MDEAH ⁺	$2\text{MDEAH}^+ + 2\text{e}^- \rightarrow 2\text{MDEA} + \text{H}_2$		(6-6)
Carbonic Acid	$2\text{H}_2\text{CO}_3 + 2\text{e}^- \rightarrow 2\text{HCO}_3^- + \text{H}_2$		(6-7)
Bicarbonate	$2\text{HCO}_3^- + 2\text{e}^- \rightarrow 2\text{CO}_3^{2-} + \text{H}_2$		(6-8)
Oxygen (pH <7)	$\text{O}_2 + 4\text{H}^+ + 4\text{e}^- \rightarrow 2\text{H}_2\text{O}$	+1.23	(6-9)
Oxygen (pH >7)	$2\text{H}_2\text{O} + \text{O}_2 + 4\text{e}^- \rightarrow 4\text{OH}^-$	+0.40	(6-10)
Anodic (Oxidation) Reactions		$E^0(V)$	
Iron	$\text{Fe} \rightarrow \text{Fe}^{2+} + 2\text{e}^-$	0.44	(6-11)

The potential switchover from MDEA pH stabilization to FFCIs following formation water breakthrough represents a potentially innovative method to extend natural gas field life spans where MDEA is utilized [7]. However, potential methods to gradually remove MDEA from closed loop MEG systems raise several possible issues including unfavourable operating conditions for poor corrosion resistance materials due to the low pH required to dissociate MDEA. As such, the corrosion rate of carbon steel within CO₂ free lean MEG solutions containing MDEA under regeneration conditions has been evaluated. Corrosion rates were measured using a combination of weight loss measurements and Linear Polarization Resistance (LPR) at varying pH_{25°C} and temperatures to study the effect of MDEA on corrosion. The results of this study have significant implications for industrial MEG regeneration systems operating using MDEA due to the potential corrosion of operationally critical equipment. The potential corrosion of the MEG distillation reboiler system may have significant impacts on tolerable operating conditions or if severe corrosion occurs, long term production capabilities.

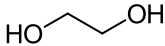
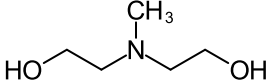
6.2 Experimental Methodology

6.2.1 Materials, Chemicals and Solution Preparation

Experimental solutions were produced using technical grade MEG sourced from Chem Supply and MDEA from Sigma Aldrich with the respective chemical purities and structures outlined by Table 6-2. Corrosion evaluation was performed within 80% wt. MEG solutions, representing a typical industrial lean MEG composition [1, 7, 9, 12, 36]. A MDEA concentration of

500mM was utilized to represent a potential concentration of MDEA within the lean glycol product to provide effective corrosion control of a gas/condensate pipeline operating under pH stabilization with a high CO₂ gas phase content [4, 7]. Within this study however, no dissolved CO₂ was present within the test solutions to ensure that the initially prepared solution pH remained constant during corrosion testing. Due to the reduced solubility of CO₂ with respect to increasing temperature, dissolved CO₂ is boiled off during the MEG regeneration process generating a pH increase across the MRU [7, 221]. As such, the prepared lean glycol solutions in this study represent regenerated lean MEG post CO₂ boil-off with pH measured after cooling. Furthermore, the reduction of carbonate species (Equations 6-6 and 6-7) may contribute to the electrochemical corrosion of carbon steel [4, 232, 233], the presence of dissolved CO₂ was further avoided to allow the effect of solely MDEA on corrosion to be determined.

Table 6-2. Chemical purity and structures

Compound	CAS	Purity (wt. %)	Chemical Structure
MEG	107-21-1	>99.5%	
MDEA	105-59-9	>99%	

6.2.2 Experimental Procedure

6.2.2.1 Experimental Apparatus and Test Conditions

Experimental testing was conducted using a stainless-steel autoclave as depicted Figure 6-1 to allow for corrosion measurement under high temperature conditions. Temperature was maintained within the system by an external electrical heating band connected to a temperature controller with an error of ± 0.1 °C. To prevent boiling of the solutions at high temperature and subsequent solution loss, the system was maintained at 6 bara pressure using high purity nitrogen controlled by an Alicat gas mass flow controller (± 0.01 bar). High purity nitrogen was utilized to prevent oxygen ingress into the system that would otherwise increase the cathodic corrosion reaction and cause thermal degradation of the MEG resulting in a reduction in solution pH [5, 12, 41]. Carbon steel coupons (AISI 1030 / UNS G10300 grade) were submerged in the solution and the resultant mass loss measured over a period of three days. Additional testing was also conducted using the same methodology for stainless steel 316L coupons to further investigate the corrosive behaviour of MDEA on more corrosion resistant metals.

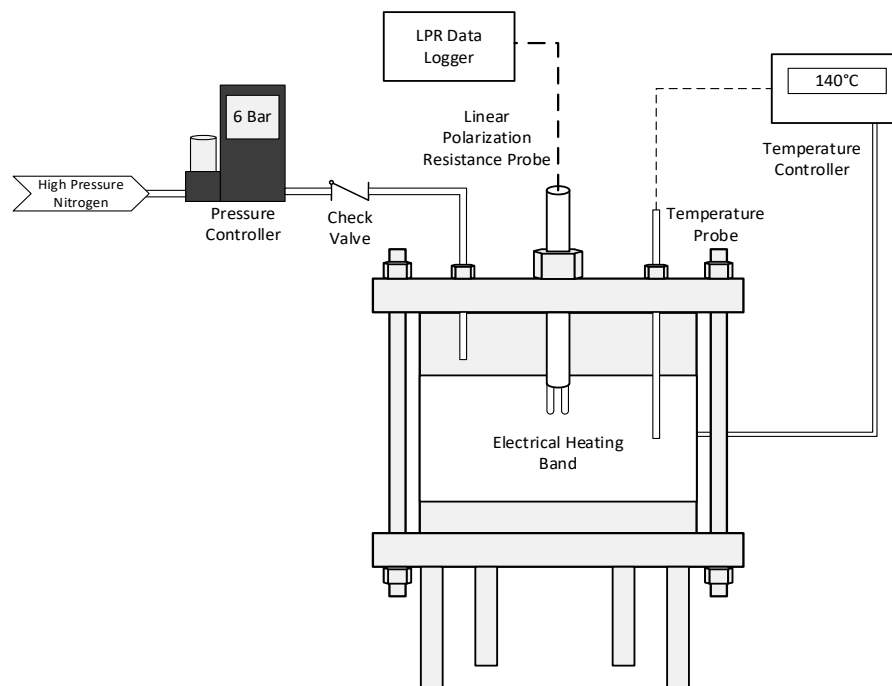


Figure 6-1. Experimental autoclave apparatus for corrosion testing

The corrosion rate of carbon steel in the presence of MDEA was evaluated within lean glycol solutions initially at 25°C and heated to 30, 80, 140 and 180°C. The high temperature conditions (140 and 180°C) were selected based on the temperature required during the regeneration of MEG with 500mM MDEA ^[7] and a potential reboiler skin temperature required to achieve 140°C within the reboiler liquid phase. Additional testing was also performed at 30 and 80°C to further highlight the effect of temperature on MDEA speciation and resulting corrosion. Testing was conducted in lean glycol pHs prepared at 25°C ranging from pH 6 to 11 to cover the wide range of potential operating pHs found within industrial MEG regeneration systems ^[221]. 37 vol. % hydrochloric acid was used to neutralize MDEA and adjust solution pH.

6.2.2.2 Corrosion Measurement

The measurement of carbon steel corrosion rates was performed using a combination of carbon steel coupon mass loss and LPR measurements. LPR measurements were performed using industrial grade Cosasco 7012-0-0 carbon steel LPR probes designed for monitoring corrosion of pipelines under harsh conditions including high temperature and pressure. LPR monitoring is an electrochemical method that measures the current required to maintain a specific potential between two electrodes from which the corrosion rate can be derived using the Stern-Geary equation ^[234]. The LPR probes were calibrated for measurement of corrosion rates in MEG through comparison to corresponding coupon mass loss measurements ^[4]. Secondary LPR probe corrosion measurements were also made through mass loss measurements of the LPR probe's carbon steel tips submerged in the test solutions for additional comparison.

6.2.2.3 pH Measurement

Due to the error associated with measuring the pH of MEG solutions, the correction factor developed by Sandengen [11] was applied.

6.3 Results and Discussion

6.3.1 Speciation of MDEA at Varying Temperature

The speciation of weak acid and bases including MDEA is dependent on multiple factors including temperature, ionic strength and the dielectric constant (ϵ) of the solvent [127-130, 199]. Several studies have been conducted to measure the change in the dissociation constant (pK_a) of MDEA with respect to temperature in water [199, 200, 226-228] and MEG solutions [199]. The change of MDEA pK_a with respect to temperature within 80% wt. MEG is illustrated by Figure 6-2A from 25-80°C from the reported data in Chapter 8 and extrapolated to 180°C with the resulting shift in MDEA speciation illustrated by Figure 6-2B. It is clear, that with increasing temperature a significant shift in MDEA pK_a can be expected favouring the undissociated form of MDEA. As a result, with increasing temperature an increase in hydrogen ions will be available for reduction at the metal surfaces within the reboiler unit as the MDEA-MDEAH⁺ equilibrium shifts.

At the reboiler-fluid interface the skin temperature of the reboiler bundle maybe significantly hotter than the bulk fluid temperature (potentially up to 180°C). The greater temperature at the interface will ultimately cause a greater conversion of MDEAH⁺ to MDEA, resulting in a greater hydrogen ion concentration localized at the interface. As a result, the localized corrosion rate at the reboiler bundle surface will be exacerbated potentially leading to rapid failure of the bundle if constructed of carbon steel.

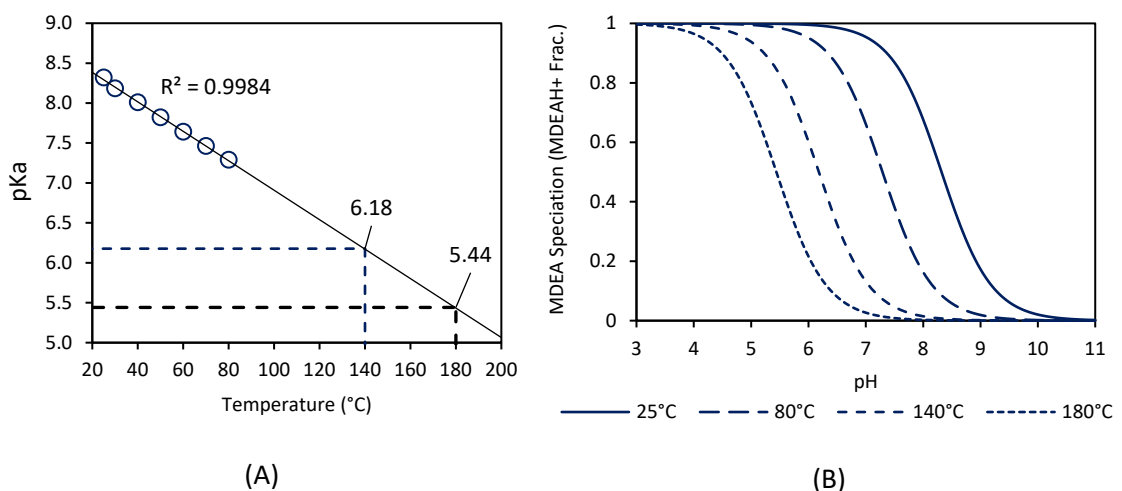


Figure 6-2 A) Effect of temperature on MDEA dissociation constant within 80% wt. MEG solution (Soames [199] – Chapter 8) and B) Speciation of MDEA in 80% wt. MEG at varying temperature

6.3.2 Effect of MDEA on Corrosion at Regeneration Temperature (140°C)

To verify the potential corrosion at high temperature arising from the behaviour of MDEA, the corrosion of carbon steel was evaluated at 140°C within varying pH_{25°C} lean glycol solutions containing 500mM MDEA and corresponding solutions without. Figure 6-3 illustrates the corrosion rate determined by the average weight loss of three carbon steel coupons over a period of three days. The transition from 25°C to 140°C ultimately lead to a more corrosive lean glycol solution due to the shift in MDEA speciation and overall exacerbated the rate of carbon steel corrosion. Most interestingly, notable corrosion was also observed within lean glycol solutions containing MDEA within the high pH region (pH > 10) where corrosion would typically not be expected. As such, carbon steel corrosion may not just be limited to MEG loops undergoing transition to FFCIs, but also under pH stabilization operation whilst MDEA is present.

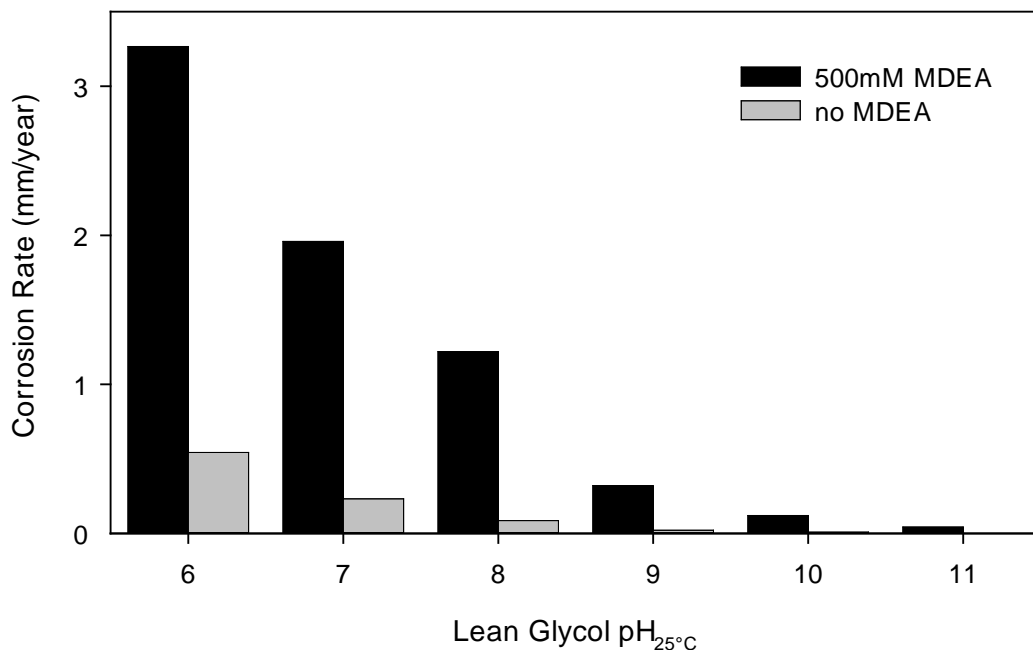


Figure 6-3. Effect of MDEA on corrosion at varying initial lean glycol pH_{25°C} and 140°C

6.3.3 Effect of Temperature and Initial Lean Glycol pH_{25°C} on Corrosion

Figure 6-4 illustrates the dual effect of initial lean glycol pH at 25°C and temperature on the corrosion rate of carbon steel using coupon weight loss measurements. It is highly evident that within increased temperature, the rate of corrosion of carbon steel is increased significantly likely as a result of the effect of temperature on MDEA speciation behaviour. Even moderate initial lean glycol pH conditions (pH_{25°C} 7- 9) in combination with the high temperature during regeneration will ultimately pose a significant corrosion risk to reboiler components manufactured from carbon steel. To verify the corrosion rates derived from weight loss coupons, LPR measurements were conducted in 30 minute intervals over a period of three days. Figure 6-5 compares the corrosion rates measured at 140°C by coupon weight loss measurements, averaged stabilized LPR measurements and the weight loss of the carbon steel LPR probe tips.

Good agreement between all three corrosion measurement methods was observed at the temperature conditions tested within this study, further confirming the strong tendency of carbon steel to undergo corrosion at high temperatures in the presence of MDEA. In contrast, corresponding testing performed using stainless steel 316L showed effectively no corrosion with a corrosion rate of 0.004 mm/year and no pitting observed under the worst case conditions tested ($\text{pH}_{25^\circ\text{C}} = 6$ and 180°C).

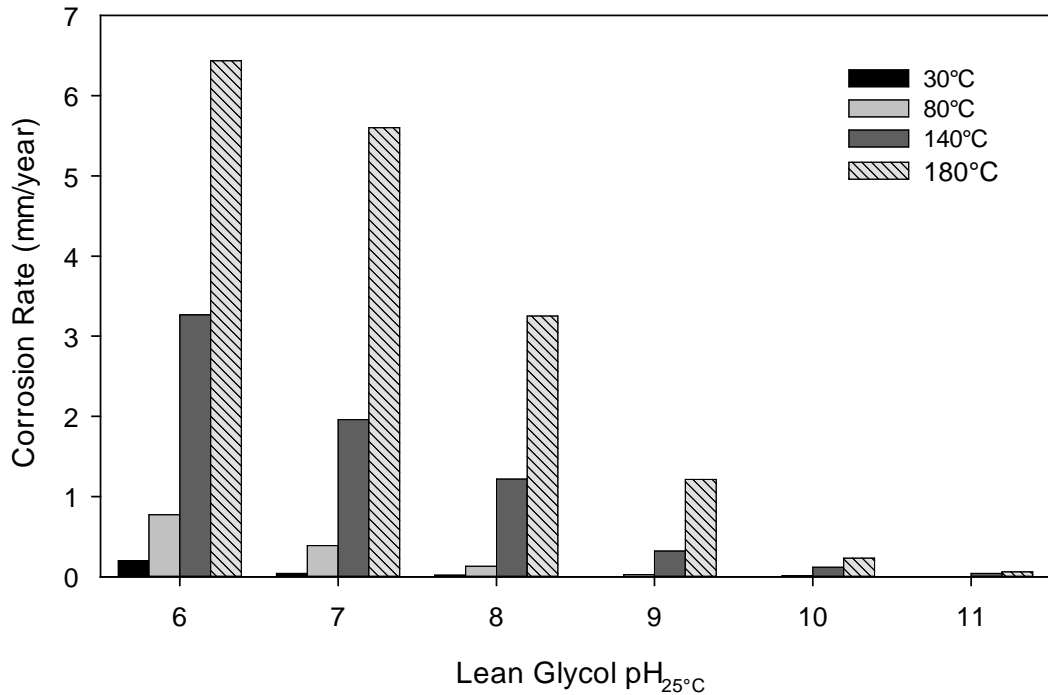


Figure 6-4. Corrosion rate of carbon steel at varying $\text{pH}_{25^\circ\text{C}}$ and temperature

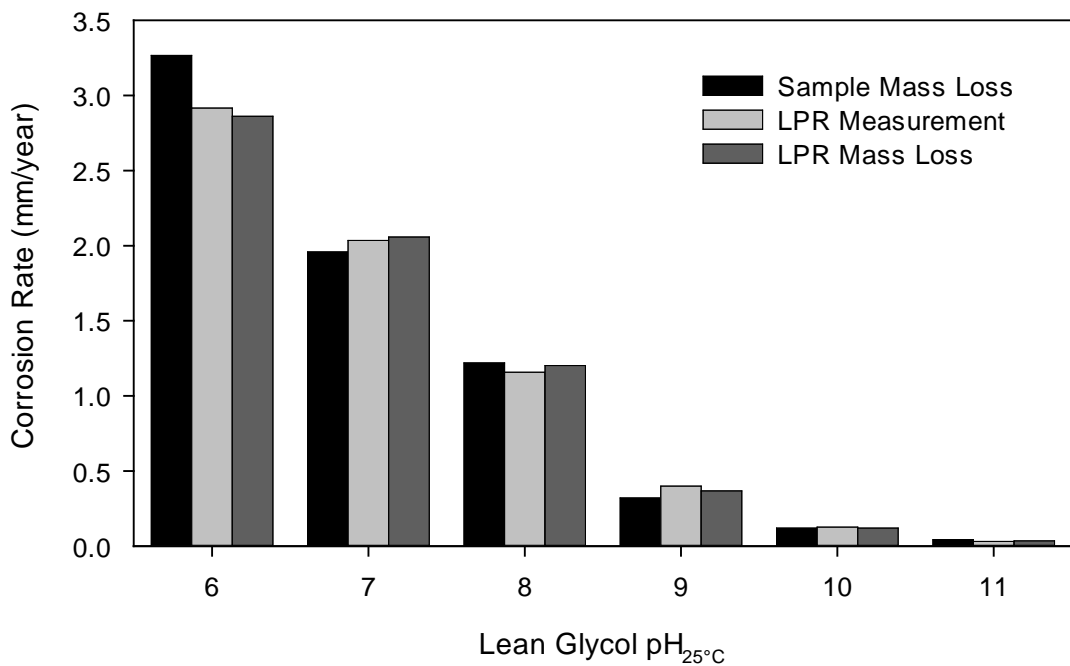


Figure 6-5. Comparison of corrosion measurement techniques at 140°C

6.3.4 Pilot Scale Distillation Corrosion Testing

To verify the experimental corrosion rates generated using the autoclave corrosion cell, larger scale testing was conducted using a pilot MEG regeneration column. The pilot distillation column forms part of a larger MEG regeneration loop utilized in various previous MEG related studies [1, 7, 12] with the distillation columns design discussed by Zaboony [1]. Corrosion rates were measured by submerging an LPR probe adjacent to the reboiler bundle operating with a liquid phase set-point temperature of 140°C. Figure 6-6 compares the corrosion rates generated using the distillation column and autoclave testing with a slightly higher corrosion rate measured within the pilot distillation column. The increased rate of corrosion compared to autoclave testing can be attributed to the dynamic conditions within the reboiler leading to increased circulation and reduced build-up of corrosion products on the LPR probe tips and corrosion proceeds. Furthermore, Figure 6-7 shows the evolution of hydrogen from the carbon steel LPR probe tips within pH_{25°C} 7, 140°C lean MEG solution during operation visually demonstrating a high rate of corrosion.

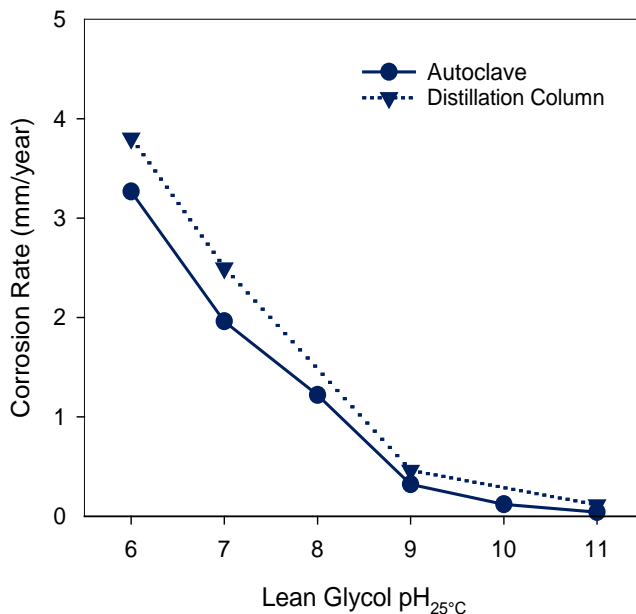


Figure 6-6. Comparison of autoclave vs. distillation column corrosion measurements (140°C – LPR measurement)



Figure 6-7. Corrosion of LPR probe during regeneration (pH_{25°C} = 7, 140°C)

6.3.5 Process Fouling Concerns due to Corrosion

If unaccounted for, the high concentration of Fe²⁺ formed through the corrosion of the carbon steel reboiler components may have several operational issues for the reboiler itself and downstream systems. Latta [10] provides an extensive review of the effect of various MEG

process contaminants including Fe^{2+} on individual MEG regeneration systems with Figure 6-8 summarizing the primary effects on the MRU. The primary risk associated with excessive Fe^{2+} content primarily involves the deposition of FeCO_3 on process heat exchangers including rich glycol preheaters and the MRU reboiler bundle potential leading to reduced heat transfer efficiency [1, 10]. The high reboiler skin temperatures significantly increase the kinetics of Fe^{2+} precipitation to FeCO_3 resulting in high fouling potential of the reboiler bundle [8-10]. Furthermore, if low fouling resistant trays are utilized within the MEG regeneration tower, solids created within the reboiler recirculation loop may foul trays below the feed entry point [10]. In the presence of oxygen, Fe^{2+} may also form iron oxide particles leading to further fouling issues and potential blockage of MEG injection nozzles [8, 19].

Figure 6-9 illustrates the total Fe^{2+} concentration produced following corrosion testing at varying initial lean glycol $\text{pH}_{25^\circ\text{C}}$ levels for testing conducted at 140°C . The total Fe^{2+} concentration was measured via spectroscopy by first acidifying the samples to dissolve any precipitated iron particles. As expected due to the high rates of corrosion experienced, the corrosion of carbon steel reboiler components due to MDEA may ultimately produce Fe^{2+} concentrations far beyond what is tolerable in closed loop MEG systems. Figure 6-10 depicts the final lean glycol solution saturated with solid particles after three days of corrosion at $\text{pH}_{25^\circ\text{C}}$ 7 and 140°C .

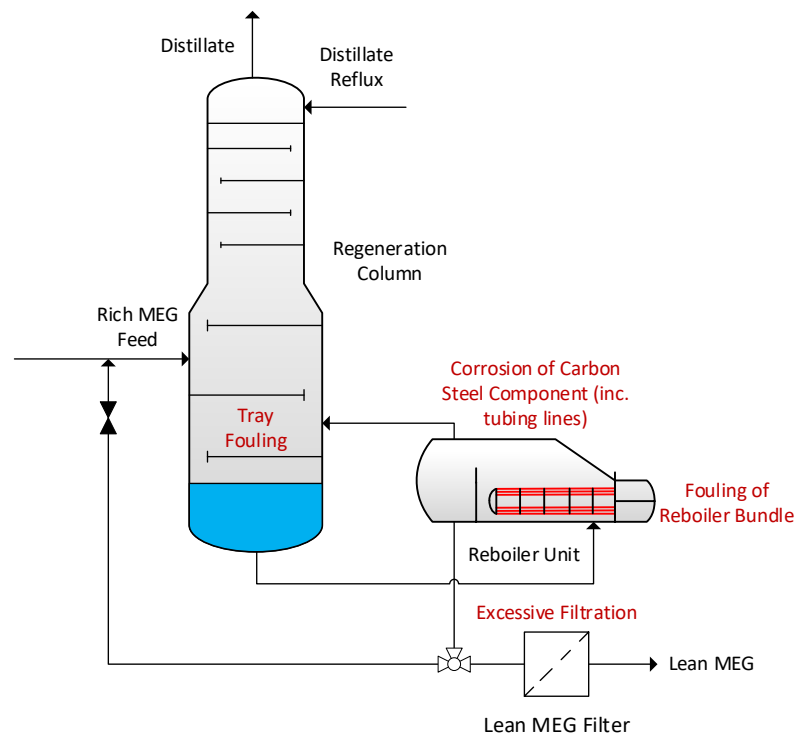


Figure 6-8. Potential impact of MDEA corrosion and excessive iron particles on MEG regeneration unit

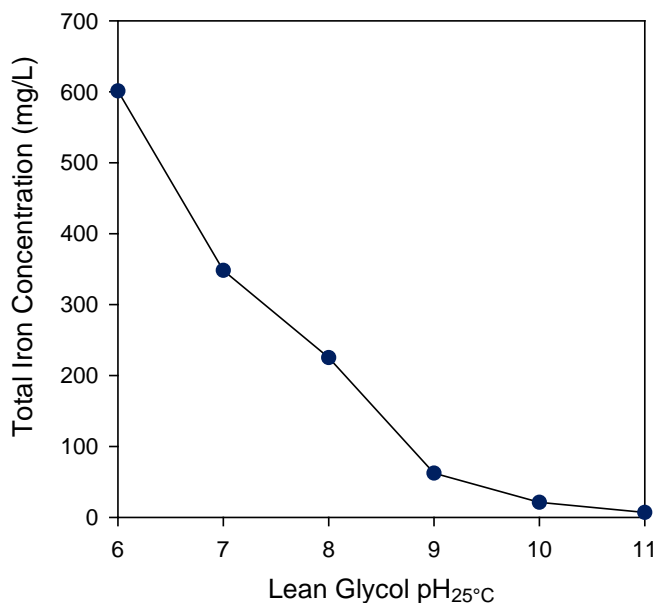


Figure 6-9. Fe²⁺ concentration after 3-days of corrosion (140°C)



Figure 6-10. Final solution after 3-days of corrosion (pH_{25°C} = 7, 140°C)

6.3.6 Application of Corrosion Inhibitors during High Temperature Regeneration

Following formation water breakthrough the presence of divalent cations will pose a scaling risk at the high pH conditions maintained under pH stabilization. Likewise, during well clean-up operations back production of drilling and completion fluids will also pose a risk of scale formation [4, 5, 32, 220]. Under both scenarios the use of FFCIs to provide corrosion protection is preferred due to the reduced scaling risk [5, 220]. However, the transition between corrosion protection using pH stabilization via MDEA to FFCIs post formation water breakthrough is problematic and time consuming [7]. Removal of MDEA can be achieved via vacuum reclamation systems by maintaining a low lean glycol pH which simultaneously alleviates the downstream scaling risk [7, 8, 221]. If MDEA is to be removed from the MEG loop, FFCIs will be injected into the lean MEG to provide continued corrosion inhibition of the primary pipeline [5, 220]. As a result, the presence of FFCIs within the MEG loop may provide some level of unintended corrosion protection inside the MRU as they are often designed to be thermally stable at regeneration conditions [2].

The review of FFCI application in oil and gas pipelines by Askari [222] outlines the most common types of film forming chemicals and the general mechanism by which they facilitate corrosion protection. It is often the case that the performance of corrosion inhibitors decrease with increasing temperature [222, 235-238]. As such the high temperature conditions within the MRU

will likely reduce the efficacy of any FFCIs injected upstream limiting their potential benefit. To evaluate the potential corrosion protection generated by FFCIs during MEG regeneration, three commercially available FFCIs outlined by Table 6-3 were tested from 30 to 180°C at $\text{pH}_{25^\circ\text{C}} 7$. Figure 6-11 illustrates the corrosion rates measured in the presence of the respective FFCIs compared to baseline testing with no CI present. Under low temperature conditions ($\leq 80^\circ\text{C}$) each FFCI successfully reduced the corrosion rates to below 0.1 mm/yr. However, the corrosion rates measured under high temperature regeneration conditions at 140 and 180°C continued to exceed tolerable corrosion rates. Figure 6-12 illustrates the corrosion inhibition efficiencies (%) of the respective FFCIs indicating that the maximum inhibition efficiency of each FFCI was reached at 140°C with no further decline at higher temperatures.

Table 6-3. FFCIs evaluated at high temperature regeneration conditions

FFCI	Type	Primary CI components
1	Amine	Polyamines
2	Amine	Amine derivatives
3	Quaternary ammonium salt	Benzyltrimethyldecylammonium chloride
		Benzylquinolinium Chloride 2-Mercaptoethanol

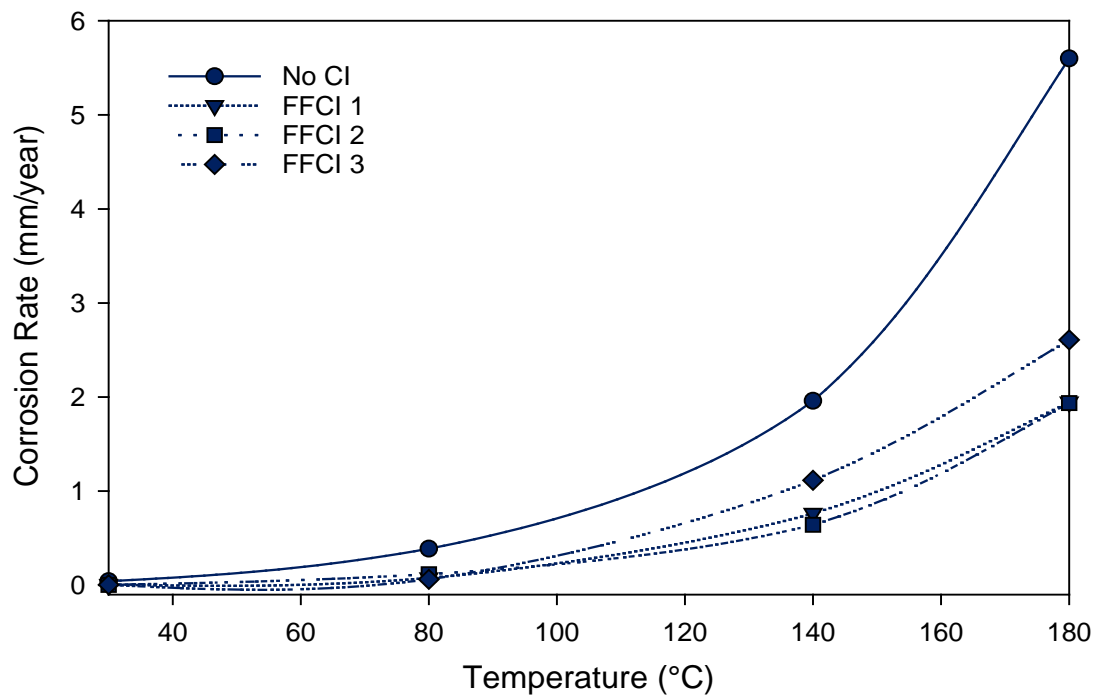


Figure 6-11. Corrosion rates of carbon steel under high temperature conditions with FFCIs present ($\text{pH}_{25^\circ\text{C}} 7$)

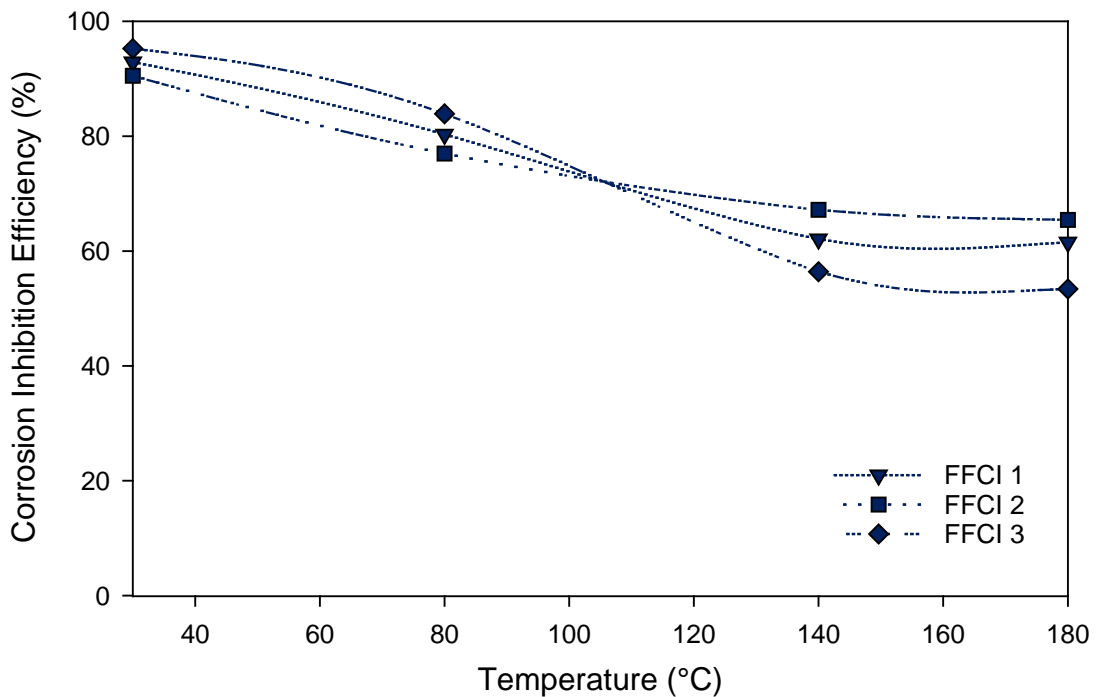


Figure 6-12. Corrosion inhibition efficiencies of FFCIs under high temperature conditions ($\text{pH}_{25^\circ\text{C}} 7$)

6.4 Conclusion

MDEA may be utilized as a pH stabilizer in natural gas pipelines if the expected gas phase CO_2 content would otherwise require traditional salt based pH stabilizers to be dosed beyond their solubility limits in MEG. Various previous studies have suggested that the protonated form of MDEA may induce corrosion of carbon steel through contribution to the cathodic corrosion reaction [4, 229, 230, 239]. However the results of this study indicate that significant corrosion of carbon steel may instead occur through the effect of temperature on MDEA dissociation behaviour [199, 200, 226-228]. The dissociation constant of MDEA is inversely proportional to temperature and will hence lead to the deprotonation of MDEAH^+ as temperature increases. The subsequent release of hydrogen ions will ultimately increase the risk of corrosion through the cathodic reduction of hydrogen at metal surfaces. In particular, the surface of reboiler bundle tubing is especially susceptible to this form of corrosion if manufactured from carbon steel. The skin temperature of the tubing bundle will be hotter compared to the bulk liquid phase and will hence result in a greater concentration of hydrogen ions localized at the liquid-metal interface.

The transition from an initial temperature of 25°C to MEG regeneration temperatures ultimately led to a significant increase in measured carbon steel corrosion rates with the greatest rates of corrosion expectedly found at the lower initial $\text{pH}_{25^\circ\text{C}}$ values. For initial lean glycol $\text{pH}_{25^\circ\text{C}}$

of 9 and below, carbon steel corrosion rates in excess of 1 mm/year were observed at $\geq 140^{\circ}\text{C}$ with a corrosion rate of 6.4 mm/year measured under the worst case conditions tested ($\text{pH}_{25^{\circ}\text{C}} = 6$ and 180°C). In contrast, stainless steel 316L was found to be resistant to the low pH conditions generated during MEG regeneration in the presence of MDEA with a corrosion rate of 0.004 mm/year measured under similar worst-case conditions and with no pitting observed. As such, it is highly evident that carbon steel components are the most susceptible to the potentially corrosive conditions generated by MDEA during the high temperature regeneration of MEG and should be avoided if practicable.

FFCIs may be injected upstream into the natural gas pipeline to provide continued corrosion inhibition if MDEA is to be removed from the closed loop MEG system. As such, the presence of FFCIs within the MEG loop may provide some level of unintended corrosion protection inside the MRU. To account for this, various commercially available FFCIs were evaluated and were found to reduce the rate of carbon steel corrosion at all temperatures tested. However, at 140 and 180°C , the corrosion rate of carbon steel remained above tolerable limits. Overall, if process conditions during the MEG regeneration process are not carefully considered and controlled, MDEA may pose a significant unintended corrosion risk to reboiler components constructed from carbon steel in MEG loops utilizing MDEA for pH stabilization.

7.0 EFFECT OF WETTABILITY ON PARTICLE SETTLEMENT BEHAVIOUR WITHIN MONO-ETHYLENE GLYCOL REGENERATION PRE-TREATMENT SYSTEMS

7.1 Introduction

Mono-Ethylene Glycol (MEG) is widely used as a thermodynamic hydrate inhibitor to prevent the formation of gas hydrates within natural gas transportation pipelines [1, 4, 6, 7, 9, 32, 40, 199]. Due to the large dosage requirement to ensure sufficient hydrate control and cost of inhibitor dosage, the regeneration and reuse of MEG is essential to minimise operational costs [1, 2, 4-6]. The industrial regeneration of MEG entails a variety of chemical and physical processes to remove contaminants such as process chemicals, mineral salts and organic acids as well as the reconcentration of the MEG by removal of excess water [1, 2, 7, 9]. In particular, following the breakthrough of formation water, the removal of divalent cations including calcium and magnesium is important to prevent the formation of scale within downstream equipment operating at high temperature including the regeneration column [4, 32, 74, 205, 218, 240].

If a slip-stream reclamation system is utilised for salt control, the removal of divalent cations including calcium, iron and magnesium is typically performed during pre-treatment (Figure 7-1) [7, 8] by reaction within carbonate or hydroxide to form divalent salts that subsequently precipitate out under moderate to high temperatures ($\geq 80^{\circ}\text{C}$ [10, 12, 53, 240, 241]). The precipitated solids can then be removed within downstream filtration systems [10]. Likewise, the removal of pipeline corrosion products such as iron carbonate (FeCO_3) as well as other solid particles present with the reservoir fluids including sand may be required [10]. Downstream of the pre-treatment system, the treated rich glycol is subsequently stored within the rich glycol tank of which may act as a settlement tank for particles not removed by initial filtration. If considerable levels of solid particulates are present or poor settlement occurs within the rich glycol tank, excessive strain may be placed on downstream filtrations systems requiring frequent replacement of filters.

Based upon analysis of one of the largest MEG regeneration systems operating in Western Australia, quartz and FeCO_3 have been identified as problematic particles that often fail to completely settle resulting in excessive filter replacement. The exposure of the particles to condensate (typically $\text{C}_6\text{-C}_{20}$) and associated organic compounds (long-chain fatty acids/carboxylics) has been suggested as a possible reason for reduced settlement rate within the rich glycol tank. Furthermore, the use of surfactant based corrosion inhibitors may also produce oil-wetted particles in order to repel water and hence reduce corrosion [242]. Following exposure to condensate or corrosion inhibitors, the surface properties of the particles are

altered potentially reducing their settlement within MEG-water systems. The behaviour of oil-wetted quartz and FeCO_3 has hence been analysed within MEG solution in terms of settlement, particle attraction (Zeta potential) as well as the behaviour of the particles at MEG-vapour interface. Furthermore, modification of surface properties has been studied through application of surfactants to improve particle settlement.

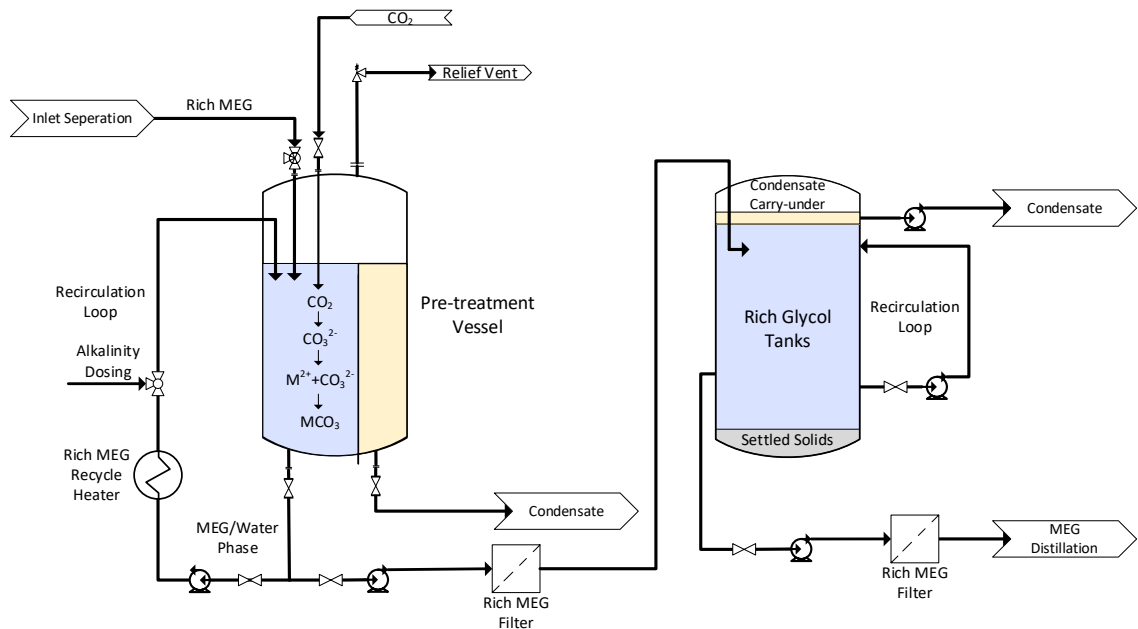


Figure 7-1. Curtin Corrosion Centre's rich MEG pre-treatment and settlement systems

7.2 Wettability of Solid Particles

The 'wettability' of a solid surface is a measure of the affinity of a liquid to a solid surface in the presence of another fluid (vapour of liquid) dictating the liquids ability to spread on the solid surface ^[142, 243]. In the presence of hydrocarbons and water, a particle may vary from strongly 'water-wetted' to strongly 'oil-wetted' with the degree of wettability providing a measure of a particles hydrophilicity or hydrophobicity ^[143, 144]. Within solid/water/oil systems, the surfaces of metal oxides and other naturally occurring inorganic materials are typically completely wetted by water ^[176]. However, some metal oxides such as barite (BaSO_4) and hematite (Fe_2O_3) can also be wetted by oil indicating partial or intermediate wettability ^[176, 244]. The modification of a particles wettability influences the particles behaviour and interactions within liquid films and at liquid interfaces. The wettability of solid particles is a key parameter influencing solid-liquid separation as well as other applications including oil agglomeration and dust abatement ^[149, 183]. The wettability of a particle or surface is influenced by numerous factors including particle shape, size, surface chemistry and roughness ^[178, 179, 183, 184, 245], temperature ^[246-252], pressure ^[143, 169] and the presence of ionic species such as sodium, magnesium and sulphate ^[168, 170, 186, 187].

The wettability of a solid particle plays an important role in the particle agglomeration process necessary for settlement to be achieved ^[145, 146]. If insufficient wetting of the particles is present, poor adhesion between the particles may result ^[146]. Furthermore, the wetted state of a particle may also influence its settlement behaviour. The process of film flotation is used to separate water-wet (hydrophilic) and oil-wet particles (hydrophobic) whereby particles are introduced at the water-air interface, as a result, the water-wet particles sink and oil-wet particles float ^[149]. Particles are submerged into the wetting liquid only when the critical wetting surface tension of the particle is equal or greater than the surface tension of the liquid ^[141]. Furthermore, the wettability of particles plays an important role in the formation of oil-water emulsions due to their behaviour at oil-water interfaces ^[139]. Particles that are strongly wetted by water tend to have poor stability at the oil-water interface, with the opposite true for oil-wetted particles ^[139]. Oil-wetted particles have a tendency to adsorb to the oil-water interface improving emulsion stability through reduced contact area between the two fluids ^[139, 140].

7.2.1 Wettability in Oil and Gas Reservoirs and Pipelines

Typically, carbonate surfaces within oil reservoirs are neutral to oil-wet due to the adsorption of carboxylic components onto the carbonate surface ^[185, 253]. The conversion of calcite surfaces from water-wet to oil-wet in the presence of fatty organic compounds (such as stearic acid) has been conclusively demonstrated whereby such compounds will adsorb onto the surface of calcite ^[143, 168-170, 254]. Likewise, the adsorption of polar organic compounds present in crude oils has been identified as the mechanism for why carbonate oil reservoirs exhibit oil-wet characteristics ^[168, 195, 255]. Organic compounds containing negatively charged carboxyl groups (COO^-) are the most strongly adsorbed oil components onto calcium carbonate surfaces ^[172, 194]. Carboxylate molecules present within crude oil have a tendency to adsorb onto the positive sites of the calcite surface at low pH ^[168, 256]. At low pH (<8-9 ^[171, 172]) the surface of calcite becomes positively charged due to the presence of calcium ions whereas at higher pH the increased concentration of CO_3^{2-} produces a negatively charged calcite surface ^[171, 173]. The presence of calcium ions at the calcite surface provides a point for which chemisorption of the carboxylic molecules can occur replacing surface hydroxyls (formed by surface hydration by water) ^[256]. Ultimately, the adsorbed acids confer a hydrophobic characteristic to the calcite surface resulting in poor wettability in water. Due to the similar nature of FeCO_3 and CaCO_3 , the lessons learned regarding calcite wettability behaviour and modification can be applied directly to FeCO_3 .

The exposure of initially water-wet carbonates, quartz and shale surfaces to oil-based drilling fluids has also been shown to alter the wettability of the solid surface to oil-wet ^[156, 176, 257-260]. The wettability of solid particles has been demonstrated to influence their dispersion

(and hence agglomeration) within liquid phases, specifically drilling muds ^[259, 261]. For drilling mud applications, weighting agents (such as calcium carbonate) are added to increase liquid phase density and in most cases are made oil-wet via wetting agents to prevent particle agglomeration and settling ^[189, 259]. The exposure of solid particles including FeCO_3 and quartz (potentially already oil-wet from the reservoir) to oil-wetting compounds within hydrocarbon transportation pipelines including condensate and residual drilling mud fluids may ultimately lead to settlement problems downstream.

7.3 Chemicals and Particle Modification Procedure

Quartz particles (50-70 mesh particle size) and technical grade FeCO_3 particles ($\geq 99\%$ wt.) were sourced from Sigma Aldrich and City Chemical respectively. To produce particles of sizes relevant to industrial MEG regeneration systems, particle size analysis was performed on rich MEG samples taken downstream of an industrial MEG regeneration system rich MEG storage tank (refer to Figure 7-2). Quartz and FeCO_3 particles were crushed and subsequently passed through a set of 63 μm , 32 μm and 10 μm particle sieves to produce two particle size ranges of interest (10-32 μm and 32-63 μm).

To evaluate the influence of particle wetted state on particle settlement, particles were wetted by oil in order to render them hydrophobic. This was achieved by submerging the respective particles in a solution of 0.01 M stearic acid (Chem Supply, $\geq 99.5\%$ wt.) in decane (Sigma Aldrich, $\geq 99\%$ wt.) for 2 hours at 50°C ^[254, 262-264]. Oil-wetted particles were then separated from the liquid phase by centrifuge and the recovered particles dried for one day at 75°C. For testing purposes, an artificial condensate produced by ExxonMobil referred to as IsoPar M was utilised. The artificial condensate primarily contains C11-C16 hydrocarbons and was selected due to its close representation to the condensate produced in the field of interest.

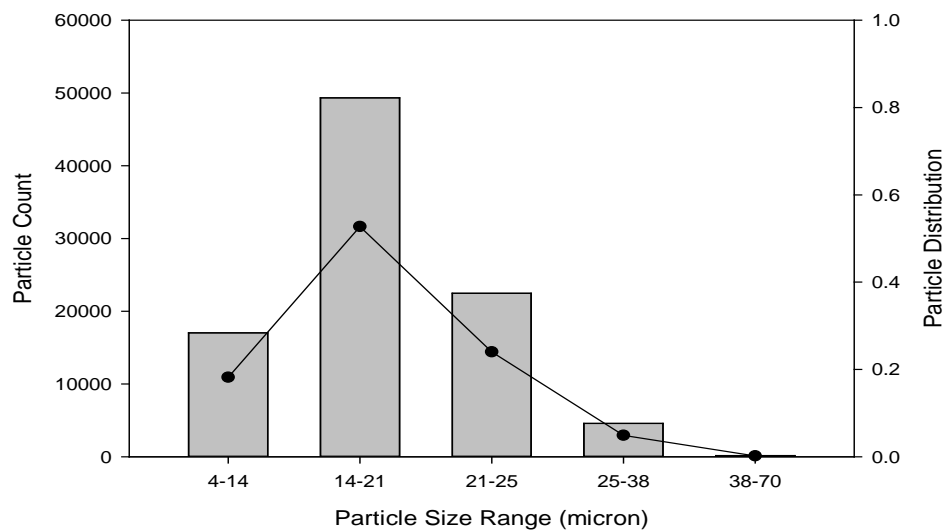


Figure 7-2. Particle size analysis of field rich MEG samples

7.4 Results and Discussion

7.4.1 Behaviour of Particles at MEG-Vapour and MEG-Condensate Interface

To better understand the behaviour of oil-wetted particles and how they distribute within MEG systems, their behaviour at MEG-vapour and MEG-condensate interfaces was analysed. Condensate present within the pre-treatment system maybe inadvertently carried under alongside the MEG phase within the rich glycol tank. Condensate entering into the rich glycol tank will ultimately form a distinct layer above the MEG phase due to the inherent difference in solution density (Figure 7-1). Unmodified (hydrophilic) and oil-wetted (hydrophobic) particles were introduced above the MEG-vapour and condensate-vapour interfaces and allowed to settle. Both quartz and FeCO_3 hydrophilic particles were observed to easily transition through the MEG/vapour interface completely settling with minimal issue. In contrast, the hydrophobic particles of sizes ranging from 10-32, 32-63, 63-100 and 200-300 μm were unable to break the surface of the 50% wt. MEG (Appendix C – Figure C1). Once settled at the MEG/vapour interface, the oil-wetted particles demonstrated strong hydrophobic attraction accumulating into large particle build-ups (Appendix C – Figure C2).

Where condensate was present as a distinct layer above the MEG phase, both water-wetted and oil-wetted particles failed to transition through into the MEG phase (Appendix C – Figure C3). Interestingly, both water and oil wetted particles tended to accumulate into larger particle formations, likely in order to minimise surface contact with the opposing water/oil phase for oil-wetted/water-wetted particles respectively. A significant visual difference between water-wetted and oil-wetted FeCO_3 was also observed within the condensate phase. The condensate is unable to wet the surface of the water-wetted particles resulting in a 'dry' appearance compared to the oil-wetted particles. Overall, if adequate removal methods such as skimming pumps are not in place, the long term accumulation of particles at the vapour/liquid interface may pose significant problems for industrial MEG regeneration systems including interference with liquid level and other measurement sensors.

7.4.2 Settlement of Particles within Rich Glycol Systems

Poor settlement of suspended particles within processing systems can have notable impact on downstream operations, or if filtration systems are in place, increase the need for frequent filter replacement. As such, it is important to optimise the particle settlement process during the design phase or if problems arise during operation, removal of the factors that cause poor settlement. Due to the increased viscosity of MEG solutions (2.906 mPa.s, 50% wt. 20°C) compared to water systems (1.0016 mPa.s, 20°C), reduced particle settlement is expected. However, due to the limited ability to influence particle size through polymeric flocculants owing to unideal behaviour at the high temperatures experienced during downstream regeneration

including foaming, identification and rectification of other factors leading to poor settlement beyond particle size is important. The effect of a particles wetted state has hence been investigated to identify the implications on particle settlement within MEG systems and identification of potential solutions to improve settlement.

XRD analysis of field samples obtained from filter systems located downstream of a rich MEG system identified quartz, cinnabar/metacinnbar and FeCO_3 as the primary crystalline components. As such, the settlement behaviour of water/MEG-wetted and oil-wetted quartz and FeCO_3 has been investigated within 50% wt. MEG solution representing a typical rich MEG composition. To investigate the particle settlement behaviour, the respective particles were initial suspended in 50% wt. MEG solution and injected horizontally into a vertical chamber filled with the 50% wt. MEG solution.

The resulting settlement behaviour of water/MEG-wetted and oil-wetted FeCO_3 (10-32 μm) is illustrated by Figure 7-3 and Figure 7-4 respectively, with the water/MEG-wetted FeCO_3 demonstrating efficient settlement. In contrast, oil-wetted FeCO_3 demonstrated a continuous tendency to float to the vapour-liquid interface with significant accumulation at the interface occurring due to hydrophobic interaction of the particles to each other^[156, 164-167]. Furthermore, a portion of the oil-wetted FeCO_3 particles effectively remained suspended in the solution at the injection level of which would ultimately pass through with the eluent causing excessive filtration requirements. Overall, oil-wetted FeCO_3 particles between 10-63 μm demonstrated a strong tendency to float and accumulate at the interface with oil-wetted particles above 63 μm successfully settling (Appendix C – Figure C4). This result is particularly troublesome for MEG systems where particle sizes are often significantly below 63 μm (Figure 7-2).

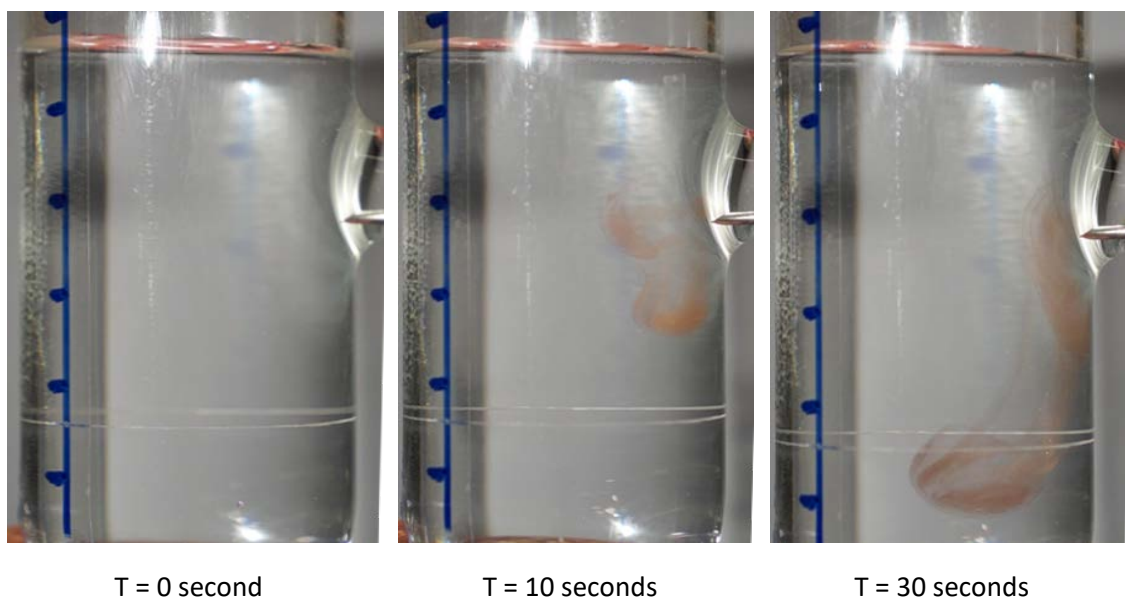


Figure 7-3. Settlement of water/MEG-wetted FeCO_3 (10-32 μm) in 50% wt. MEG solution

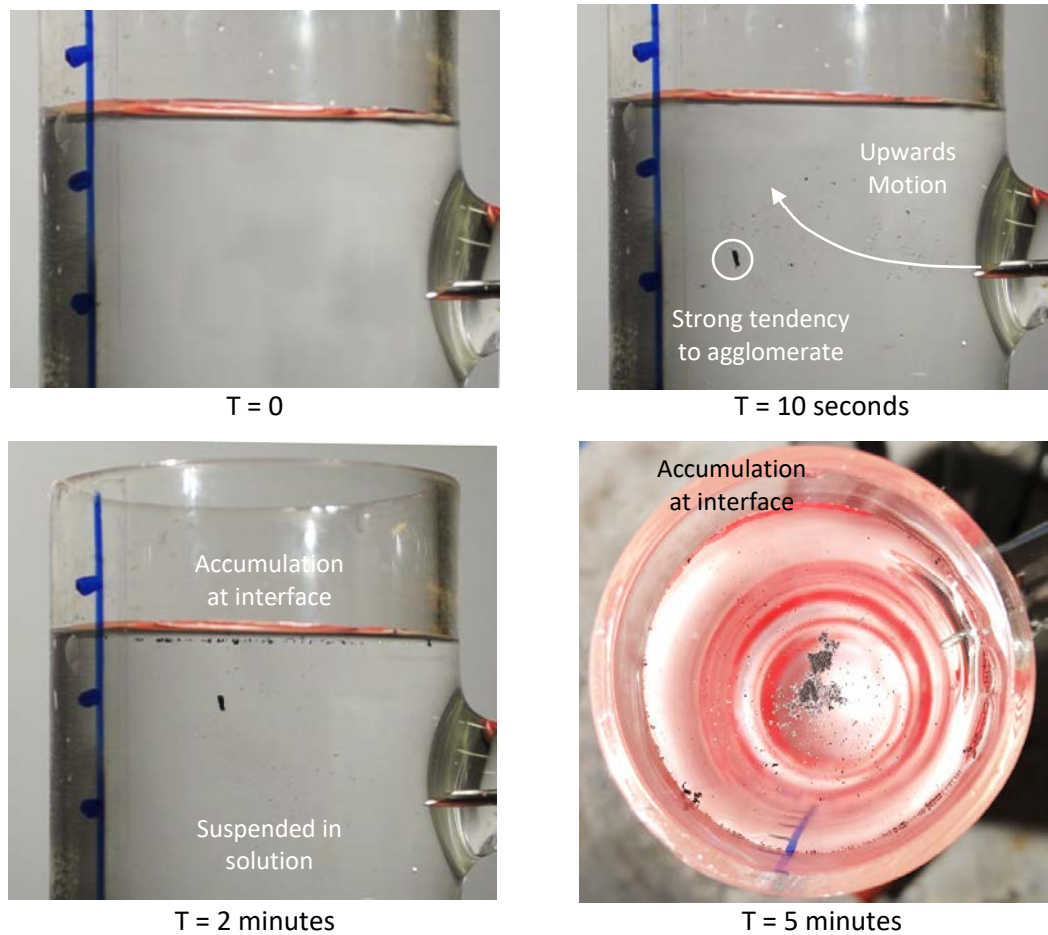


Figure 7-4. Settlement of oil-wetted FeCO_3 (10-32 μm) in 50% wt. MEG solution

The settlement behaviour of 10-32 μm quartz is illustrated in Figure 7-5 showing a general trend to settle within the 50% wt. MEG solution. However, due to the difference in density between quartz ($\approx 2.6 \text{ g/cm}^3$) and FeCO_3 ($\approx 3.9 \text{ g/cm}^3$) low particle size quartz 10-32 μm demonstrated poor settlement regardless of wetted state, often taking upwards of an hour for water/MEG-wetted quartz to achieve full settlement. In a similar manner to FeCO_3 , the settlement behaviour of quartz particles between 10-32 μm was observed to be negatively influenced following the oil-wetting process with oil-wetted particles tending to transition towards the vapour-liquid interface (Figure 7-6). Oil-wetted 32-63 μm quartz particle primarily settled at a reduced rate compared to corresponding water/MEG-wetted particles with only a minor portion (<10%) floating or remaining suspended after 5 minutes (Appendix C – Figure C5). Overall, the behaviour of quartz appeared to be less influenced by the effects of oil-wetting suggesting the adsorption of condensate and carboxylics to the quartz surface occurs to a lesser extent compared to FeCO_3 . This is likely due to the presence of positive iron ions at the particle surface providing sites for chemisorption of the stearic acid molecules to occur.

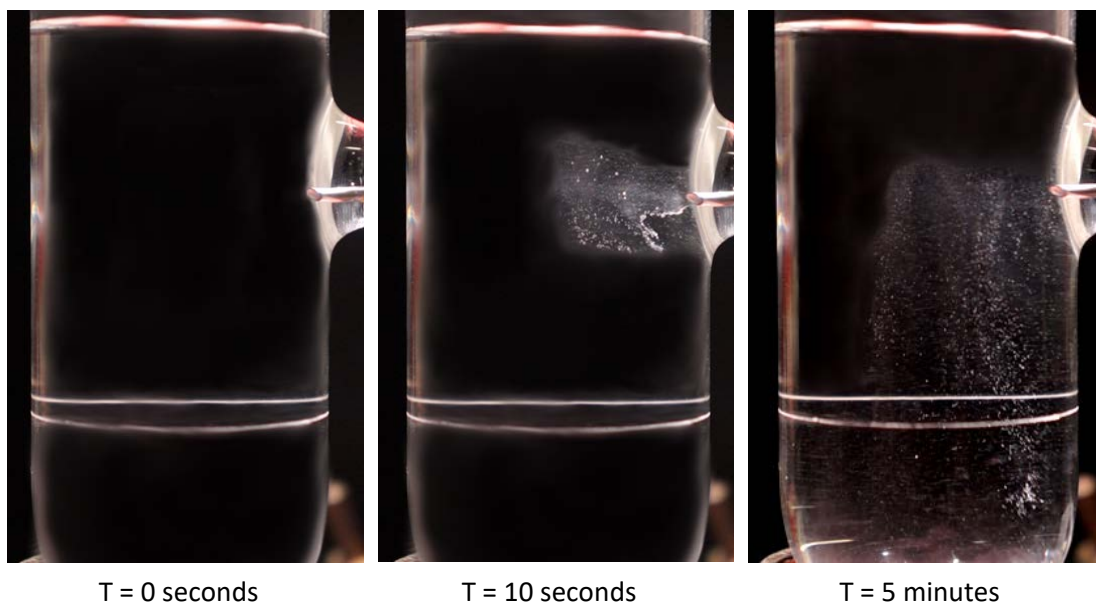


Figure 7-5. Settlement of water/MEG-wetted quartz (10-32 μm) in 50% wt. MEG solution

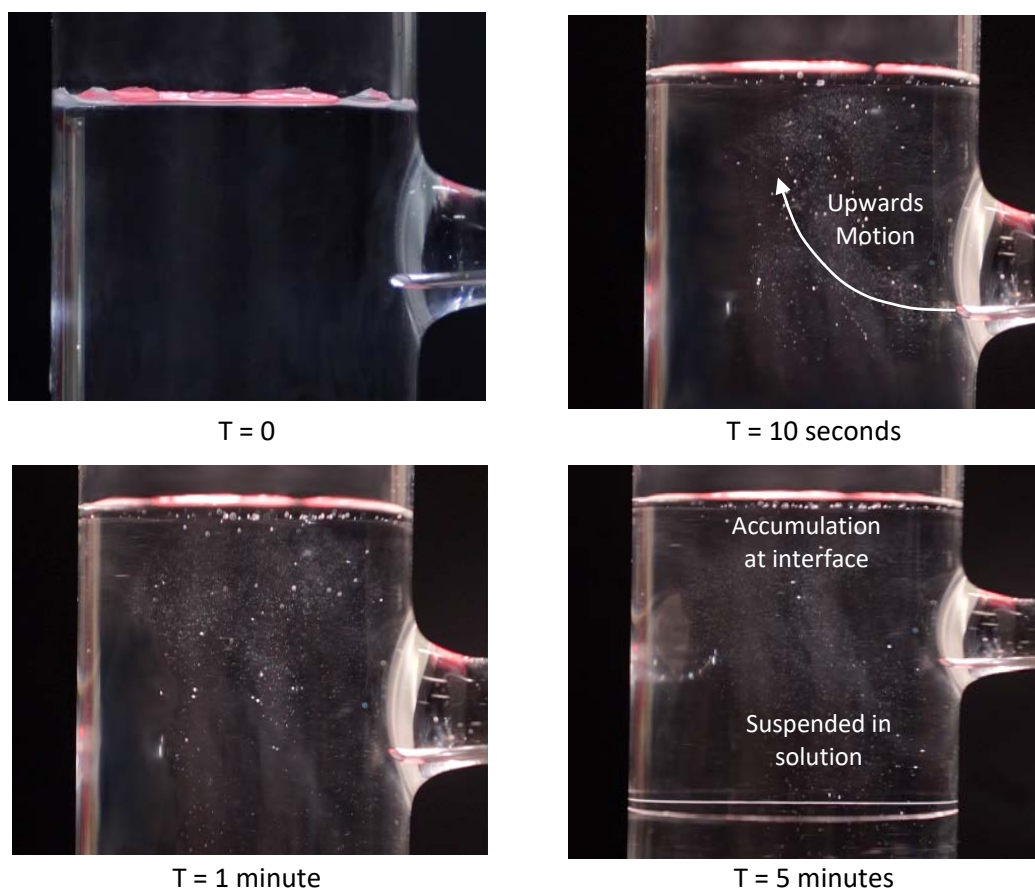


Figure 7-6. Settlement of oil-wetted quartz (10-32 μm) in 50% wt. MEG solution

7.4.3 Selection of Suitable Surfactants through Zeta Potential Measurement

The zeta potential of a solid particle is often used as a measure of the particles charge due to its relation to both surface charge and the electrical double layer surrounding the particle [154, 159, 265]. Zeta potential has also been routinely applied as a measure of a solid suspension's stability with lower absolute zeta potential indicative of particle agglomeration and increased

settlement^[159]. As the absolute zeta potential decreases towards the isoelectric point (IEP), the electrostatic repulsion between similarly charged particles is diminished resulting in greater relative attraction by van der Waals forces according to DLVO theory^[152, 158, 159]. The surface charge of a particle and hence zeta potential is also an important parameter in selecting a suitably charged ionic polymer surfactants^[266]. The zeta potential of a particle and hence its effective surface charge has been shown extensively to be dependent upon both solution pH and the presence of ionic species^[154, 159, 251, 256], factors highly variable in industrial MEG systems.

Measurement of zeta potential within this study was performed using a dynamic light scattering (DLS), Zetasizer Nano ZS (Malvern Instruments). The zeta potential of quartz and FeCO₃ within 50% MEG solution at varying pH is presented in Figure 7-7 showing a general trend towards negative surface charge at higher pH. The increasingly negative surface charge of both particles within the pH range of interest to MEG systems suggests that a cationic surfactant such as cetyltrimethylammonium bromide (CTAB) is best suited for neutralizing particle surface charge. The adsorption of oil-wetting agents (stearic acid) to the surface of both particles ultimately influenced the measured zeta potentials with the greatest variation occurring in the higher pH regions once the respective particle zeta potential transitioned to negative. The results are in line with the findings of Kasha [267] who reported similar behaviour when comparing aged calcite exposed to stearic acid in decane compared to pure calcite. Likewise, the effect of ionic species at concentrations measured within two industrial MEG regeneration systems (Appendix C – Table C-1) was evaluated. The presence of ionic species at reported concentrations had the expected effect of reducing the absolute zeta potential^[154, 159, 251, 256], but to within a range where cationic surfactants are still suitable.

Furthermore, to generate a better understanding of how both anionic and cationic surfactants influence particle behaviour in terms of particle attraction, the zeta potential of FeCO₃ and quartz was measured at pH 9 with varying surfactant concentrations (Figure 7-8). The cationic surfactant CTAB, had the greatest influence on particle zeta potential resulting in a shift to a positively charged surface, a result in line with Foss [268]. The shift to a positive zeta potential can be attributed to the adsorption of CTAB molecules to the surface of the particle, or to within the particles electrical double layer^[159, 269, 270]. The work of Bi [269] suggests that CTAB will directly adsorb to the initially negatively charged particle surface through electrostatic attraction, neutralising the particles surface charge. However, at sufficiently high concentrations CTAB will continue to form a double layer through hydrophobic attraction between the chains of adsorbed surfactant molecules in the initial monolayer and free monomers^[159, 269, 270]. The resultant double layer leaves the positively charged head of the CTAB molecule exposed producing a positive surface charge with more hydrophilic characteristics^[159, 269]. In contrast

sodium dodecyl sulphate (SDS), an anionic surfactant showed minimal effect on the initially negatively charged particle surface instead remaining constant in the case of quartz and transitioning through the IEP of FeCO_3 . The use of SDS may be beneficial in the settlement of FeCO_3 due to the dominance of van der Waals attraction relative to electrostatic repulsive forces allowing greater particle agglomeration [158, 159, 178, 266].

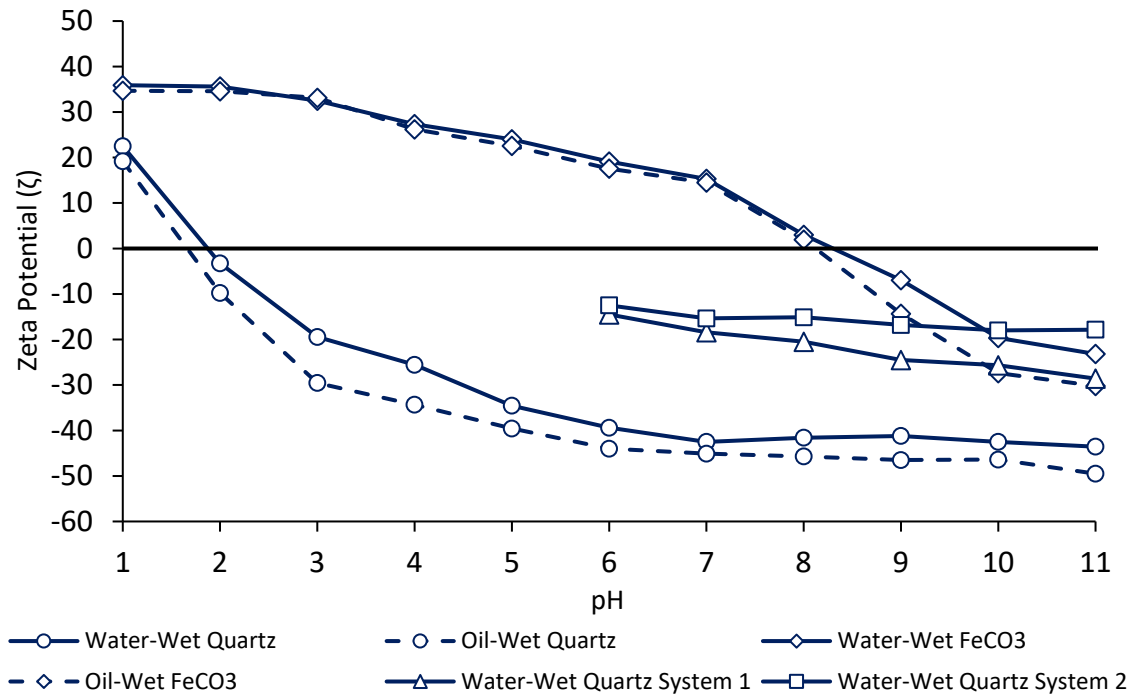


Figure 7-7. Zeta potential of quartz and FeCO_3 within 50% wt. MEG solution

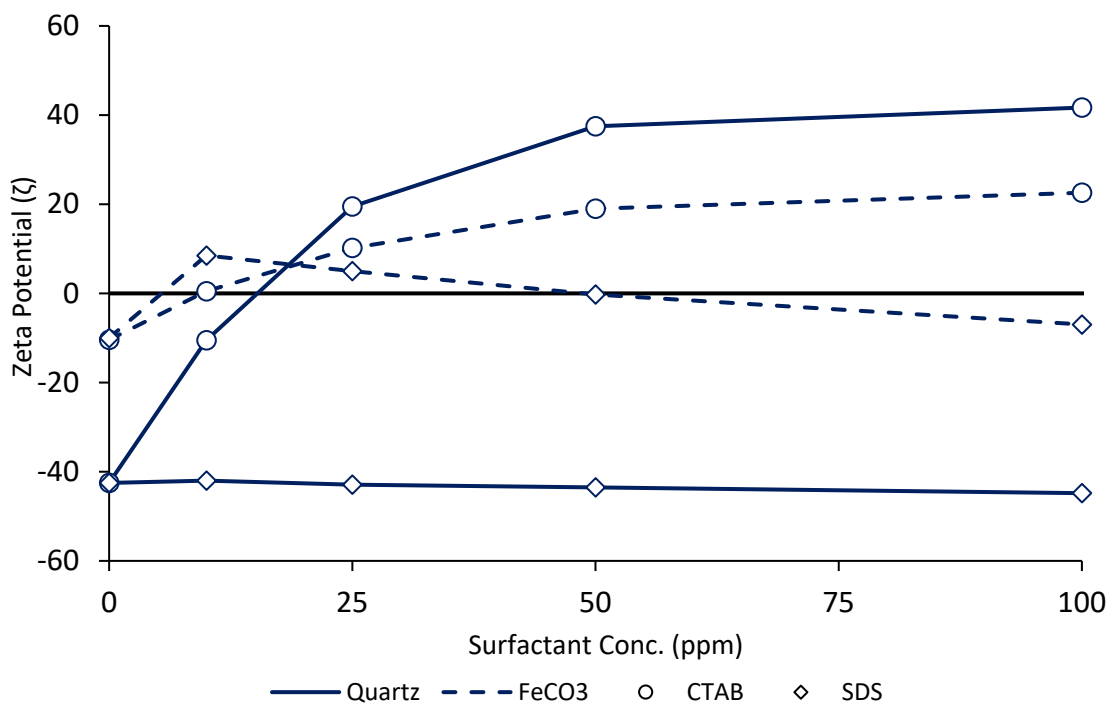


Figure 7-8. Effect of CTAB and SDS on particle Zeta potential (pH 9)

7.4.4 Application of Surfactants to Modify Particle Surface Properties

The study of Standnes and Austad [271] concluded that $R - N^+(CH_3)_3$ cationic surfactants including CTAB were capable of desorbing negatively charged carboxylics contained in crude oil irreversible from solid surfaces through formation of ion pairs [272, 273]. The cationic head group of the CTAB molecule potentially forms ion-pairs with the negatively charge carboxylic acid group through electrostatic attraction, ultimately leading to their desorption from the solid surface and hence an increase in water-wetness [272-274]. Al-Anssari [159] also suggest that the positively charged head of the CTAB molecule may adsorb directly to negatively charged particles leading to the protrusion of the hydrophobic tail into the solution. Through hydrophobic interaction of the tails, neighbouring CTAB coated particles will ultimately agglomerate facilitating a great level of settlement [275, 276]. In contrast, non-ionic and anionic surfactants instead modify solid surfaces from oil-wet to water-wet through adsorption of the surfactants onto the solid surface forming a more water-wettable layer [274]. Anionic surfactants such as SDS have been shown to adsorb onto solid surfaces through hydrophobic interaction between the tail of the surfactant and adsorbed carboxylics thus increasing water-wettability through exposure of the hydrophilic head into the solution [273, 274].

To improve the settlement of oil-wetted particles entering into the rich glycol storage system, two surfactants were evaluated for their ability to transition the particles from oil-wetted to water-wetted. Firstly, CTAB, a cationic surfactant, was selected due to the negative surface charge of both quartz and $FeCO_3$ at the pH levels of interest to MEG pre-treatment systems (typically pH 8 and above, refer to Figure 7-7) and potential to induce particle aggregation [159, 275]. For comparison purposes, the anionic surfactant SDS was also selected due to its proven capability to transition a variety of surfaces from oil-wet to water-wet [159, 274]. The effectiveness of surfactant treatment was evaluated using a graduated cylinder submerged within a water bath at 80°C to replicate temperature conditions with industrial MEG pre-treatment systems [9, 10, 12]. Initially oil-wet particles were introduced at the liquid-vapour interface of 50% MEG solution containing the respective surfactant with the solution then mixed using a high-powered mixer at 1000 rpm for 10 minutes to rigorously expose the particles to the surfactant solution. Based on the settlement behaviour of water/MEG-wetted and oil-wetted particles demonstrated by Figures 3-6, particles observed to completely settle were considered successfully modified by the surfactant and now water/MEG-wetted, whilst those returning to the interface considered to be unaffected. Particles that were found to remain suspended within the solution were considered to undergo a partial removal of the oil-wetted layer.

Figure 7-9 illustrates the particle modification efficiency of CTAB up to 100 ppm concentration for both $FeCO_3$ and quartz. Each experiment was repeated three times and the

average result with error bars representing the standard deviation of all three experiments presented. The percentage of particle settlement was determined by independently weighing the particles remaining at the surface, suspended in solution and those settled at the bottom of the cylinder after a period of 30 minutes. CTAB demonstrated a strong ability to increase particle settlement by transitioning the initially oil-wetted particles to either fully water/MEG-wetted or partially water/MEG-wetted thus aiding in settlement behaviour. From the experimental results, FeCO_3 appeared to be more susceptible to the effects of CTAB in comparison to quartz. The behaviour of the particles coupled with the physical appearance of the post-surfactant treatment particles suggests that the CTAB molecule has effectively desorbed the oil-wetting agents from the surface of the particle. The desorption of the oil-wetting agents by CTAB produced a particle in similar physical appear to the unmodified FeCO_3 particles (Figure 7-3 compared to Figure 7-4) whilst also resulting in minimal particle size change as illustrated by Figure 7-11. This behaviour is in line with the studies of Hou [272], Standnes and Austad [194] and Jarrahan [273] who suggested that cationic surfactants like CTAB are capable of desorbing oil-wetting agents by the formation of ion pairs through electrostatic attraction.

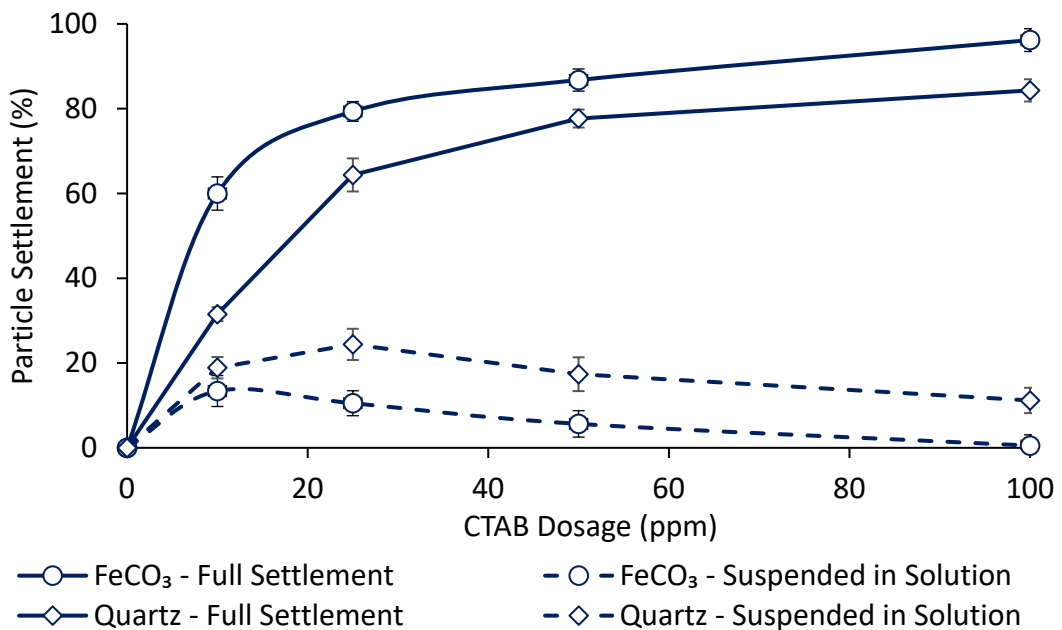


Figure 7-9. Effect of CTAB on initially oil-wet 10-32 μm FeCO_3 and quartz settlement

In comparison, SDS showed little to no ability to aid in settlement performance with the majority of particles (>90%) returning back to the liquid vapour interface after surfactant exposure (Figure 7-10). Exposure of the particles to SDS did however result in the formation of large particle agglomerations particularly in the case of FeCO_3 as indicated by Figure 7-12. Based on the results and conclusions of Al-Anssari [159], it is likely that SDS adsorbed to the surface of the FeCO_3 and quartz particles during treatment resulting in the formation of the large particle

agglomerations. Adsorption of the surfactant may ultimately lead to cross-linking of the surfactant molecules through hydrophobic attraction between the polymer chains. Furthermore, due to the effect of SDS on the zeta potential of FeCO_3 particles at pH 9 (Figure 7-8), the effect of SDS on the particle size of FeCO_3 was far more pronounced compared to that of CTAB. FeCO_3 reached its IEP at approximately 50 ppm SDS concentration helping to facilitate the strong particle attraction observed due to the dominance of van der Waals attraction between the particles [152, 158, 159].

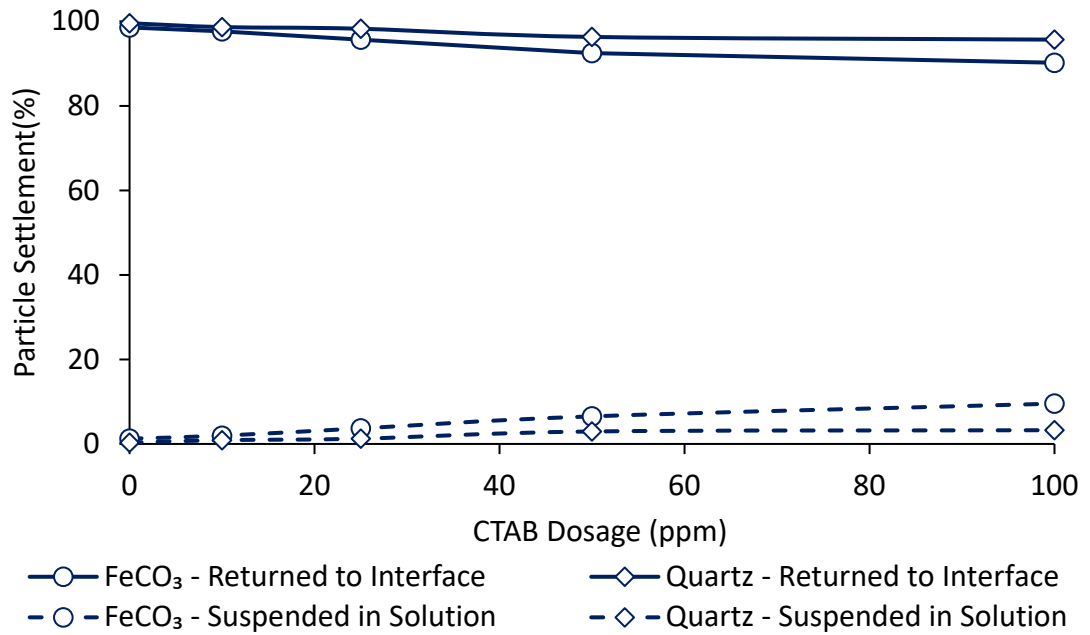


Figure 7-10. Effect of SDS on initially Oil-Wet 10-32 μm FeCO_3 and quartz settlement

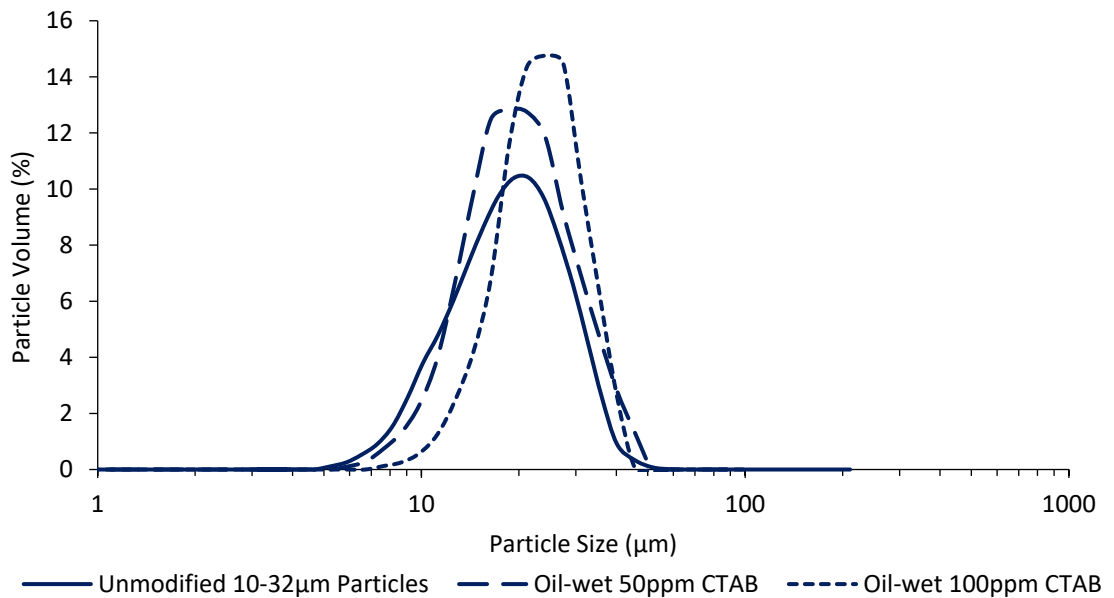


Figure 7-11. Effect of CTAB on FeCO_3 particle size after oil-wetted to water/MEG-wetted transition

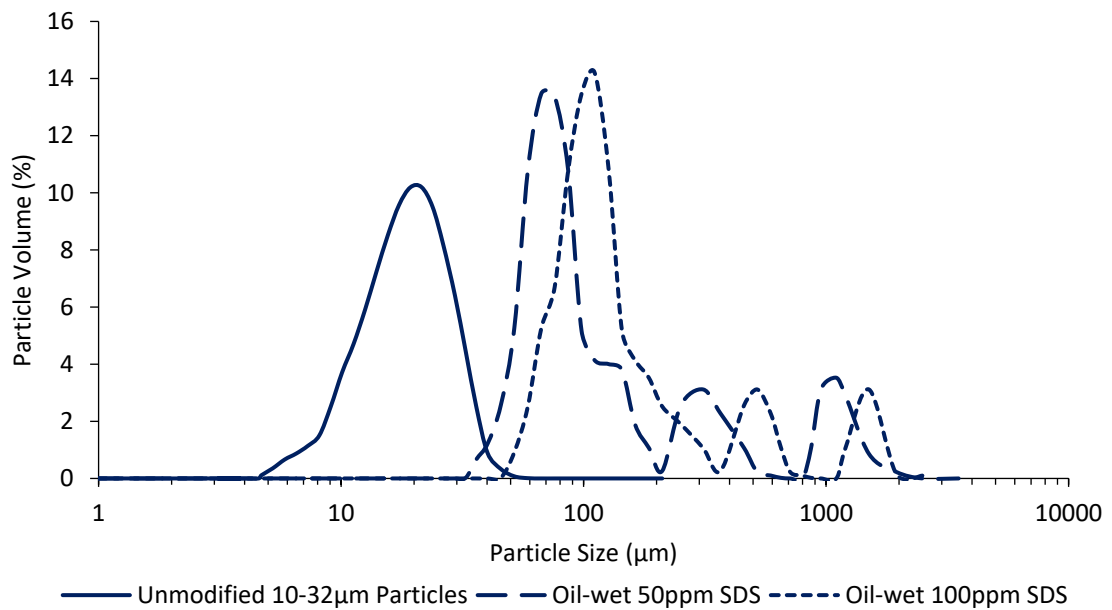


Figure 7-12. Effect of SDS on FeCO_3 particle size after oil-wetted to water/MEG-wetted transition

Further comparison of anionic and cationic surfactants for particle modification of FeCO_3 is illustrated by Figure 7-13, whereby several generic and commercially available surfactants were evaluated at a 50 ppm dosage rate. Table 7-1 outlines the varying types of surfactants used, including the manufacturer provided surfactant descriptions. Overall, the results further highlight that cationic surfactants are more suitable for modifying particle wettability properties within the high pH conditions of MEG pre-treatment systems where particle surface charge is more likely to be negative. The negative surface charge and resultant electrostatic repulsion between particle and surfactant molecule may ultimately overwhelm the hydrophobic attraction required for anionic surfactants to perform, particularly in the case of quartz and particles within higher pH solutions (>8-9) [273, 274].

Table 7-1. Generic and commercially available surfactants

Surfactant	Type		Description
SDS	Generic	Anionic	Sodium Dodecyl Sulphate
Anionic	Commercial	Anionic	Anionic high molecular weight polymer
CTAB	Generic	Cationic	Cetrimonium bromide
DODAB	Generic	Cationic	Dimethyldioctadecylammonium bromide
Hyamine	Generic	Cationic	Benzethonium chloride
Cationic 1	Commercial	Cationic	Cationic brine dispersion polyacrylamide flocculent
Cationic 2	Commercial	Cationic	Mixture of four cationic surfactants developed as a wax dispersant in MEG systems

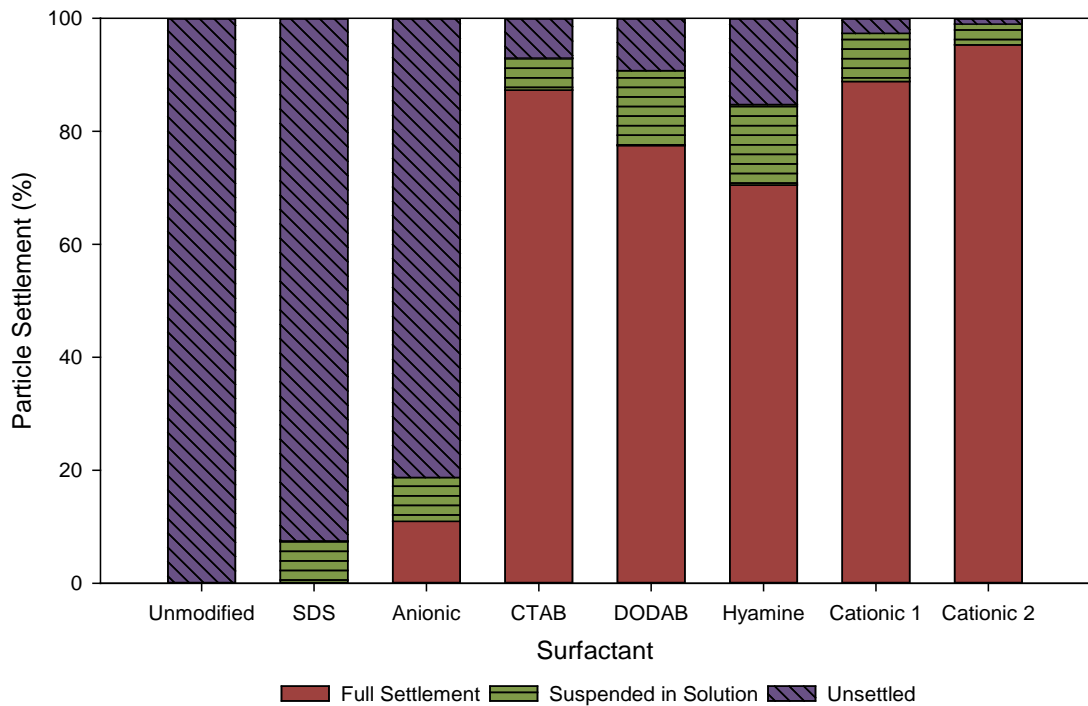
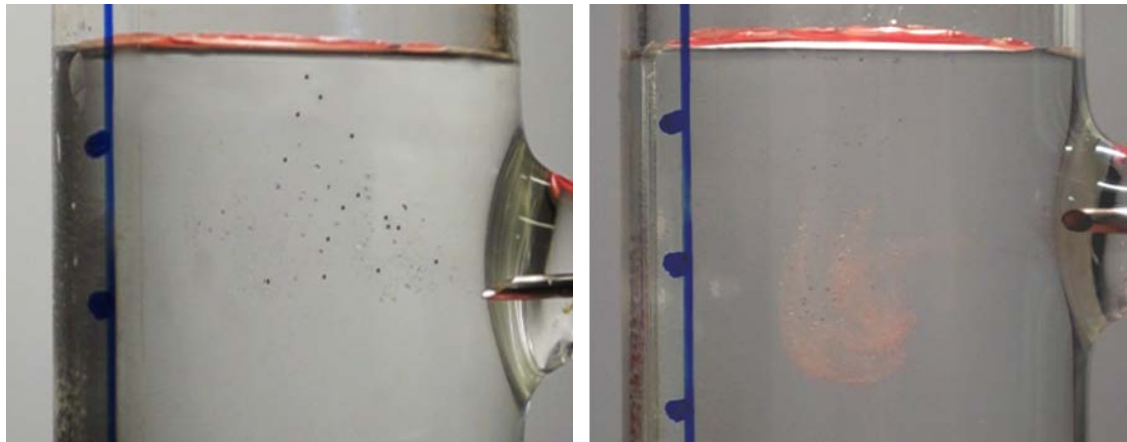


Figure 7-13. Comparison of generic and commercially available surfactants (50 ppm) - FeCO_3

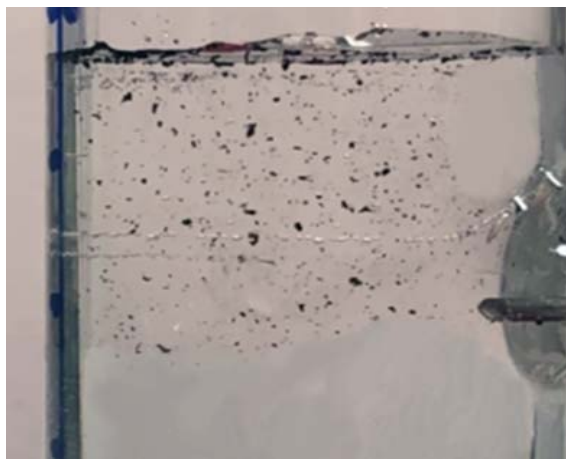
To further evaluate the ability of the surfactants to modify the particles to more water/MEG-wetted, the procedure utilised in Section 4.2 was again used to visualise particle settlement behaviour. Initially oil-wetted particles were exposed to a solution of 50% MEG containing varying concentrations of each surfactant and mixed vigorously for ten minutes. The resultant particles were then injected horizontally into the settlement chamber and their settlement analysed. Exposure of the initially oil-wetted FeCO_3 particles to CTAB prior to injection successfully modified the surface of the particles to a more water/MEG-wetted state. The resulting water/MEG-wetted particles (Figure 7-14b) demonstrated greater settleability compared to the corresponding oil-wetted particles (Figure 7-14a), with settlement behaviour in line with the unmodified FeCO_3 settlement experiments (Figure 7-3). Likewise, the CTAB treated FeCO_3 again demonstrated visual similarity to the unmodified FeCO_3 when submerged in the solution further confirming their conversion to a more water/MEG wetted state. In contrast, FeCO_3 and quartz particles treated using SDS showed no improvement in settlement with particles exhibiting similar behaviour to un-treated oil-wetted particles. The effect of SDS on particle size is further evident with large FeCO_3 particle accumulations formed (refer to Figure 7-14c), which although significantly larger in particle size, still failed to settle. Overall, the results indicate that the formation of an oil-wetted layer upon particle surfaces plays a much greater role in determining settleability compared to particle size, particularly within the particle size ranges found in industrial MEG systems. As such, during the design and operation of industrial

MEG regeneration systems, the oil-wetting of particles, and potential chemical treatments, must be taken into consideration to maximise particle settlement efficiency.



a) Oil-wet 10-32 μm FeCO_3 particles

b) Oil-wet 10-32 μm FeCO_3 particles with 50ppm CTAB



c) Oil-wet 10-32 μm FeCO_3 particles with 50 ppm SDS

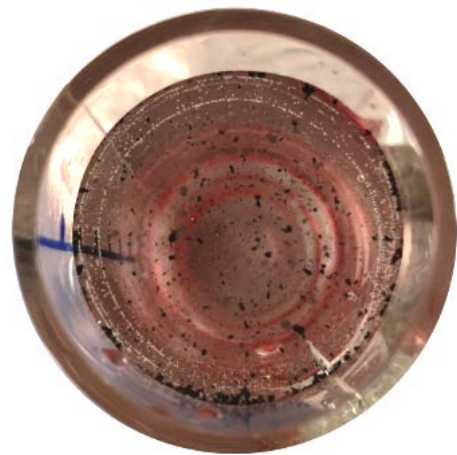


Figure 7-14. Modification of FeCO_3 surface properties by CTAB and SDS surfactants

7.5 Conclusion

A variety of studies have been conducted to analyse the impact of wettability of particle and solid surfaces with direct application to Enhanced Oil Recovery (EOR) [143, 159, 171, 190, 272, 274]. However, the impact of wettability on the behaviour of solid particles in terms of settlement has received minimal attention, particularly for industrial systems. The exposure of FeCO_3 and quartz to condensate and formation of oil-wetted particles has been identified as a potential cause of poor particle settlement within an industrial MEG regeneration system operating in Western Australia. The effect of oil-wetting on settlement behaviour was hence evaluated and potential methods to increase settlement rate explored.

Oil-wetted particles formed through exposure to a stearic acid/decane solution showed a strong tendency to either remain suspended in solution indefinitely or transition to the MEG-air interface. As such, it is clear that the formation of oil-wetted particles through exposure to condensate within the transportation pipeline or within the pre-treatment system may ultimately result in poor settlement and the need for excessive filtration. To combat this, a variety of cationic surfactants including CTAB showed strong potential in transitioning the initially oil-wetted particles to a more settleable water/MEG-wetted state, a result consistent with prior studies into EOR ^[143, 272-274]. The strong performance of cationic surfactants for particle modification can be attributed to the negative surface charge of iron and quartz at the pH levels typical in MEG pre-treatment systems (>8). In contrast, due to the negative particle surface charge, SDS and a commercially available anionic surfactant, showed poor performance in increasing particle settlement.

Furthermore, the addition of CTAB and SDS also showed the ability to increase the particle size of FeCO_3 potentially aiding in settlement performance ^[159, 178, 246, 256]. However, the conversion of oil-wetted particles to water-wetted was found to be a greater contributing factor to improved settlement performance than the increase in particle size, with large particles formed after SDS treatment failing to settle. Overall, the settlement of initially oil-wetted quartz and FeCO_3 particles was increased from 0% when completely oil-wetted to 80 and 90% respectively following treatment using 100 ppm of CTAB, with good settlement percentages also generated via treatment using commercially available cationic surfactants. As such, the work within this study may provide a potential cause behind poor settlement of particles within industrial rich MEG processing systems and a possible method to combat this issue through application of cationic surfactants.

8.0 ACID DISSOCIATION CONSTANT (PK_a) OF COMMON MEG REGENERATION ORGANIC ACIDS AND METHYLDIETHANOLAMINE AT VARYING MEG CONCENTRATION, TEMPERATURE AND IONIC STRENGTH

8.1 Introduction

The presence of organic acids within MEG regeneration systems poses a potential corrosion risk to natural gas transportation pipelines [69-72]. Organic acids such as acetic, propanoic and butanoic typically enter into the MEG regeneration loop via the condensed water phase where free organic acids are present within the reservoir [63]. Alternatively, following the breakthrough of formation water, organic acids may also be introduced alongside mineral salt ions [9, 63]. The thermal degradation of MEG at high temperature in the presence of oxygen may also lead to the formation of organic acids including glycolic, acetic and formic acids [1, 3, 5, 39, 63].

The introduction of organic acids into natural gas transportation pipelines will ultimately reduce the pH of the liquid phase and hence pose a corrosion risk through increased solubility of the protective iron carbonate film [65-68]. Furthermore, organic acids such as acetic acid have been demonstrated to increase the rate of Top of the Line Corrosion (TLC) in the presence of carbon dioxide [17, 63, 72-76]. As such, whilst operating under pH stabilisation corrosion control it is important to ensure sufficient alkalinity is present to neutralise incoming organic acids.

Corrosion prevention through pH stabilisation can be achieved through the addition of hydroxide or carbonate salts, or amine-based compounds including MDEA [4, 17]. The application of MDEA within closed loop MEG systems for pH stabilisation is advantageous due to its thermal stability allowing multiple regeneration cycles before degradation occurs and its ability to be recovered during reclamation at high pH [277, 278]. However, upon the onset of formation water the risk of scaling within subsea and MEG regeneration systems at high pH is present. As such, if scaling cannot be alternatively managed through scale inhibitors it may be beneficial to transition from pH stabilisation using MDEA to more scaling friendly film forming corrosion inhibitors [8, 9].

The removal of MDEA from the MEG regeneration loop can be accomplished alongside monovalent cations including sodium via vacuum reclamation [9, 40]. Removal of MDEA during the reclamation process involves first neutralising the MDEA to facilitate reaction with anionic species including chlorides, sulphates, sulphides and organic acid ions to form heat stable salts in a similar manner to industrial CO₂ capture systems using amines [40, 213-215, 217]. Upon the evaporation of lean MEG under vacuum, the heat stable MDEA salts will remain, hence facilitating their removal. Likewise, removal of organic acids via the vacuum reclamation system

may also be achieved in a similar manner to prevent their accumulation within the loop. As such, the acid dissociation behaviour of a chemical is an important factor dictating the efficiency of its removal during reclamation.

The acid dissociation constant (pK_a) of a chemical is influenced by a variety of factors including temperature, ionic strength and the dielectric constant (ϵ) of the solvent ^[130]. Organic solvents such as ethylene glycol have been shown experimentally to influence the pK_a of various weak acids and bases typically increasing pK_a compared to aqueous solutions ^[127-130]. The dielectric constant of ethylene glycol (37.7 at 20°C ^[279]) is noticeably lower than that of water (78.54 at 20°C ^[279]) and will hence influence the dissociation behaviour of weak acids and bases.

The pK_a of chemicals within MEG are hence important to MEG regeneration system operators and designers. The removal of MDEA and organic acids via vacuum reclamation is dependent on both system pH and temperature and will ultimately be influenced by the acid dissociation behaviour. Likewise, the complete neutralisation of incoming organic acids from the well is important whilst operating under pH stabilisation corrosion control. The pK_a of organic acids commonly found within MEG regeneration systems and MDEA have hence been determined at varying MEG concentrations, temperatures and ionic strengths.

8.2 Experimental Methodology

8.2.1 Chemicals

The organic acids and MDEA utilised within this study were procured from Chem Supply and Sigma Aldrich respectively. The purities of the chemicals used, and their respective chemical structures are outlined by Table 8-1.

8.2.2 Apparatus and Procedure.

The pK_a of organic acids and MDEA within varying MEG concentrations was determined via titration using a HI902 potentiometric automatic titration system. The automatic titration system utilises a dynamic titration mode whereby the addition of the titrant is reduced as the equivalence point approaches. For this study, a minimum titrant volume step size of 0.025 ml was utilised to ensure accurate identification of the equivalence point ($\pm 0.1\%$ dosed volume). pH measurements were performed using a Thermo Scientific Orion 8302BNUMD pH probe (± 0.01 pH units) with automatic temperature compensation. Temperature was maintained within the titration cell via an external water heating jacket ($\pm 0.1^\circ\text{C}$). For the organic acids and MDEA respectively, 0.1 M (± 0.002 M) NaOH and HCl supplied by Hanna instruments was utilised as the titrant.

Solutions of varying MEG concentration (wt. %) were prepared using de-ionised water (18.2M Ω .cm) and ethylene glycol supplied by Chem Supply (CAS: 107-21-1). The concentration

of prepared MEG solutions was verified using an ATAGO PAL-91S refractometer pre-calibrated for the determination of MEG concentration with an accuracy of $\pm 0.4\%$ (V/V). Prior to titration all solutions were sparged using ultra-pure nitrogen (>99.999 mol. %) to remove dissolved CO₂. Each titration was repeated three times with the average pK_a presented. To account for the inherent error associated with pH measurement in MEG solutions, the correction factor described by Sandengen [11] was applied.

To assess the accuracy of the titration and pK_a determination procedure utilised, the pK_a of the respective organic acids and MDEA within water at 25°C was compared to literature values. The measured pK_a and comparison literature values are summarised in Table 8-2 with good agreement found. Furthermore, the effect of temperature on the measured pK_a of the organic acids and MDEA within aqueous solutions was compared to published literature studies (Figure 8-1 to Figure 8-3).

Table 8-1. Chemical purity and structures

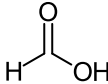
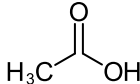
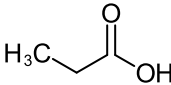
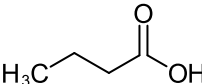
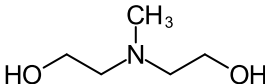
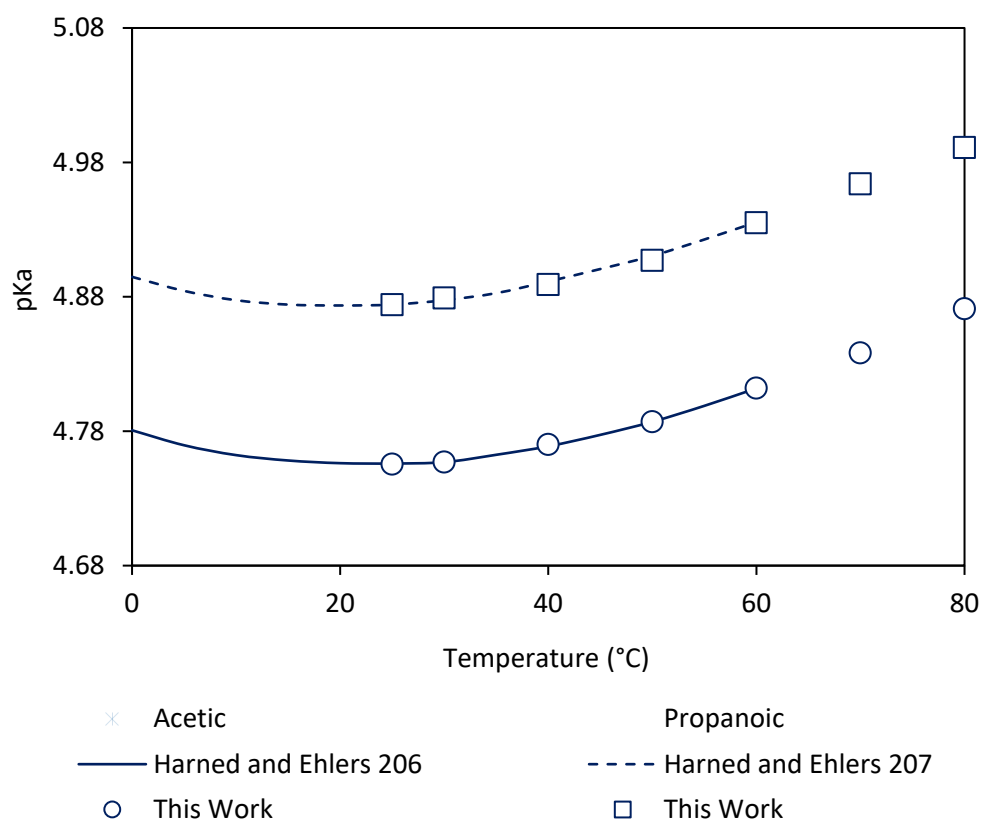
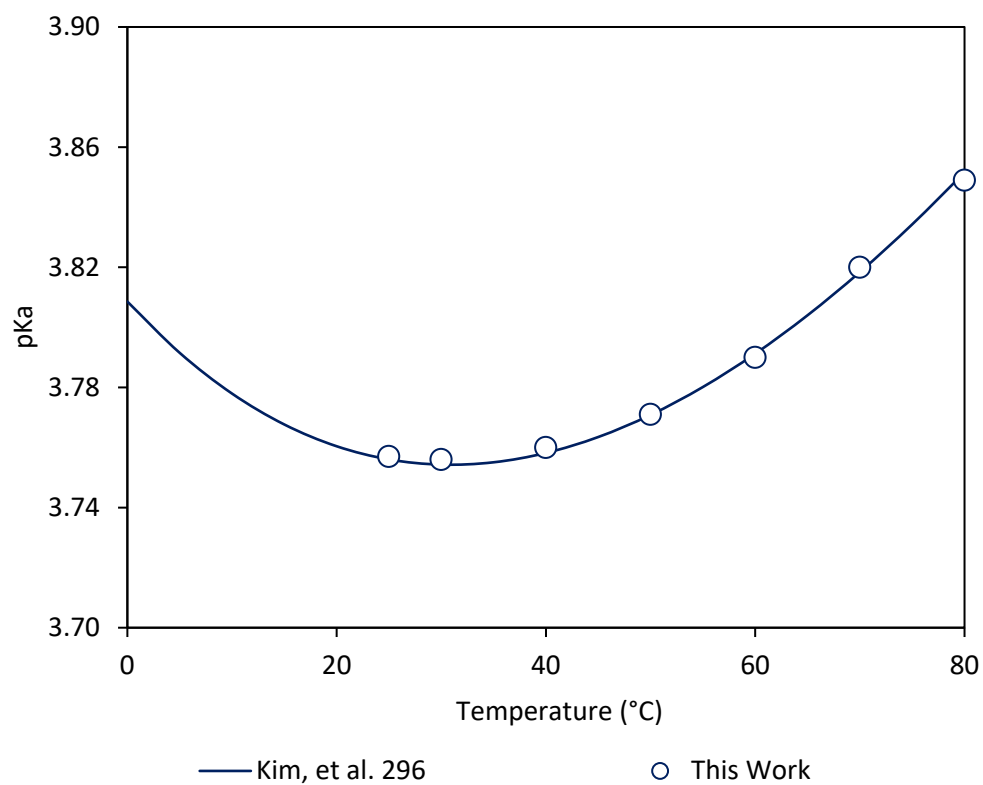
Compound	CAS	Purity	Chemical Structure
Formic acid	64-18-6	>99.5%	
Acetic acid	64-19-7	>99.5%	
Propanoic acid	109-52-4	>99.5%	
Butanoic acid	107-92-6	>99.5%	
MDEA	105-59-9	>99%	

Table 8-2. Water pK_a comparison to literature^a

Compound	pK _{a,(water)} (25°C)	
	Literature	This Study
Acetic acid	4.76 ^[280]	4.76
Propanoic acid	4.88 ^[280]	4.87
Butanoic acid	4.82 ^[281]	4.82
Formic acid	3.75 ^[281]	3.76
MDEA	8.58 ^[227]	8.58

^aStandard uncertainties: $u(T) = 0.01^\circ\text{C}$ and $u(\text{pK}_a) = 0.03$

Figure 8-1. Effect of temperature on pK_a of acetic and propanoic acid (aqueous solution)Figure 8-2. Effect of temperature on pK_a of formic acid (aqueous solution)

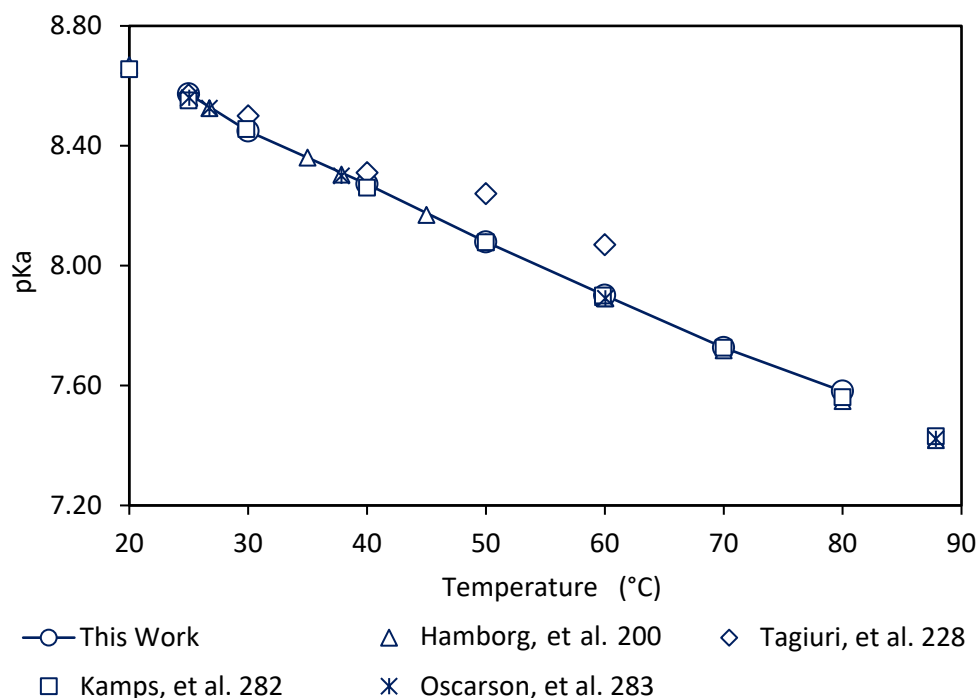


Figure 8-3. Effect of temperature on pK_a of MDEA (aqueous solution)

8.3 Determination of pK_a Values

The determination of pK_a from potentiometric titration data is often performed by plotting the pH as a function of titrant volume and estimating the pK_a value from the curves inflection point^[130]. At the equivalence point, the concentration of the acid or base and its conjugate form is equal and hence through Equation (8-1), pK_a is equal to pH. However, the measurement of pK_a is influenced by the ionic strength of the solution and in turn the dissociation of the acid or base to its conjugate form^[130, 284, 285]. As such, calculation of the acid dissociation constants (pK_a) reported in this study was performed using Equation (8-2)^[285] where the activity coefficient of the ionic species (γ_i^-) is incorporated. Through Equation (8-2), pK_a was calculated over the entire pH range of the titration and the average pK_a reported. The activity coefficient of the undissociated species (γ_i) was assumed to be one^[285-287].

$$pK_a = pH + \log \left[\frac{[A^\pm]}{[HA]} \right] \quad (8-1)$$

$$pK_a = pH + \log \left[\frac{1 - \alpha}{\alpha} \right] + \log \left(\frac{\gamma_i}{\gamma_i^-} \right) \quad (8-2)$$

$$\text{where } \alpha = V/V_{eq}$$

To calculate the activity coefficient of the dissociated species (γ_i^-), the Debye-Hückel equation given by Equation (8-3) was utilised^[228, 284, 285, 287, 288]. Where the A and B terms are constants, a_i is the ionic size parameter, z_i the valence of the ionic species and I the ionic strength of the solution (calculated through Equation (8-4)). The ionic size parameters reported by Kielland [289] were utilised for the organic acids ($a_i = 3.5 \text{ \AA}$ ^[285]) and MDEA ($a_i = 4.5 \text{ \AA}$ ^[228]).

The values of the A and B constant terms were taken from the works of Manov [290] and Robinson and Stokes [291].

$$-\log(\gamma_i) = \frac{Az_i^2 I^{\frac{1}{2}}}{1 + Ba_i I^{\frac{1}{2}}} \quad (8-3)$$

$$I = \frac{1}{2} \sum z_i^2 \cdot c_i \quad (8-4)$$

where c_i = ion concentration and z_i = ion valence

8.4 Results and Discussion

8.4.1 Effect of MEG Concentration on pK_a .

The effect of varying MEG concentration on the pK_a of the organic acids and MDEA at 25°C is presented within Table 8-3 and Table 8-5 respectively. For the organic acids, increasing MEG concentration resulted in an increase in the measured pK_a as per Figure 8-4. The change in measured pK_a was found to change linearly with respect to MEG mole fraction (not shown). As a result, the change in pK_a directly correlated with the change in dielectric constant of the solution (refer to Figure 8-6 and Figure 8-7)^[130]. In contrast, the measured pK_a of MDEA was found to decrease with respect to increasing MEG concentration (Figure 8-5), however, again in line with the change in MEG mole fraction and resultant change in dielectric constant of the solution (Figure 8-8).

8.4.2 Effect of temperature on pK_a .

The effect of temperature on the pK_a of the organic acids and MDEA was evaluated within varying MEG concentration solutions (30, 50 and 80% wt.) and is presented in Table 8-4 and Table 8-5 respectively. The pK_a of the organic acids within MEG solution demonstrated similar behaviour with respect to temperature as within water (Figure 8-9 to Figure 8-11). A similar response was observed for MDEA whereby the change in temperature induced a large reduction in the measured pK_a matching that of water (Figure 8-12). The results are in line with the findings of Castells [226] who suggested a large change in pK_a can be expected for amines with a lower temperature response exhibited by organic acids.

Table 8-3. Effect of MEG concentration on measured organic acid pK_a (25°C)^a

Compound	MEG Concentration (wt. %)						
	0	30	40	50	60	70	80
Formic	3.75	3.89	3.99	4.10	4.25	4.40	4.65
Acetic	4.76	4.96	5.08	5.22	5.42	5.63	5.93
Propanoic	4.88	5.23	5.38	5.55	5.74	6.01	6.29
Butanoic	4.82	5.13	5.28	5.46	5.64	5.90	6.21

^aStandard uncertainties: $u(T) = 0.01^\circ\text{C}$, $u(\text{MEG } \%) = 0.2$, $u(pK_a) = 0.04$

Table 8-4. Effect of temperature on measured organic acid pK_a in aqueous and varying MEG concentration solution ^a

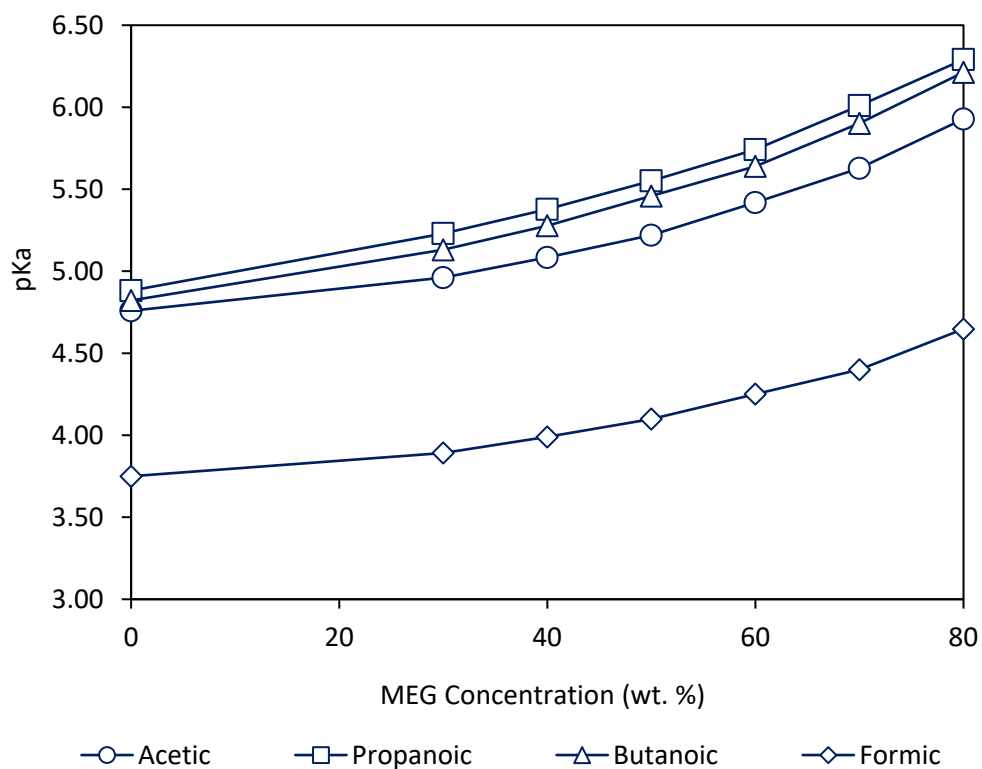
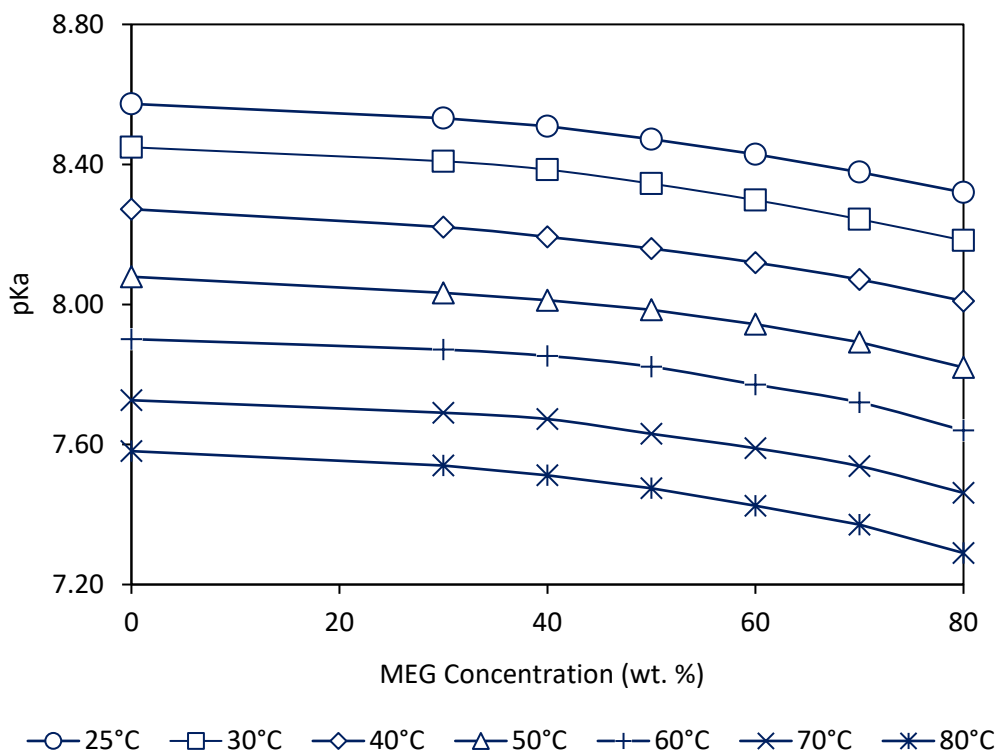
Compound	Temperature (°C)						
	25	30	40	50	60	70	80
Aqueous Solution							
Formic	3.76	3.76	3.76	3.77	3.79	3.82	3.85
Acetic	4.76	4.76	4.77	4.79	4.81	4.84	4.87
Propanoic	4.87	4.88	4.89	4.91	4.94	4.96	4.99
Butanoic	4.82	4.82	4.84	4.86	4.88	4.91	4.94
30% wt. MEG							
Formic	3.89	3.89	3.90	3.90	3.92	3.95	3.99
Acetic	4.96	4.96	4.97	4.99	5.01	5.04	5.08
Propanoic	5.23	5.23	5.25	5.26	5.29	5.32	5.37
Butanoic	5.13	5.14	5.15	5.16	5.19	5.22	5.27
50% wt. MEG							
Formic	4.09	4.09	4.10	4.11	4.12	4.15	4.09
Acetic	5.22	5.22	5.23	5.25	5.27	5.30	5.22
Propanoic	5.55	5.56	5.57	5.58	5.61	5.65	5.55
Butanoic	5.46	5.46	5.47	5.49	5.52	5.55	5.46
80% wt. MEG							
Formic	4.65	4.65	4.65	4.66	4.68	4.71	4.76
Acetic	5.93	5.93	5.94	5.96	5.99	6.02	6.07
Propanoic	6.29	6.30	6.31	6.33	6.35	6.39	6.44
Butanoic	6.21	6.22	6.23	6.25	6.28	6.31	6.36

^aStandard uncertainties: $u(T) = 0.01^\circ\text{C}$, $u(\text{MEG } \%) = 0.2$, $u(pK_a) = 0.04$

Table 8-5. Effect of MEG concentration and temperature on measured MDEA pK_a ^a

MEG Concentration (wt. %)	Temperature (°C)						
	25	30	40	50	60	70	80
0	8.57	8.45	8.27	8.08	7.90	7.73	7.58
30	8.53	8.41	8.22	8.03	7.87	7.69	7.54
40	8.51	8.39	8.19	8.01	7.85	7.67	7.51
50	8.47	8.35	8.16	7.99	7.82	7.63	7.48
60	8.43	8.30	8.12	7.94	7.77	7.59	7.43
70	8.38	8.24	8.07	7.89	7.72	7.54	7.37
80	8.32	8.18	8.01	7.82	7.64	7.46	7.29

^aStandard uncertainties: $u(T) = 0.01^\circ\text{C}$, $u(\text{MEG } \%) = 0.2$, $u(pK_a) = 0.04$

Figure 8-4. Effect of MEG concentration on pK_a of organic acids (25°C)Figure 8-5. Effect of MEG concentration and temperature on pK_a of MDEA

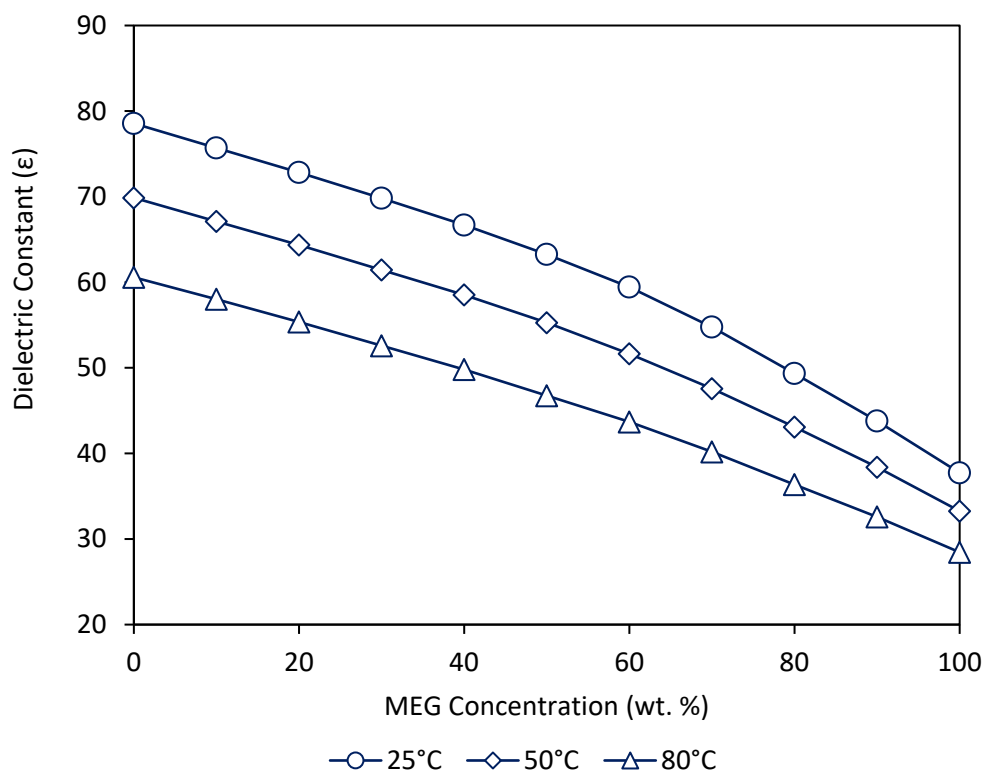


Figure 8-6. Dielectric constant of varying MEG concentration solutions [292, 293]

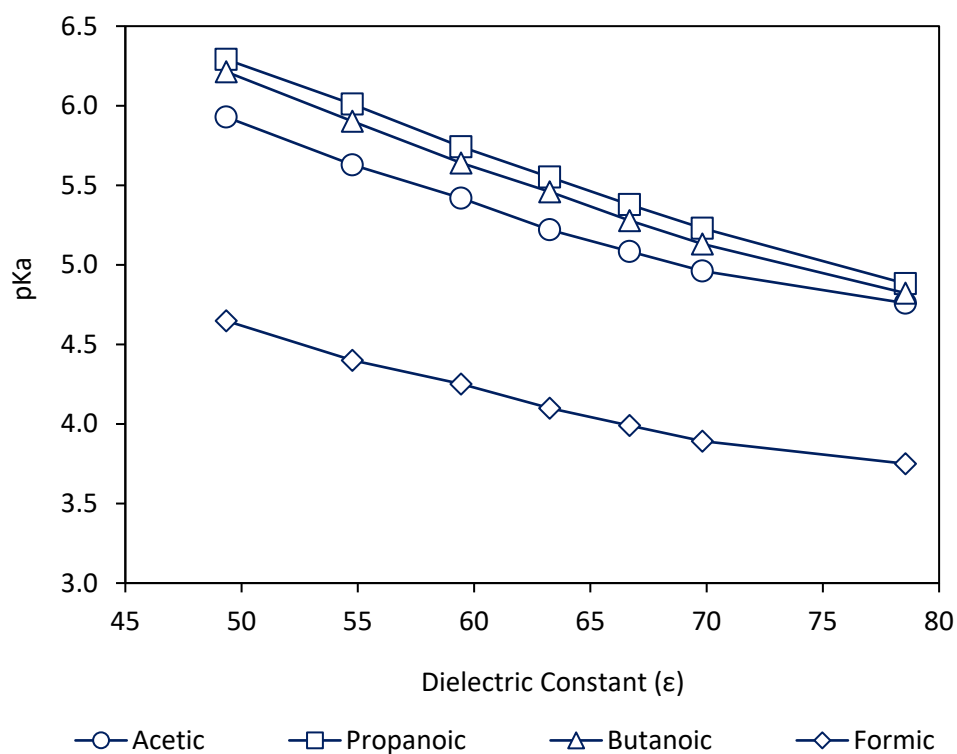
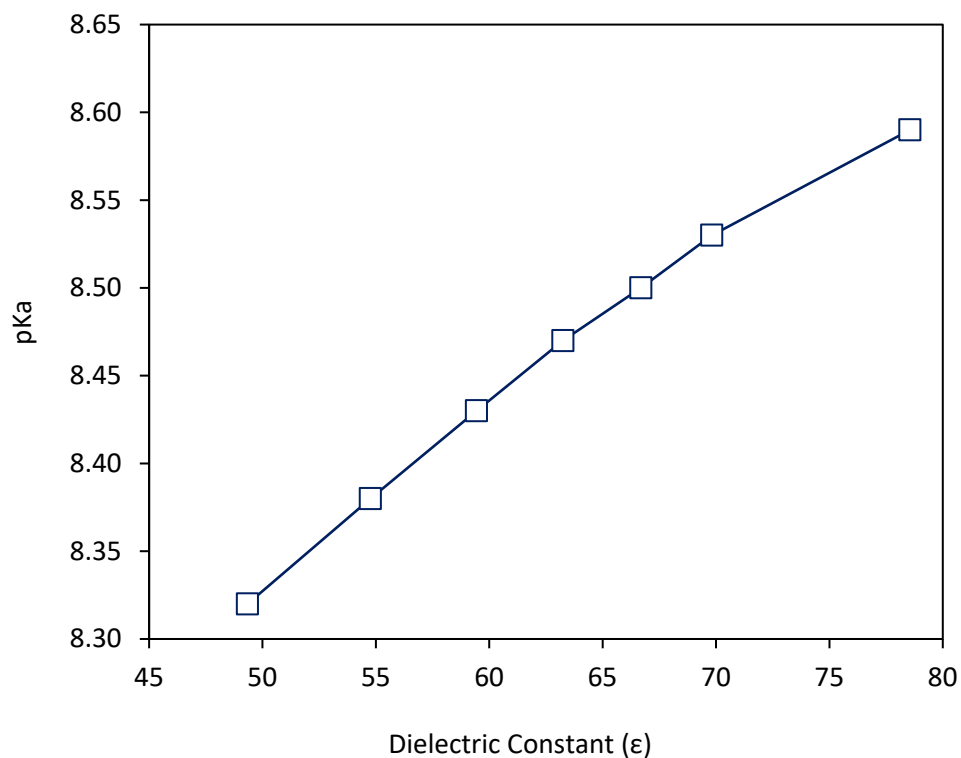
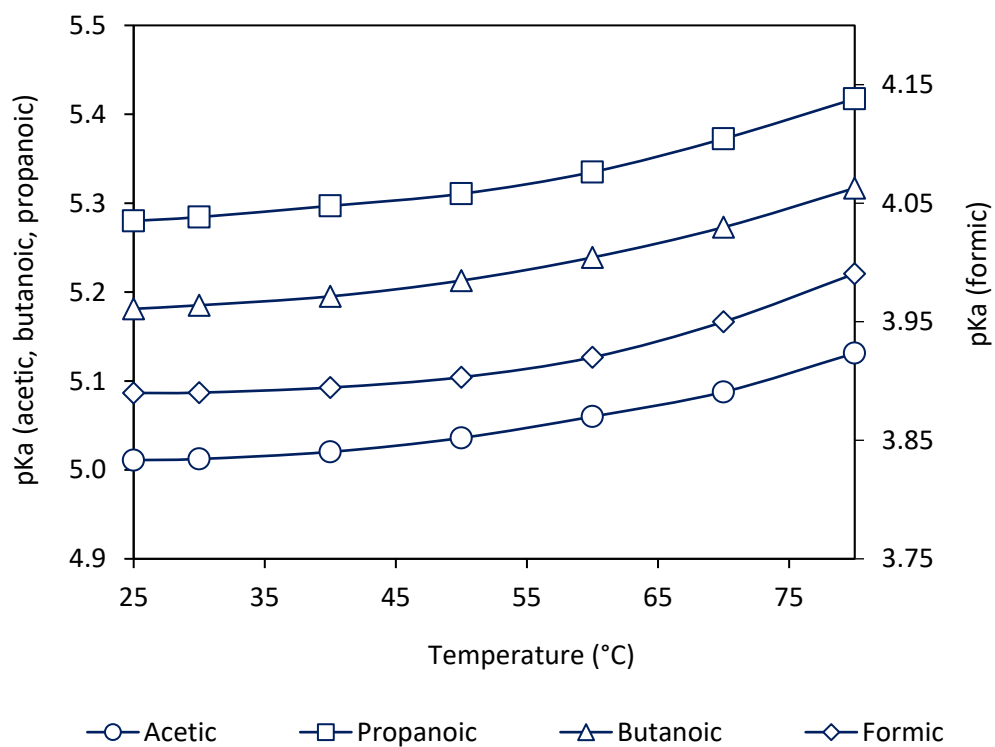
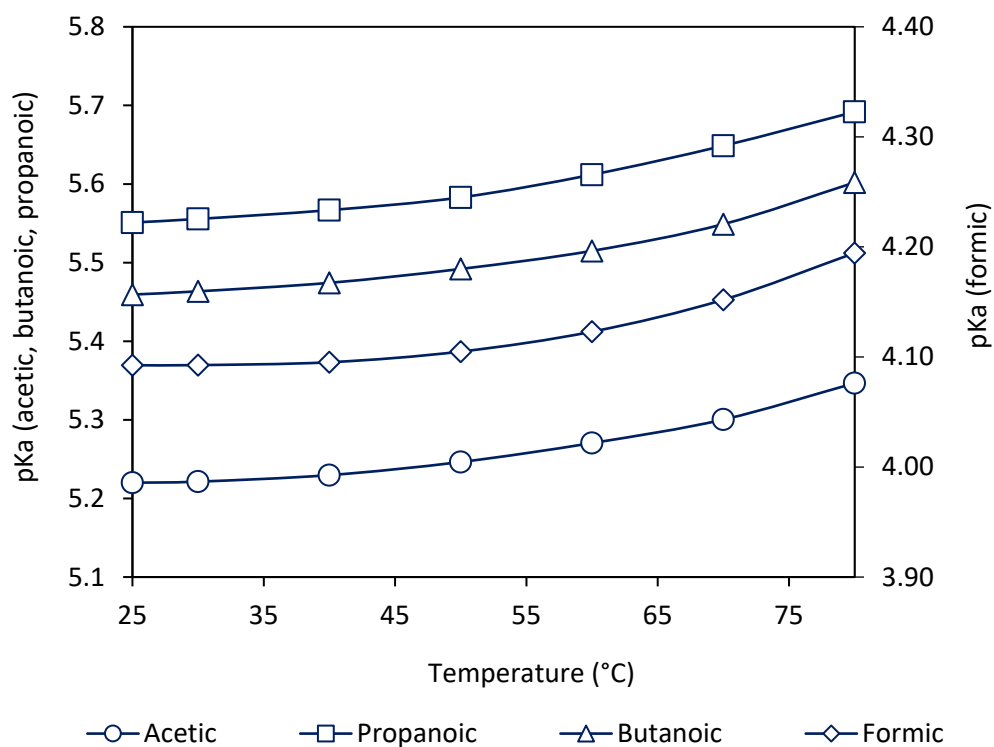
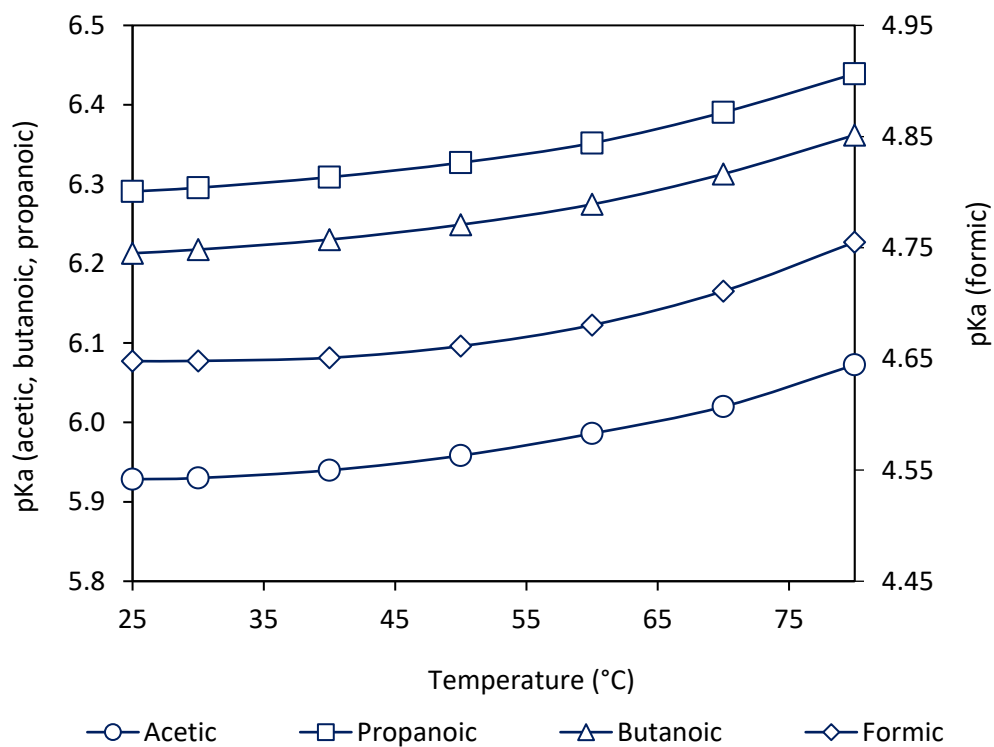


Figure 8-7. Dielectric constant vs. organic acid pKa (25°C)

Figure 8-8. Dielectric constant vs. MDEA pK_a Figure 8-9. Effect of temperature on pK_a of organic acids (30% wt. MEG)

Figure 8-10. Effect of temperature on pK_a of organic acids (50% wt. MEG)Figure 8-11. Effect of temperature on pK_a of organic acids (80% wt. MEG)

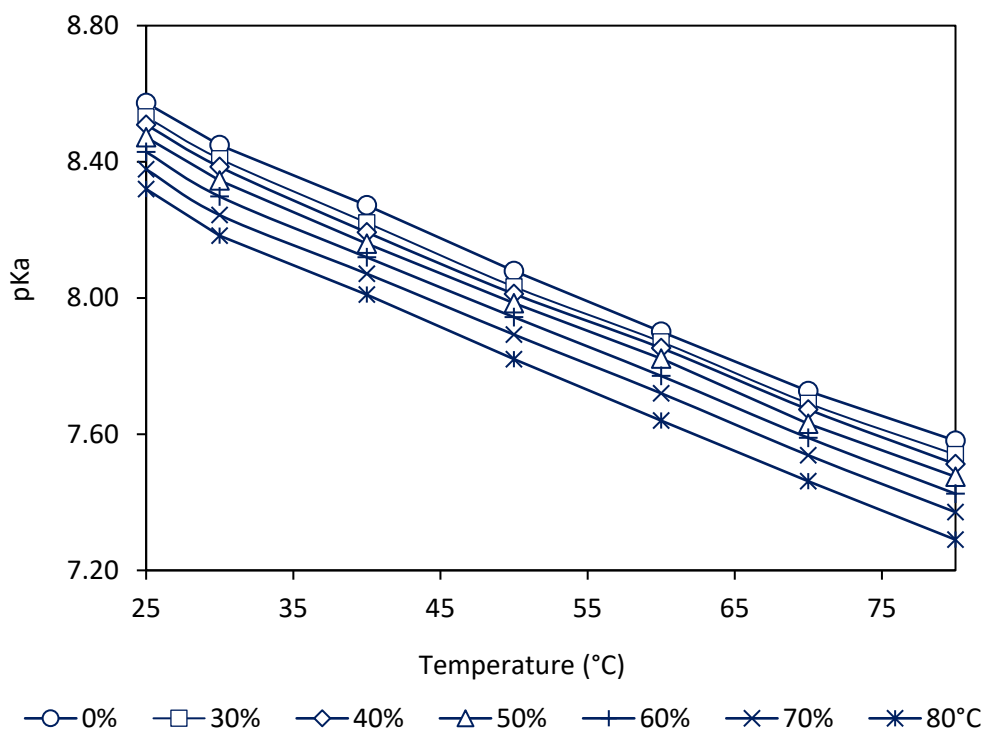


Figure 8-12. Effect of temperature on pK_a of MDEA in varying concentration MEG solution

8.4.3 Estimation of Thermodynamic Properties

The measured MDEA dissociation constants were correlated with temperature using the van't Hoff equation described by Equation (8-5). Subsequently, the Gibbs free energy ($\Delta G^\circ \text{ kJ.mol}^{-1}$), standard state enthalpy change ($\Delta H^\circ \text{ kJ.mol}^{-1}$) and entropy change ($\Delta S^\circ \text{ kJ.mol}^{-1}.K$) were calculated at 25°C by Equations (8-6) to (8-8) and are listed in Table 8-8. Comparison of the thermodynamic properties of MDEA within aqueous solution at 25°C was made to literature (Table 8-6) with good agreement found. In contrast, the organic acids were found to be temperature dependent and hence the temperature dependant form of the van't Hoff equation was applied (Equations (8-9) to (8-11)). Comparison of the thermodynamic properties of the organic acids to prior studies of organic acids in aqueous solutions showed good agreement (Table 8-7). The thermodynamic properties of the organic acids at 25°C in varying MEG concentration solutions is presented in Table 8-9.

$$\ln(K_a) = -\ln(10^{pK_a}) = a + \frac{b}{T/K} \quad (8-5)$$

$$\Delta G^\circ = \Delta H^\circ - T\Delta S^\circ \quad (8-6)$$

$$\Delta H^\circ = -R \times b \quad (8-7)$$

$$\Delta S^\circ = R \times a \quad (8-8)$$

$$\ln(K_a) = -\ln(10^{pK_a}) = a + \frac{b}{T/K} + \frac{c}{(T/K)^2} \quad (8-9)$$

$$\Delta H^\circ = -R \left(b + \frac{2c}{T/K} \right) \quad (8-10)$$

$$\Delta S^\circ = R \left(a - \frac{c}{(T^2/K)} \right) \quad (8-11)$$

Table 8-6. Comparison of MDEA thermodynamic quantities in aqueous solution (25°C)^a

Properties	This Work	Literature			
		Tagiuri [228]	Hamborg [294]	Kim [295]	Hartono [227]
$\Delta_r G_m^\circ$ kJ. mol ⁻¹	48.93	48.88	48.87	48.63	48.97
$\Delta_r H_m^\circ$ kJ. mol ⁻¹	36.20	26.49	34.9	35.2	35.69
ΔS° kJ. mol ⁻¹ . K ⁻¹	-0.042	-0.07	-	-0.045	-

^aStandard uncertainties: $u(T) = 0.01^\circ\text{C}$, $u(\Delta_r G_m^\circ) = 0.05$, $u(\Delta_r H_m^\circ) = 0.05$, $u(\Delta S^\circ) = 0.05$

Table 8-7. Comparison of organic acid thermodynamic quantities in aqueous solution (25°C)^a

Properties	Formic		Acetic		Propanoic		Butanoic
	This work	Kim [296]	This work	Harned and Ehlers [206]	This work	Harned and Ehlers [297]	This work
$\Delta_r G_m^\circ$ kJ. mol ⁻¹	21.74	21.44	27.83	27.82	27.14	27.15	27.51
$\Delta_r H_m^\circ$ kJ. mol ⁻¹	1.28	1.23	-0.85	-0.87	-0.58	-0.54	-0.75
ΔS° kJ. mol ⁻¹ . K ⁻¹	-0.069	-0.068	-0.096	-0.096	-0.093	-0.093	-0.095

^aStandard uncertainties: $u(T) = 0.01^\circ\text{C}$, $u(\Delta_r G_m^\circ) = 0.05$, $u(\Delta_r H_m^\circ) = 0.05$, $u(\Delta S^\circ) = 0.05$

Table 8-8. MDEA thermodynamic quantities in varying MEG concentration solutions (25°C)^a

Properties	MEG Concentration (wt. %)					
	30	40	50	60	70	80
$\Delta_r G_m^\circ$ kJ. mol ⁻¹	48.70	48.52	48.36	48.11	47.82	47.49
$\Delta_r H_m^\circ$ kJ. mol ⁻¹	36.13	35.84	36.35	36.62	36.56	37.47
ΔS° kJ. mol ⁻¹ . K ⁻¹	-0.042	-0.042	-0.040	-0.038	-0.037	-0.033

^aStandard uncertainties: $u(T) = 0.01^\circ\text{C}$, $u(\text{MEG } \%) = 0.2$, $u(\Delta_r G_m^\circ) = 0.05$, $u(\Delta_r H_m^\circ) = 0.05$, $u(\Delta S^\circ) = 0.05$.

Table 8-9. Organic acid thermodynamic quantities in varying concentration MEG solution (25°C)^a

Properties	Formic	Acetic	Propanoic	Butanoic
30% (wt.)				
$\Delta_r G_m^\circ$ kJ. mol ⁻¹	22.20	28.32	29.85	29.29
$\Delta_r H_m^\circ$ kJ. mol ⁻¹	1.99	0.84	0.65	0.44
ΔS° kJ. mol ⁻¹ . K ⁻¹	-0.068	-0.092	-0.098	-0.097
50% (wt.)				
$\Delta_r G_m^\circ$ kJ. mol ⁻¹	23.36	29.79	31.68	31.16
$\Delta_r H_m^\circ$ kJ. mol ⁻¹	2.19	0.96	0.39	0.88
ΔS° kJ. mol ⁻¹ . K ⁻¹	-0.071	-0.097	-0.105	-0.102
80% (wt.)				
$\Delta_r G_m^\circ$ kJ. mol ⁻¹	26.53	33.84	35.91	35.46
$\Delta_r H_m^\circ$ kJ. mol ⁻¹	2.23	1.07	0.40	0.45
ΔS° kJ. mol ⁻¹ . K ⁻¹	-0.082	-0.110	-0.119	-0.117

^aStandard uncertainties: $u(T) = 0.01^\circ\text{C}$, $u(\text{MEG } \%) = 0.2$, $u(\Delta_r G_m^\circ) = 0.05$, $u(\Delta_r H_m^\circ) = 0.05$, $u(\Delta S^\circ) = 0.05$.

8.4.4 Effect of Sodium Chloride Content and Ionic Strength on pK_a

The introduction of mineral salts into MEG regeneration systems is a major process concern due to its effect on regeneration performance and increased scaling potential [1, 9]. Sodium Chloride (NaCl) represents one of the major salt species introduced into MEG regeneration loops following formation water breakthrough [9, 39]. The effect of ionic strength in the form of NaCl upon the acid dissociation behaviour of acetic acid and MDEA at 25°C was analysed in varying MEG concentration solutions and is presented in Table 8-10.

The effect of ionic strength on MDEA pK_a (Figure 8-13) was in line with the findings of Hartono [227] who concluded that at low ionic strengths (<1 mol/L) the change in pK_a is linear. A similar response was observed for acetic acid pK_a with respect to increasing ionic strength (Figure 8-14). A small deviation in ΔpK_a was observed at the higher ionic strengths when comparing the varying MEG concentration solutions. This small deviation may be as a result of the reduced mobility of ionic species in higher concentration MEG solutions [298, 299].

Table 8-10. Effect of salinity (NaCl) on pK_a of acetic acid and MDEA in varying MEG concentration solution (25°C)^a

Sodium (ppm wt.)	Ionic Strength (mol/L)	Acetic Acid		MDEA	
		pK_a	ΔpK_a	pK_a	ΔpK_a
Aqueous Solution					
0	0.000	4.755	0	8.573	0
250	0.011	4.754	-0.001	8.577	0.003
500	0.022	4.753	-0.002	8.579	0.006
1000	0.043	4.750	-0.005	8.589	0.016
2000	0.087	4.747	-0.008	8.602	0.029
5000	0.217	4.738	-0.017	8.643	0.070
10000	0.435	4.725	-0.030	8.717	0.144
30% wt. MEG					
0	0.000	4.961	0	8.532	0
250	0.011	4.960	-0.001	8.535	0.003
500	0.022	4.959	-0.002	8.539	0.007
1000	0.043	4.956	-0.005	8.548	0.016
2000	0.087	4.952	-0.009	8.563	0.031
5000	0.217	4.943	-0.018	8.603	0.070
10000	0.435	4.930	-0.031	8.677	0.145
50% wt. MEG					
	0.000	5.220	0	8.472	0
250	0.011	5.219	-0.001	8.475	0.003
500	0.022	5.218	-0.002	8.479	0.007
1000	0.043	5.216	-0.004	8.488	0.016
2000	0.087	5.212	-0.008	8.504	0.032
5000	0.217	5.202	-0.018	8.545	0.073
10000	0.435	5.189	-0.031	8.620	0.148
80% wt. MEG					
	0.000	5.928	0	8.320	0
250	0.011	5.927	-0.001	8.325	0.005
500	0.022	5.926	-0.002	8.329	0.009
1000	0.043	5.924	-0.004	8.337	0.017
2000	0.087	5.920	-0.008	8.352	0.032
5000	0.217	5.910	-0.018	8.395	0.075
10000	0.435	5.896	-0.032	8.472	0.152

^aStandard uncertainties: $u(T) = 0.01^\circ\text{C}$, $u(\text{MEG } \%) = 0.2$, $u(pK_a) = 0.04$, $u(\text{sodium}) = 10 \text{ ppm wt.}$

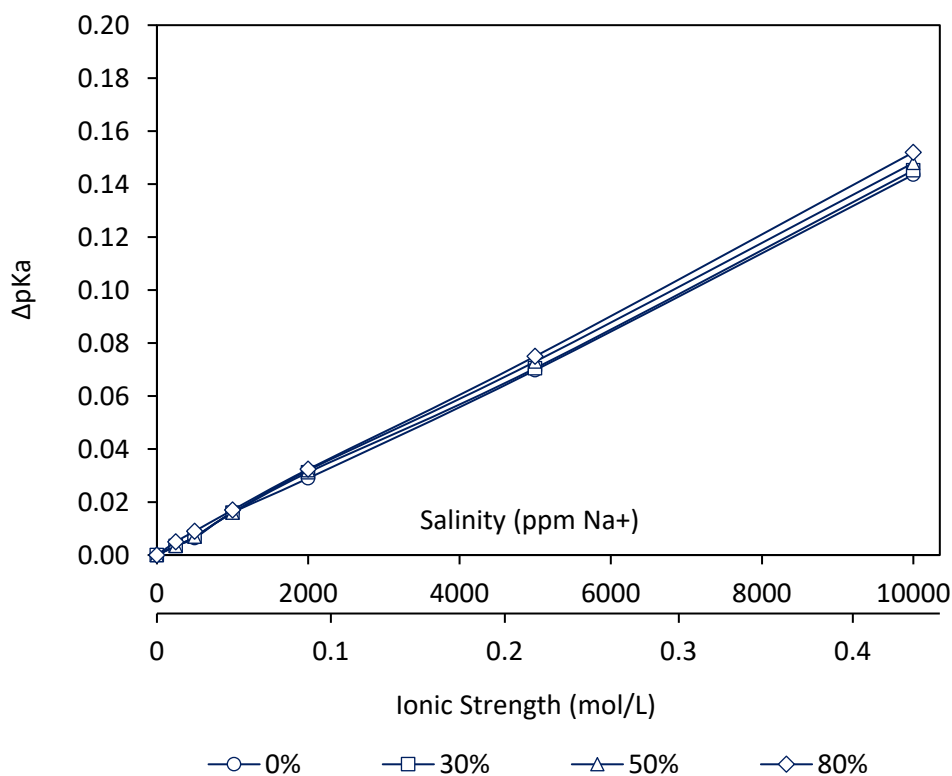


Figure 8-13. Effect of salinity (NaCl) on pK_a of MDEA in varying MEG concentration solution (25°C)

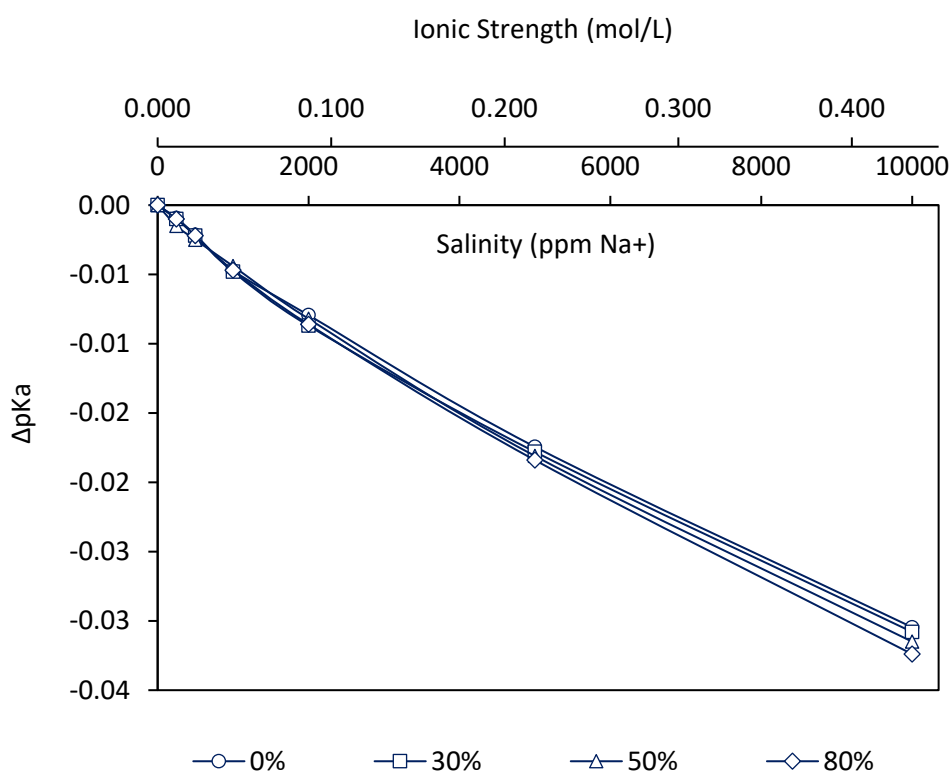


Figure 8-14. Effect of salinity (NaCl) on pK_a of acetic acid in varying MEG concentration solution (25°C)

8.4.5 pK_a Modelled as Function of MEG Concentration, Temperature and Ionic Strength (NaCl)

Industrial MEG regeneration systems may be operated at a wide range of target MEG concentrations, pHs and salinities depending on field conditions and requirements. As such, the pK_a of acetic acid and MDEA has been modelled as a function of MEG concentration, temperature and ionic strength to allow prediction at a wide range of conditions. The relationship between acetic acid pK_a within 80% wt. MEG solution is illustrated by Figure 8-15 further demonstrating the parabolic and linear relationship of acetic acid pK_a with temperature and salinity respectively. Sigmaplot's parabolic regression function was used to fit the experimental data presented in Appendix D, Table D-1 to the function given by Equation (8-12). The model coefficients at the respective MEG wt. concentrations is provided in Table 8-11. To allow estimation of acetic acid pK_a for varying MEG concentrations, a correction factor based on the mole fraction of MEG was used to develop the model given by Equation (8-13). The average error of Equation (8-12) and (8-13) is reported in Table 8-11. Furthermore, a graphical representation of the model is illustrated by Figure 8-12 showing the agreement between experimental (data points) and calculated (mesh plot).

Likewise, a similar model was developed to predict the pK_a of MDEA at varying temperature, salinity and MEG concentration. The three-dimensional relationship between MDEA pK_a , temperature and salinity within 80% wt. MEG is illustrated by Figure 8-16. Sigmaplot's 3D linear regression was used to fit the experimental data (Appendix D, Table D2) to the model given by Equation (8-14) with the coefficients and model accuracy reported in Table 8-11. Furthermore, correcting for MEG concentration, Equation (8-15) can be used to calculate MDEA pK_a at varying MEG concentrations.

$$pK_a(\text{Acetic Acid}) = A + B \times (T^\circ\text{C}) + C \times \left(I \frac{\text{mol}}{\text{L}} \right) + D \times (T^\circ\text{C})^2 + E \times \left(I \frac{\text{mol}}{\text{L}} \right)^2 \quad (8-12)$$

$$pK_a(\text{Acetic Acid}) = A_{80\%} + B_{80\%} \times (T^\circ\text{C}) + C_{80\%} \times \left(I \frac{\text{mol}}{\text{L}} \right) + D_{80\%} \times (T^\circ\text{C})^2 + E_{80\%} \times \left(I \frac{\text{mol}}{\text{L}} \right)^2 - \frac{(x_{80\% \text{ MEG}} - x_{i\% \text{ MEG}})}{0.441} \quad (8-13)$$

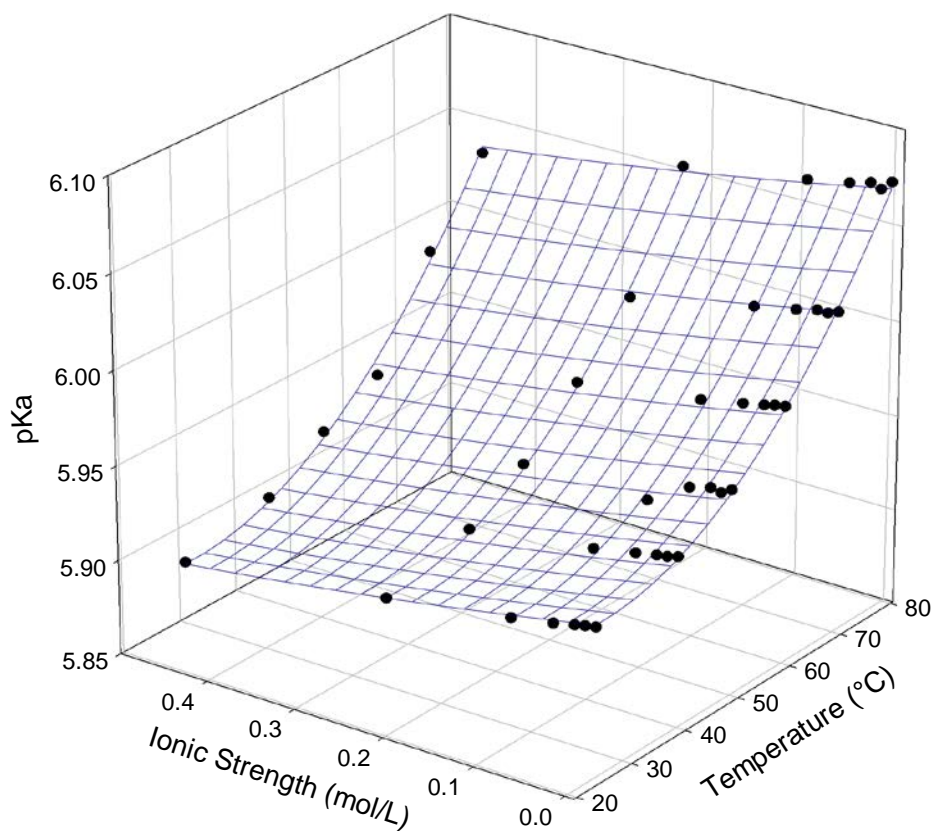
$$pK_a(\text{MDEA}) = A + B \times (T^\circ\text{C}) + C \times \left(I \frac{\text{mol}}{\text{L}} \right) \quad (8-14)$$

$$pK_a(\text{MDEA}) = A_{80\%} + B_{80\%} \times (T^\circ\text{C}) + C_{80\%} \times \left(I \frac{\text{mol}}{\text{L}} \right) + \frac{(x_{80\% \text{ MEG}} - x_{i\% \text{ MEG}})}{2.033} \quad (8-15)$$

Where: $x_{i\% \text{ MEG}}$ = Corresponding mole fraction at given mass fraction

Table 8-11. pK_a model coefficients and errors

Acetic Acid Model Coefficients			
MEG Conc. (wt. %)	80%	50%	30%
A	5.9621	5.2441	4.9929
B	-0.0025	-0.0018	-0.0023
C	-0.0942	-0.0901	-0.103
D	4.814×10^{-5}	3.801×10^{-5}	4.18×10^{-5}
E	0.0422	0.0418	0.055
Model Error (%)			
Individual	0.133	0.165	0.151
Combined	0.133	0.348	0.413
MDEA Model Coefficients			
MEG Conc. (wt. %)	80%	50%	30%
A	8.7666	8.9018	8.9639
B	-0.0186	-0.0180	-0.0181
C	0.3544	0.3353	0.353
Model Error (%)			
Individual	0.151	0.187	0.213
Combined	0.151	0.233	0.265

Figure 8-15. Acetic acid pK_a within 80% wt. MEG as a function of ionic strength and temperature

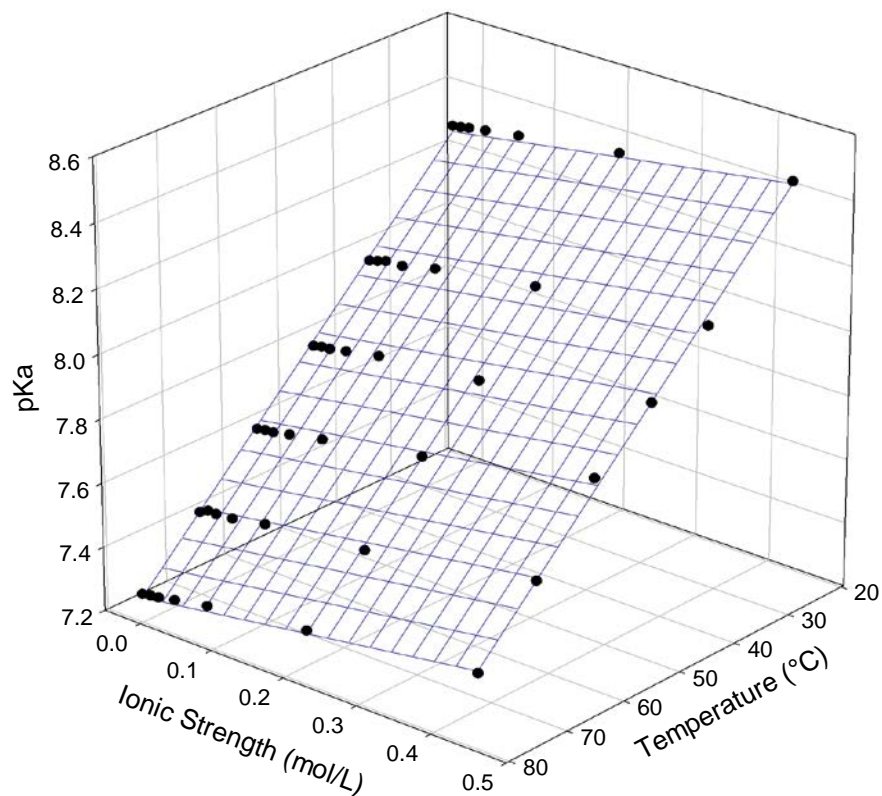


Figure 8-16. MDEA pK_a within 80% wt. MEG as a function of ionic strength and temperature

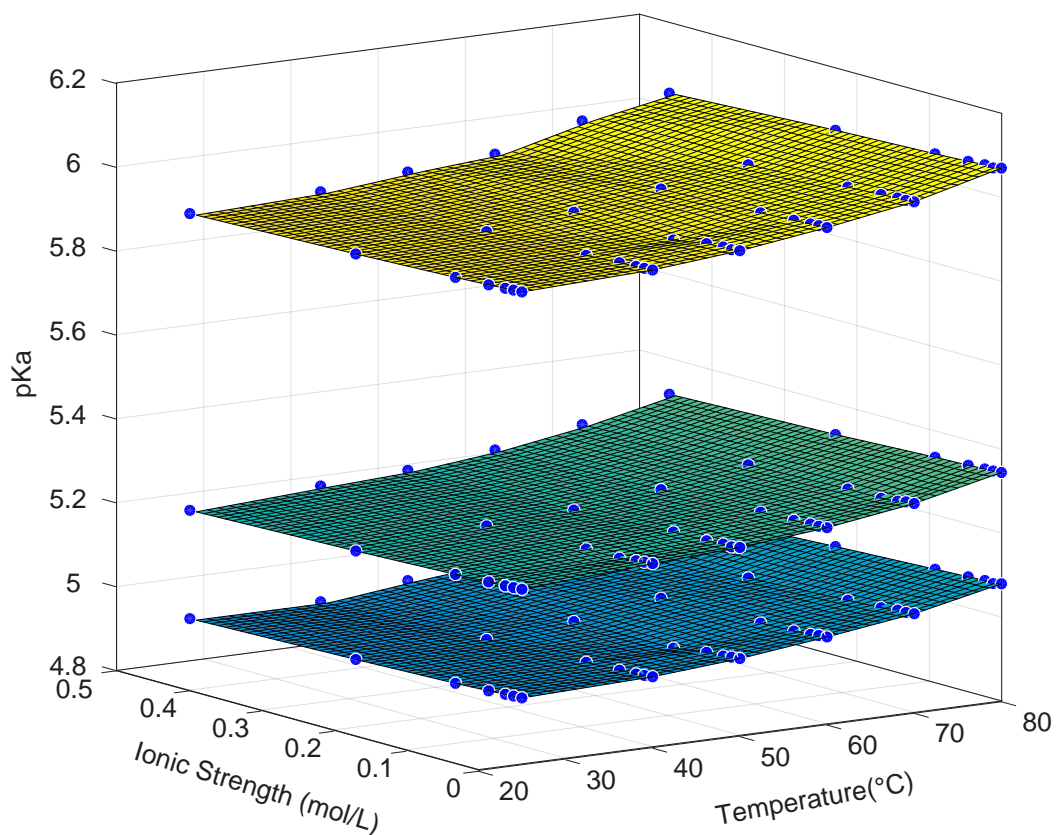


Figure 8-17. Acetic acid pK_a within 80% (yellow), 50% (green), 30% (blue) wt. MEG as a function of ionic strength and temperature. Data points = measured pK_a (Appendix D Table D1), mesh plot = calculated pK_a (Equation (8-12)).

8.5 Conclusion

The dissociation constants of four organic acids commonly present within MEG regeneration systems and MDEA were measured at varying MEG concentrations (0-80 wt. %) and temperatures (25-80°C). The change in measured pK_a of each species was found to be primarily influenced by the change in dielectric constant of the solution as MEG concentration increased (linear with respect to MEG mole fraction). Furthermore, the influence of temperature on the measured pK_a of each species was determined and the thermodynamic properties of the dissociation process including Gibbs free energy $\Delta G^\circ \text{ kJ.mol}^{-1}$ standard enthalpy $\Delta H^\circ \text{ kJ.mol}^{-1}$ and entropy $\Delta S^\circ \text{ kJ.mol}^{-1}.K^{-1}$ were calculated at 25°C using the van't Hoff Equation.. Good agreement was found between the measured dissociation constants and thermodynamic properties of each species within aqueous solution to prior published literature. The influence of ionic strength on acetic acid and MDEA dissociation was also determined with the measured pK_a changing linearly with respect to ionic strength. A model has been proposed to calculate the pK_a of acetic acid and MDEA within MEG solutions of varying concentration, temperature and ionic strength. The proposed models had a maximum average error of 0.413% and 0.265% for acetic acid and MDEA respectively.

9.0 EXPERIMENTAL VAPOUR-LIQUID EQUILIBRIUM DATA FOR BINARY MIXTURES OF METHYLDIETHANOLAMINE IN WATER AND ETHYLENE GLYCOL UNDER VACUUM

9.1 Introduction

Mono-Ethylene glycol (MEG) and N-methyldiethanolamine (MDEA) are common chemicals used in the natural gas processing industry. The injection of MEG is performed to prevent the formation of natural gas hydrates within transportation pipelines [1, 4, 6]. Whereas MDEA and other alkanolamines are typically used as chemical absorbents for the removal of carbon dioxide and hydrogen sulphide during natural gas processing [300, 301]. Furthermore, the application of MDEA within natural gas transportation extends to its use as a basic compound suitable for pH stabilisation corrosion control [4, 17].

pH stabilisation corrosion control is performed to promote the formation of an iron carbonate protective film by artificially increasing system pH [4, 16, 17, 72]. MDEA as a pH stabiliser may be preferable to salt based (hydroxide or carbonate) chemicals due to its ability to be recovered during vacuum reclamation minimising operational losses and dosing requirements [4, 51]. Moreover, the thermal stability of MDEA is advantageous during industrial MEG regeneration where exposure to high temperature (120-140°C)^[1] is required allowing multiple regeneration cycles before thermal degradation occurs [277, 278].

Vacuum reclamation is often performed to prevent the accumulation of salts within the MEG regeneration loop [2, 9, 32]. The vacuum reclamation process entails the vaporisation of MEG to remove non-volatile salt compounds. Vacuum reclamation of MEG is typically performed at low pressure (≈ 100 mbar [8, 32, 38]) to minimise the required operational temperature (120-150°C [2, 38]). Low temperature vaporisation of MEG is desired to prevent its degradation [8, 9]. However, the vacuum reclamation process may inadvertently lead to MDEA losses due its higher boiling point in comparison to MEG. Therefore, ensuring the vaporisation of MDEA alongside MEG is important aspect of MEG regeneration during pH stabilisation to minimise MDEA losses.

Alternatively, the removal of MDEA within MEG regeneration systems operating under pH stabilisation control is essential following formation water breakthrough [8, 9]. The combined presence of MDEA (high pH) and divalent cations including calcium, magnesium and barium presents a scaling risk within both transportation lines and equipment operating at high temperature (heat exchangers, MEG regeneration system) [9, 218]. MDEA will react in the presence of CO₂ to form bicarbonate [4, 9, 218] facilitating the formation of scaling products including CaCO₃. pH stabilisation chemicals such as MDEA must therefore be removed to facilitate switch over to more scaling friendly Film Forming Corrosion Inhibitors (FFCIs). The removal of MDEA can be achieved via vacuum reclamation systems alongside mineral salts [9].

Therefore, knowledge of the vapour-liquid equilibrium (VLE) of MDEA with respect to MEG at low pressure is essential for the design of separation equipment. Current literature for MDEA VLE data in MEG and water solutions is limited at the low-pressure conditions necessary for MEG vacuum reclamation. This work outlines the VLE of MDEA with respect to water and MEG under low pressure conditions (40-10 kPa) and (20-5 kPa) respectively. However, the operating conditions of reclamation systems for MEG regeneration may ultimately depend on whether MDEA removal or retention is desired.

9.2 Experimental Methodology

9.2.1 Materials

MDEA and MEG were purchased from Chem Supply with a mass purity greater than 99.5% wt. and were used without further purification. Where water was used, deionised water with a resistivity of 18.2 MΩ.cm was utilised. The physical properties of water, MEG and MDEA including refractive index of the pure solutions their boiling points and critical properties are outlined by Table 9-1 and Table 9-2.

Table 9-1. Chemicals, suppliers and purity

Chemical	Supplier	CAS No.	Purity (mass %)
Ethylene glycol	Chem Supply	107-21-1	>99.5
Methyldiethanolamine		105-59-9	>99
Water			18.2 MΩ.cm

Table 9-2. Refractive indices (n_D), boiling points and critical properties^a

Chemical	Refractive indices (n_D) at 20°C, 101.325 kPa		Boiling point (°C) at 101.325 kPa	T_c/K	P_c/MPa	Z_c
	Literature	Measured ^a				
Water	1.3325	1.3323	100	647.096 ^[302]	22.064 ^[302]	0.23 ^[302]
MEG	1.4318 ^[303, 304]	1.4315	197.3 ^[305]	645 ^[131, 306]	8.573 ^[131]	0.262 ^[131]
MDEA	1.4642 ^[307]	1.4684	247 ^[279]	678 ^[131, 306]	3.88 ^[131]	0.254 ^[131]

^aStandard uncertainties are $u(n_D) = 0.0003$, $u(T) = 0.1^\circ\text{C}$ and $u(P) = 0.1\text{ kPa}$

9.2.2 Apparatus and Procedure

The VLE data of the MEG-MDEA system under vacuum was generated using a Heidolph vacuum rotary evaporation system. The system is designed to perform vacuum distillation and was modified to permit the generation of VLE data using the flow-scheme shown in Figure 9-1.

The system is capable of generating a vacuum down to 20 mbar with an accuracy of ± 1 mbar. Furthermore, the system is capable of producing a maximum solution temperature within the heating flask of $180^{\circ}\text{C} \pm 0.1^{\circ}\text{C}$ using an oil heating bath.

The system was modified from its original design by placing a manually adjustable valve between the condenser and condensed liquid storage to continuously return the condensed vapour to the flask. Liquid reflux of the condensed vapour was maintained until a constant temperature of the liquid and vapour phases was achieved indicating equilibrium. Following temperature stabilisation, the valve was opened to allow accumulation of the condensed vapour with the storage vessel. Liquid and vapour phase samples were extracted from the system and analysed by a combination of ion chromatography and refractive index measurement.

Ion chromatography was performed using a Dionex ICS-2100 IC System. For comparison purposes, the mole fraction of MDEA was also measured via refractive index at 20°C using an ATAGO PAL-BX/RI refractometer with an accuracy of ± 0.0003 . The calibration curve of n_D vs mole fraction (MDEA) is given by Figure 9-2. The MDEA concentration was calculated using the n_D of the sample and a polynomial equation fitted to the respective calibration curve. Furthermore, nitrogen was continuously introduced into the rotary flask to prevent the thermal degradation of MDEA and MEG in the presence of oxygen. Thermal degradation would otherwise result in discolouration that would impact refractive index measurement [3, 5, 39]

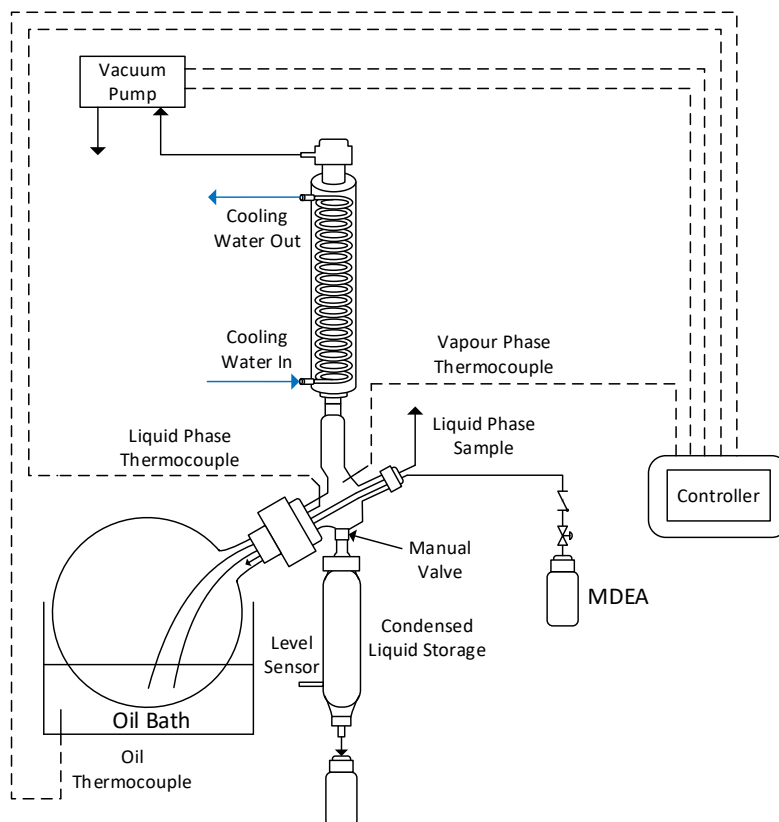


Figure 9-1. Experimental apparatus (Heidolph Hei-VAP Rotary Evaporator)

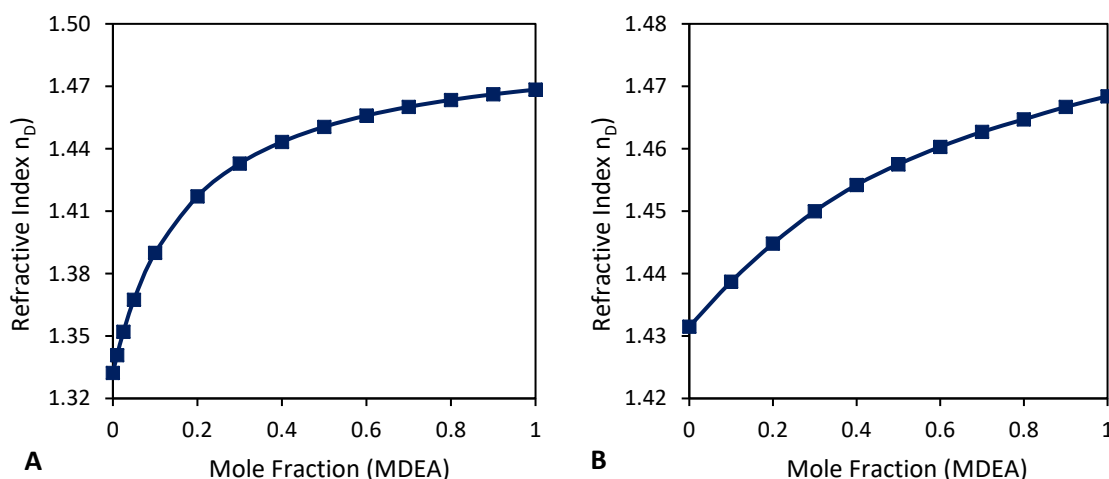


Figure 9-2. Refractive index vs. MDEA mole fraction calibration curve at 20°C, 101.325 kPa.
A) Water-MDEA, B) MEG-MDEA

9.3 Results and Discussion

The experimental VLE data of the water-MDEA at $P = (40, 20, 10)$ kPa and MEG-MDEA $P = (20, 10$ and $5)$ kPa binary systems is presented in Table 9-3. To assess the applicability of using the modified rotary evaporator for generation of VLE data, the water-MDEA VLE data at 40 kPa was compared to literature data reported by Voutsas [308] with good agreement found (Figure 9-3). Furthermore comparison was also made to the limited water-MDEA VLE data reported by Barreau [309] for water-MDEA at 10 kPa with good agreement again found (Figure 9-5). Likewise, comparison of the VLE data generated for the MEG-MDEA system was compared to the literature data reported by Yang [131] (Figure 9-6). Due to the temperature limitations of the rotary evaporator system VLE data up to approximately 175°C was generated for the MEG-MDEA system at 20 kPa.

The liquid-phase activity coefficients γ for each chemical was calculated from the experimental data by Equation (9-1)^[310]. Where, p_i^S represents the vapour pressure of the pure component, i at equilibrium temperature^[131]. As the VLE data was generated at low pressure, the behaviour of the vapour phase can be considered ideal and the ϕ factor considered negligible^[131, 132]. Estimation of water vapour pressure was performed using the empirical correlation proposed by Wagner and Pruß [311] as per Equation (9-2). The correlation provides accurate estimation of water vapour pressure over a wide range of temperature (273.15-633.15K). Conversely, estimation of ethylene glycol vapour pressure was achieved using the Antoine coefficients listed Table 9-4^[312]. For MDEA, the vapour pressure was calculated via the Clausius–Clapeyron type equations proposed by Voutsas [308] and Xu [313] given by Equations (9-3) and (9-4) respectively. The equation used to calculate MDEA vapour pressure was dependant on equilibrium temperature with the applicable temperature ranges of Equations (9-3) and (9-4) being 413-513K^[308] and 323-383K^[313] respectively.

Table 9-3. VLE data and calculated activity coefficients (γ) for Water-MDEA and MEG MDEA systems^a

Water-MDEA					MEG-MDEA				
x ₂	y ₂	γ ₁	γ ₂	T/K	x ₂	y ₂	γ ₁	γ ₂	T/K
40 kPa					20 kPa				
0.000	0.000	1.000		349.02	0.000	0.000	1.000		423.01
0.356	0.0015	0.993	1.101	360.12	0.031	0.004	0.993	0.763	423.56
0.532	0.0035	0.992	1.042	368.57	0.088	0.013	0.998	0.755	424.81
0.756	0.013	0.932	0.925	388.95	0.135	0.022	0.986	0.790	426.25
0.825	0.023	0.950	0.924	398.56	0.283	0.059	0.963	0.814	430.89
0.880	0.042	0.977	0.939	409.65	0.385	0.102	0.956	0.854	434.25
0.912	0.065	1.009	0.939	418.65	0.434	0.127	0.939	0.855	436.37
0.928	0.087	1.006	0.934	425.32	0.491	0.154	0.928	0.882	438.65
0.939	0.109	1.001	0.930	430.65	0.572	0.210	0.893	0.913	442.60
0.950	0.142	1.037	0.968	435.92	0.621	0.256	0.872	0.930	445.11
0.966	0.221	1.034	0.941	447.59	0.676	0.315	0.851	0.992	447.50
0.980	0.359	1.107	1.000	458.69	1.000	1.000		1.000	467.46
1.000	1.000		1.000	488.42	10 kPa				
20 kPa					0.000	0.000	1.000		406.01
0.000	0.000	1.000		333.20	0.041	0.005	0.992	0.620	406.65
0.075	0.0001	1.016	1.197	334.56	0.078	0.011	0.990	0.687	407.50
0.224	0.0005	1.010	1.151	338.57	0.110	0.016	0.992	0.727	408.15
0.295	0.0008	1.006	1.133	340.80	0.204	0.036	0.978	0.842	410.67
0.446	0.0017	0.931	0.991	348.20	0.366	0.092	0.940	0.980	415.69
0.613	0.0038	0.914	0.913	357.50	0.460	0.140	0.926	1.002	418.83
0.675	0.0054	0.893	0.881	362.50	0.610	0.239	0.888	0.986	425.15
0.785	0.012	0.862	0.824	374.50	0.668	0.300	0.862	1.000	428.03
0.856	0.022	0.902	0.832	384.56	0.755	0.413	0.808	0.992	433.13
0.912	0.045	0.955	0.856	397.56	0.832	0.541	0.789	0.988	437.49
0.955	0.112	1.031	0.922	414.80	1.000	1.000		1.000	448.32
0.980	0.260	1.184	0.982	432.60	5 kPa				
1.000	1.000		1.000	467.58	0.000	0.000	1.000		390.40
10 kPa					0.039	0.005	0.984	0.804	391.10
0.000	0.0000	1.000		318.95	0.118	0.017	0.990	0.860	392.40
0.188	0.0003	0.972	1.111	323.65	0.201	0.034	0.995	0.873	394.00
0.276	0.0005	0.948	1.057	326.50	0.276	0.052	0.999	0.911	395.90
0.436	0.0011	0.954	1.012	331.60	0.363	0.082	0.968	0.918	398.79
0.565	0.0022	0.864	0.885	339.48	0.453	0.117	0.951	0.915	401.78
0.659	0.0037	0.798	0.782	346.89	0.598	0.210	0.931	0.928	407.14
0.766	0.0075	0.772	0.752	356.80	0.682	0.283	0.887	0.953	411.27
0.826	0.013	0.755	0.725	364.91	0.732	0.345	0.878	0.981	413.51
0.876	0.022	0.776	0.742	373.21	0.835	0.515	0.860	0.975	419.26
0.926	0.046	0.825	0.773	385.68	0.925	0.725	0.841	0.997	424.90
0.965	0.120	1.001	0.924	400.89	1.000	1.000		1.000	430.52
0.991	0.415	1.213	1.037	425.54					
1.000	1.000		1.000	448.42					

^aStandard uncertainties are $u(T) = 0.1$ K, $u(P) = 0.1$ kPa and $u(x,y) = 0.005$

$$\gamma_i = \frac{y_i P}{x_i p_i^s} \phi_i \quad (i = 1, 2) \quad (9-1)$$

$$\ln \left(\frac{P_{\text{Water}}}{P_c} \right) = \frac{T_c}{T} (a_1 \theta + a_2 \theta^{1.5} + a_3 \theta^3 + a_4 \theta^{3.5} + a_5 \theta^4 + a_6 \theta^{7.5}) \quad (9-2)^{[311]}$$

$$\theta = 1 - \frac{T}{T_c}$$

$$\ln p^s = 26.1369 - \left(\frac{7588.516}{T} \right), \quad p^s = Pa \quad (9-3)^{[308]}$$

$$\ln p^s = 26.2942 - \left(\frac{7657.86}{T} \right), \quad p^s = Pa \quad (9-4)^{[313]}$$

Table 9-4. Water vapour pressure and MEG Antoine parameters

Water Equation (9-2) Parameters	a_1	a_2	a_3	a_4	a_5	a_6
	-7.8595178	1.84408259	-11.786649	22.6807411	-15.961871	1.80122502
MEG Antoine Parameters	A		B		C	
	8.0908		2088.94		-67.70	
	$\log(p_i^s/\text{mmHg}) = A - B/[(T/K) - C]$					

9.3.1 Correlation of VLE Data

Correlation of the experimental VLE data reported was performed using the NRTL, Wilson and UNIQUAC models. Regression of the respective binary parameters was performed using the objective function outlined by Equation (9-5) ^[131, 132] where γ_{exp} was calculated through Equation (9-1). The models and their respective equations are outlined by Table 9-5 with the utilised UNIQUAC parameters reported in Table 9-6. For the NRTL model, the non-randomness parameter α_{ij} was set to 0.3 ^[131, 314]. The regressed binary parameters for each model is presented in Table 9-7 and Table 9-8 for water-MDEA and MEG-MDEA respectively. The comparison of experimental data to calculated values is illustrated by Figures 9-3 to 9-5 for the water-MDEA system and Figures 9-6 to 9-8 for the MEG-MDEA system.

$$OF = \sum \left(\frac{\gamma_{exp} - \gamma_{cal}}{\gamma_{exp}} \right)^2 \quad (9-5)$$

Table 9-5. Activity coefficient models

NRTL	$\ln \gamma_i = x_j \left[\frac{\tau_{ji} g_{ji}^2}{(x_i + x_j g_{ji})^2} + \frac{\tau_{ij} g_{ij}^2}{(x_j + x_i g_{ij})^2} \right]$ $\tau_{ij} = \frac{g_{ij} - g_{jj}}{RT} \quad \tau_{ji} = \frac{g_{ji} - g_{ii}}{RT}$ $g_{ij} = \exp(-\alpha_{ij} \tau_{ij}) \quad g_{ji} = \exp(-\alpha_{ji} \tau_{ji}) \quad \alpha_{ij} = \alpha_{ji} = 0.3$
-------------	---

Table 9-6 Activity coefficient models continued

Wilson	$\ln \gamma_i = -\ln(x_i + A_{ij}x_j) + x_j \left(\frac{A_{ij}}{x_i + x_j A_{ij}} - \frac{A_{ji}}{x_j + x_i A_{ji}} \right)$ $A_{ij} = \frac{V_j}{V_i} \exp \left(-\frac{g_{ij} - g_{jj}}{RT} \right)$ $V_i = \frac{RT_{ci}}{P_{ci}} Z_{ci}^{\tau_i} \quad \tau_i = 1 + \left(1 - \frac{T}{T_{ci}} \right)^{\frac{2}{7}}$
UNIQUAC	$\ln \gamma_i = \ln \left(\frac{\phi_i}{x_i} \right) + \left(\frac{Z}{2} \right) q_i \ln \left(\frac{\theta_i}{\phi_i} \right) + \phi_j \left(l_i - \frac{r_i}{r_j} l_j \right) - q_i \ln(\theta_i + \theta_j \tau_{ji})$ $+ \theta_j q_i \left(\frac{\tau_{ji}}{\theta_i + \theta_j \tau_{ji}} - \frac{\tau_{ij}}{\theta_j + \theta_i \tau_{ij}} \right)$ $l_i = \left(\frac{Z}{2} \right) (r_i - q_i) - (r_i - 1)$ $\theta_i = \frac{x_i q_i}{x_i q_i + x_j q_j} \quad \phi_i = \frac{x_i r_i}{x_i r_i + x_j r_j}$ $\tau_{ij} = \exp \left(-\frac{g_{ij} - g_{jj}}{RT} \right) \quad \tau_{ji} = \exp \left(-\frac{g_{ji} - g_{ii}}{RT} \right)$

 Table 9-6. Molecule volume parameters r , area parameters q and Z parameter for the UNIQUAC Model

Chemical	r	q	Z
Water	0.92 ^[308, 315]	1.40 ^[308, 315]	
MEG	2.4080 ^[131, 312]	2.248 ^[131, 312]	10 ^[131, 315]
MDEA	4.94410 ^[131, 308]	4.268 ^[131, 308]	

Table 9-7. Water-MDEA binary interaction parameters

System	Water-MDEA		
Pressure	40 kPa	20 kPa	10 kPa
NRTL			
$g_{ij} - g_{jj}/J. \text{mol}^{-1}$	84.37	-135.34	98.10
$g_{ji} - g_{ii}/J. \text{mol}^{-1}$	-197.94	-119.53	-919.05
Wilson			
$g_{ij} - g_{jj}/J. \text{mol}^{-1}$	4856.33	4880.69	4378.64
$g_{ji} - g_{ii}/J. \text{mol}^{-1}$	-4289.02	-4872.10	-4998.23
UNIQUAC			
$g_{ij} - g_{jj}/J. \text{mol}^{-1}$	332.95	169.77	-332.11
$g_{ji} - g_{ii}/J. \text{mol}^{-1}$	594.60	527.19	357.00

Table 9-8. MEG-MDEA binary interaction parameters

System	MEG-MDEA		
Pressure	20 kPa	10 kPa	5 kPa
NRTL			
$g_{ij} - g_{jj}/J \cdot \text{mol}^{-1}$	-921.85	-566.61	-545.48
$g_{ji} - g_{ii}/J \cdot \text{mol}^{-1}$	-338.24	-662.28	-371.01
Wilson			
$g_{ij} - g_{jj}/J \cdot \text{mol}^{-1}$	-783.00	-743.31	-654.29
$g_{ji} - g_{ii}/J \cdot \text{mol}^{-1}$	1894.99	1547.58	1757.05
UNIQUAC			
$g_{ij} - g_{jj}/J \cdot \text{mol}^{-1}$	40.15	50.24	40.00
$g_{ji} - g_{ii}/J \cdot \text{mol}^{-1}$	72.33	70.65	65.11

9.3.1 Thermodynamic Consistency

The experimental VLE data was analysed using the semiempirical thermodynamic consistency test for isobaric binary VLE data proposed by Herington [316]. For isobaric VLE data, experimental data can be considered thermodynamically consistent when $(D-J)$ is less than 10 [131, 316, 317]. The variables D and J were evaluated using Equations (9-6) and (9-7) respectively where the values of “area+” and “area-” are calculated from the x_1 - $\ln(\gamma_1/\gamma_2)$ graph. The calculated D and J values for each system are summarised in Table 9-9 confirming thermodynamic consistency.

$$D = \left[\frac{(\text{area } +) - (\text{area } -)}{(\text{area } +) + (\text{area } -)} \right] \cdot 100 \quad (9-6)$$

$$J = 150 \cdot \frac{T_{\max} - T_{\min}}{T_{\min}} \quad (9-7)$$

Table 9-9. Herington thermodynamic consistency test

System	Pressure (kPa)	D-J
Water-MDEA	40	-31.62
	20	-26.59
	10	-27.91
MEG-MDEA	20	-4.01
	10	-4.38
	5	-5.12

Furthermore, the thermodynamic consistency test proposed by Van Ness [310] was also applied by comparing the predictions of the non-random two liquid (NRTL)^[314], Wilson^[318] and Universal Quasichemical (UNIQUAC)^[315] models to the experimental data. The model residuals were plotted against the liquid-phase composition, x_1 to determine if the deviations scatter uniformly about zero [132]. If the VLE data is thermodynamically consistent, the residual plots

should show no clear trend else systemic errors may be present ^[132]. The residual plots of δT , δy_1 and $\delta \ln(\gamma_1/\gamma_2)$ for the MEG-MDEA system is illustrated by Figures 9-9 to 9-11 showing the experimental data is thermodynamically consistent. The water-MDEA system showed similar consistency.

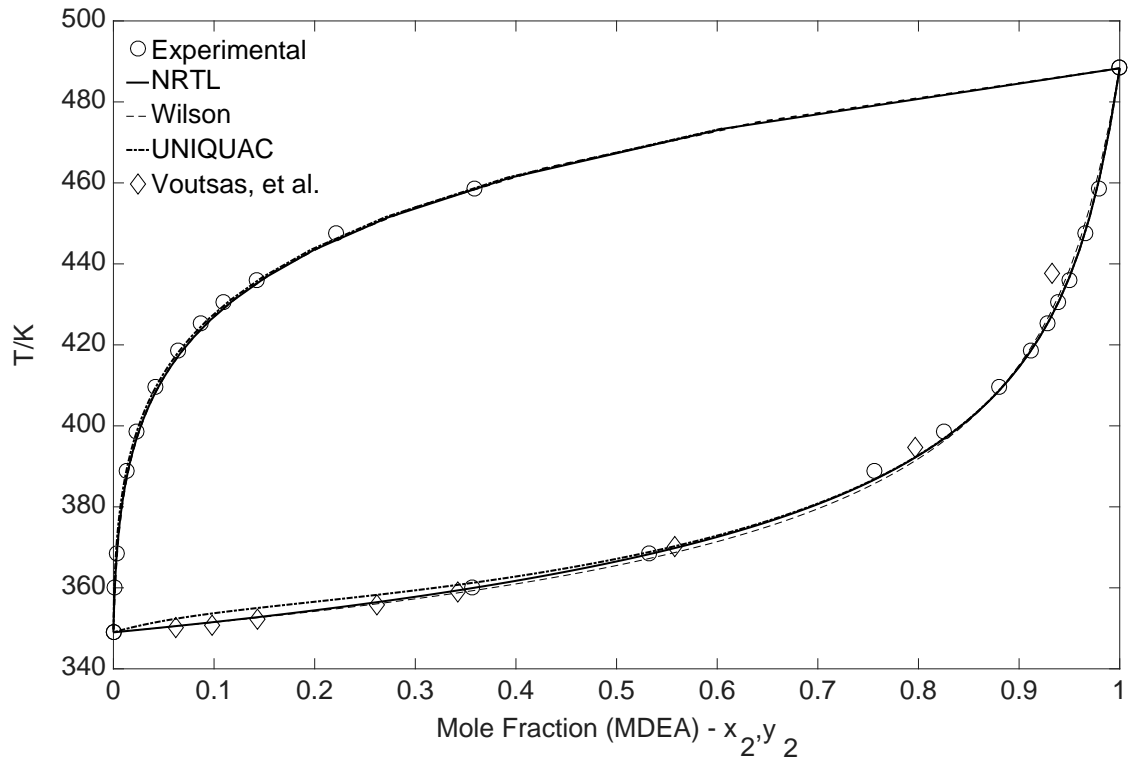


Figure 9-3. VLE data for water-MDEA at 40 kPa

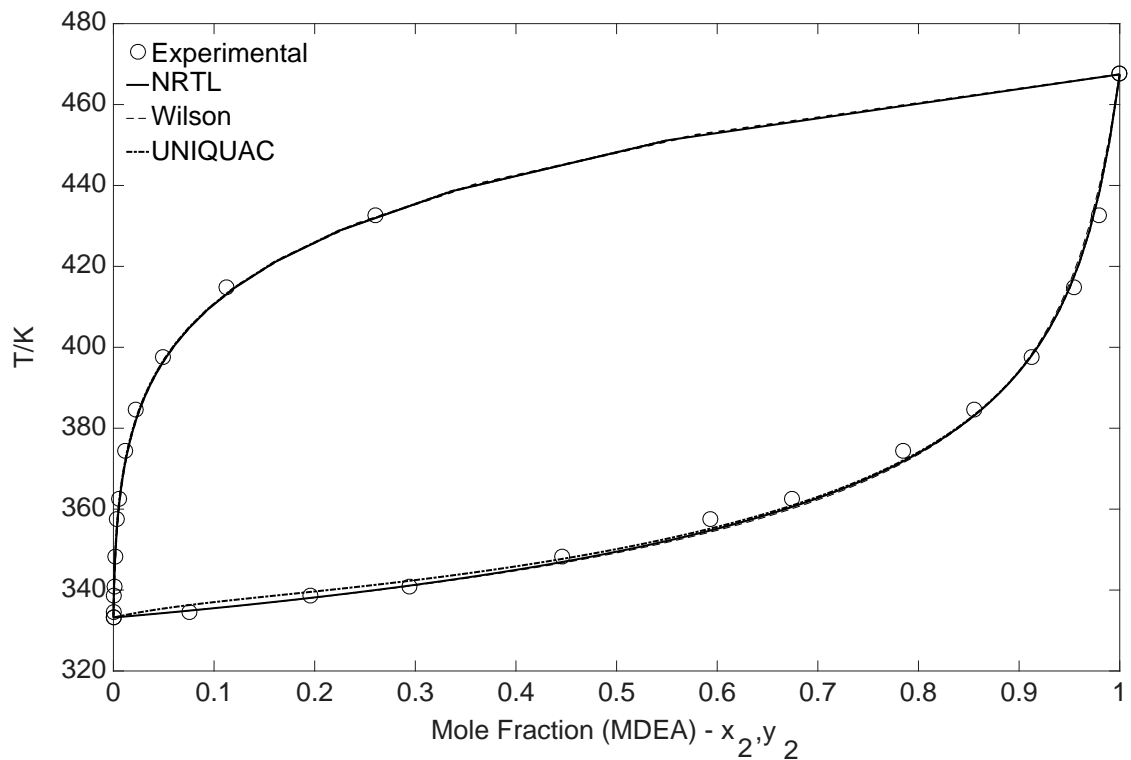


Figure 9-4. VLE data for water-MDEA at 20 kPa

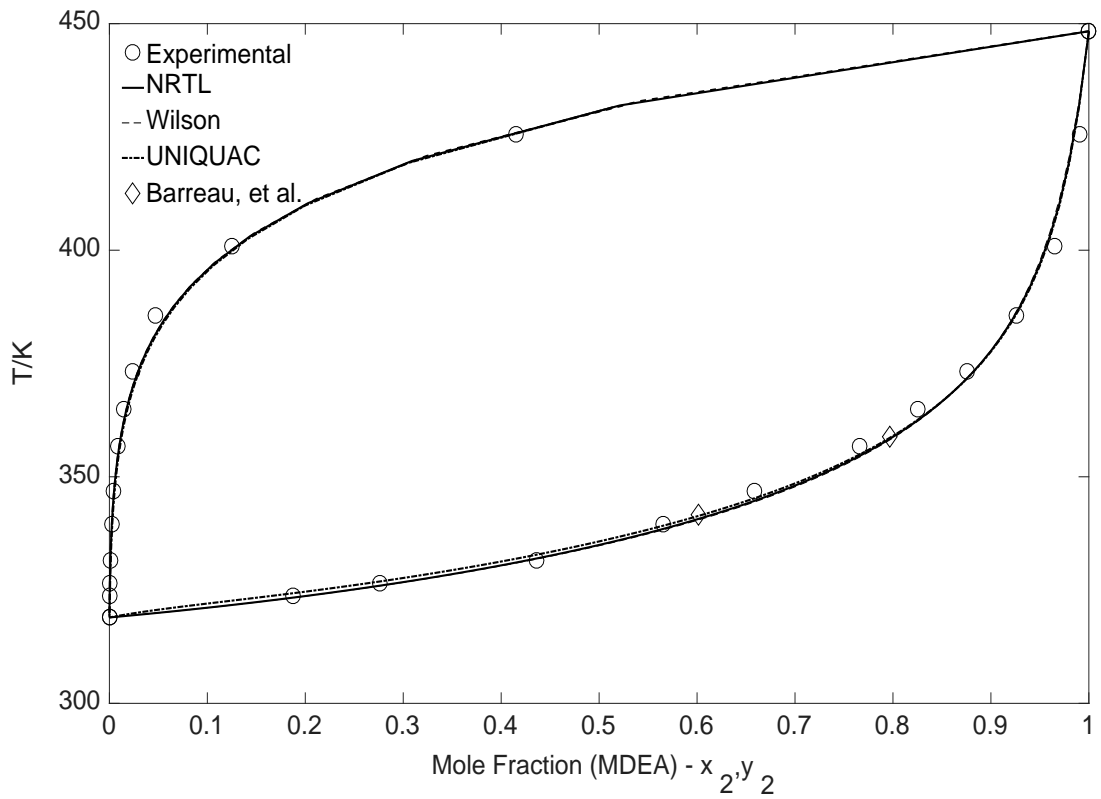


Figure 9-5. VLE data for water-MDEA at 10 kPa

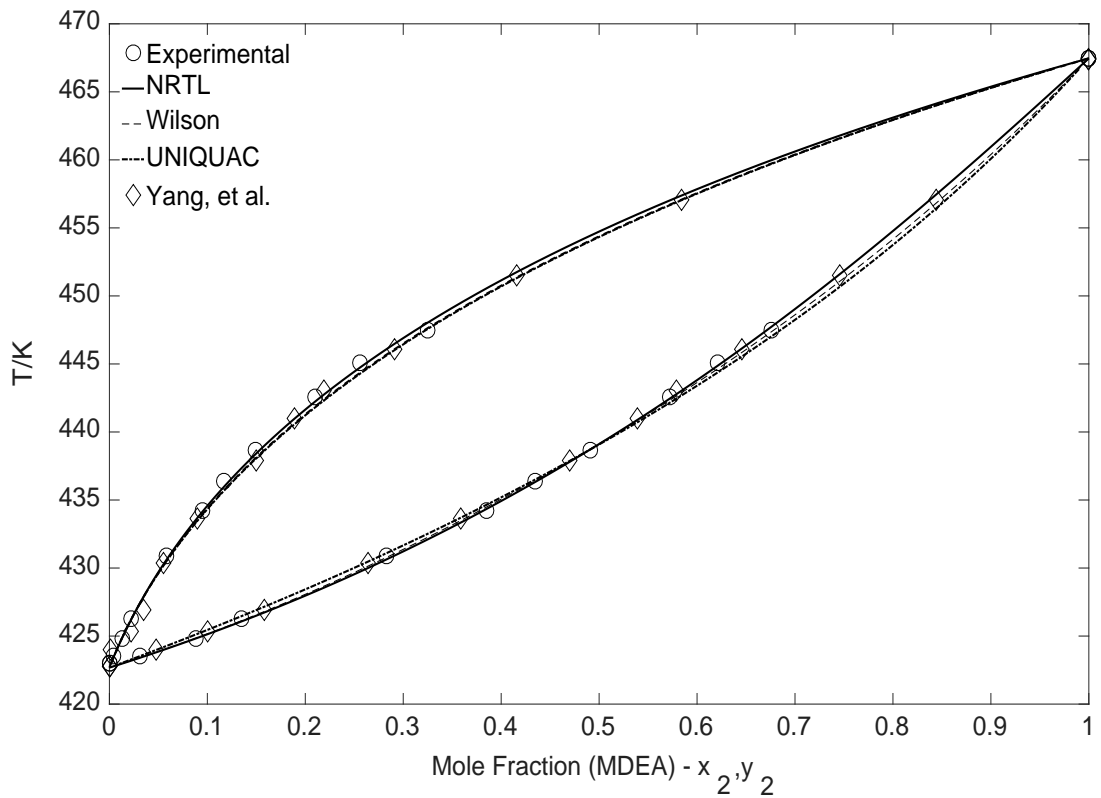


Figure 9-6. VLE data for MEG-MDEA at 20 kPa

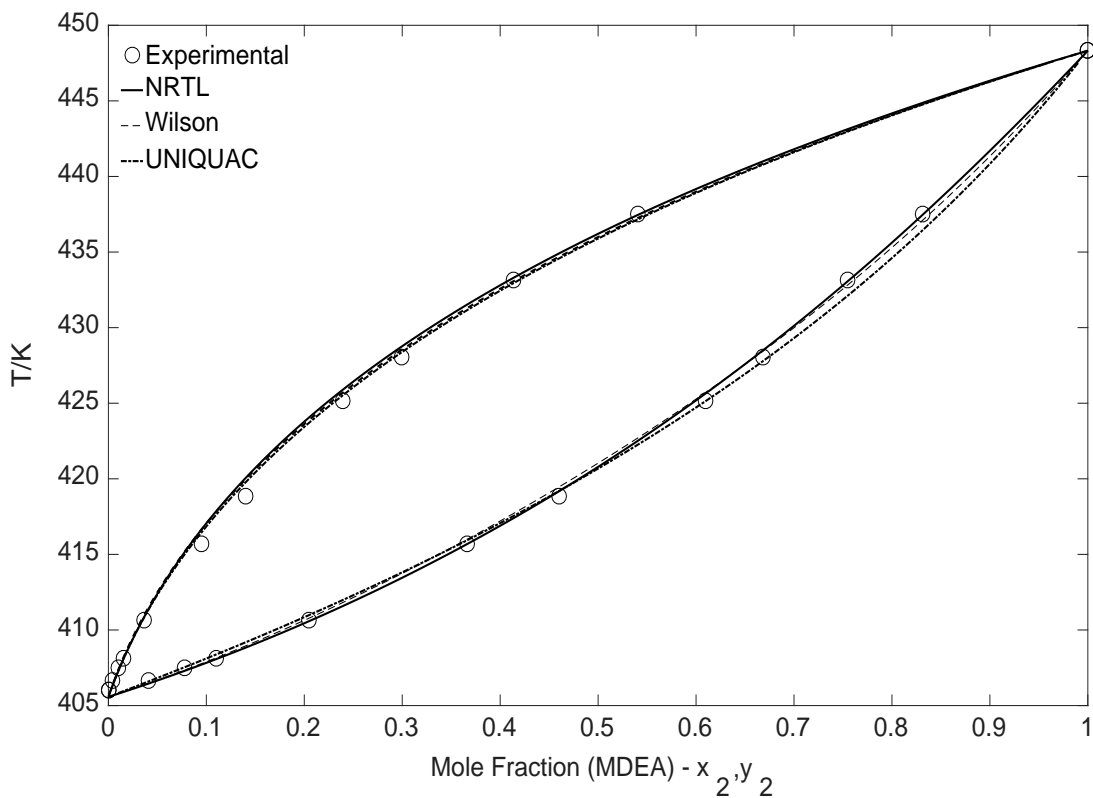


Figure 9-7. VLE data for MEG-MDEA at 10 kPa

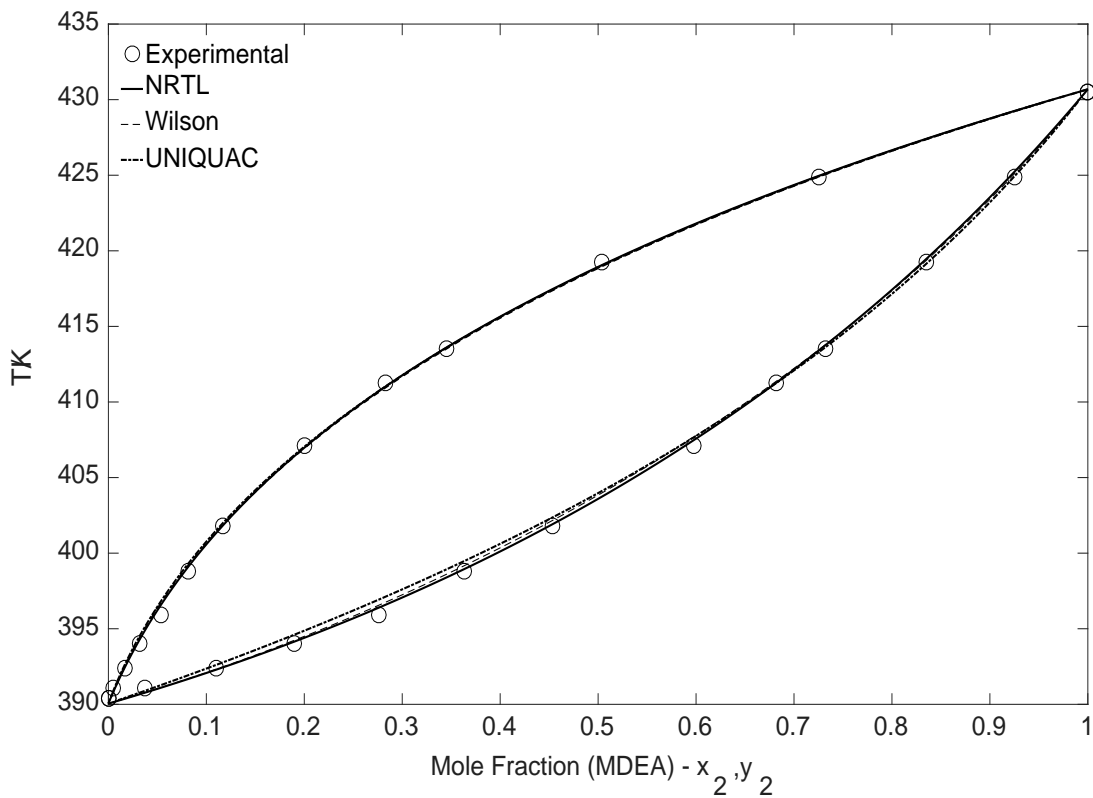


Figure 9-8. VLE data for MEG-MDEA at 5 kPa

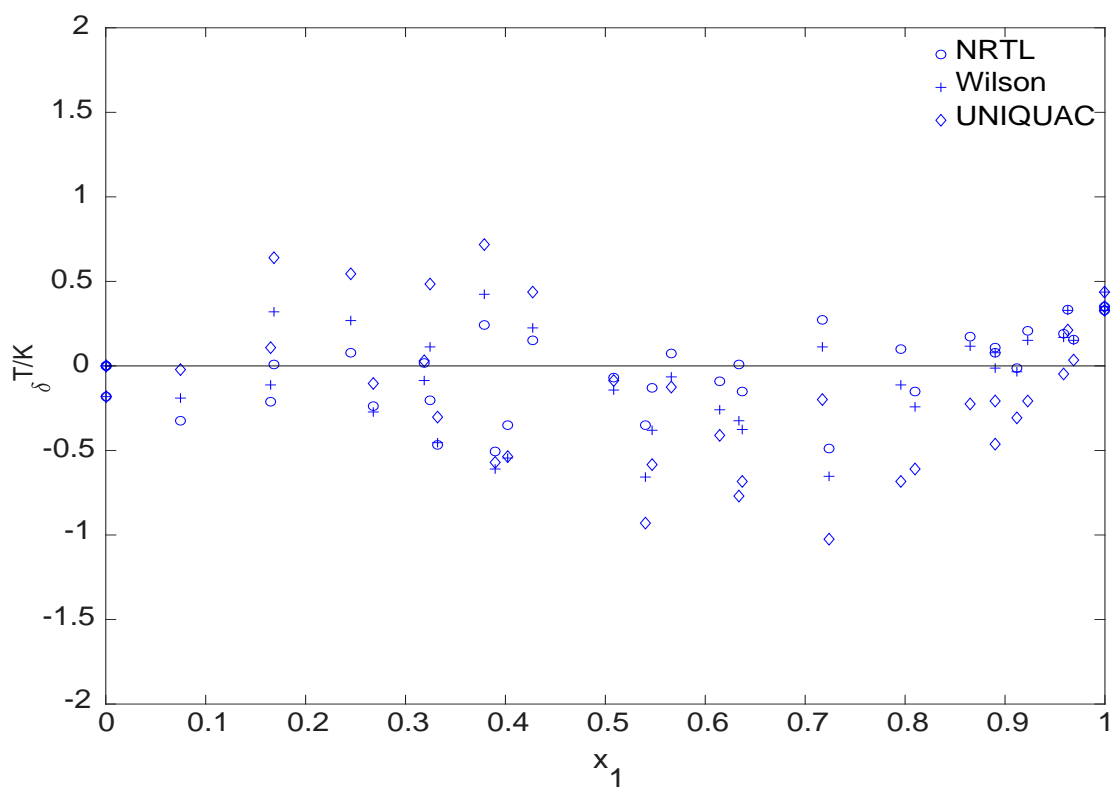


Figure 9-9. MEG-MDEA δT residual

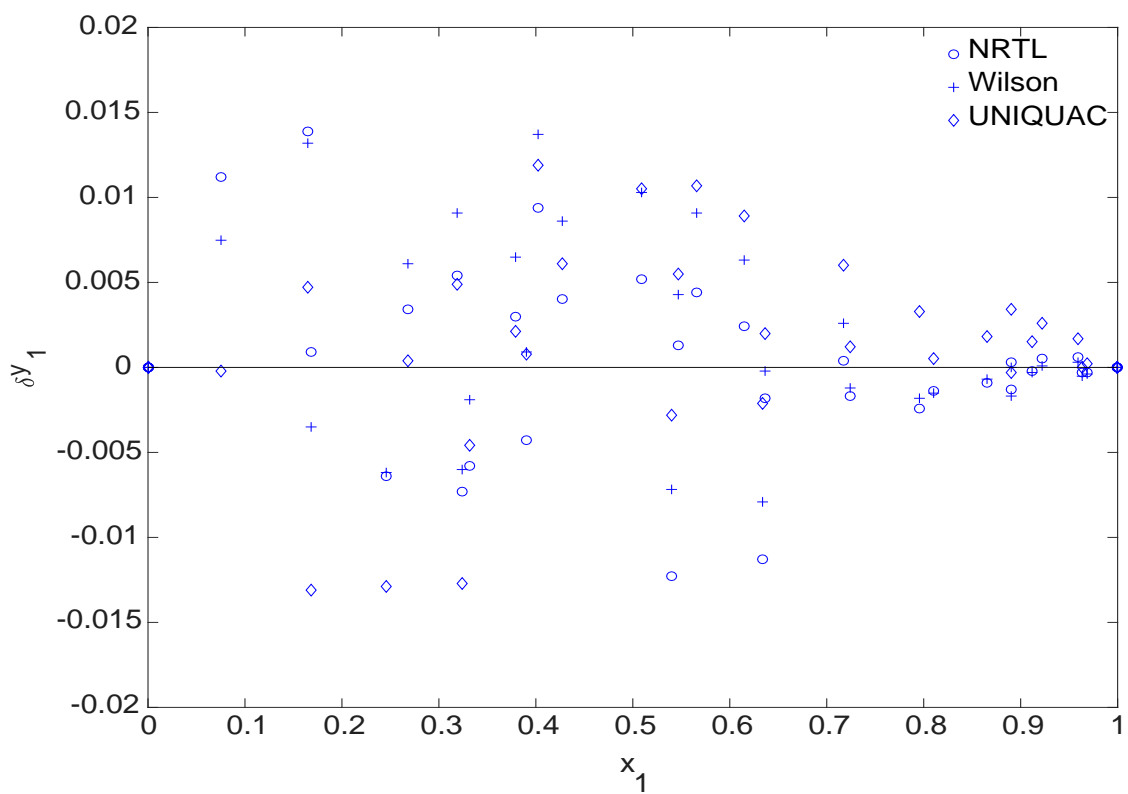
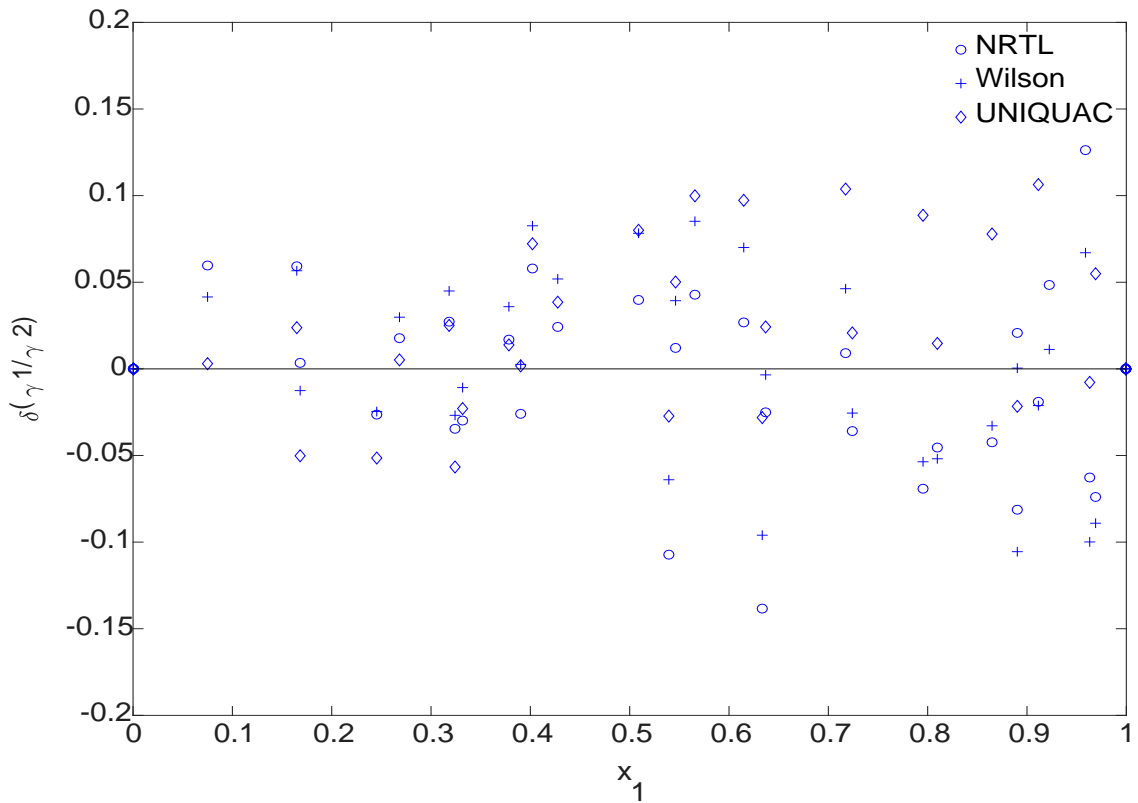


Figure 9-10. MEG-MDEA δy_1 residual


 Figure 9-11. MEG-MDEA $\delta(\gamma_1/\gamma_2)$ residual

9.3.2 Analysis of Model Accuracy

To assess the accuracy of the regressed binary parameters and corresponding model fit, the root-mean-square (RMS) deviations δT , δy_1 , $\delta \ln(\gamma_1/\gamma_2)$ were calculated via Equation (9-8)^[132]. The respective RMS and are presented in Tables 9-10 and 9-11 for the water and MEG MDEA systems. Comparative RMS values to the work of Kim [132] and Wang [319] were calculated in terms of $\delta y_1 - \delta \ln(\gamma_1/\gamma_2)$ and $\delta T - \delta y_1$ respectively. The UNIQUAC model was found on average to give a higher RMS value, particularly in terms of $\delta T/K$ suggesting the NRTL and Wilson models provide a better fit. The lower accuracy of the UNIQUAC model may be a result of the two regressed parameters being insufficient to accurately model the experimental data [320].

$$\text{RMS } \delta X = \sqrt{\sum_{i=1}^n \frac{(X_i - X_{\text{calc}})^2}{n}} \quad (9-8)$$

To further assess the validity of the model fits, the VLE analysis method suggested by Mathias [321] was applied. Figures 9-12 to 9-14 compare the relative volatility calculated via the reported experimental MEG-MDEA VLE data and those calculated through the respective activity coefficient models. The deviation of the modelled results in comparison to experimental

data appears to be greatest at the lower MDEA concentration region as suggested by Mathias [321]. This is primarily due to the low concentration of MDEA within the vapour phase ($y_2 < 0.01$) where the reported measurement uncertainty ($u(x,y) = 0.005$) can lead to a significant change in calculated relative volatility.

The percentage error in modelled MDEA K-values with respect to the experimental data is illustrated by Figure 9-15 where good agreement between experimental and NRTL and Wilson models was found. The absolute error for the NRTL and Wilson models was typically below 2%. Similar agreement was also found for the reported water-MDEA experimental data within the higher vapour-MDEA concentration regions ($x_2 > 0.4$) (Figure 9-16). However, the effect of the measurement uncertainty was found to be more pronounced for the water-MDEA system at low vapour MDEA concentrations. Although a significant fraction of MDEA was present within the liquid phase only minimal amounts were present within the vapour due to the extremely high relative volatility of water to MDEA. The resulting low concentration of MDEA, coupled with the relatively high measurement uncertainty at such low concentrations lead to the large error in calculated K-values.

Table 9-10. Water-MDEA RMS error for model fitting

System	Water-MDEA		
	40 kPa	20 kPa	10 kPa
NRTL			
RMS $\delta T/K$	0.829	0.810	0.990
RMS δy_1	0.024	0.021	0.036
RMS $\delta \ln(\gamma_1/\gamma_2)$	0.155	0.160	0.259
Wilson			
RMS $\delta T/K$	0.719	0.812	0.899
RMS δy_1	0.037	0.029	0.036
RMS $\delta \ln(\gamma_1/\gamma_2)$	0.190	0.170	0.259
UNIQUAC			
RMS $\delta T/K$	1.298	1.301	1.354
RMS δy_1	0.053	0.050	0.064
RMS $\delta \ln(\gamma_1/\gamma_2)$	0.251	0.260	0.373

Table 9-11. MDEA-MDEA RMS error for model fitting

System	MEG-MDEA		
	40 kPa	20 kPa	10 kPa
NRTL			
RMS $\delta T/K$	0.178	0.272	0.265
RMS δy_1	0.003	0.006	0.006
RMS $\delta \ln(\gamma_1/\gamma_2)$	0.034	0.069	0.045
Wilson			
RMS $\delta T/K$	0.203	0.338	0.336
RMS δy_1	0.006	0.004	0.007
RMS $\delta \ln(\gamma_1/\gamma_2)$	0.054	0.046	0.056
UNIQUAC			
RMS $\delta T/K$	0.345	0.478	0.463
RMS δy_1	0.017	0.016	0.014
RMS $\delta \ln(\gamma_1/\gamma_2)$	0.072	0.111	0.109

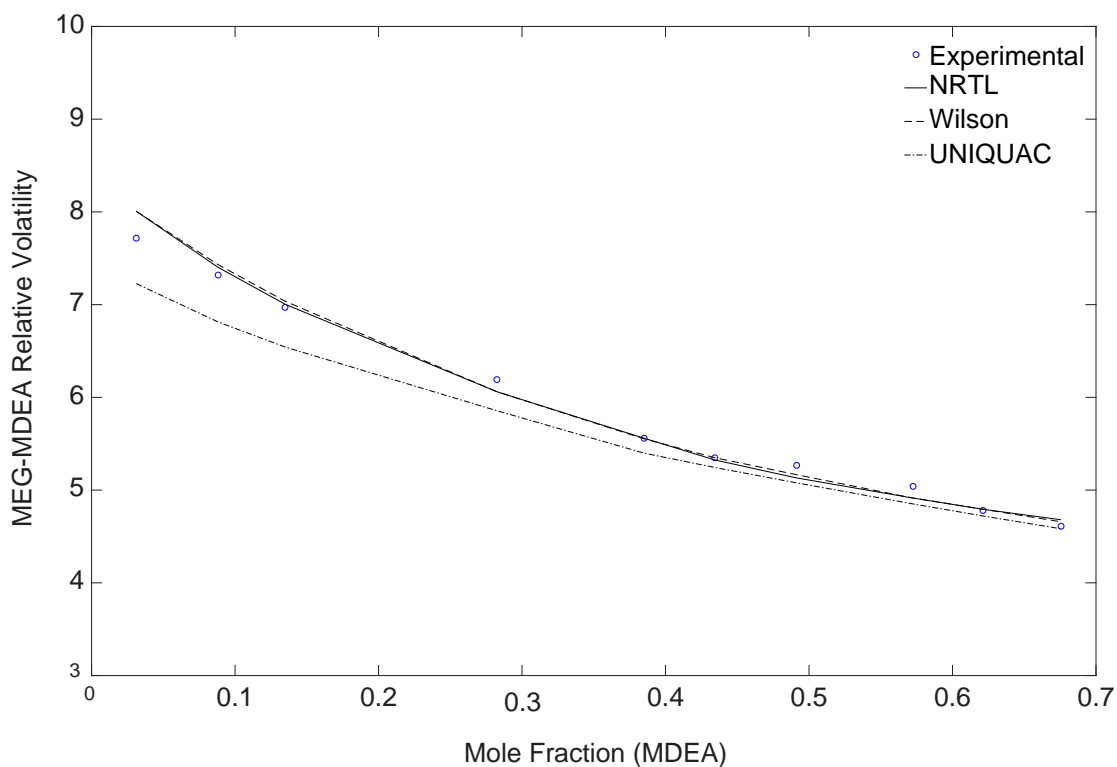


Figure 9-12. Comparison of experimental to modelled relative volatility for MEG-MDEA at 20 kPa

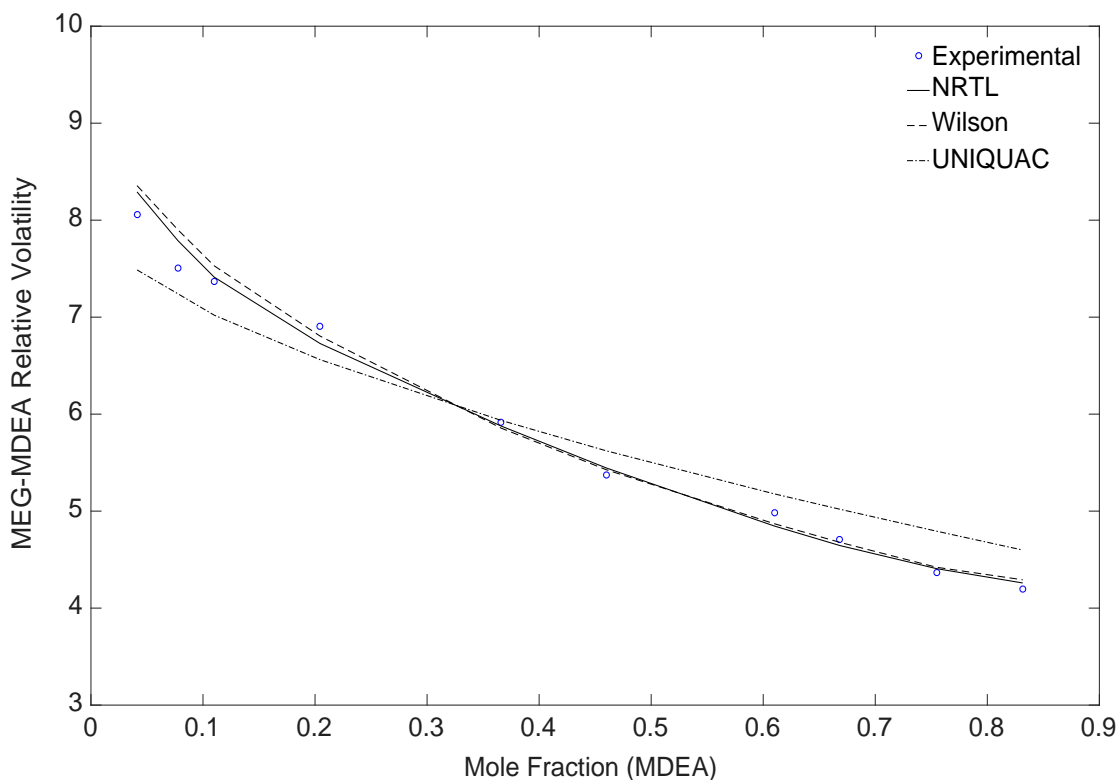


Figure 9-13. Comparison of experimental to modelled relative volatility for MEG-MDEA at 10 kPa

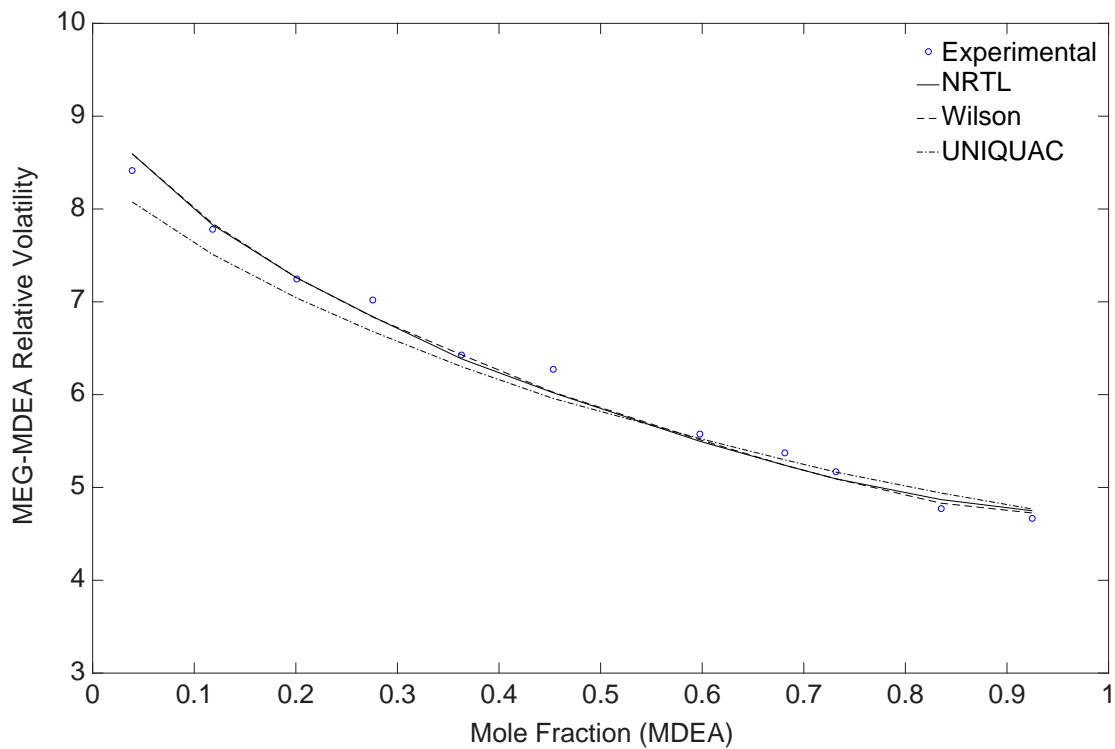


Figure 9-14. Comparison of experimental to modelled relative volatility for MEG-MDEA at 5 kPa

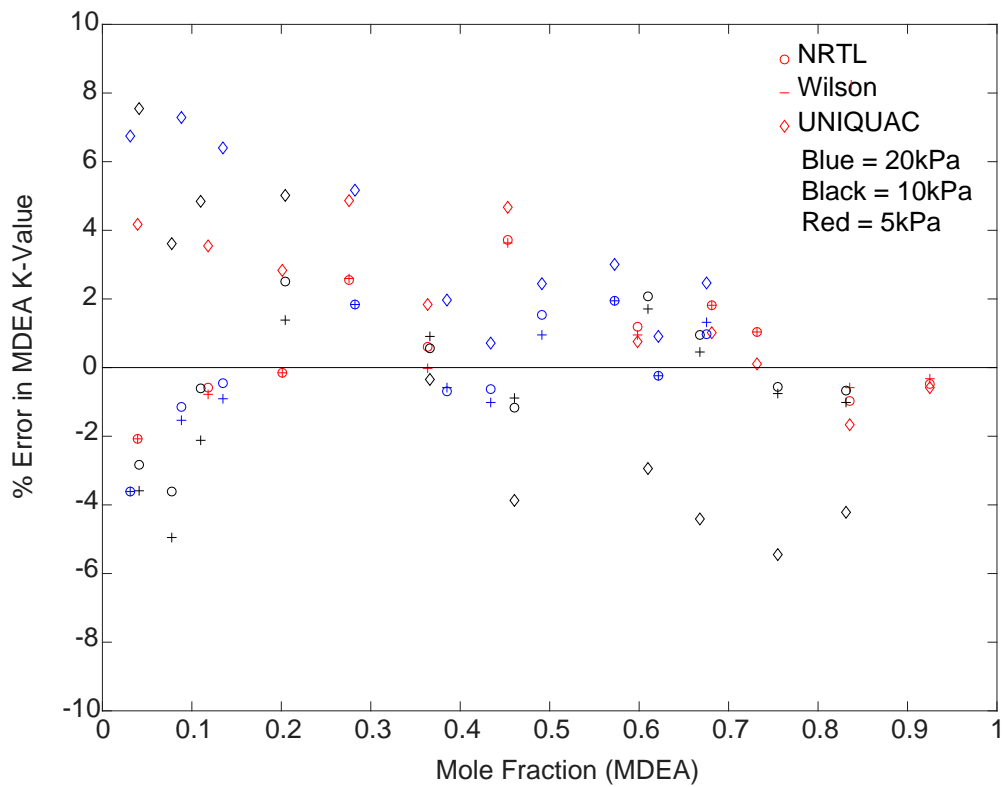


Figure 9-15. Percentage error in model K-values in comparison to experimental data for MEG-MDEA

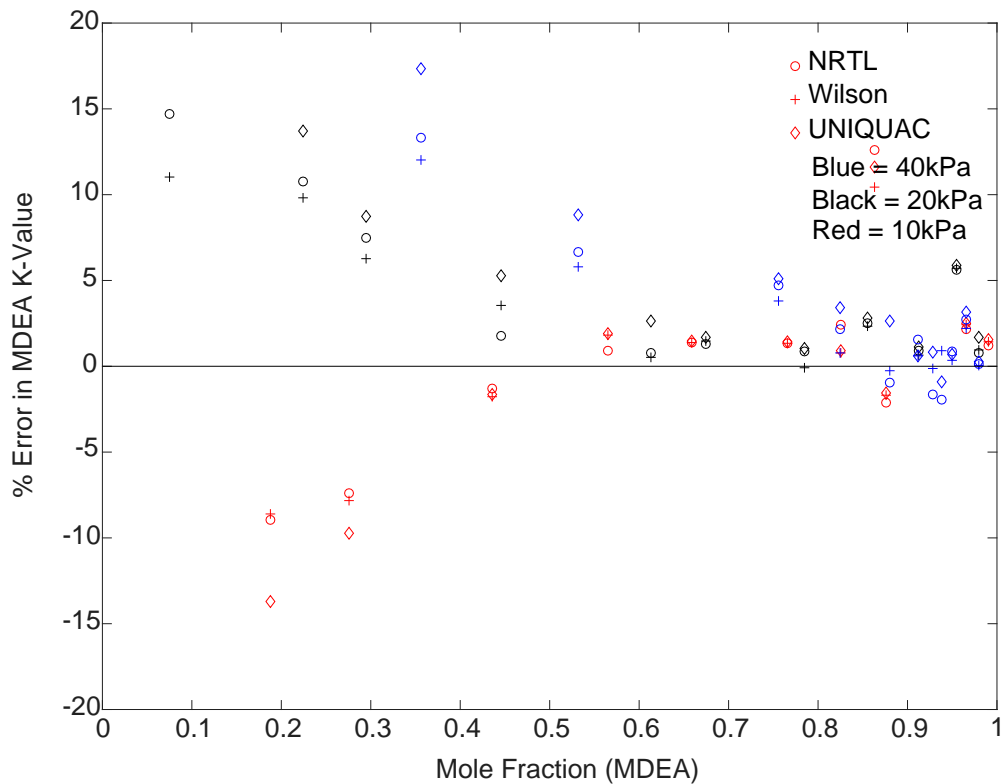


Figure 9-16. Percentage error in model K-values in comparison to experimental data for Water-MDEA

9.4 Conclusion

VLE for the water-MDEA and MEG-MDEA binary systems has been generated experimentally under low pressure conditions (40-5) kPa. Activity coefficients and binary interaction parameters for the binary systems were subsequently fit to the NRTL, Wilson and UNIQUAC models. The experimental data was analysed using the Herington [316] and Van Ness [310] thermodynamic consistency tests and found to be consistent. Comparison was also made to the limited MDEA VLE data reported by Voutsas [308], Yang [131] and Barreau [309] with good agreement found. The VLE data generated within this study is applicable for low pressure separation of MDEA from water and MEG solutions such as vacuum reclamation during industrial MEG regeneration.

10.0 CONCLUSION: SUMMARY, RELEVANCE OF WORK TO INDUSTRY AND RECOMMENDATIONS FOR FUTURE WORKS

The use of MEG injection to prevent the formation of gas hydrates is an important aspect of continued flow assurance for many recent and future natural gas developments. As such, improved understanding of chemical and physical behaviour within MEG systems, improved corrosion inhibition strategies and solutions to issues arising during MEG regeneration can have significant implications on industrial MEG usage. The primary objectives of this research were to identify, through consultation with industry, various operational issues and uncertainties faced within major MEG regeneration systems including the largest MEG regeneration system operating in Western Australia. Through this, several areas were identified including; the optimisation of process chemistry, optimisation of separation processes, optimisation of production chemical performance and the identification of potentially undesirable process conditions (corrosion risks). In light of these objectives, several studies were conducted looking at various aspects of the MEG regeneration process and associated corrosion inhibition strategies including:

- Optimisation of process contaminant removal including organic acids and MDEA post formation water breakthrough
- Evaluating the potential switchover from MDEA to FFCIs to provide continued corrosion inhibition post formation water breakthrough
- Potential corrosion risks arising from MDEA during potential MDEA to FFCI switchover
- Diagnosing of routine settlement problems within industrial rich glycol settlement systems
- Determination of chemical and physical data relating to the MEG regeneration process to supplement the aforementioned research.
- Effect of organic acids on production chemical performance including sulphite-based oxygen scavengers

The proceeding chapter outlines the general conclusions and recommendations derived from the individual chapters of this study, overall relevance of the conducted work to industry and recommendations for potential future work.

10.1 Optimisation of Organic Acid Removal to Prevent Long-Term Accumulation

The level of organic acids within closed-loop MEG systems is often controlled via vacuum reclamation systems through the formation of non-volatile organic salt products allowing their separation from the evaporated MEG/water phase. However, if a reclamation system is unavailable, or operated at low pH, organic acids will ultimately accumulate within the MEG loop. The accumulation of organic acids within a MEG loop can have several detrimental impacts including aggravated CO₂ corrosion rates ^[69-72], Top-of-the-Line-Corrosion (TLC) ^[17, 63, 72-76], loss of production chemical efficacy and deposition of organic salts. As such, continued control of organic acid levels within MEG loops is critical for continued long-term operation.

The presented research studies the removal of organic acids (acetic) under a wide range of pH and salinity conditions during the MEG regeneration and reclamation processes. Based on the experimental results generated, the removal efficiency of acetic acid over an entire regeneration cycle has been modelled in conjunction with estimated pH rises across the distillation system as a function of dissolved CO₂ content and initial pH. Through the developed model, the plant wide acetic acid removal efficiency can be predicted to identify current removal levels, or if required, what conditions are necessary to prevent accumulation and subsequent production issues. The work further illustrates the large impact insufficient reclamation slip-streams rate have on the ability to prevent organic acid accumulation. Where the slip-stream rate is low or a low pH maintained during reclamation (such as during MDEA to FFCI transition), the majority of organic acid removal is generated through the regeneration column through the produced water product. Under such circumstances it may be advantageous to operate with a low pH within the regeneration column to ensure sufficient removal of organic acids occur and accumulation avoided.

10.2 Corrosion Inhibition Switchover from MDEA to FFCI

The transition from pH stabilisation using MDEA to FFCIs may provide an attractive method to extend the life span of high CO₂ containing natural gas fields producing formation water where the risk of scaling cannot be otherwise controlled by production reallocation or scale inhibitor injection. Although the switchover from pH stabilisation using hydroxides to FFCIs has been performed previously, a similar scenario using MDEA as the pH stabiliser is unique. In such systems, due to the chemistry of MDEA and the significantly greater dosage rate required during pH stabilisation, its complete removal from the MEG loop is considerably more difficult. Furthermore, when formation water is produced, increased concentrations of organic acids including acetic can be expected within MEG regeneration systems and can impose a corrosion

risk together with carbon dioxide ^[69-72]. Due to the opposing pH conditions required to remove both MDEA and organic acids during vacuum reclamation, the removal of MDEA during the switchover to FFCI will ultimately lead to organic acid accumulation with the closed loop MEG system. The removal of organic acids through the distillation system as discussed previously may be the only viable option to prevent organic acid accumulation during the MDEA to FFCI transition process.

As such, a case study was performed to evaluate the potential simultaneous removal of organic acids and MDEA/alkalinity during the switch over from pH stabilisation to FFCIs. It was found that by target a pH of 6 within the rich glycol feed to the MRU, sufficient boil-off of organic acids could be achieved during distillation to prevent accumulation within the MEG regeneration loop and subsequent corrosion issues. Simultaneously, removal of MDEA and reduction of lean glycol alkalinity was achieved through the reclamation system to facilitate FFCI switchover more rapidly than a comparative industrial operational methodology. Under the proposed method, the target alkalinity to reduce the risk of down-stream scaling was reached within 5-6 regeneration cycles compared to 12 of the comparative industrial operational methodology. However, due to the vacuum reclamation slip-stream rate utilised (11% - based off an industrial MEG system), complete removal of MDEA from the loop required 10-11 MEG regeneration cycles (compared to 25-30 cycles under the industry method). Ultimately, the prolonged presence of MDEA within the MEG loop represents a significant operational expense due to increased acid/base dosages required to perform pH adjustments and increased regeneration requirements. Therefore, performing a MDEA to FFCI switchover post formation water breakthrough whilst possible, may be problematic and costly if an insufficient reclamation slip-stream rate is utilised and unable to be increased due to system operational and design constraints.

10.3 Potential Corrosion Issues arising from MDEA and MDEA-to-FFCI Switchover

Although the transition from MDEA to FFCI may provide an innovative method to extend the life span of a formation water producing well, the potential effect of such dramatic changes in system chemistry must be evaluated. In particular, while MDEA is utilised to prevent corrosion in the primary wet gas pipeline through pH control, its presence within the MEG regeneration system coupled with changes in system chemistry may inadvertently pose a significant corrosion risk to systems manufactured from carbon steel. Due to the effect of temperature on the dissociation constant of MDEA, any increase in temperature will favour its undissociated form leading to the release of hydrogen ions as the acid-base equilibrium of MDEA shifts. The

subsequent release of hydrogen ions will therefore facilitate corrosion through the cathodic reduction of hydrogen ions at metal surfaces. Systems manufactured from carbon steel operating at high temperatures within the regeneration column including the reboiler shell, heating bundles and process piping are most at risk of this form of corrosion.

The evaluation of carbon steel corrosion in the presence of 80% wt. lean MEG containing 500mM MDEA under regeneration conditions including 140°C and 180°C (a potential reboiler skin temperature) found significant risk of corrosion with corrosion rates in excess of 1 mm/year measured. Under the conditions recommended for transition between MDEA to FFCl's ($\text{pH}_{25^\circ\text{C}} = 7$, within the reboiler) a corrosion rate of 1.96 mm/year was observed. Ultimately, if low to moderate pH levels are maintained within the regeneration column to facilitate corrosion inhibition switchover, the high temperature conditions will generate extensive corrosion of carbon steel components if MDEA/MDEAH⁺ is present. Furthermore, several FFCl's potentially applied in natural gas systems were found to provide insufficient corrosion protection under the high temperature test conditions. As such, if a corrosion inhibition switchover from MDEA to FFCl's is to be performed, proper selection of corrosion resistant materials such as stainless steels for the reboiler system is essential.

10.4 Diagnosing Routine Settlement Problems in MEG Regeneration Systems

Through consultation with major liquid natural gas producer, the poor settlement of quartz and iron carbonate particles was identified as a major issue affecting the performance of a MEG regeneration system resulting in excessive blockage and replacement of in-line filters. A study was therefore undertaken to diagnose the routine settling problems faced within the third-party oil and gas companies' rich MEG settlement system. Two primary issues were identified including; a) low particle size (<53 μm) resulting in poor settlement within high viscosity MEG solution and b) exposure to hydrocarbon condensate constituents causing modification of particle surface properties through oil-wetting of the particle surface. Analysis of oil-wetted quartz and iron carbonate settlement behaviour found a greater tendency to remain suspended in the solution and be removed in the rich MEG effluent stream or to strongly float and accumulate at the liquid-vapour interface in comparison to naturally water-wetted particles.

Carboxylics and long-chain fatty acids were suspected to be the primary cause of particles becoming oil-wetted after exposure to the condensate phase of the primary pipeline. Furthermore, if surfactant-based film forming corrosion inhibitors are injected into the pipeline to provide corrosion control, their effect on the chemical properties of solid surfaces may also provide another avenue in which solid particles are rendered oil-wetted. Overall, the exposure

of solid particles, namely iron carbonate and quartz to the condensate phase and/or FFCIs within the primary natural gas pipeline may result in poor settlement of suspended particles with downstream MEG regeneration systems, leading to increase filtration requirements. The effect of oil-wetting on particle settlement was successfully managed through application of a cationic surfactants, including cetrimonium bromide (CTAB), to transition the initially oil-wetted surface to water-wetted. Cationic surfactants were found to be most suitable due to the negative surface charge of mineral particles at pH levels typical of MEG regeneration system pre-treatment systems (pH > 8).

10.5 Generation of Chemical and Physical Data Relevant to Industrial MEG System Operation and Design

Due to the recent adoption of MEG for natural gas hydrate inhibition coupled with limited academic research into MEG systems, there is limited literature data available regarding chemical and physical data in MEG systems. In particular, MEG as a solvent can have significant impact on the speciation behaviour of weak acids and bases of which ultimately influences pH driven separation processes (i.e. reclamation for organic acid and/or MDEA removal). To generate a better understanding of how various factors in MEG systems influence the speciation behaviour of common organic acids and MDEA, their respective dissociation constants have been measured at varying MEG concentrations, temperatures and salinities. Within industrial MEG systems, these factors are highly variable and as such, models have been proposed to calculate the acid dissociation constant of acetic acid and MDEA from 0-100% wt. MEG, 25-80°C and 0-0.5 M ionic strength. Furthermore, the thermodynamic properties of the dissociation process including Gibbs free energy (ΔG° kJ.mol⁻¹) standard enthalpy (ΔH° kJ.mol⁻¹) and entropy (ΔS° kJ.mol⁻¹.K⁻¹) were calculated at 25°C using the van't Hoff Equation. The experimental dissociation data generated as part of this study can help better model and estimate the removal of both organic acids and MDEA during distillation (organic acids) and vacuum reclamation.

Likewise, experimental data was generated to study the vapour-liquid equilibrium behaviour of MDEA within MEG and water solutions under vacuum conditions to simulate its behaviour during MEG reclamation. Isobaric vapour-liquid equilibrium data for the binary MEG-MDEA system was measured at (20, 10 and 5) kPa and water-MDEA system at (40, 20, 10) kPa. The generated experimental VLE data was subsequently correlated to the UNIQUAC, NRTL and Wilson activity coefficient models and the respective binary parameters regressed. The measurement of VLE data under such conditions for MDEA-MEG and MDEA-water systems can

help improve the development of process simulation models for the design of industrial MEG reclamation units where MDEA is present.

10.6 Optimisation of Sulphite Based Oxygen Scavenger Performance in MEG Systems

The presence of dissolved oxygen within regenerated lean MEG poses a significant corrosion risk to subsea MEG injection systems with those manufactured from corrosion resistant alloys also susceptible. To reduce the risk of oxygen-based corrosion, the injection of oxygen scavengers into the produced lean MEG may be required if sufficiently pure nitrogen is unavailable or too costly to implement such as on offshore platforms where space is limited. Sulphite based oxygen scavengers represent one of the most widely used chemical based oxygen removal methods in both water systems and more recently MEG injection systems. However, the wide range of process conditions, contaminants present within MEG regeneration systems and the inhibitory effect of MEG itself has meant that the application of sulphite in MEG systems has been troublesome.

As such, to generate a better understanding of sulphite-based oxygen scavenger behaviour within MEG systems, a commercially available metabisulphite scavenger was evaluated under a wide range of pH, salt and organic acid levels. The ultimate goal of the research was to develop a defined operating pH range for known organic acid and salt concentrations (NaCl) for direct application for field use. The presence of organic acid conjugate bases including acetate were found to be the primary factor reducing the performance of the sulphite oxygen scavenging mechanism at pHs between 7-10 with a pH greater than 10.5 required to achieve good oxygen removal. In contrast, the presence of sodium and chloride ions had only a minor impact on oxygen removal performance of sulphite with strong removal achieved up to 50 g/L NaCl at a lean glycol pH of 11. Based on the experimental results presented, a simple guide for field-operators has been proposed detailing the operating pHs required to achieve below 20 ppb oxygen content within four hours based on known organic acid concentrations and salinities.

10.7 Relevance of Work to Industry

Several of the combined studies within this thesis provide a better understanding of MDEA as pH stabiliser and its chemical and physical behaviour within MEG systems. This work has significant implications for industrial MEG regeneration and natural gas systems utilising MDEA as pH stabiliser including those operating with high CO₂ partial pressures where traditional salt-based pH stabilisers would be otherwise unsuitable. Improved knowledge of MDEAs behaviour within MEG, potential methods to transition to FFCIs, and the identification of potentially

corrosive conditions associated with the use of MDEA, ultimately increases its viability in pH stabilisation applications for industry use for corrosion control. Furthermore, improved understanding of organic acid behaviour within MEG systems and recommendations to improve organic acid removal may help to reduce the risk of corrosion associated with long-term organic acid accumulation. All of these studies and the recommendations and conclusions drawn from them, can help industry operators of MEG systems reduce long-term corrosion risks as well as operational costs associated with corrosion inhibition and the operation of MEG systems.

Finally, the two studies conducted based off of current issues faced within an industrial MEG system have direct implications to all MEG systems due to the common nature of the problems and wide spread use of the impacted production chemicals. Sulphite based oxygen scavengers are widely used in industry including MEG systems for oxygen removal and were found to, in the presented work, to be detrimentally impacted by their interaction with organic acids. As such, their application to MEG systems where organic acids are widely experienced, is problematic with several operational recommendations that can be directly implemented in industry made to alleviate potential poor performance and minimise associated corrosion risks. Conversely, the settlement behaviour of solid particles entering into a regeneration system was found to be drastically impacted by their exposure to condensate constituents. Said exposure ultimately lead to poor settlement and excessive down-stream filtration requirements, of which could however, be successfully alleviated by cationic surfactants through modification of particle surface properties. Improved solid behaviour in MEG systems, and recommendations to improve settlement behaviour through chemical application can help significantly reduce filter change out requirements, reducing operational costs and system downtime.

10.8 Recommendations for Future Work

With several long-term natural gas production systems in Australia utilising MEG for hydrate inhibition and with numerous new developments planned, continued research into MEG optimisation and various problems experienced in the field is important. For natural gas systems utilising MDEA for pH stabilisation, further research into optimising the switchover process to FFCLs post formation water breakthrough can significantly improve the viability of the process. Some examples of potential MDEA research in MEG systems include:

- MDEA behaviour during MEG regeneration
 - Further study upon the effect of MDEA on corrosion in MEG regeneration systems
 - Potential degradation under high temperature regeneration conditions

- Optimisation of MDEA removal from closed loop MEG systems
 - Optimisation of pH conditions for MDEA removal during reclamation
 - Identification of potential effects of MDEA removal conditions on system wide chemistry (i.e. reduced organic acid removal).

Furthermore, continued development of experimental data relating to the chemical and physical behaviour in MEG systems can aid in the design and operation of future MEG regeneration systems. Several examples include:

- Effects of long-term degradation of MEG over multiple regeneration cycles on hydrate inhibition performance
- Measurement of weak acid/base dissociation data at higher temperatures to better model high temperature separation processes
- Low pressure VLE data in tertiary MEG/water/MDEA solutions and VLE data with dissolved salts to better model reclamation of MDEA containing MEG solutions
- Experimental measurement of salt solubility limits in MEG solutions to better model salt removal during reclamation including:
 - Organic acid salts
 - MDEA tertiary amine salts

REFERENCES

1. Zaboon, S., A. Soames, V. Ghodkay, R. Gubner, and A. Barifcani, *Recovery of Mono-Ethylene Glycol by Distillation and the Impact of Dissolved Salts Evaluated Through Simulation of Field Data*. Journal of Natural Gas Science and Engineering, 2017. **44**: p. 214-232.
2. Bikkina, C., N. Radhakrishnan, S. Jaiswal, R. Harrington, and M. Charlesworth, *Development of MEG Regeneration Unit Compatible Corrosion Inhibitor for Wet Gas Systems*, in *SPE Asia Pacific Oil and Gas Conference and Exhibition*. 2012, Society of Petroleum Engineers: Perth, Australia.
3. Haque, M.E., *Ethylene Glycol Regeneration Plan: A Systematic Approach to Troubleshoot the Common Problems*. Journal of Chemical Engineering, 2012. **27**(1): p. 21-26.
4. Pojtanabuntoeng, T., B. Kinsella, H. Ehsani, and J. McKechnie, *Assessment of Corrosion Control by pH Neutralisation in the Presence of Glycol at Low Temperature*. Corrosion Science, 2017. **126**: p. 94-103.
5. AlHarooni, K., A. Barifcani, D. Pack, R. Gubner, and V. Ghodkay, *Inhibition Effects of Thermally Degraded MEG on Hydrate Formation for Gas Systems*. Journal of Petroleum Science and Engineering, 2015. **135**: p. 608-617.
6. Haghighi, H., A. Chapoy, R. Burgess, and B. Tohidi, *Experimental and Thermodynamic Modelling of Systems Containing Water and Ethylene Glycol: Application to Flow Assurance and Gas Processing*. Fluid Phase Equilibria, 2009. **276**(1): p. 24-30.
7. Soames, A., E. Odeigah, A. Al Helal, S. Zaboon, S. Iglauer, A. Barifcani, and R. Gubner, *Operation of a MEG Pilot Regeneration System for Organic Acid and Alkalinity Removal During MDEA to FFCI Switchover*. Journal of Petroleum Science and Engineering, 2018. **169**: p. 1-14.
8. Lehmann, M.N., A. Lamm, H.M. Nguyen, C.W. Bowman, W.Y. Mok, M. Salasi, and R. Gubner, *Corrosion Inhibitor and Oxygen Scavenger for use as MEG Additives in the Inhibition of Wet Gas Pipelines*, in *Offshore Technology Conference-Asia*. 2014, Offshore Technology Conference: Kuala Lumpur, Malaysia.
9. Latta, T.M., M.E. Seiersten, and S.A. Bufton, *Flow Assurance Impacts on Lean/Rich MEG Circuit Chemistry and MEG Regenerator/Reclaimer Design*, in *Offshore Technology Conference*. 2013, Offshore Technology Conference: Houston, Texas.
10. Latta, T.M., A.A. Palejwala, S.K. Tipson, and N.P. Haigh, *Design Considerations for Mitigating the Impact of Contaminants in Rich MEG on Monoethylene Glycol Recovery Unit MRU Performance*, in *Offshore Technology Conference Asia*. 2016, Offshore Technology Conference: Kuala Lumpur, Malaysia.
11. Sandengen, K., B. Kaasa, and T. Østvold, *pH Measurements in Monoethylene Glycol (MEG) + Water Solutions*. Industrial & Engineering Chemistry Research, 2007. **46**(14): p. 4734-4739.
12. AlHarooni, K., R. Gubner, S. Iglauer, D. Pack, and A. Barifcani, *Influence of Regenerated Monoethylene Glycol on Natural Gas Hydrate Formation*. Energy & Fuels, 2017. **31**(11): p. 12914-12931.
13. Halvorsen, E.N., A.M.K. Halvorsen, T.R. Andersen, C. Biornstad, and K. Reiersolmen, *Qualification of Scale Inhibitors for Subsea Tiebacks With MEG Injection*. 2009, Society of Petroleum Engineers.
14. Halvorsen, A.M.K., J.I. Skar, and K. Reiersølmoen, *Qualification of Scale And Corrosion Inhibitor For a Subsea HPHT Field With a MEG-loop*. 2012, NACE International.
15. Olsen, S., *Corrosion Control by Inhibition, Environmental Aspects, and pH Control: Part II: Corrosion Control by pH Stabilization*. 2006, NACE International.

REFERENCES

16. Dugstad, A., M. Seiersten, and R. Nyborg, *Flow Assurance of pH Stabilized Wet Gas Pipelines*, in *CORROSION*. 2003, NACE International: San Diego, California.
 17. Olsen, S. and A.M.K. Halvorsen, *Corrosion Control by pH Stabilization*, in *CORROSION*. 2015, NACE International: Dallas, Texas.
 18. Gulbrandsen, E., J. Kvarekval, and H. Miland, *Effect of Oxygen Contamination on Inhibition Studies in Carbon Dioxide Corrosion*. *Corrosion*, 2005. **61**(11): p. 1086-1097.
 19. Salasi, M., T. Pojtanabuntoeng, S. Wong, and M. Lehmann, *Efficacy of Bisulfite Ions as an Oxygen Scavenger in Monoethylene Glycol (At Least 20 wt%)/Water Mixtures*. *SPE Journal*, 2017. **22**(5): p. 1467-1477.
 20. Nazeri, M., B. Tohidi, and A. Chapoy, *An Evaluation of Risk of Hydrate Formation at the Top of a Pipeline*. 2014.
 21. Ellison, B.T., C.T. Gallagher, L.M. Frostman, and S.E. Lorimer, *The Physical Chemistry of Wax, Hydrates, and Asphaltene*, in *Offshore Technology Conference*. 2000, Offshore Technology Conference: Houston, Texas.
 22. Hale, A.H. and A.K.R. Dewan, *Inhibition of Gas Hydrates in Deepwater Drilling*. 1990.
 23. Sloan, E.D., Jr., *Natural Gas Hydrates*. 1991.
 24. Ng, H.-J. and D.B. Robinson, *Hydrate formation in systems containing methane, ethane, propane, carbon dioxide or hydrogen sulfide in the presence of methanol*. *Fluid Phase Equilibria*, 1985. **21**(1): p. 145-155.
 25. Janda, K.C., *Methane hydrate Type sII*. 2008, UCI Department of Chemistry: <http://ps.uci.edu/scholar/kcjanda/home>.
 26. Makogon, Y.F., *Natural gas hydrates – A promising source of energy*. *Journal of Natural Gas Science and Engineering*, 2010. **2**(1): p. 49-59.
 27. Cha, M., K. Shin, J. Kim, D. Chang, Y. Seo, H. Lee, and S.-P. Kang, *Thermodynamic and kinetic hydrate inhibition performance of aqueous ethylene glycol solutions for natural gas*. *Chemical Engineering Science*, 2013. **99**: p. 184-190.
 28. Kvamme, B., T. Kuznetsova, J.M. Bauman, S. Sjöblom, and A. Avinash Kulkarni, *Hydrate Formation during Transport of Natural Gas Containing Water and Impurities*. *Journal of Chemical & Engineering Data*, 2016. **61**(2): p. 936-949.
 29. Williams, H., T. Herrmann, M. Jordan, and C. McCallum, *The Impact of Thermodynamic Hydrate Inhibitors (MEG and Methanol) on Scale Dissolver Performance*, in *SPE International Oilfield Scale Conference and Exhibition*. 2016, Society of Petroleum Engineers: Aberdeen, Scotland, UK.
 30. Akhfash, M., M. Arjmandi, Z.M. Aman, J.A. Boxall, and E.F. May, *Gas Hydrate Thermodynamic Inhibition with MDEA for Reduced MEG Circulation*. *Journal of Chemical & Engineering Data*, 2017. **62**(9): p. 2578-2583.
 31. Giavarini, C. and K. Hester, *Gas hydrates immense energy potential and environmental challenges*. Vol. 80. 2011, London: London, United Kingdom: Springer.
 32. Brustad, S., K.P. Løken, and J.G. Waalman, *Hydrate Prevention using MEG instead of MeOH: Impact of Experience from Major Norwegian Developments on Technology Selection for Injection and Recovery of MEG*, in *Offshore Technology Conference*. 2005, Offshore Technology Conference: Houston, Texas.
 33. Sloan, E.D., *Clathrate hydrates of natural gases / E. Dendy Sloan, Carolyn A. Koh*. 3rd ed.. ed, ed. C.A. Koh. 2008, Boca Raton: Boca Raton : CRC Press.
 34. Al Harooni, K.M.A., *Gas Hydrates Investigations of Natural Gas with High Methane Content and Regenerated Mono-Ethylene Glycol*, in *Department of Petroleum Engineering*. 2017, Curtin University: Western Australia.
 35. Akers, T.J., *Formation and Removal of Hydrates Inside Wellhead Connectors*, in *SPE Annual Technical Conference and Exhibition*. 2009, Society of Petroleum Engineers: New Orleans, Louisiana. p. 15.
 36. Carroll, J.J., *Natural Gas Hydrates : a Guide for Engineers*. 2003, Amsterdam, Boston: Gulf Professional Pub.
-

REFERENCES

37. Montazaud, T., *Precipitation of Carbonates in the Pretreatment Process for Regeneration of Ethylene Glycol*, in *Chemical Engineering and Biotechnology*. 2011, Norwegian University of Science and Technology. p. 89.
 38. Psarrou, M.N., L.O. Jøsang, K. Sandengen, and T. Østvold, *Carbon Dioxide Solubility and Monoethylene Glycol (MEG) Degradation at MEG Reclaiming/Regeneration Conditions*. *Journal of Chemical & Engineering Data*, 2011. **56**(12): p. 4720-4724.
 39. Nazzer, C.A. and J. Keogh, *Advances in Glycol Reclamation Technology*, in *Offshore Technology Conference*. 2006, Offshore Technology Conference: Houston, Texas.
 40. Soames, A., A. Al Helal, S. Iglauer, A. Barifcani, and R. Gubner, *Experimental Vapor–Liquid Equilibrium Data for Binary Mixtures of Methyldiethanolamine in Water and Ethylene Glycol under Vacuum*. *Journal of Chemical & Engineering Data*, 2018. **63**(5): p. 1752-1760.
 41. Odeigah, E.A., T. Pojtanabuntoeng, F. Jones, and R. Gubner, *The Effect of Monoethylene Glycol on Calcium Carbonate Solubility at High Temperatures*. *Industrial & Engineering Chemistry Research*, 2018. **57**(46): p. 15909-15915.
 42. Trofimuk, T., S. Ayres, and J. Esquier. *CCR MEG Reclaiming Technology: from Mobile to the Largest Reclaiming Unit in the World*. in *Rio oil & gas Expo and conference*. 2014. Rio de Janeiro, Brazil: Brazilian Petroleum, Gas and Biofuels Institute.
 43. Son, H., Y. Kim, S. Park, M. Binns, and J.-K. Kim, *Simulation and Modeling of MEG (Monoethylene Glycol) Regeneration for the Estimation of Energy and MEG Losses*. *Energy*, 2018. **157**: p. 10-18.
 44. FOLEY, R.T., *Role of the Chloride Ion in Iron Corrosion*. *CORROSION*, 1970. **26**(2): p. 58-70.
 45. Hassan, H.H., *Effect of chloride ions on the corrosion behaviour of steel in 0.1M citrate*. *Electrochimica Acta*, 2005. **51**(3): p. 526-535.
 46. Sharifi-Asl, S., F. Mao, P. Lu, B. Kursten, and D.D. Macdonald, *Exploration of the effect of chloride ion concentration and temperature on pitting corrosion of carbon steel in saturated Ca(OH)₂ solution*. *Corrosion Science*, 2015. **98**: p. 708-715.
 47. Seiersten, M., E. Brendsdal, S. Deshmukh, A. Dugstad, G. Endrestøl, A. Ek, and G. Watterud *Development of a Simulator for Ethylene Glycol Loops Based on Solution Thermodynamics and Particle Formation Kinetics*. 2010.
 48. Flaten, E.M., G. Watterud, J.-P. Andreassen, and M.E. Seiersten, *Precipitation Of Iron And Calcium Carbonate In Pipelines At Varying Meg Contents*. 2008, Society of Petroleum Engineers.
 49. Halvorsen, E.N., A.M.K. Halvorsen, T.R. Andersen, K. Reiersolmoen, and C. Biornstad, *New Method for Scale Inhibitor Testing*, in *SPE International Symposium on Oilfield Chemistry*. 2009, Society of Petroleum Engineers: The Woodlands. Texas. p. 11.
 50. Flaten, E.M., M. Seiersten, and J.-P. Andreassen, *Growth of the calcium carbonate polymorph vaterite in mixtures of water and ethylene glycol at conditions of gas processing*. *Journal of Crystal Growth*, 2010. **312**(7): p. 953-960.
 51. Dugstad, A. and M. Seiersten, *pH-stabilisation, a Reliable Method for Corrosion Control of Wet Gas Pipelines*, in *1st International Symposium on Oilfield Corrosion*. 2004, Society of Petroleum Engineers.
 52. Flaten, E.M., M. Seiersten, and J.-P. Andreassen, *Polymorphism and morphology of calcium carbonate precipitated in mixed solvents of ethylene glycol and water*. *Journal of Crystal Growth*, 2009. **311**(13): p. 3533-3538.
 53. Al Helal, A., A. Soames, R. Gubner, S. Iglauer, and A. Barifcani, *Influence of magnetic fields on calcium carbonate scaling in aqueous solutions at 150°C and 1bar*. *Journal of Colloid and Interface Science*, 2018. **509**: p. 472-484.
 54. Flaten, E.M., M. Seiersten, and J.-P. Andreassen, *Induction time studies of calcium carbonate in ethylene glycol and water*. *Chemical Engineering Research and Design*, 2010. **88**(12): p. 1659-1668.
-

REFERENCES

55. Flaten, E.M., X. Ma, M. Seiersten, C. Aanonsen, R. Beck, and J.-P. Andreassen, *Impact of Monoethylene Glycol and Fe²⁺ on Crystal Growth of CaCO₃*. 2015, NACE International.
 56. Sorbie, K.S. and N. Laing, *How Scale Inhibitors Work: Mechanisms of Selected Barium Sulphate Scale inhibitors Across a Wide Temperature Range*, in *SPE International Symposium on Oilfield Scale*. 2004, Society of Petroleum Engineers: Aberdeen, United Kingdom. p. 10.
 57. Gill, J.S., *Development of Scale Inhibitors*, in *CORROSION 96*. 1996, NACE International: Denver, Colorado. p. 19.
 58. Siegmeier, R., M. Kirschey, and M. Voges, *Acrolein Based Polymers as Scale Inhibitors*, in *CORROSION 98*. 1998, NACE International: San Diego, California. p. 12.
 59. Foss, M.S., M.E. Seiersten, and K. Nisancioglu, *Interaction Between Scale Inhibitors and FeCO₃ Precipitation on Carbon Steel*, in *SPE International Oilfield Corrosion Symposium*. 2006, Society of Petroleum Engineers: Aberdeen, UK. p. 7.
 60. Graham, G.M., K.S. Sorbie, and M.M. Jordan, *How scale inhibitors work and how this affects test methodology*, in *BC Conference on Solving Oilfield Scaling*. 1997: Aberdeen, United Kingdom.
 61. Khormali, A. and D.G. Petrakov, *Laboratory investigation of a new scale inhibitor for preventing calcium carbonate precipitation in oil reservoirs and production equipment*. *Petroleum Science*, 2016. **13**(2): p. 320-327.
 62. Wang, Q., F. Liang, W. Al-Nasser, F. Al-Dawood, T. Al-Shafai, H. Al-Badairy, S. Shen, and H. Al-Ajwad, *Laboratory study on efficiency of three calcium carbonate scale inhibitors in the presence of EOR chemicals*. *Petroleum*, 2018.
 63. Svenningsen, G. and R. Nyborg, *Modeling of Top of Line Corrosion with Organic Acid and Glycol*, in *CORROSION*. 2014, Nace International: Houston, Texas.
 64. Okafor, P.C. and S. Nestic, *EFFECT OF ACETIC ACID ON CO₂ CORROSION OF CARBON STEEL IN VAPOR-WATER TWO-PHASE HORIZONTAL FLOW*. *Chemical Engineering Communications*, 2007. **194**(2): p. 141-157.
 65. Svenningsen, G., M. Foss, R. Nyborg, H. Fukagawa, and I. Kurniawan, *Top of Line Corrosion with High CO₂ and Organic Acid*, in *CORROSION*. 2013, NACE International: Orlando, Florida.
 66. Garsany, Y., D. Pletcher, and B. Hedges, *Speciation and electrochemistry of brines containing acetate ion and carbon dioxide*. *Journal of Electroanalytical Chemistry*, 2002. **538–539**: p. 285-297.
 67. Hedges, B. and L. McVeigh, *The Role of Acetate in CO₂ Corrosion: The Double Whammy*, in *CORROSION*. 1999, NACE International: San Antonio, Texas.
 68. Joosten, M.W., J. Kolts, J.W. Hembree, and M. Achour, *Organic Acid Corrosion In Oil And Gas Production*, in *CORROSION*. 2002, NACE International: Denver, Colorado.
 69. Ikeh, L., G.C. Enyi, and G.G. Nasr, *Inhibition Performance of Mild Steel Corrosion in the Presence of Co₂, HAc and MEG*, in *SPE International Oilfield Corrosion Conference and Exhibition*. 2016, Society of Petroleum Engineers: Aberdeen, Scotland, UK.
 70. Dong, L., C. ZhenYu, and G. XingPeng, *The Effect of Acetic Acid and Acetate on CO₂ Corrosion of Carbon Steel*. *Anti-Corrosion Methods and Materials*, 2008. **55**(3): p. 130-134.
 71. Crolet, J.L., N. Thevenot, and A. Dugstad, *Role of Free Acetic Acid on the CO₂ Corrosion of Steels*, in *CORROSION*. 1999, NACE International: San Antonio, Texas.
 72. Mendez, C., M. Singer, A. Comacho, S. Nestic, S. Hernandez, Y. Sun, Y. Gunaltun, and M.W. Joosten, *Effect of Acetic Acid, pH and MEG on the CO₂ Top of the Line Corrosion*, in *CORROSION 2005*, NACE International: Houston, Texas.
 73. Amri, J., E. Gulbrandsen, and R.P. Nogueira, *Effect Of Acetic Acid On Propagation And Stifling Of Localized Attacks In CO₂ Corrosion Of Carbon Steel*, in *CORROSION*. 2009, NACE International: Atlanta, Georgia.
-

REFERENCES

74. Sykes, G. and M. Gunn, *Optimising MEG Chemistry When Producing Formation Water*, in *SPE Asia Pacific Oil & Gas Conference and Exhibition*. 2016, Society of Petroleum Engineers: Perth, Australia.
 75. Andersen, T.R., A.M.K. Halvorsen, A. Valle, and A. Dugstad, *The Influence Of Condensation Rate And Acetic Acid Concentration On Tol-Corrosion In Multiphase Pipelines*, in *CORROSION*. 2007, NACE International: Nashville, Tennessee.
 76. Singer, M., D. Hinkson, Z. Zhang, H. Wang, and S. Nešić, *CO₂ Top-of-the-Line Corrosion in Presence of Acetic Acid: A Parametric Study*, in *CORROSION*. 2013, NACE International: Atlanta, Georgia. p. 719-735.
 77. Nace International. *Corrosion in the Oil and Gas Industry*. [cited 2019 21/02/2019]; Available from: <https://www.nace.org/Corrosion-Central/Industries/Oil---Gas-Production/>.
 78. Revie, R.W., *Uhlig's Corrosion Handbook: Third Edition*. 2011.
 79. Căstiri, V.C., *Corrosion prevention and protection : practical solutions / V. S. Sastri, Edward Ghali, Mimoun Elboujdaini*, ed. E. Ghali and M. Elboujdaini. 2007, Chichester, England: Wiley.
 80. Roberge, P.R., *Corrosion basics : an introduction / Pierre R. Roberge*. 2nd ed.. ed. 2006, Houston, Tex.: Houston, Tex. : NACE International.
 81. Kvarekval, J., S. Olsen, and S. Skjerve, *The Effect of O₂ on CO₂ Corrosion in pH Stabilized Gas/Condensate Pipelines*. 2005, NACE International.
 82. Mansoori, H., R. Mirzaee, and A. Mohammadi, *Pitting Corrosion Failures of Natural Gas Transmission Pipelines*. 2013, International Petroleum Technology Conference.
 83. Melchers, R.E. and M. Ahammed, *Pitting Corrosion of Offshore Water Injection Steel Pipelines*. 2016, International Society of Offshore and Polar Engineers.
 84. Joosten, M.W., B. Tier, M. Seiersten, and C. Wintermark, *Materials Considerations for MEG (Mono Ethylene Glycol) Reclamation Systems*. 2007, NACE International.
 85. Martin, R.L., *Corrosion Consequences of Oxygen Entry into Oilfield Brines*. 2002, NACE International.
 86. Palencsár, A., J. Amri, M. Seiersten, and C. Omgba, *Corrosion in MEG Injection Lines in the Presence of O₂ - Experiments and Modelling*, in *SPE International Oilfield Corrosion Conference and Exhibition*. 2016, Society of Petroleum Engineers: Aberdeen, Scotland, UK. p. 17.
 87. Guo, P., E.C. La Plante, B. Wang, X. Chen, M. Balonis, M. Bauchy, and G. Sant, *Direct observation of pitting corrosion evolutions on carbon steel surfaces at the nano-to-micro- scales*. Scientific reports, 2018. **8**(1): p. 7990-7990.
 88. Kermani, M.B. and A. Morshed, *Carbon Dioxide Corrosion in Oil and Gas Production—A Compendium*. *CORROSION*, 2003. **59**(8): p. 659-683.
 89. Papavinasam, S., A. Doiron, T. Panneerselvam, and R.W. Revie, *Effect of Hydrocarbons on the Internal Corrosion of Oil and Gas Pipelines*. *CORROSION*, 2007. **63**(7): p. 704-712.
 90. Nam, N.D., M. Mathesh, B. Hinton, M.J.Y. Tan, and M. Forsyth, *Rare Earth 4-Hydroxycinnamate Compounds as Carbon Dioxide Corrosion Inhibitors for Steel in Sodium Chloride Solution*. *Journal of The Electrochemical Society*, 2014. **161**(12): p. C527-C534.
 91. Shi, L., C. Wang, and C. Zou, *Corrosion failure analysis of L485 natural gas pipeline in CO₂ environment*. *Engineering Failure Analysis*, 2014. **36**: p. 372-378.
 92. Cavalcanti, H.S., T.S. Villela, and J.M. Silva, *INTERNAL CORROSION MONITORING IN NATURAL GAS PIPELINES*, in *17th World Petroleum Congress*. 2002, World Petroleum Congress: Rio de Janeiro, Brazil. p. 4.
 93. Zhao, W., T. Zhang, Y. Wang, J. Qiao, and Z. Wang, *Corrosion Failure Mechanism of Associated Gas Transmission Pipeline*. *Materials (Basel, Switzerland)*, 2018. **11**(10): p. 1935.
-

-
94. Pojtanabuntoeng, T., M. Salasi, and R. Gubner. *The influence of mono ethylene glycol (MEG) on CO₂ corrosion of carbon steel at elevated temperatures (80 to 120 C)*. in *Corrosion Conference and Expo*. 2014.
 95. López, D.A., T. Pérez, and S.N. Simison, *The Influence of Microstructure and Chemical Composition of Carbon and Low Alloy Steels in CO₂ Corrosion. A State-of-the-Art Appraisal*. Materials & Design, 2003. **24**(8): p. 561-575.
 96. Ramachandran, S., S. Mancuso, K.A. Bartrip, and P. Hammonds, *Inhibition of Acid Gas Corrosion in Pipelines using Glycol for Hydrate Inhibition*. 2006, NACE International.
 97. Gulbrandsen, E. and J. Morard, *Why Does Glycol Inhibit CO₂ Corrosion?*, in *Corrosion 98 Conference and Expo*. 1998, NACE International: Houston, TX.
 98. Popoola, L.T., A.S. Grema, G.K. Latinwo, B. Gutti, and A.S. Balogun, *Corrosion problems during oil and gas production and its mitigation*. International Journal of Industrial Chemistry, 2013. **4**(1): p. 35.
 99. Cheng, Y.F., *Stress corrosion cracking of pipelines / Y. Frank Cheng*. 2013, Hoboken, N.J.: Hoboken, N.J. : John Wiley & Sons, Inc.
 100. Song, F.M., *Predicting the mechanisms and crack growth rates of pipelines undergoing stress corrosion cracking at high pH*. Corrosion Science, 2009. **51**(11): p. 2657-2674.
 101. Honarvar Nazari, M., S.R. Allahkaram, and M.B. Kermani, *The effects of temperature and pH on the characteristics of corrosion product in CO₂ corrosion of grade X70 steel*. Materials & Design, 2010. **31**(7): p. 3559-3563.
 102. Li, D., D. Han, L. Zhang, M. Lu, L. Wang, and W. Ma, *Effects of Temperature on CO₂ Corrosion of Tubing and Casing Steel*, in *CORROSION 2013*. 2013, NACE International: Orlando, Florida. p. 11.
 103. Yin, Z.F., Y. Feng, W. Zhao, Z. Bai, and G. Lin, *Effect of temperature on CO₂ corrosion of carbon steel*. Surface and Interface Analysis: An International Journal devoted to the development and application of techniques for the analysis of surfaces, interfaces and thin films, 2009. **41**(6): p. 517-523.
 104. Dugstad, A., *Fundamental Aspects of CO₂ Metal Loss Corrosion - Part 1: Mechanism*, in *CORROSION 2006*. 2006, NACE International: San Diego, California. p. 18.
 105. Larrey, D. and Y.M. Gunaltun, *Correlation of Cases of Top of Line Corrosion With Calculated Water Condensation Rates*. 2000, NACE International.
 106. Yeaw, S.H., *Water dew-pointing with subsea gas dehydration to improve pipeline and flow assurance economics*. 2017, Aker Solutions.
 107. Belarbi, Z., M. Singer, D. Young, F. Farelas, T.N. Vu, and S. Nestic, *Thiols as Volatile Corrosion Inhibitors for Top of the Line Corrosion*, in *CORROSION 2017*. 2017, NACE International: New Orleans, Louisiana, USA. p. 14.
 108. Gunaltun, Y., T.E. Pou, M. Singer, C. Duret, and S. Espitalier, *Laboratory Testing Of Volatile Corrosion Inhibitors*, in *CORROSION 2010*. 2010, NACE International: San Antonio, Texas. p. 20.
 109. Gonzalez, J.J., M.E. Alfonso, and G. Pellegrino, *Corrosion of Carbon Steels in Monoethylene Glycol*, in *CORROSION 2000*. 2000, NACE International: Orlando, Florida. p. 13.
 110. Ivonye, I., C. Wang, and A. Neville, *The Corrosion of Carbon Steel in the Presence of Monoethylene Glycol (MEG) – Assessing the Influence of an Iron Carbonate Scale*. 2015, NACE International.
 111. Xiang, Y., Y.S. Choi, Y. Yang, and S. Nešić, *Corrosion of carbon steel in MDEA-based CO₂ capture plants under regenerator conditions: Effects of O₂ and heat-stable salts*. Corrosion, 2015. **71**(1): p. 30-37.
 112. Sridhar, N., D.S. Dunn, A.M. Anderko, M.M. Lencka, and H.U. Schutt, *Effects of Water and Gas Compositions on the Internal Corrosion of Gas Pipelines—Modeling and Experimental Studies*. CORROSION, 2001. **57**(3): p. 221-235.
-

REFERENCES

113. Al Helal, A., A. Soames, R. Gubner, S. Iglauer, and A. Barifcani, *Performance of Erythorbic Acid as an Oxygen Scavenger in Thermally Aged Lean MEG*. Journal of Petroleum Science and Engineering, 2018. **170**: p. 911-921.
 114. Braga, T.G., *Effects of Commonly Used Oilfield Chemicals on the Rate of Oxygen Scavenging by Sulfite/Bisulfite*. 1987.
 115. Kvarckval, J. and A. Dugstad, *Corrosion Mitigation with pH Stabilization in Slightly Sour Gas/Condensate Pipelines*, in *CORROSION 2006*. 2006, NACE International: San Diego, California. p. 15.
 116. Halvorsen, A.M.K. and T.R. Andersen, *pH Stabilization for Internal Corrosion Protection of Pipeline Carrying Wet Gas With CO₂ and Acetic Acid*, in *CORROSION*. 2003, NACE International: San Diego, California.
 117. Bartos, M. and J.D. Watson, *Oilfield Corrosion Inhibition Under Extremely High Shear Conditions*, in *CORROSION 2000*. 2000, NACE International: Orlando, Florida. p. 12.
 118. Kundu, S.S. and M. Seiersten, *Development of a Non-Sulphite Oxygen Scavenger for Monoethylene Glycol (MEG) used as Gas Hydrate Inhibitor*. Journal of Petroleum Science and Engineering, 2017.
 119. Shen, Z., S. Guo, W. Kang, K. Zeng, M. Yin, J. Tian, and J. Lu, *Kinetics and Mechanism of Sulfite Oxidation in the Magnesium-Based Wet Flue Gas Desulfurization Process*. Industrial & Engineering Chemistry Research, 2012. **51**(11): p. 4192-4198-4192-4198.
 120. Karatza, D., M. Prisciandaro, A. Lancia, and D. Musmarra, *Sulfite Oxidation Catalyzed by Cobalt Ions in Flue Gas Desulfurization Processes*. Journal of the Air & Waste Management Association, 2010. **60**(6): p. 675-680.
 121. Wilkinson, P.M., B. Doldersum, P.H.M.R. Cramers, and L.L. Van Dierendonck, *The kinetics of uncatalyzed sodium sulfite oxidation*. Chemical Engineering Science, 1993. **48**(5): p. 933-941.
 122. Linek, V. and V. Vacek, *Chemical engineering use of catalyzed sulfite oxidation kinetics for the determination of mass transfer characteristics of gas—liquid contactors*. Chemical Engineering Science, 1981. **36**(11): p. 1747-1768.
 123. Kobe, K.A. and W.L. Gooding, *Oxygen Removal from Boiler Feed Water by Sodium Sulfite*. Industrial & Engineering Chemistry, 1935. **27**(3): p. 331-333.
 124. Coker, A.K., *Chapter 10 - Distillation: Part 1: Distillation Process Performance*, in *Ludwig's Applied Process Design for Chemical and Petrochemical Plants (Fourth Edition)*. 2010, Gulf Professional Publishing: Boston. p. 1-268.
 125. Towler, G. and R. Sinnott, *Chapter 17 - Separation Columns (Distillation, Absorption, and Extraction)*, in *Chemical Engineering Design (Second Edition)*. 2013, Butterworth-Heinemann: Boston. p. 807-935.
 126. Yong, A. and E.O. Obanijesu, *Influence of natural gas production chemicals on scale production in MEG regeneration systems*. Chemical Engineering Science, 2015. **130**: p. 172-182.
 127. Sarmini, K. and E. Kenndler, *Ionization Constants of Weak Acids and Bases in Organic Solvents*. Journal of Biochemical and Biophysical Methods, 1999. **38**(2): p. 123-137.
 128. Şanlı, S., Y. Altun, N. Şanlı, G. Alsancak, and J.L. Beltran, *Solvent Effects on pK_a Values of Some Substituted Sulfonamides in Acetonitrile–Water Binary Mixtures by the UV-Spectroscopy Method*. Journal of Chemical & Engineering Data, 2009. **54**(11): p. 3014-3021.
 129. Lee, C.K., E.H. Jeoung, and I.-S.H. Lee, *Effect of Mixtures of Water and Organic Solvents on the Acidities of 5-Membered Heteroaromatic Carboxylic Acids*. Journal of Heterocyclic Chemistry, 2000. **37**(1): p. 159-166.
 130. Reijenga, J., A. van Hoof, A. van Loon, and B. Teunissen, *Development of Methods for the Determination of pK(a) Values*. Analytical Chemistry Insights, 2013. **8**: p. 53-71.
 131. Yang, C., Y. Feng, B. Cheng, P. Zhang, Z. Qin, H. Zeng, and F. Sun, *Vapor–Liquid Equilibria for Three Binary Systems of N-Methylethanolamine, N-*
-

-
- Methyldiethanolamine, and Ethylene Glycol at P = (40.0, 30.0, and 20.0) kPa*. Journal of Chemical & Engineering Data, 2013. **58**(8): p. 2272-2279.
132. Kim, I., H.F. Svendsen, and E. Børresen, *Ebulliometric Determination of Vapor–Liquid Equilibria for Pure Water, Monoethanolamine, N -Methyldiethanolamine, 3-(Methylamino)-propylamine, and Their Binary and Ternary Solutions*. Journal of Chemical & Engineering Data, 2008. **53**(11): p. 2521-2531.
133. Ahmed, T., *Equations of state and PVT analysis*. 2013: Gulf Publishing Company. 1-553.
134. Schroepfer, G.J., *Factors Affecting the Efficiency of Sewage Sedimentation*. Sewage Works Journal, 1933. **5**(2): p. 209-232.
135. Mohammed, M.A. and D.A.E. Halagy, *Studying the factors affecting the settling velocity of solid particles in non-Newtonian fluids*. Al-Nahrain Journal for Engineering Sciences, 2013. **16**(1): p. 41-50.
136. Pizzi, N.G., *Water treatment*. 4th ed.. ed, ed. A. American Water Works. 2010, Denver, Colo.: Denver, Colo. : American Water Works Association.
137. Crittenden, J.C., H. Montgomery Watson, and I. Wiley, *MWH's water treatment : principles and design*. 3rd ed. / revised by John C. Crittenden ... [et al.].. ed. Water treatment. 2012, Hoboken, N.J.: Hoboken, N.J. : John Wiley and Sons.
138. Binnie, C., *Basic water treatment*. Fifth edition.. ed, ed. M. Kimber. 2013: London : ICE Publishing.
139. Binks, B.P., *Colloidal Particles at a Range of Fluid–Fluid Interfaces*. Langmuir, 2017. **33**(28): p. 6947-6963.
140. Safouane, M., D. Langevin, and B.P. Binks, *Effect of Particle Hydrophobicity on the Properties of Silica Particle Layers at the Air–Water Interface*. Langmuir, 2007. **23**(23): p. 11546-11553.
141. Diao, J. and D.W. Fuerstenau, *Characterization of the wettability of solid particles by film flotation 2. Theoretical analysis*. Colloids and Surfaces, 1991. **60**: p. 145-160.
142. Yuan, Y. and T.R. Lee, *Contact Angle and Wetting Properties*, in *Surface Science Techniques*, G. Bracco and B. Holst, Editors. 2013, Springer Berlin Heidelberg: Berlin, Heidelberg. p. 3-34.
143. Al-Anssari, S., M. Arif, S. Wang, A. Barifcani, M. Lebedev, and S. Iglauer, *Wettability of nano-treated calcite/CO₂/brine systems: Implication for enhanced CO₂ storage potential*. International Journal of Greenhouse Gas Control, 2017. **66**: p. 97-105.
144. Feng, D.-x. and A.V. Nguyen, *Contact angle variation on single floating spheres and its impact on the stability analysis of floating particles*. Colloids and Surfaces A: Physicochemical and Engineering Aspects, 2017. **520**: p. 442-447.
145. Kan, H., H. Nakamura, and S. Watano, *Effect of particle wettability on particle-particle adhesion of colliding particles through droplet*. Powder Technology, 2016. **302**: p. 406-413.
146. Huntsberger, J.R., *The Relationship between Wetting and Adhesion*, in *Contact Angle, Wettability, and Adhesion*. 1964, AMERICAN CHEMICAL SOCIETY. p. 180-188.
147. Rabinovich, Y.I., M.S. Esayanur, and B.M. Moudgil, *Capillary Forces between Two Spheres with a Fixed Volume Liquid Bridge: Theory and Experiment*. Langmuir, 2005. **21**(24): p. 10992-10997.
148. Ennis, B.J., G. Tardos, and R. Pfeffer, *A microlevel-based characterization of granulation phenomena*. Powder Technology, 1991. **65**(1): p. 257-272.
149. Fuerstenau, D.W., J. Diao, and M.C. Williams, *Characterization of the wettability of solid particles by film flotation 1. Experimental investigation*. Colloids and Surfaces, 1991. **60**: p. 127-144.
150. Vargha-Butler, E.I. and E. Moy A.W. Neumann, *Sedimentation behaviour of low surface energy powders in different non-polar liquid systems*. Colloids and Surfaces, 1987. **24**(4): p. 315-324.
-

REFERENCES

151. Bergström, L., *Hamaker constants of inorganic materials*. Advances in Colloid and Interface Science, 1997. **70**: p. 125-169.
 152. Tadros, T., *Electrostatic Repulsion and Colloid Stability*, in *Encyclopedia of Colloid and Interface Science*, T. Tadros, Editor. 2013, Springer Berlin Heidelberg: Berlin, Heidelberg. p. 363-363.
 153. Popa, I., G. Gillies, G. Papastavrou, and M. Borkovec, *Attractive and Repulsive Electrostatic Forces between Positively Charged Latex Particles in the Presence of Anionic Linear Polyelectrolytes*. The Journal of Physical Chemistry B, 2010. **114**(9): p. 3170-3177.
 154. Moulin, P. and H. Roques, *Zeta potential measurement of calcium carbonate*. Journal of Colloid and Interface Science, 2003. **261**(1): p. 115-126.
 155. Buschow, K.H.J., *Encyclopedia of Materials: Science and Technology*. 2001: Elsevier.
 156. Menezes, J.L., J. Yan, and M.M. Sharma, *The Mechanism of Wettability Alteration Due to Surfactants in Oil-Based Muds*, in *SPE International Symposium on Oilfield Chemistry*. 1989, Society of Petroleum Engineers: Houston, Texas.
 157. Wu, Z., X. Wang, H. Liu, H. Zhang, and J.D. Miller, *Some physicochemical aspects of water-soluble mineral flotation*. Advances in Colloid and Interface Science, 2016. **235**: p. 190-200.
 158. Frimmel, F.H., *Chemistry of the Solid-Water Interface. Processes at the Mineral-Water and Particle-Water Interface in Natural Systems*. Von W. Stumm. Wiley, Chichester, 1992. X, 428 S., Broschur 32.50 £ - ISBN 0-471-57672-7. Angewandte Chemie, 1993. **105**(5): p. 800-800.
 159. Al-Anssari, S., M. Arif, S. Wang, A. Barifcani, and S. Iglauer, *Stabilising nanofluids in saline environments*. Journal of Colloid and Interface Science, 2017. **508**: p. 222-229.
 160. Omland, T.H., *Particle settling in non-Newtonian drilling fluids*, in *Petroleum Engineering*. 2010, University of Stavanger: Norway.
 161. Greenwood, R., *Review of the measurement of zeta potentials in concentrated aqueous suspensions using electroacoustics*. Advances in Colloid and Interface Science, 2003. **106**(1): p. 55-81.
 162. Hunter, R.J., *Foundations of Colloid Science*. 2001: Oxford University Press.
 163. Southall, N.T., K.A. Dill, and A.D.J. Haymet, *A View of the Hydrophobic Effect*. The Journal of Physical Chemistry B, 2002. **106**(3): p. 521-533.
 164. Meyer, E.E., K.J. Rosenberg, and J. Israelachvili, *Recent progress in understanding hydrophobic interactions*. Proceedings of the National Academy of Sciences, 2006. **103**(43): p. 15739.
 165. Patel, A.J., P. Varilly, S.N. Jamadagni, H. Acharya, S. Garde, and D. Chandler, *Extended surfaces modulate hydrophobic interactions of neighboring solutes*. Proceedings of the National Academy of Sciences, 2011. **108**(43): p. 17678.
 166. Xi, E. and A.J. Patel, *The hydrophobic effect, and fluctuations: The long and the short of it*. Proceedings of the National Academy of Sciences, 2016. **113**(17): p. 4549.
 167. Crist, J.T., Y. Zevi, J.F. McCarthy, J.A. Throop, and T.S. Steenhuis, *Transport and Retention Mechanisms of Colloids in Partially Saturated Porous Media*. Vadose Zone Journal, 2005. **4**(1): p. 184-195.
 168. Rezaei Gomari, K.A. and A.A. Hamouda, *Effect of fatty acids, water composition and pH on the wettability alteration of calcite surface*. Journal of Petroleum Science and Engineering, 2006. **50**(2): p. 140-150.
 169. Al-Anssari, S., A. Barifcani, S. Wang, L. Maxim, and S. Iglauer, *Wettability alteration of oil-wet carbonate by silica nanofluid*. Journal of Colloid and Interface Science, 2016. **461**: p. 435-442.
 170. Rezaei Gomari, K.A., R. Denoyel, and A.A. Hamouda, *Wettability of calcite and mica modified by different long-chain fatty acids (C18 acids)*. Journal of Colloid and Interface Science, 2006. **297**(2): p. 470-479.
-

REFERENCES

171. Hirasaki, G. and D.L. Zhang, *Surface Chemistry of Oil Recovery From Fractured, Oil-Wet, Carbonate Formations*. 2004.
 172. Thomas, M.M., J.A. Clouse, and J.M. Longo, *Adsorption of organic compounds on carbonate minerals: 1. Model compounds and their influence on mineral wettability*. *Chemical Geology*, 1993. **109**(1): p. 201-213.
 173. Somasundaran, P. and G.E. Agar, *The zero point of charge of calcite*. *Journal of Colloid and Interface Science*, 1967. **24**(4): p. 433-440.
 174. Lander, L.M., L.M. Siewierski, W.J. Brittain, and E.A. Vogler, *A systematic comparison of contact angle methods*. *Langmuir*, 1993. **9**(8): p. 2237-2239.
 175. Farokhpoor, R., B.J.A. Bjørkvik, E. Lindeberg, and O. Torsæter, *CO₂ Wettability Behavior During CO₂ Sequestration in Saline Aquifer -An Experimental Study on Minerals Representing Sandstone and Carbonate*. *Energy Procedia*, 2013. **37**: p. 5339-5351.
 176. Cline, J.T., D.C. Teeters, and M.A. Andersen, *Wettability Preferences of Minerals Used in Oil-Based Drilling Fluids*. 1989, Society of Petroleum Engineers.
 177. Iglauer, S., C.H. Pentland, and A. Busch, *CO₂ wettability of seal and reservoir rocks and the implications for carbon geo-sequestration*. *Water Resources Research*, 2015. **51**(1): p. 729-774.
 178. Chau, T.T., W.J. Bruckard, P.T.L. Koh, and A.V. Nguyen, *A review of factors that affect contact angle and implications for flotation practice*. *Advances in Colloid and Interface Science*, 2009. **150**(2): p. 106-115.
 179. Kumar, G. and K.N. Prabhu, *Review of non-reactive and reactive wetting of liquids on surfaces*. *Advances in Colloid and Interface Science*, 2007. **133**(2): p. 61-89.
 180. Shafrin, E.G. and W.A. Zisman, *CONSTITUTIVE RELATIONS IN THE WETTING OF LOW ENERGY SURFACES AND THE THEORY OF THE RETRACTION METHOD OF PREPARING MONOLAYERS*. *The Journal of Physical Chemistry*, 1960. **64**(5): p. 519-524.
 181. Ballal, D. and W.G. Chapman, *Hydrophobic and hydrophilic interactions in aqueous mixtures of alcohols at a hydrophobic surface*. *The Journal of Chemical Physics*, 2013. **139**(11): p. 114706.
 182. Lundgren, M., N.L. Allan, T. Cosgrove, and N. George, *Wetting of Water and Water/Ethanol Droplets on a Non-Polar Surface: A Molecular Dynamics Study*. *Langmuir*, 2002. **18**(26): p. 10462-10466.
 183. Yekeler, M., U. Ulusoy, and C. Hiçyılmaz, *Effect of particle shape and roughness of talc mineral ground by different mills on the wettability and floatability*. *Powder Technology*, 2004. **140**(1): p. 68-78.
 184. Hideo, N., I. Ryuichi, H. Yosuke, and S. Hiroyuki, *Effects of surface roughness on wettability*. *Acta Materialia*, 1998. **46**(7): p. 2313-2318.
 185. Alotaibi, M.B., R. Azmy, and H.A. Nasr-El-Din, *Wettability Challenges in Carbonate Reservoirs*. 2010, Society of Petroleum Engineers.
 186. Karoussi, O. and A.A. Hamouda, *Macroscopic and nanoscale study of wettability alteration of oil-wet calcite surface in presence of magnesium and sulfate ions*. *Journal of Colloid and Interface Science*, 2008. **317**(1): p. 26-34.
 187. Karoussi, O. and A.A. Hamouda, *Imbibition of Sulfate and Magnesium Ions into Carbonate Rocks at Elevated Temperatures and Their Influence on Wettability Alteration and Oil Recovery*. *Energy & Fuels*, 2007. **21**(4): p. 2138-2146.
 188. Qi, Z., Y. Wang, H. He, D. Li, and X. Xu, *Wettability Alteration of the Quartz Surface in the Presence of Metal Cations*. *Energy & Fuels*, 2013. **27**(12): p. 7354-7359.
 189. Growcock, F.B., C.F. Ellis, D.D. Schmidt, and J.J. Azar, *Electrical Stability, Emulsion Stability, and Wettability of Invert Oil-Based Muds*. 1994.
 190. Chen, P. and K.K. Mohanty, *Wettability Alteration in High Temperature Carbonate Reservoirs*, in *SPE Improved Oil Recovery Symposium*. 2014, Society of Petroleum Engineers: Tulsa, Oklahoma, USA.
-

-
191. Lee, K.S., N. Ivanova, V.M. Starov, N. Hilal, and V. Dutschk, *Kinetics of wetting and spreading by aqueous surfactant solutions*. Advances in Colloid and Interface Science, 2008. **144**(1): p. 54-65.
 192. Starov, V.M., *Surfactant solutions and porous substrates: spreading and imbibition*. Advances in Colloid and Interface Science, 2004. **111**(1): p. 3-27.
 193. Starov, V.M., S.R. Kosvintsev, and M.G. Velarde, *Spreading of Surfactant Solutions over Hydrophobic Substrates*. Journal of Colloid and Interface Science, 2000. **227**(1): p. 185-190.
 194. Standnes, D.C. and T. Austad, *Wettability alteration in chalk: 2. Mechanism for wettability alteration from oil-wet to water-wet using surfactants*. Journal of Petroleum Science and Engineering, 2000. **28**(3): p. 123-143.
 195. Anderson, W.G., *Wettability literature survey - Part 1: Rock/oil/brine interactions and the effects of core handling on wettability*. J. Pet. Technol.; (United States), 1986: p. Medium: X; Size: Pages: 1125-1144.
 196. Kasiri, N. and A. Bashiri, *Wettability and Its Effects on Oil Recovery in Fractured and Conventional Reservoirs*. Petroleum Science and Technology, 2011. **29**(13): p. 1324-1333.
 197. Morrow, N.R., *Wettability and Its Effect on Oil Recovery*. Journal of Petroleum Technology, 1990. **42**(12): p. 1476-1484.
 198. Atkins, P. and J. de Paula, *Atkins' Physical Chemistry*. 2010: OUP Oxford.
 199. Soames, A., S. Iglauer, A. Barifcani, and R. Gubner, *Acid Dissociation Constant (pKa) of Common Monoethylene Glycol (MEG) Regeneration Organic Acids and Methyl-diethanolamine at Varying MEG Concentration, Temperature, and Ionic Strength*. Journal of Chemical & Engineering Data, 2018. **63**(8): p. 2904-2913.
 200. Hamborg, E.S. and G.F. Versteeg, *Dissociation Constants and Thermodynamic Properties of Amines and Alkanolamines from (293 to 353) K*. Journal of Chemical & Engineering Data, 2009. **54**(4): p. 1318-1328.
 201. Nurmi, D.B., J.W. Overman, J. Erwin, and J.L. Hudson, *Sulfite Oxidation in Organic Acid Solutions*, in *Flue Gas Desulfurization*. 1982, AMERICAN CHEMICAL SOCIETY. p. 173-189.
 202. Brandt, C. and R. Vaneldik, *TRANSITION-METAL-CATALYZED OXIDATION OF SULFUR(IV) OXIDES - ATMOSPHERIC-RELEVANT PROCESSES AND MECHANISMS*, in *Chem. Rev.* 1995. p. 119-190.
 203. Al Helal, A., A. Soames, R. Gubner, S. Iglauer, and A. Barifcani, *Measurement of Monoethylene Glycol Volume Fraction at Varying Ionic Strengths and Temperatures*. Journal of Natural Gas Science and Engineering, 2018. **54**: p. 320-327.
 204. Hagerup, O. and S. Olsen, *Corrosion Control by pH Stabilizer, Materials and Corrosion Monitoring in 160 km Multiphase Offshore Pipeline*, in *CORROSION*. 2003, NACE International: San Diego, California.
 205. Al Helal, A., A. Soames, S. Iglauer, R. Gubner, and A. Barifcani, *The influence of magnetic fields on calcium carbonate scale formation within monoethylene glycol solutions at regeneration conditions*. Journal of Petroleum Science and Engineering, 2019. **173**: p. 158-169.
 206. Harned, H.S. and R.W. Ehlers, *The Dissociation Constant of Acetic Acid from 0 to 60° Centigrade¹*. Journal of the American Chemical Society, 1933. **55**(2): p. 652-656.
 207. Harned, H.S. and R.W. Ehlers, *The Dissociation Constant of Acetic Acid from 0 to 35° Centigrade*. Journal of the American Chemical Society, 1932. **54**(4): p. 1350-1357.
 208. Fein, J.B., *Experimental Study of Aluminum-, Calcium-, and Magnesium-Acetate Complexing at 80°C*. Geochimica et Cosmochimica Acta, 1991. **55**(4): p. 955-964.
 209. Choi, W.S. and K.-J. Kim, *Separation of Acetic Acid from Acetic Acid-Water Mixture by Crystallization*. Separation Science and Technology, 2013. **48**(7): p. 1056-1061.
-

REFERENCES

210. Rossiter, W.J., P.W. Brown, and M. Godette, *The Determination of Acidic Degradation Products in Aqueous Ethylene Glycol and Propylene Glycol Solutions using Ion Chromatography*. Solar Energy Materials, 1983. **9**(3): p. 267-279.
211. Daraboina, N., C. Malmos, and N. von Solms, *Synergistic kinetic inhibition of natural gas hydrate formation*. Fuel, 2013. **108**: p. 749-757.
212. Koch, G., J. Veryney, N. Thompson, O. Moghissi, M. Gould, and J. Payer, *International Measures of Prevention, Application, and Economics of Corrosion Technologies Study*, G. Jacobson, Editor. 2017, NACE International: 15835 Park Ten Place, Houston, TX 77084.
213. Aronu, U.E., K.G. Lauritsen, A. Grimstvedt, and T. Mejdell, *Impact of heat stable salts on equilibrium CO₂ absorption*. Energy Procedia, 2014. **63**(Supplement C): p. 1781-1794.
214. Pal, P., A. AbuKashabeh, S. Al-Asheh, and F. Banat, *Accumulation of heat stable salts and degraded products during thermal degradation of aqueous methyldiethanolamine (MDEA) using microwave digester and high pressure reactor*. Journal of Natural Gas Science and Engineering, 2014. **21**(Supplement C): p. 1043-1047.
215. Choi, Y.S., D. Duan, S. Nesic, F. Vitse, S.A. Bedell, and C. Worley, *Effect of Oxygen and Heat Stable Salts on the Corrosion of Carbon Steel in MDEA-Based CO₂ Capture Process*. Corrosion, 2010. **66**(12): p. C1-C10.
216. Haws, R., *Contaminants in amine gas treating*. CCR Technologies inc, 2001. **11375**.
217. Nainar, M. and A. Veawab, *Corrosion in CO₂ capture unit using MEA-piperazine blends*. Energy Procedia, 2009. **1**(1): p. 231-235.
218. Babu, D.R., M. Hosseinzadeh, A. Ehsaninejad, R. Babaei, M.R. Kashkooli, and H. Akbary, *Carbonates precipitation in MEG loops – A comparative study of South Pars and Bass Strait gas fields*. Journal of Natural Gas Science and Engineering, 2015. **27**, Part 2: p. 955-966.
219. Rinker, E.B., S.S. Ashour, and O.C. Sandall, *Absorption of Carbon Dioxide into Aqueous Blends of Diethanolamine and Methyldiethanolamine*. Industrial & Engineering Chemistry Research, 2000. **39**(11): p. 4346-4356.
220. AlHarooni, K., D. Pack, S. Iglauer, R. Gubner, V. Ghodkay, and A. Barifcani, *Analytical Techniques for Analyzing Thermally Degraded Monoethylene Glycol with Methyl Diethanolamine and Film Formation Corrosion Inhibitor*. Energy & Fuels, 2016. **30**(12): p. 10937-10949.
221. Soames, A., A. Barifcani, and R. Gubner, *Removal of Organic Acids during Mono-Ethylene Glycol Distillation and Reclamation to Minimize Long-Term Accumulation*. Industrial & Engineering Chemistry Research, 2019. **58**(16): p. 6730-6739.
222. Askari, M., M. Aliofkhaezrai, S. Ghaffari, and A. Hajizadeh, *Film Former Corrosion Inhibitors for Oil and Gas Pipelines - A Technical Review*. Journal of Natural Gas Science and Engineering, 2018. **58**: p. 92-114.
223. Saxena, A.K., V.K. Sharma, S.K. Chugh, C. Velchamy, R. Kumar, R. Prakash, B.K. Sharma, and R.S. Dinesh, *Corrosion Failure of Compressed-Natural-Gas Transmission Lines*, in *SPE India Oil and Gas Conference and Exhibition*. 1998, Society of Petroleum Engineers: New Delhi, India.
224. Remita, E., B. Tribollet, E. Sutter, V. Vivier, F. Ropital, and J. Kittel, *Hydrogen Evolution in Aqueous Solutions Containing Dissolved CO₂: Quantitative Contribution of the Buffering Effect*. Corrosion Science, 2008. **50**(5): p. 1433-1440.
225. Tran, T., B. Brown, S. Nešić, and B. Tribollet, *Investigation of the Electrochemical Mechanisms for Acetic Acid Corrosion of Mild Steel*. CORROSION, 2013. **70**(3): p. 223-229.
226. Castells, C.B., C. Ràfols, M. Rosés, and E. Bosch, *Effect of Temperature on pH Measurements and Acid–Base Equilibria in Methanol–Water Mixtures*. Journal of Chromatography A, 2003. **1002**(1): p. 41-53.
-

REFERENCES

227. Hartono, A., M. Saeed, I. Kim, and H.F. Svendsen, *Protonation Constant (pKa) of MDEA in Water as Function of Temperature and Ionic Strength*. Energy Procedia, 2014. **63**: p. 1122-1128.
228. Tagiuri, A., M. Mohamedali, and A. Henni, *Dissociation Constant (pKa) and Thermodynamic Properties of Some Tertiary and Cyclic Amines from (298 to 333) K*. Journal of Chemical & Engineering Data, 2016. **61**(1): p. 247-254.
229. Choi, Y.-S., D. Duan, S. Jiang, and S. Nešić, *Mechanistic Modeling of Carbon Steel Corrosion in a Methyldiethanolamine (MDEA)-Based Carbon Dioxide Capture Process*. CORROSION, 2013. **69**(6): p. 551-559.
230. Duan, D., S. Jiang, Y.-S. Choi, and S. Nešić, *Corrosion Mechanism of Carbon Steel in MDEA-Based CO₂ Capture Plants*, in CORROSION. 2013, NACE International: Orlando, Florida. p. 11.
231. Yamamoto, H. and J. Tokunaga, *Solubilities of Nitrogen and Oxygen in 1,2-Ethanediol + Water at 298.15 K and 101.33 kPa*. Journal of Chemical and Engineering Data, 1994. **39**(3): p. 544-547.
232. Han, J., J. Zhang, and J.W. Carey, *Effect of Bicarbonate on Corrosion of Carbon Steel in CO₂ Saturated Brines*. International Journal of Greenhouse Gas Control, 2011. **5**(6): p. 1680-1683.
233. Bian, C., Z.M. Wang, X. Han, C. Chen, and J. Zhang, *Electrochemical Response of Mild Steel in Ferrous Ion Enriched and CO₂ Saturated Solutions*. Corrosion Science, 2015. **96**: p. 42-51.
234. Stern, M. and A.L. Geary, *Electrochemical Polarization: I. A Theoretical Analysis of the Shape of Polarization Curves*. Journal of The Electrochemical Society, 1957. **104**(1): p. 56-63.
235. Desimone, M.P., G. Gordillo, and S.N. Simison, *The Effect of Temperature and Concentration on the Corrosion Inhibition Mechanism of an Amphiphilic Amido-Amine in CO₂ Saturated Solution*. Corrosion Science, 2011. **53**(12): p. 4033-4043.
236. Jenkins, A., *Performance of High-Temperature, Biodegradable Corrosion Inhibitors*, in CORROSION. 2011, NACE International: Houston, Texas. p. 12.
237. Zhang, J., L. Niu, F. Zhu, C. Li, and M. Du, *Theoretical and Experimental Studies for Corrosion Inhibition Performance of Q235 Steel by Imidazoline Inhibitors against CO₂ Corrosion*. Journal of Surfactants and Detergents, 2013. **16**(6): p. 947-956.
238. Zhang, J., D. Shi, X. Gong, F. Zhu, and M. Du, *Inhibition Performance of Novel Dissymmetric Bisquaternary Ammonium Salt with an Imidazoline Ring and an Ester Group*. Journal of Surfactants and Detergents, 2013. **16**(4): p. 515-522.
239. Tomoe, Y., M. Shimizu, and Y. Nagae, *Unusual Corrosion of a Drill Pipe in Newly Developed Drilling Mud during Deep Drilling*. CORROSION, 1999. **55**(7): p. 706-713.
240. Baraka-Lokmane, S., C. Hurtevent, M. Seiersten, E. Flaten, M. Farrell, O. Bradshaw, S. Hare, M. Bonis, F. Jacob, and N. Carles, *Technical challenges and solutions in a closed loop MEG regeneration system for gas field offshore, UK*. WIT Transactions on Engineering Sciences, 2013. **79**: p. 511-522.
241. Kim, H., Y. Lim, Y. Seo, and M. Ko, *Life cycle cost analysis of MEG regeneration process incorporating a modified slip stream concept*. Chemical Engineering Science, 2017. **166**: p. 181-192.
242. Foss, M., E. Gulbrandsen, and J. Sjöblom, *CO₂ Corrosion Inhibition And Oil Wetting Of Carbon Steel With Ferric Corrosion Products*, in CORROSION 2009. 2009, NACE International: Atlanta, Georgia. p. 17.
243. Schlangen, L.J.M., L.K. Koopal, M.A. Cohen Stuart, and J. Lyklema, *Wettability: thermodynamic relationships between vapour adsorption and wetting*. Colloids and Surfaces A: Physicochemical and Engineering Aspects, 1994. **89**(2): p. 157-167.

REFERENCES

244. Schulman, J.H. and J. Leja, *Control of contact angles at the oil-water-solid interfaces. Emulsions stabilized by solid particles (BaSO₄)*. Transactions of the Faraday Society, 1954. **50**(0): p. 598-605.
 245. Ulusoy, U. and M. Yekeler, *Correlation of the surface roughness of some industrial minerals with their wettability parameters*. Chemical Engineering and Processing: Process Intensification, 2005. **44**(5): p. 555-563.
 246. Hamouda, A. and O. Karoussi, *Effect of Temperature, Wettability and Relative Permeability on Oil Recovery from Oil-wet Chalk*. Energies, 2008. **1**(1): p. 19-34.
 247. Rao, D.N., *Wettability Effects in Thermal Recovery Operations*. 1999.
 248. Tang, G.Q. and N.R. Morrow, *Salinity, Temperature, Oil Composition, and Oil Recovery by Waterflooding*. 1997.
 249. Schembre, J.M., G.Q. Tang, and A.R. Kovscek, *Wettability alteration and oil recovery by water imbibition at elevated temperatures*. Journal of Petroleum Science and Engineering, 2006. **52**(1): p. 131-148.
 250. Al-Hadhrani, H.S. and M.J. Blunt, *Thermally Induced Wettability Alteration to Improve Oil Recovery in Fractured Reservoirs*. 2000, Society of Petroleum Engineers.
 251. Rao, D.N., *Wettability Effects in Thermal Recovery Operations*, in *SPE/DOE Improved Oil Recovery Symposium*. 1996, Society of Petroleum Engineers: Tulsa, Oklahoma.
 252. Hjelmeland, O.S. and L.E. Larrondo, *Experimental investigation of the effects of temperature, pressure, and crude oil composition on interfacial properties. [Interfacial tension between crude oil and brine]*. SPE (Society of Petroleum Engineers) Reserv. Eng.; (United States), 1986: p. Medium: X; Size: Pages: 321-328.
 253. Sharma, G. and K. Mohanty, *Wettability Alteration in High-Temperature and High-Salinity Carbonate Reservoirs*. 2013.
 254. Al-Anssari, S., S. Wang, A. Barifcani, M. Lebedev, and S. Iglauer, *Effect of temperature and SiO₂ nanoparticle size on wettability alteration of oil-wet calcite*. Fuel, 2017. **206**: p. 34-42.
 255. Dubey, S.T. and M.H. Waxman, *Asphaltene Adsorption and Desorption From Mineral Surfaces*. 1991.
 256. Legens, C., H. Toulhoat, L. Cuiec, F. Villieras, and T. Palermo, *Wettability Change Related to Adsorption of Organic Acids on Calcite: Experimental and Ab Initio Computational Studies*. 1999.
 257. Cuiec, L., *Effect of Drilling Fluids on Rock Surface Properties*. 1989.
 258. Ballard, T.J. and R.A. Dawe, *Wettability Alteration Induced by Oil-Based Drilling Fluid*. 1988, Society of Petroleum Engineers.
 259. Yan, J.N., J.L. Monezes, and M.M. Sharma, *Wettability Alteration Caused by Oil-Based Muds and Mud Components*. 1993.
 260. Sharma, M.M. and R.W. Wunderlich, *The alteration of rock properties due to interactions with drilling-fluid components*. Journal of Petroleum Science and Engineering, 1987. **1**(2): p. 127-143.
 261. Anderson, W., *Wettability Literature Survey- Part 2: Wettability Measurement*. 1986.
 262. Al-Anssari, S.F.J., *Application of Nanotechnology in Chemical Enhanced Oil Recovery and Carbon Storage*. 2018.
 263. Shi, X., R. Rosa, and A. Lazzeri, *On the Coating of Precipitated Calcium Carbonate with Stearic Acid in Aqueous Medium*. Langmuir, 2010. **26**(11): p. 8474-8482.
 264. Hansen, G., A.A. Hamouda, and R. Denoyel, *The effect of pressure on contact angles and wettability in the mica/water/n-decane system and the calcite+stearic acid/water/n-decane system*. Colloids and Surfaces A: Physicochemical and Engineering Aspects, 2000. **172**(1): p. 7-16.
 265. Kirby, B.J. and E.F. Hasselbrink, *Zeta potential of microfluidic substrates: 1. Theory, experimental techniques, and effects on separations*. ELECTROPHORESIS, 2004. **25**(2): p. 187-202.
-

REFERENCES

266. Zhou, Y. and G.V. Franks, *Flocculation Mechanism Induced by Cationic Polymers Investigated by Light Scattering*. *Langmuir*, 2006. **22**(16): p. 6775-6786.
267. Kasha, A., H. Al-Hashim, W. Abdallah, R. Taherian, and B. Sauerer, *Effect of Ca²⁺, Mg²⁺ and SO₄²⁻ ions on the zeta potential of calcite and dolomite particles aged with stearic acid*. *Colloids and Surfaces A: Physicochemical and Engineering Aspects*, 2015. **482**: p. 290-299.
268. Foss, M., E. Gulbrandsen, and J. Sjöblom, *Adsorption of Corrosion Inhibitors onto Iron Carbonate (FeCO₃) Studied by Zeta Potential Measurements*. *Journal of Dispersion Science and Technology*, 2010. **31**(2): p. 200-208.
269. Bi, Z., W. Liao, and L. Qi, *Wettability alteration by CTAB adsorption at surfaces of SiO₂ film or silica gel powder and mimic oil recovery*. *Applied Surface Science*, 2004. **221**(1): p. 25-31.
270. Tyrode, E., M.W. Rutland, and C.D. Bain, *Adsorption of CTAB on Hydrophilic Silica Studied by Linear and Nonlinear Optical Spectroscopy*. *Journal of the American Chemical Society*, 2008. **130**(51): p. 17434-17445.
271. Standnes, D.C. and T. Austad, *Wettability alteration in carbonates: Interaction between cationic surfactant and carboxylates as a key factor in wettability alteration from oil-wet to water-wet conditions*. *Colloids and Surfaces A: Physicochemical and Engineering Aspects*, 2003. **216**(1): p. 243-259.
272. Hou, B., Y. Wang, X. Cao, J. Zhang, X. Song, M. Ding, and W. Chen, *Surfactant-Induced Wettability Alteration of Oil-Wet Sandstone Surface: Mechanisms and Its Effect on Oil Recovery*. *Journal of Surfactants and Detergents*, 2016. **19**(2): p. 315-324.
273. Jarrahan, K., O. Seiedi, M. Sheykhan, M.V. Sefti, and S. Ayatollahi, *Wettability alteration of carbonate rocks by surfactants: A mechanistic study*. *Colloids and Surfaces A: Physicochemical and Engineering Aspects*, 2012. **410**: p. 1-10.
274. Salehi, M., S.J. Johnson, and J.-T. Liang, *Mechanistic Study of Wettability Alteration Using Surfactants with Applications in Naturally Fractured Reservoirs*. *Langmuir*, 2008. **24**(24): p. 14099-14107.
275. Liu, Y., M. Tourbin, S. Lachaize, and P. Guiraud, *Silica nanoparticles separation from water: Aggregation by cetyltrimethylammonium bromide (CTAB)*. *Chemosphere*, 2013. **92**(6): p. 681-687.
276. Cui, Z.G., L.L. Yang, Y.Z. Cui, and B.P. Binks, *Effects of Surfactant Structure on the Phase Inversion of Emulsions Stabilized by Mixtures of Silica Nanoparticles and Cationic Surfactant*. *Langmuir*, 2010. **26**(7): p. 4717-4724.
277. Closmann, F. and G.T. Rochelle, *Degradation of aqueous methyldiethanolamine by temperature and oxygen cycling*. *Energy Procedia*, 2011. **4**(Supplement C): p. 23-28.
278. Voice, A.K., F. Closmann, and G.T. Rochelle, *Oxidative Degradation of Amines With High-Temperature Cycling*. *Energy Procedia*, 2013. **37**(Supplement C): p. 2118-2132.
279. Lide, D.R., *CRC Handbook of Chemistry and Physics, 88th Edition*. 2007: Taylor & Francis.
280. International Union of Pure Applied Chemistry. Commission on Equilibrium Data, E.P. Serjeant, B. Dempsey, and International Union of Pure Applied Chemistry. Commission on Electrochemical Data, *Ionisation constants of organic acids in aqueous solution*. 1979: Pergamon Press.
281. Riddick, J.A., W.B. Bunger, and T.K. Sakano, *Organic Solvents: Physical Properties and Methods of Purification*. 1986: Wiley.
282. Pérez-Salado Kamps, Á. and G. Maurer, *Dissociation Constant of N-Methyldiethanolamine in Aqueous Solution at Temperatures from 278 K to 368 K*. *Journal of Chemical & Engineering Data*, 1996. **41**(6): p. 1505-1513.
283. Oscarson, J.L., G. Wu, P.W. Faux, R.M. Izatt, and J.J. Christensen, *Thermodynamics of protonation of alkanolamines in aqueous solution to 325° C*. *Thermochimica Acta*, 1989. **154**(1): p. 119-127.
-

REFERENCES

284. Bates, R.G., *Determination of pH, Theory and Practice*. 2d ed. ed. 1973, New York: Wiley.
285. Fernandes Diniz, J.M.B. and T.M. Herrington, *pKa determination of weak acids over a large pH range*. Journal of Chemical & Engineering Data, 1993. **38**(1): p. 109-111.
286. Randall, M. and C.F. Failey, *The Activity Coefficient of Non-Electrolytes in Aqueous Salt Solutions from Solubility Measurements. The Salting-out Order of the Ions*. Chemical Reviews, 1927. **4**(3): p. 285-290.
287. Kortum, G., W. Vogel, K. Andrussov, International Union of Pure Applied Chemistry, and Commission on Electrochemical Data, *Dissociation constants of organic acids in aqueous solution*. 1961, London: Butterworths.
288. Wolery, T.J., *Debye-hückel equation*, in *Geochemistry*. 1998, Springer Netherlands: Dordrecht. p. 124-126.
289. Kielland, J., *Individual Activity Coefficients of Ions in Aqueous Solutions*. Journal of the American Chemical Society, 1937. **59**(9): p. 1675-1678.
290. Manov, G.G., R.G. Bates, W.J. Hamer, and S.F. Acree, *Values of the Constants in the Debye—Hückel Equation for Activity Coefficients*¹. Journal of the American Chemical Society, 1943. **65**(9): p. 1765-1767.
291. Robinson, R.A. and R.H. Stokes, *Electrolyte Solutions: Second Revised Edition*. 2012: Dover Publications, Incorporated.
292. Fenneman, D.B., *Pulsed high-voltage dielectric properties of ethylene glycol/water mixtures*. Journal of Applied Physics, 1982. **53**(12): p. 8961-8968.
293. Akerlof, G., *Dielectric Constants of Some Organic Solvent-Water Mixtures at Various Temperatures*. Journal of the American Chemical Society, 1932. **54**(11): p. 4125-4139.
294. Hamborg, E.S., J.P.M. Niederer, and G.F. Versteeg, *Dissociation Constants and Thermodynamic Properties of Amino Acids Used in CO₂ Absorption from (293 to 353) K*. Journal of Chemical & Engineering Data, 2007. **52**(6): p. 2491-2502.
295. Kim, J.-H., C. Dobrogowska, and L.G. Hepler, *Thermodynamics of ionization of aqueous alkanolamines*. Canadian Journal of Chemistry, 1987. **65**(8): p. 1726-1728.
296. Kim, M.H., C.S. Kim, H.W. Lee, and K. Kim, *Temperature dependence of dissociation constants for formic acid and 2,6-dinitrophenol in aqueous solutions up to 175°C*. Journal of the Chemical Society, Faraday Transactions, 1996. **92**(24): p. 4951-4956.
297. Harned, H.S. and R.W. Ehlers, *The Dissociation Constant of Propionic Acid from 0 to 60°C*. Journal of the American Chemical Society, 1933. **55**(6): p. 2379-2383.
298. Rozhkova, A.G., E.V. Butyrskaya, M.V. Rozhkova, and V.A. Shaposhnik, *Quantum chemical calculation of cation interaction with water molecules and ethylene glycol*. Journal of Structural Chemistry, 2007. **48**(1): p. 166-169.
299. Rozhkova, M.V., A.G. Rozhkova, and E.V. Butyrskaya, *Separation of mineral salts and nonelectrolytes (ethylene glycol) by dialysis through ion-exchange membranes*. Journal of Analytical Chemistry, 2007. **62**(8): p. 710-715.
300. Closmann, F., T. Nguyen, and G.T. Rochelle, *MDEA/Piperazine as a solvent for CO₂ capture*. Energy Procedia, 2009. **1**(1): p. 1351-1357.
301. Arcis, H., L. Rodier, K. Ballerat-Busserolles, and J.-Y. Coxam, *Modeling of (vapor+liquid) equilibrium and enthalpy of solution of carbon dioxide (CO₂) in aqueous methyldiethanolamine (MDEA) solutions*. The Journal of Chemical Thermodynamics, 2009. **41**(6): p. 783-789.
302. The International Association for the Properties of Water and Steam, *Guideline on the Use of Fundamental Physical Constants and Basic Constants of Water*. IAPWS G5-01(2016).
303. Fogg, E.T., A.N. Hixson, and A.R. Thompson, *Densities and Refractive Indexes for Ethylene Glycol-Water Solutions*. Analytical Chemistry, 1955. **27**(10): p. 1609-1611.
-

REFERENCES

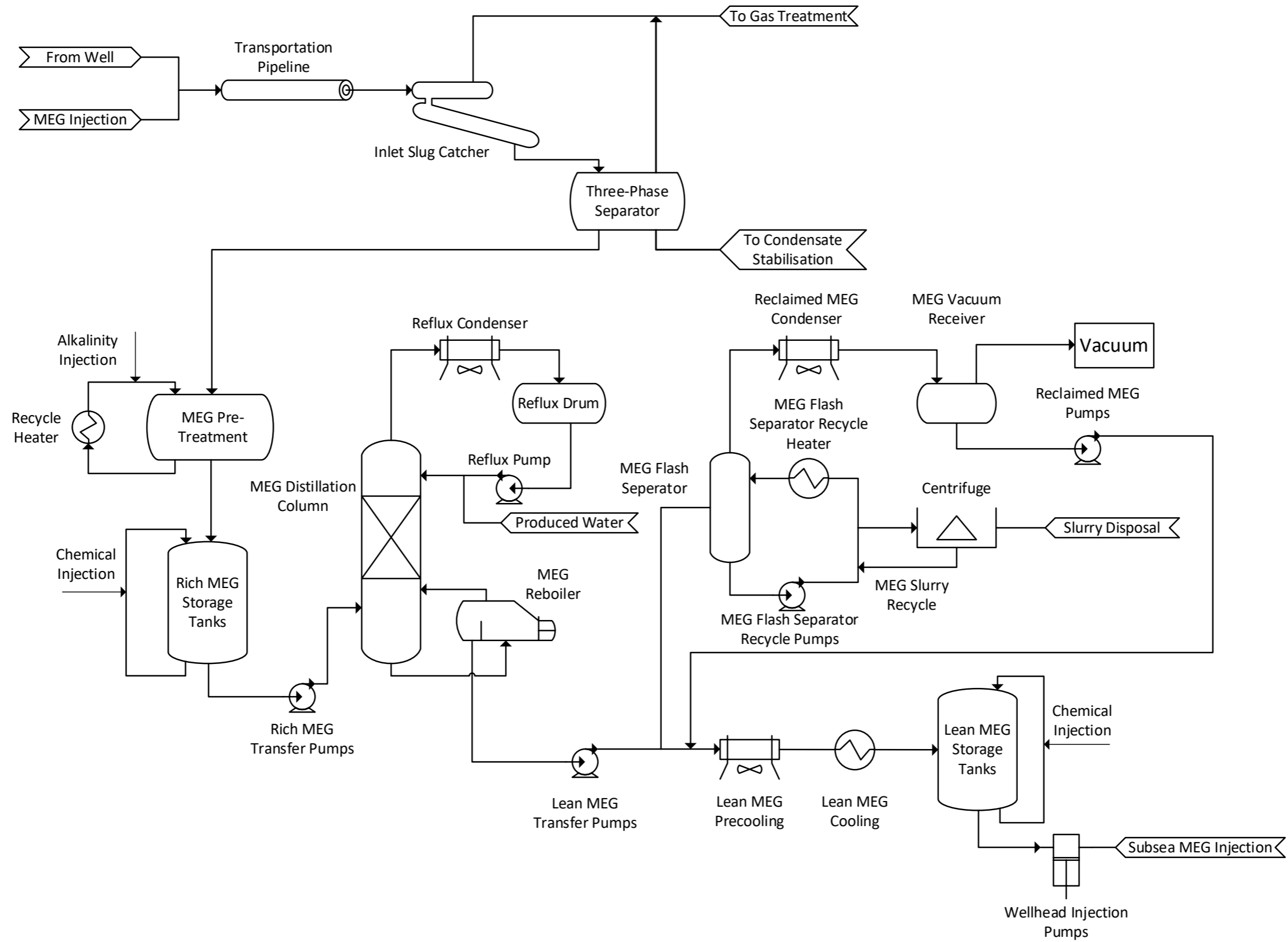
304. Kozma, I.Z., P. Krok, and E. Riedle, *Direct measurement of the group-velocity mismatch and derivation of the refractive-index dispersion for a variety of solvents in the ultraviolet*. Journal of the Optical Society of America B, 2005. **22**(7): p. 1479-1485.
305. Trimble, H.M. and W. Potts, *Glycol-Water Mixtures Vapor Pressure-Boiling Point-Composition Relations*. Industrial & Engineering Chemistry, 1935. **27**(1): p. 66-68.
306. Yaws, C.L., *Chemical properties handbook : physical, thermodynamic, environmental, transport, and health related properties for organic and inorganic chemicals / [edited] by Carl L. Yaws*. 1999, New York, N.Y.: New York, N.Y. : McGraw-Hill Education LLC.
307. Zhang, Q., S. Cai, W. Zhang, Y. Lan, and X. Zhang, *Density, viscosity, conductivity, refractive index and interaction study of binary mixtures of the ionic liquid 1-ethyl-3-methylimidazolium acetate with methyldiethanolamine*. Journal of Molecular Liquids, 2017. **233**(Supplement C): p. 471-478.
308. Voutsas, E., A. Vrachnos, and K. Magoulas, *Measurement and thermodynamic modeling of the phase equilibrium of aqueous N-methyldiethanolamine solutions*. Fluid Phase Equilibria, 2004. **224**(2): p. 193-197.
309. Barreau, A., P. Mougin, C. Lefebvre, Q.M. Luu Thi, and J. Rieu, *Ternary Isobaric Vapor-Liquid Equilibria of Methanol + N-Methyldiethanolamine + Water and Methanol + 2-Amino-2-methyl-1-propanol + Water Systems*. Journal of Chemical & Engineering Data, 2007. **52**(3): p. 769-773.
310. Van Ness, H.C., *Thermodynamics in the treatment of vapor/liquid equilibrium (VLE) data*. Pure and applied chemistry, 1995. **67**(6): p. 859-872.
311. Wagner, W. and A. Pruß, *The IAPWS Formulation 1995 for the Thermodynamic Properties of Ordinary Water Substance for General and Scientific Use*. Journal of Physical and Chemical Reference Data, 2002. **31**(2): p. 387-535.
312. Garcia-Chavez, L.Y., B. Schuur, and A.B. de Haan, *Liquid-liquid equilibrium data for mono ethylene glycol extraction from water with the new ionic liquid tetraoctyl ammonium 2-methyl-1-naphtoate as solvent*. The Journal of Chemical Thermodynamics, 2012. **51**(Supplement C): p. 165-171.
313. Xu, S., S. Qing, Z. Zhen, C. Zhang, and J.J. Carroll, *Vapor pressure measurements of aqueous N-methyldiethanolamine solutions*. Fluid Phase Equilibria, 1991. **67**(C): p. 197-201.
314. Renon, H. and J.M. Prausnitz, *Local compositions in thermodynamic excess functions for liquid mixtures*. AIChE Journal, 1968. **14**(1): p. 135-144.
315. Abrams, D.S. and J.M. Prausnitz, *Statistical thermodynamics of liquid mixtures: A new expression for the excess Gibbs energy of partly or completely miscible systems*. AIChE Journal, 1975. **21**(1): p. 116-128.
316. Herington, E.F.G., *Tests for the Consistency of Experimental Isobaric Vapor-Liquid Equilibrium Data*. Journal of the Institute of Petroleum., 1951. **37**: p. 457-470.
317. Wisniak, J., *A new test for the thermodynamic consistency of vapor-liquid equilibrium*. Industrial & Engineering Chemistry Research, 1993. **32**(7): p. 1531-1533.
318. Wilson, G.M., *Vapor-Liquid Equilibrium. XI. A New Expression for the Excess Free Energy of Mixing*. Journal of the American Chemical Society, 1964. **86**(2): p. 127-130.
319. Wang, H.-x., J.-j. Xiao, Y.-y. Shen, C.-s. Ye, L. Li, and T. Qiu, *Experimental Measurements of Vapor-Liquid Equilibrium Data for the Binary Systems of Methanol + 2-Butyl Acetate, 2-Butyl Alcohol + 2-Butyl Acetate, and Methyl Acetate + 2-Butyl Acetate at 101.33 kPa*. Journal of Chemical & Engineering Data, 2013. **58**(6): p. 1827-1832.
320. Kontogeorgis, G.M. and G.K. Folas, *Activity Coefficient Models Part 2: Local Composition Models, from Wilson and NRTL to UNIQUAC and UNIFAC*, in *Thermodynamic Models for Industrial Applications*. 2009, John Wiley & Sons, Ltd. p. 109-157.
321. Mathias, P.M., *Guidelines for the Analysis of Vapor-Liquid Equilibrium Data*. Journal of Chemical & Engineering Data, 2017. **62**(8): p. 2231-2233.
-

REFERENCES

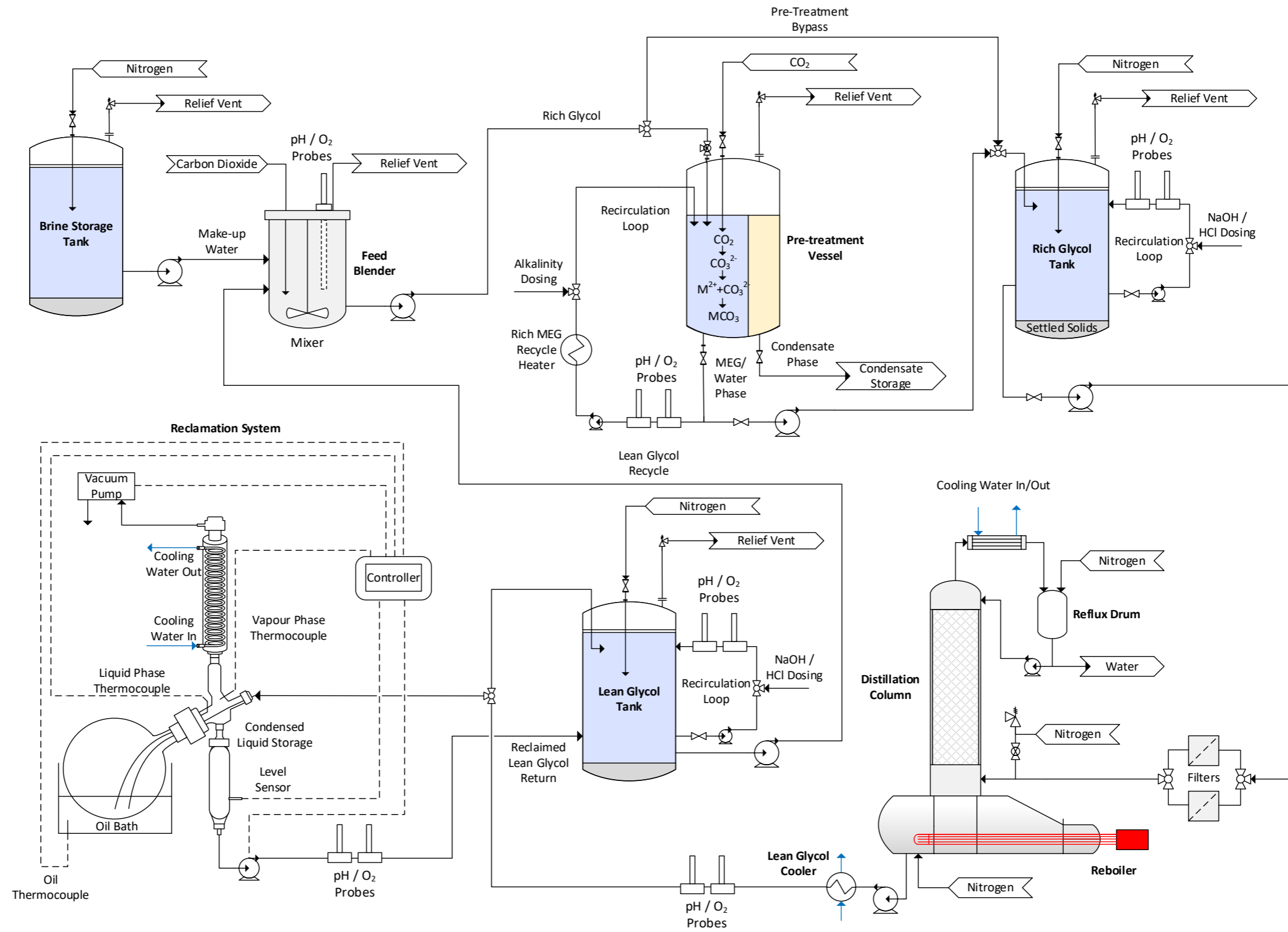
322. Sloan, E.D., *Fundamental principles and applications of natural gas hydrates*. Nature, 2003. **426**(6964): p. 353-363.
323. Kotronarou, A. and L. Sigg, *Sulfur dioxide oxidation in atmospheric water: role of iron(II) and effect of ligands*. Environmental Science & Technology, 1993. **27**(13): p. 2725-2735.
324. Halvorsen, A.M.K., T.R. Andersen, E.N. Halvorsen, G.P. Kojen, J.I. Skar, C. Biørnstad, and H. Fitje, *The Relationship Between Internal Corrosion Control Method, Scale Control And Meg Handling Of A Multiphase Carbon Steel Pipeline Carrying Wet Gas With CO₂ And Cetic Acid*. 2007, NACE International.
325. Kelland, M.A., *Oxygen Scavengers*, in *Production Chemicals for the Oil and Gas Industry*. 2009, CRC Press.
326. Backstrom, H.J., *The chain mechanism in the autoxidation of sodium sulfite solutions*. Z. Phys. Chem (International Journal of Research in Physical Chemistry and Chemical Physics), 1934. **25**: p. 99-121.
327. Ermakov, A.N., G.A. Poskrebyshev, and A.P. Purmal, *Sulfite Oxidation: The State-of-the-Art of the Problem*. Kinetics and Catalysis, 1997. **38**(3): p. 295-308.
328. Connick, R.E. and Y.-X. Zhang, *Kinetics and Mechanism of the Oxidation of HSO₃⁻ by O₂. 2. The Manganese(II)-Catalyzed Reaction*. Inorganic Chemistry, 1996. **35**(16): p. 4613-4621.
329. Zhang, J.-Z. and F.J. Millero, *The rate of sulfite oxidation in seawater*. Geochimica et Cosmochimica Acta, 1991. **55**(3): p. 677-685.
330. Hobson, D.B., P.J. Richardson, P.J. Robinson, E.A. Hewitt, and I. Smith, *Kinetics of the oxygen-sulfite reaction at waterflood concentrations: Effect of catalysts and seawater medium*. Industrial and Engineering Chemistry Research, 1987. **26**(9): p. 1818-1822.
331. Snavely, E.S., Jr., *Chemical Removal of Oxygen from Natural Waters*. 1971.
332. Salasi, M., T. Pojtanabuntoeng, S. Wong, and M. Lehmann, *Efficacy of Bisulfite Ions as an Oxygen Scavenger in Monoethylene Glycol (At Least 20 wt%)/Water Mixtures*. 2017.
333. Zhao, B., Y. Li, H. Tong, Y. Zhuo, L. Zhang, J. Shi, and C. Chen, *Study on the reaction rate of sulfite oxidation with cobalt ion catalyst*. Chemical Engineering Science, 2005. **60**(3): p. 863-868.
334. Grgić, I. and G. Berčić, *A Simple Kinetic Model for Autoxidation of S(IV) Oxides Catalyzed by Iron and/or Manganese Ions*. Journal of Atmospheric Chemistry, 2001. **39**(2): p. 155-170.
335. Novič, M., I. Grgić, M. Poje, and V. Hudnik, *Iron-catalyzed oxidation of s(IV) species by oxygen in aqueous solution: Influence of pH on the redox cycling of iron*. Atmospheric Environment, 1996. **30**(24): p. 4191-4196.
336. Brandt, C., I. Fabian, and R. van Eldik, *Kinetics and Mechanism of the Iron(III)-catalyzed Autoxidation of Sulfur(IV) Oxides in Aqueous Solution. Evidence for the Redox Cycling of Iron in the Presence of Oxygen and Modeling of the Overall Reaction Mechanism*. Inorganic Chemistry, 1994. **33**(4): p. 687-701.
337. Wang, L.-D., Y.-L. Ma, J.-M. Hao, and Y. Zhao, *Mechanism and Kinetics of Sulfite Oxidation in the Presence of Ethanol*. Industrial & Engineering Chemistry Research, 2009. **48**(9): p. 4307-4311.

Every reasonable effort has been made to acknowledge the owners of copyright material. I would be pleased to hear from any copyright owner has been omitted or incorrectly acknowledged.

Appendix A: MEG Regeneration Flow-Scheme Utilising Pre-Treatment and Slip-Stream Reclamation



Appendix B: Curtin Corrosion Centre's MEG Regeneration Pilot Plant



Appendix C: Supplementary Particle Wettability Results – Chapter Seven



Figure C-1. Behaviour of oil-wetted solid particles at MEG-air interface

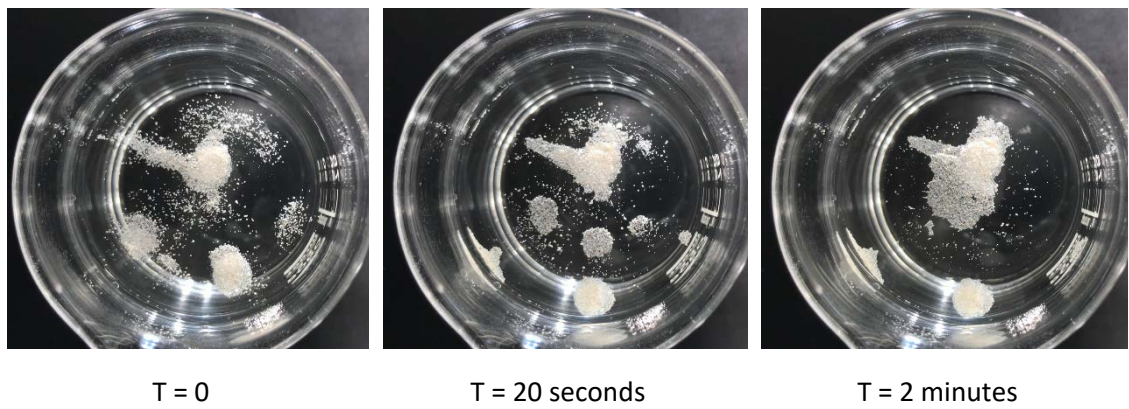


Figure C-2. Oil-wetted quartz particle attraction at MEG-air interface

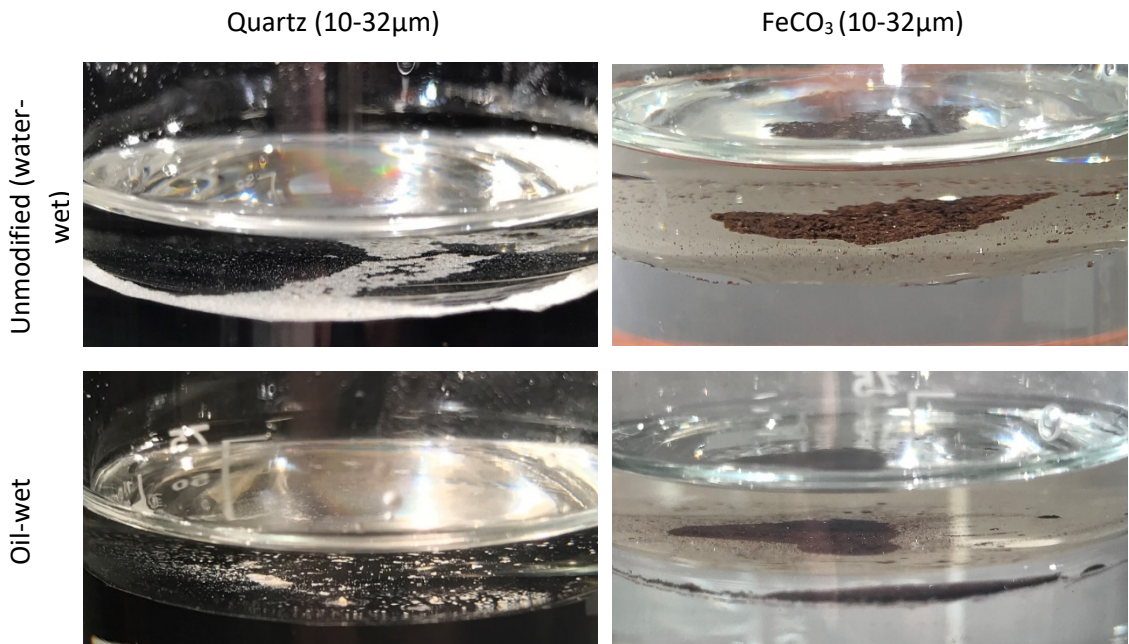


Figure C-3. Behaviour of solid particles at MEG-condensate interface



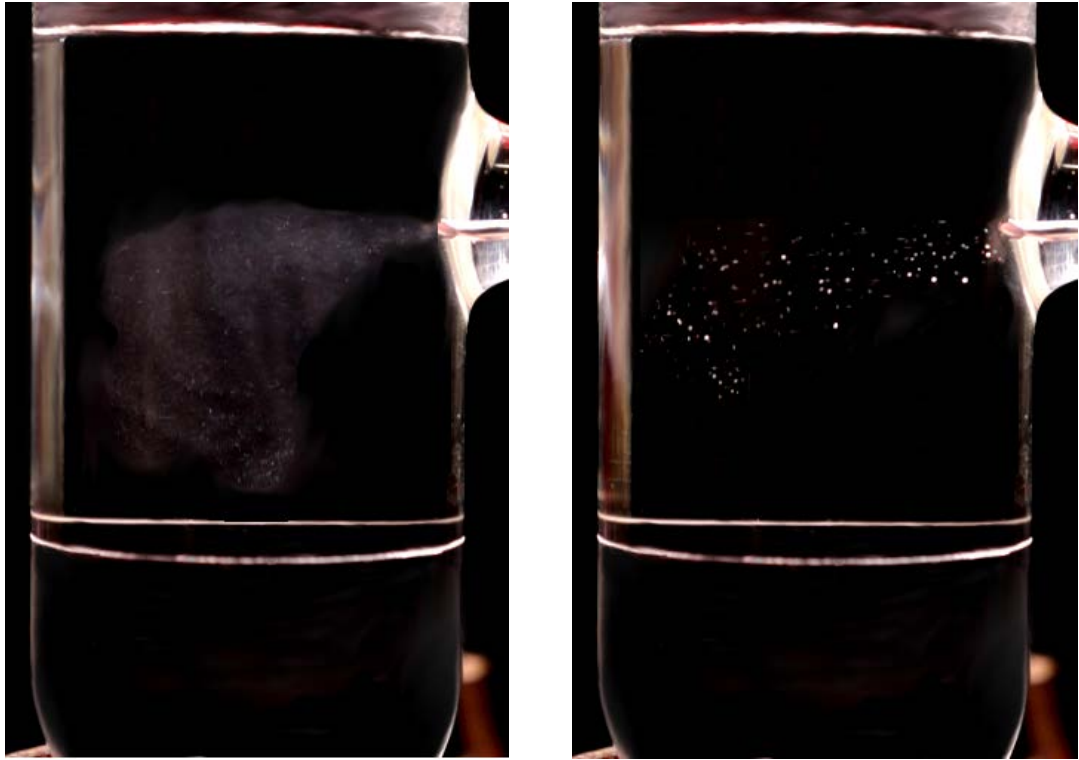
T = 10 seconds



T = 30 seconds

Figure C-4. Settlement of water/MEG-wetted FeCO_3 ($>63 \mu\text{m}$) in 50% wt. MEG solution32-63 μm Water/MEG Wetted Quartz32-63 μm Oil-Wetted Quartz

T = 0 seconds



T = 10 seconds



T = 30 seconds

T = 60 seconds

Figure C-5. Comparison of water/MEG-wetted and oil-wetted quartz (>63 μm) in 50% wt. MEG solution

Table C-1. Industrial rich MEG solution compositions.

Component (ppmw)	System 1	System 2
Na	994	4679
K	13	106
Ca	4	70
Mg	1.2	9
Fe	0.12	0.31
Sr	0.34	10
Ba	2.4	19
Li	0.26	2.5
Cl	1532	7216
HCO ₃	440	828
SO ₄	4	6.2
Acetic acid	721	500
Propanoic acid	63	55
Butanoic acid	15	4.6
Pentanoic acid	22	2.3

Appendix D: Supplementary Acid Dissociation Experimental Data – Chapter Eight

Table D-1. Effect of MEG concentration, temperature and ionic strength on acetic acid pK_a^a

MEG Concentration (wt. %)	Temperature (°C)	Ionic Strength (mol/L)	pK_a	MEG Concentration (wt. %)	Temperature (°C)	Ionic Strength (mol/L)	pK_a
30	25	0.000	4.961	30	60	0	5.010
30	25	0.011	4.960	30	60	0.011	5.008
30	25	0.023	4.959	30	60	0.023	5.005
30	25	0.046	4.956	30	60	0.046	5.002
30	25	0.092	4.952	30	60	0.092	4.999
30	25	0.229	4.943	30	60	0.229	4.992
30	25	0.459	4.930	30	60	0.459	4.972
30	40	0	4.970	30	70	0	5.038
30	40	0.011	4.968	30	70	0.011	5.035
30	40	0.023	4.966	30	70	0.023	5.035
30	40	0.046	4.964	30	70	0.046	5.030
30	40	0.092	4.961	30	70	0.092	5.026
30	40	0.229	4.949	30	70	0.229	5.013
30	40	0.459	4.929	30	70	0.459	5.001
30	50	0	4.986	30	80	0	5.081
30	50	0.011	4.984	30	80	0.011	5.076
30	50	0.023	4.981	30	80	0.023	5.078
30	50	0.046	4.979	30	80	0.046	5.076
30	50	0.092	4.967	30	80	0.092	5.072
30	50	0.229	4.964	30	80	0.229	5.060
30	50	0.459	4.952	30	80	0.459	5.039
50	25	0.000	5.220	50	60	0	5.271
50	25	0.011	5.219	50	60	0.011	5.269
50	25	0.023	5.218	50	60	0.023	5.268
50	25	0.046	5.216	50	60	0.046	5.266
50	25	0.092	5.212	50	60	0.092	5.263
50	25	0.229	5.202	50	60	0.229	5.251
50	25	0.459	5.189	50	60	0.459	5.236
50	40	0	5.240	50	70	0	5.300
50	40	0.011	5.238	50	70	0.011	5.299
50	40	0.023	5.236	50	70	0.023	5.295
50	40	0.046	5.231	50	70	0.046	5.291
50	40	0.092	5.231	50	70	0.092	5.291
50	40	0.229	5.220	50	70	0.229	5.282
50	40	0.459	5.205	50	70	0.459	5.269
50	50	0	5.251	50	80	0	5.347
50	50	0.011	5.247	50	80	0.011	5.345
50	50	0.023	5.248	50	80	0.023	5.344

50	50	0.046	5.245	50	80	0.046	5.342
50	50	0.092	5.244	50	80	0.092	5.339
50	50	0.229	5.230	50	80	0.229	5.327
50	50	0.459	5.215	50	80	0.459	5.314
80	25	0.000	5.928	80	60	0	5.986
80	25	0.011	5.927	80	60	0.011	5.985
80	25	0.023	5.926	80	60	0.023	5.984
80	25	0.046	5.924	80	60	0.046	5.981
80	25	0.092	5.920	80	60	0.092	5.977
80	25	0.229	5.910	80	60	0.229	5.968
80	25	0.459	5.896	80	60	0.459	5.941
80	40	0	5.940	80	70	0	6.020
80	40	0.011	5.938	80	70	0.011	6.018
80	40	0.023	5.937	80	70	0.023	6.018
80	40	0.046	5.935	80	70	0.046	6.015
80	40	0.092	5.931	80	70	0.092	6.011
80	40	0.229	5.922	80	70	0.229	5.998
80	40	0.459	5.906	80	70	0.459	5.993
80	50	0	5.958	80	80	0	6.073
80	50	0.011	5.955	80	80	0.011	6.068
80	50	0.023	5.956	80	80	0.023	6.070
80	50	0.046	5.953	80	80	0.046	6.067
80	50	0.092	5.940	80	80	0.092	6.063
80	50	0.229	5.940	80	80	0.229	6.053
80	50	0.459	5.926	80	80	0.459	6.032

^aStandard uncertainties: $u(T) = 0.01^\circ\text{C}$, $u(\text{MEG } \%) = 0.2$, $u(\text{p}K_a) = 0.04$, $u(\text{Ionic Strength}) = 0.001$ mol/L

Table D-2. Effect of MEG concentration, temperature and ionic strength on MDEA $\text{p}K_a$ ^a

MEG Concentration (wt. %)	Temperature ($^\circ\text{C}$)	Ionic Strength (mol/L)	$\text{p}K_a$	MEG Concentration (wt. %)	Temperature ($^\circ\text{C}$)	Ionic Strength (mol/L)	$\text{p}K_a$
30	25	0.000	8.532	30	60	0	7.871
30	25	0.011	8.535	30	60	0.011	7.875
30	25	0.023	8.539	30	60	0.023	7.877
30	25	0.046	8.548	30	60	0.046	7.885
30	25	0.092	8.563	30	60	0.092	7.898
30	25	0.229	8.602	30	60	0.229	7.941
30	25	0.459	8.677	30	60	0.459	8.016
30	40	0	8.221	30	70	0	7.691
30	40	0.011	8.231	30	70	0.011	7.697
30	40	0.023	8.237	30	70	0.023	7.701
30	40	0.046	8.242	30	70	0.046	7.708
30	40	0.092	8.290	30	70	0.092	7.720
30	40	0.229	8.375	30	70	0.229	7.760
30	40	0.459	8.396	30	70	0.459	7.835
30	50	0	8.033	30	80	0	7.548
30	50	0.011	8.039	30	80	0.011	7.540

30	50	0.023	8.047	30	80	0.023	7.548
30	50	0.046	8.055	30	80	0.046	7.551
30	50	0.092	8.079	30	80	0.092	7.590
30	50	0.229	8.146	30	80	0.229	7.642
30	50	0.459	8.224	30	80	0.459	7.695
50	25	0.000	8.472	50	60	0	7.822
50	25	0.011	8.475	50	60	0.011	7.817
50	25	0.023	8.479	50	60	0.023	7.837
50	25	0.046	8.488	50	60	0.046	7.829
50	25	0.092	8.504	50	60	0.092	7.858
50	25	0.229	8.545	50	60	0.229	7.896
50	25	0.459	8.620	50	60	0.459	7.940
50	40	0	8.160	50	70	0	7.630
50	40	0.011	8.172	50	70	0.011	7.635
50	40	0.023	8.168	50	70	0.023	7.637
50	40	0.046	8.184	50	70	0.046	7.645
50	40	0.092	8.194	50	70	0.092	7.664
50	40	0.229	8.237	50	70	0.229	7.709
50	40	0.459	8.317	50	70	0.459	7.775
50	50	0	7.985	50	80	0	7.475
50	50	0.011	7.994	50	80	0.011	7.479
50	50	0.023	7.997	50	80	0.023	7.483
50	50	0.046	8.010	50	80	0.046	7.492
50	50	0.092	8.020	50	80	0.092	7.507
50	50	0.229	8.060	50	80	0.229	7.541
50	50	0.459	8.174	50	80	0.459	7.656
80	25	0.000	8.320	80	60	0	7.640
80	25	0.011	8.324	80	60	0.011	7.645
80	25	0.023	8.329	80	60	0.023	7.647
80	25	0.046	8.337	80	60	0.046	7.658
80	25	0.092	8.352	80	60	0.092	7.679
80	25	0.229	8.395	80	60	0.229	7.735
80	25	0.459	8.472	80	60	0.459	7.852
80	40	0	8.010	80	70	0	7.462
80	40	0.011	8.017	80	70	0.011	7.475
80	40	0.023	8.025	80	70	0.023	7.474
80	40	0.046	8.027	80	70	0.046	7.479
80	40	0.092	8.052	80	70	0.092	7.498
80	40	0.229	8.099	80	70	0.229	7.530
80	40	0.459	8.151	80	70	0.459	7.627
80	50	0	7.820	80	80	0	7.290
80	50	0.011	7.826	80	80	0.011	7.295
80	50	0.023	7.828	80	80	0.023	7.298
80	50	0.046	7.838	80	80	0.046	7.309
80	50	0.092	7.858	80	80	0.092	7.329
80	50	0.229	7.888	80	80	0.229	7.369
80	50	0.459	7.998	80	80	0.459	7.435

^aStandard uncertainties: $u(T) = 0.01^\circ\text{C}$, $u(\text{MEG } \%) = 0.2$, $u(\text{pK}_a) = 0.04$, $u(\text{Ionic Strength}) = 0.001$ mol/L

Appendix E: Effect of Organic Acids upon Sulphite Oxygen Scavenger Performance within Mono-Ethylene Glycol Injection Systems

1.0 Introduction

Mono-Ethylene Glycol (MEG) is commonly injected into natural gas transportation pipelines to prevent the formation of gas hydrate blockages during well re-start and well testing operations, or in some instances even continuously during gas production [1, 5, 7, 32, 40]. These 'ice-like' blockages form when water molecules surround a gas molecule creating a solid material at the low temperatures and high pressures typically encountered in off-shore hydrocarbon production flow lines [5, 220, 322]. Under the right conditions, a hydrate blockage can occur rapidly in such flow lines and may result in restricted or ceased production. The removal of a hydrate plug can take days or weeks which can give rise to significant production losses as well as creating major safety risks for the asset. MEG is typically injected at high rates with ratios of 1:1 with produced water being typical for most operating assets. In fields with high water production, this level of injection equates to a significant volumetric flow rate in the production system. In one Australian system, where continuous MEG injection is required, the MEG injection rates equate to nearly 2500 m³/day during maximum forecasted water production.

Alongside hydrate inhibition, the prevention of corrosion in natural gas pipelines is of critical importance to continued flow assurance. The prevention of CO₂ based corrosion, the primary form of corrosion in natural gas systems [7, 15, 95, 223], can be achieved via two primary methods including pH stabilisation using basic chemicals or application of film forming corrosion inhibitors (FFCIs) [2, 4, 7, 9, 116]. However, the presence of even low levels of oxygen dissolved in MEG prior to reinjection has also been shown to present a corrosion risk for natural gas systems – particularly those manufactured from the Corrosion Resistant Alloys (CRAs) commonly used in sub-sea systems [8, 81, 82, 84, 110-113].

The presence of dissolved oxygen can directly result in pitting corrosion of metal surfaces [8, 84] and may negatively influence the stability and corrosion mitigating properties of passivating iron carbonate films formed during corrosion inhibition by pH stabilisation [81, 111]. To minimise the risk of corrosion via oxygen, it is common practice to reduce the total dissolved oxygen content in the lean MEG to below 20 ppb prior to injection [8, 83, 113, 114]. The oxygen content within industrial MEG systems is often minimised via blanketing of storage vessels with nitrogen. However, if impure nitrogen is used, which is often the case, the required <20 ppb oxygen content will not be achieved by blanketing alone [84]. As such, to ensure adequate oxygen levels

nitrogen blanketing is often performed in combination with chemical oxygen scavengers to achieve the desired sub 20 ppb oxygen content.

Through previous studies, the presence of organic acids has been hypothesized to negatively influence the performance of sulphite-based oxygen scavengers via interaction with the transition metal catalysts typically used in the scavenger formulation [19, 201, 202]. Organic acid ions such as acetate may result in the formation of metal complexes reducing the availability of the metal ion to catalyse the oxygen removal reaction. Alternative studies indicate that organic acid ions such as acetate may inhibit the oxygen scavenging reaction of sulphites through scavenging of the radical intermediate products of the sulphite-oxygen chain reaction mechanism [323]. Organic acids are commonly present in hydrocarbon reservoirs and will enter the closed MEG loop via the condensed water [7-9, 63]. Organic acids common within MEG regeneration systems include acetic, propanoic and butanoic acids [7-10, 63, 105, 199, 324] with acetic acid composing 50-90% of organic acids [64]. The presence of organic acids may also arise from thermal degradation of the MEG [5, 7, 12, 199], or by back-production of well drilling/completion fluids following new well start-ups. Another common group of contaminants are mineral salts which may enter the MEG stream following formation water breakthrough and/or also from well drilling and completion fluids.

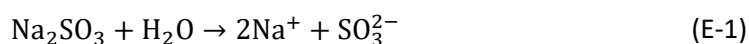
An improved understanding of how common containments including organic acids and mineral salt ions impact the oxygen scavenging mechanism of sulphite can help to better define the safe operating limits for MEG treated with these chemicals and help minimise the risk of oxygen-based corrosion. As such, a comprehensive analysis of how organic acids and salinity influences the performance of sulphite-based oxygen scavengers at varying pH levels was performed. The objective of this study was to identify a suitable operating pH range for given organic acid and salt contents where the sulphite-based oxygen scavenger would be effective in minimising the risk of oxygen-based corrosion of subsea systems.

2.0 Review of Sulphite Based Oxygen Scavengers

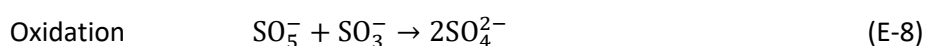
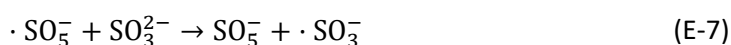
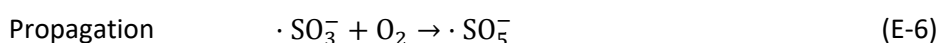
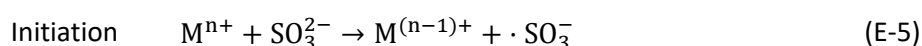
The application of sulphite compounds as oxygen scavengers has seen extensive use in water-based applications such as water boilers, seawater injection systems and more recently hydrocarbon systems to prevent oxygen-based corrosion. The most common sulphite based oxygen scavengers used in a wide range of industries including oilfield and natural gas production include sulphite (M_2SO_3), bisulphite ($MHSO_3$) and metabisulphite ($M_2S_2O_5$) sodium or ammonium salts [325]. The use of sulphite-based oxygen scavengers in water applications has a proven track record with extensive prior research conducted to evaluate sulphite-oxygen reaction mechanisms and kinetics [19, 119-123]. A comprehensive review of

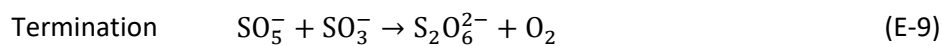
bisulphite-sulphite oxygen scavenger performance has also been performed by Salasi [19] to evaluate the effects of various solution parameters including temperature, pH and MEG concentration in MEG solutions.

The ability of sulphite-based oxygen scavengers to provide effective oxygen removal stems from the ability of the sulphite ion to directly react with molecular oxygen dissolved within solution. The addition of sulphite/(meta)bisulphite sodium salts to water will dissociate according to Equations (E-1 to E-3) to form sulphite ions that will subsequently react with dissolved oxygen to form sulphate ions. The reaction of sulphite ions with oxygen follows the reaction defined by Equation (E-4) with the extent of the sulphite-oxygen reaction being highly dependent on the concentration of the free sulphite ion SO_3^{2-} and hence pH [8, 19, 325]. HSO_3^- must first dissociate to SO_3^{2-} before oxygen removal can take place and will be more likely to occur at higher pHs. The speciation distribution of sulphite species as a function of pH has been reported by various authors including Salasi [19] and Shen [119] indicating that SO_3^{2-} begins to form at pHs greater than 5-6.

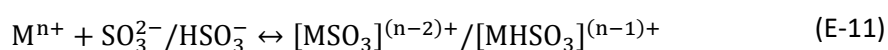


Although the reaction of sulphite species with oxygen appears simple, the oxidation of sulphite actually occurs in a multi-step process involving multiple free radical reactions. One of the earliest proposed free radical reaction pathways for sulphite species with oxygen was proposed by Backstrom [326] where the reaction is initiated following the radicalization of sulphite ions by a metal catalyst. The multi-step reaction mechanism of sulphite with oxygen suggested by is given by Equations (E-5) to (E-10) where 'M' is a transition metal. The free radical oxidation reaction mechanism of sulphite has been extensively reviewed by various authors including Ermakov [327], Connick and Zhang [328], Zhang and Millero [329], Hobson [330] and Snively [331].





The use of transition metals in combination with sulphite for oxygen removal has been well documented for their ability to act as a catalyst [113, 120, 202, 328, 332-336]. The most common transition metals used for catalysation of the sulphite-oxygen reaction listed in terms of reducing effectiveness include Fe(II), Mn(II), Co(II) and Ni(II) [332]. However, the addition of Fe(II) is often undesirable due to its ability to directly react with oxygen to form rust. Likewise, the use of cobalt as a catalyst may be undesirable to its potential to act as a carcinogen in humans and poor performance compared to the safer alternative of manganese. As per Equation (E-5), the first step in sulphite oxygen removal occurs through the reaction of sulphite ions with the transition metal catalyst to produce free radical sulphite, alternatively, recent studies including that by Grgić and Berčić [334] suggest the first step involves the formation of a metal-sulphite complex through Equation (E-11). The metal-sulphite complexes then undergo decomposition to form the reduced metal ions and sulphite radicals.



The performance of sulphite-based oxygen scavengers has been shown to be inhibited by the presence of alcohols such as MEG. Salasi [332] suggested that the inhibitory effect of MEG upon the performance of sulphite as an oxygen scavenger stems from alcohols promoting free radical sulphites to undergo the termination reactions. They further suggest that the chain termination reactions may possibly be prevented by reaction of the free radical sulphite ions with transition metals. This is consistent with the findings of Braga [114] who states that the presence of alcohols decrease oxygen scavenging rates by directly influencing the controlling chain termination process, particularly at the high concentrations required for hydrate prevention in MEG systems. The performance of sulphite oxygen scavengers was also evaluated by Wang [337] in the presence of ethanol. The findings of this study suggest that ethanol acts as an inhibitor by reacting with the free radical $\cdot\text{SO}_3^{2-}$. Through experimental testing it has been shown that in comparison to water, to achieve appreciable oxygen removal with alcohols a much larger dosage of oxygen scavenger is required [332].

3.0 Experimental System and Methodology

3.1 Experimental Apparatus

Oxygen scavenger evaluation was conducted utilising four 1-Litre glass test cells fitted with a custom-made lid to provide an air tight seal as depicted by Figure E-1. Each testing cell was fitted with individual InPro 4800i pH probe and InPro 6850i polarographic dissolved oxygen (DO)

sensors supplied by Mettler Toledo. The InPro 6850i DO sensor has an oxygen detection range of 6 ppb to saturation within an accuracy of $\pm 1\%$. The pH and DO sensors were directly connected to two M800 Process 4-Channel Mettler Toledo measurement systems to both monitor system conditions as well as transmit experimental data to a connected computer for recording.

The oxygen scavenger solution was introduced into the test cell via an injection port fitted with a rubber seal to minimise oxygen intrusion using a syringe. To further prevent oxygen ingress each test cell was fitted with a retractable nitrogen inlet to provide continuous sparging of ultra-high purity nitrogen (>99.999 mol%) into the headspace of the cell. The retractable nitrogen inlet also provided the ability to directly sparge the test solution with air or nitrogen as required to adjust the starting oxygen content of the solution. An outlet tube connected to a gas wash bottle was included to prevent pressure build-up within the cell whilst also preventing flow reversal of air back into the cell.

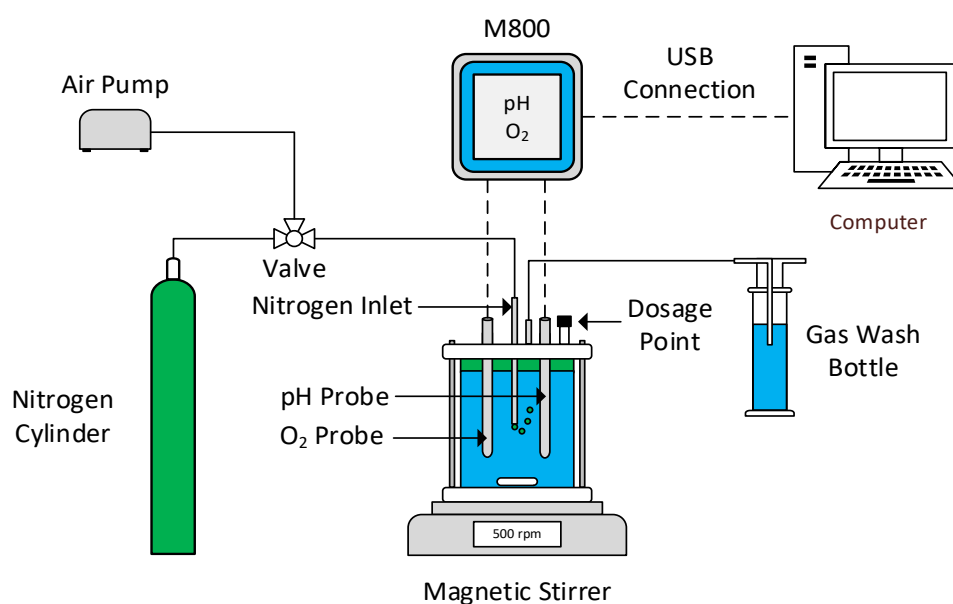


Figure E-1. Experimental apparatus

3.2 Experimental Methodology

The experimental matrix outlined in Table E-1 was used to evaluate the effect of organic acids (acetic) and salinity on the performance of the sulphite oxygen scavenger. All experimentation was conducted within 85% wt. MEG solution (commonly termed 'Lean MEG') prepared using distilled water (resistivity 18.2 M Ω .cm) and pure MEG supplied by Chem Supply at a temperature of 20°C. Prior to testing, the test solution was sparged using nitrogen to achieve a starting concentration of 1000 ppb oxygen representing typical industrial oxygen content due to impure nitrogen sparging and/or oxygen intrusion [15, 84, 118]. The pH of the solution was then adjusted to the desired starting pH using potassium hydroxide.

To commence oxygen scavenger evaluation, the oxygen scavenger was injected through the rubber injection port using a 25 cm long needle and syringe at the dosage concentration recommended by the supplier (500 ppm total oxygen scavenger solution, yielding ≈ 200 ppm metabisulphite ion). Once injected, the pH and oxygen content of the MEG solution was monitored using the M800 systems with experimental data recorded to a computer. Sparging of ultra-high purity nitrogen into the headspace of the cell was maintained throughout the experiment to prevent oxygen ingress from the external atmosphere. Each experiment was continued until the oxygen content within the cell reached below 20 ppb or until complete stabilisation of oxygen content occurred. For the field of interest to this study, the target oxygen concentration was identified as <20 ppb oxygen within a four-hour time frame.

Table E-1. Experimental matrix

pH: 9, 10, and 11		NaCl (g/L)						
		0	0.25	1	2	4	6	20
Acetic Acid (mg/L)	0	✓	✓	✓	✓	✓	✓	pH 11
	100	✓	✓	✓	✓	✓	✓	
	250	✓	✓	✓	✓	✓	✓	
	500	✓	✓	✓	✓	✓	✓	
	1000	✓	✓	✓	✓	✓	✓	
pH: 9.5, 10.5 and 12		NaCl (g/L)						
		0	0.25	1	2	4	6	20
Acetic Acid (mg/L)	0	✓	✓		✓		✓	
	100	✓	✓					
	250	✓	✓		✓		✓	
	500	✓	✓					
	1000	✓	✓		✓		✓	

4.0 Experimental Results and Discussion

4.1 Effect of Organic Acids on Sulphite Oxygen Scavenger Performance

The presence of organic acids within MEG regeneration systems can arise over prolonged periods of time due the thermal degradation of recycled MEG during the regeneration process and organic acids present in the condensed water phase [3, 5, 7, 39, 63, 199]. Furthermore, upon the breakthrough of formation water, greater concentrations of organic acids including acetic, propanoic and butanoic acids may be experienced during MEG regeneration [7-9, 199]. Several literature sources state that the catalysis reaction necessary for rapid removal of oxygen by sulphite-based oxygen scavengers is inhibited by the presence of organic acids [19, 201, 202]. The presence of organic acid ions, including acetate can result in the formation of metal complexes directly reducing the availability of the metal ions for the catalysis of the sulphite reaction [202,

^{323]}. However, Kotronarou and Sigg [323] also suggest that the presence of acetate can inhibit the sulphite-oxygen reaction at high pHs through scavenging of the radical intermediates outlined by Equations (8-5 to 8-10.) The work of Al Helal [113] showed no impact of organic acids on the performance of an erythorbic acid based oxygen scavenger using manganese as a catalyst. This result indicates that there is minimal interaction between manganese and organic acids and the reduction in sulphite oxygen scavenger performance most likely occurs through termination of the sulphite chain reaction.

To verify the impact of organic acids upon the sulphite oxygen scavenging mechanism, testing was performed using 85% wt. lean MEG with increasing amounts of acetic acid with an initial pH of 9 with no mineral salts present. A pH of 9 was selected for testing to ensure sufficient neutralization of the acetic acid to acetate had occurred without using an excessive pH that would otherwise increase performance drastically. Figure E-2 illustrates the effect of acetic acid, the primary organic acid found in MEG systems, upon the performance of the proprietary sulphite oxygen scavenger at the 500 ppm dosage. A clear reduction in performance was observed with increasing acetic acid concentration suggesting that the acetate has a large impact on sulphite oxygen scavenger performance through either undesirable interaction with the catalyst or side reactions with intermediate products. Therefore, within lean MEG where organic acids are present, reduced performance of sulphite oxygen scavengers as per Figure E-2 should be expected at this pH level. In contrast, the effects of acetic acid upon oxygen scavenger performance at pH 11 are illustrated by Figure E-3 showing essentially no impact up to an acetic acid concentration of 10000 ppm at the same oxygen scavenger concentration.

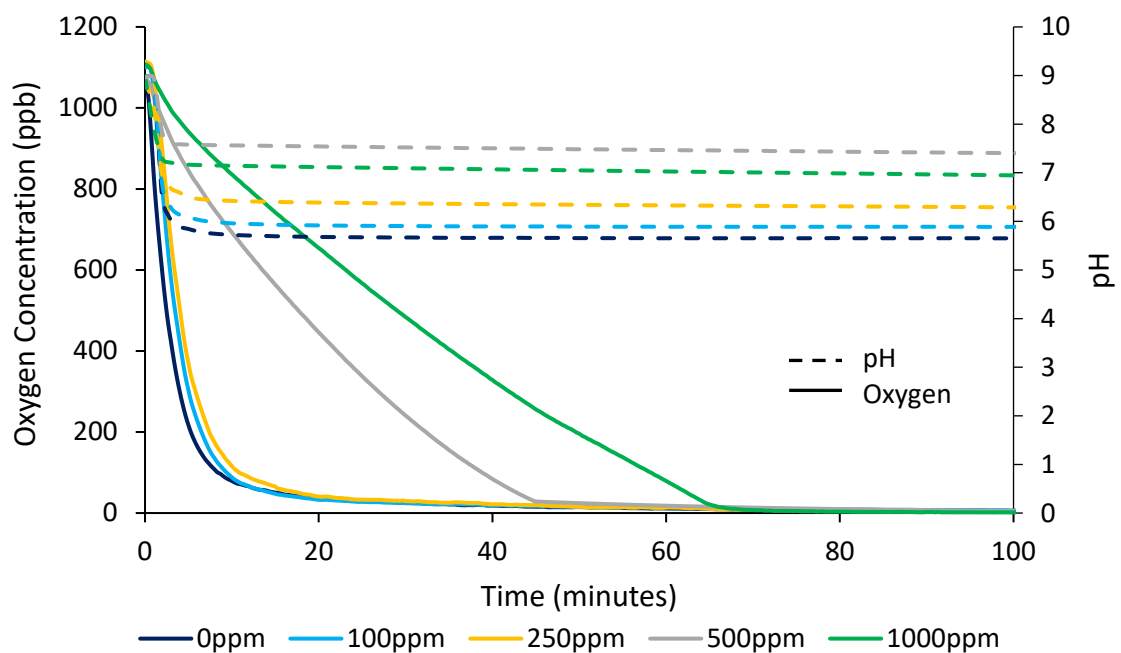


Figure E-2. Effect of acetic acid concentration on sulphite oxygen scavenger performance at pH 9

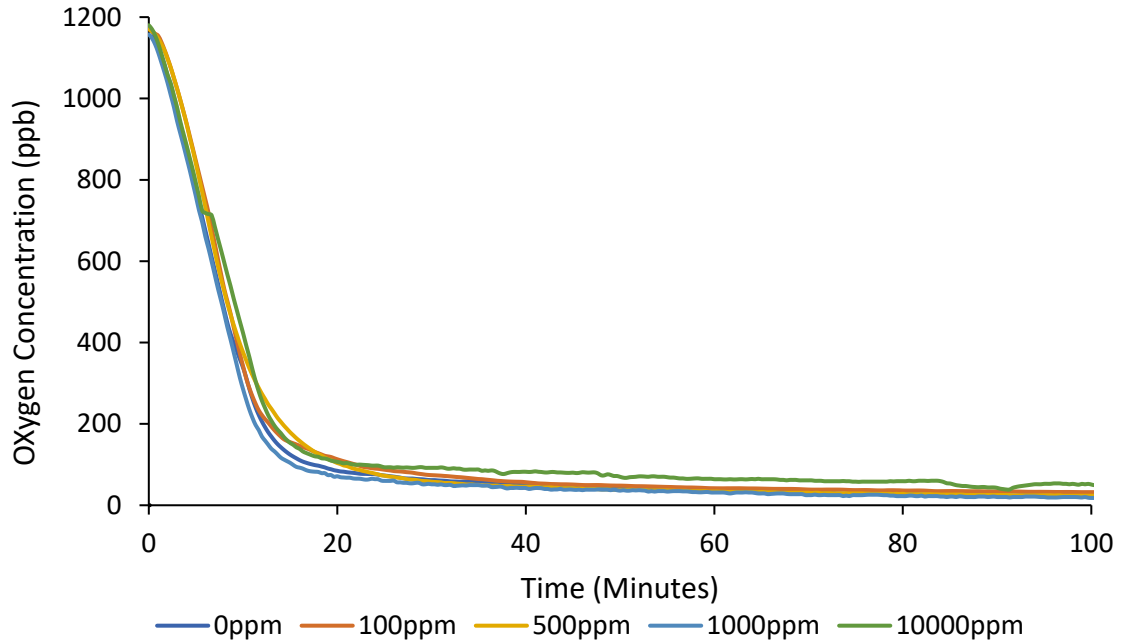
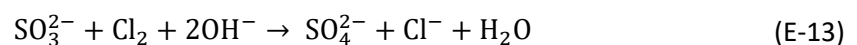


Figure E-3. Effect of acetic acid concentration on sulphite oxygen scavenger performance at pH 11

4.2 Effect of Salt Content (NaCl) on Sulphite Oxygen Scavenger Performance

The ingress of ionic species whether through dosage of process chemicals including salt-based pH stabilisers or following formation water breakthrough represents a significant operational concern for closed-loop MEG systems. In addition to the obvious risk of salt precipitation and fouling in the processing equipment, the impact of dissolved salt on oxygen scavenger performance may also be a concern. If the concentration of salt reaches beyond given design limits, replacement of MEG may be required. This replacement represents a substantial cost to operation due to the large volume of MEG often utilised in closed-loop MEG systems. As such, significant cost savings can be achieved if the permissible concentration of salt can be extended beyond the original design limits, specifically to this study, the salt concentration that can be allowed before the oxygen scavenger performance is deteriorated. Prior studies suggest that hypochlorite and chlorine may react preferentially with sulphite at high pH (Equation E-12 and E-13), effectively competing with the desired oxidation reaction and hence reducing oxygen scavenger performance^[114]. The effect of salt concentration (NaCl) upon the performance of the sulphite oxygen scavenger has hence been evaluated to identify potential salt content limits before oxygen removal performance is detrimentally reduced.



From Figure E-4, it is clear that the initial oxygen removal rate at varying salt concentrations at pH 11 does not appear to differ significantly. Instead, the primary reduction in performance due to the presence of salts occurs within the low oxygen concentration region (<100-200 ppb oxygen) where the presence of salt molecules may impair the ability of the oxygen scavenger to physical react with the oxygen. Figures E-5 and E-6 illustrate the variation in oxygen scavenger performance within varying salt and organic acid concentration lean MEG solutions. Again from Figure E-6, it is highly evident the oxygen removal in the low oxygen region is reduced in comparison to solutions with lower salt content. Although a reduction in performance has occurred, the oxygen scavenger was found to be capable of reaching the desired 20 ppb oxygen content within a reasonable timeframe (<100 minutes) indicating that significantly less frequent replacement of MEG (due to presence of dissolved salt) is required as long as a sufficiently high pH is maintained in the lean MEG solution prior to oxygen scavenger dosing. However, maintaining a lean glycol pH of 11 and above may pose a significant subsea scaling risk in the event of sudden formation water onset and should be closely monitored or controlled via injection of scale inhibitors.

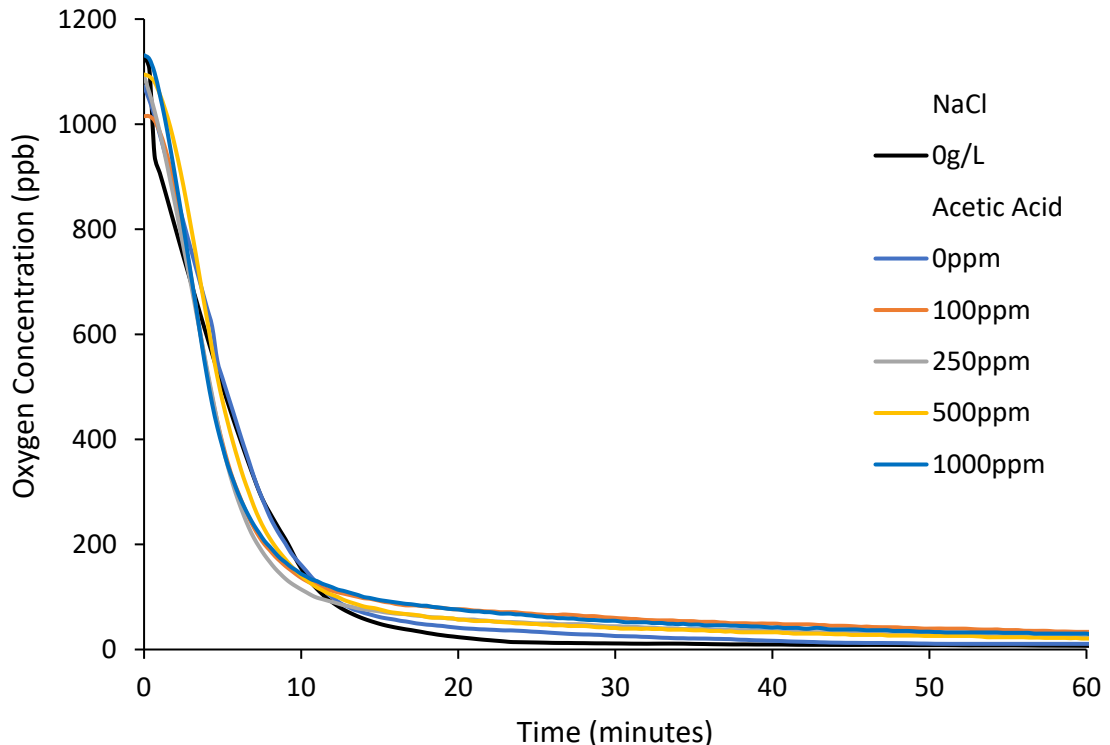


Figure E-4. Performance of sulphite oxygen scavenger at pH 11 within 50 g/L NaCl lean MEG

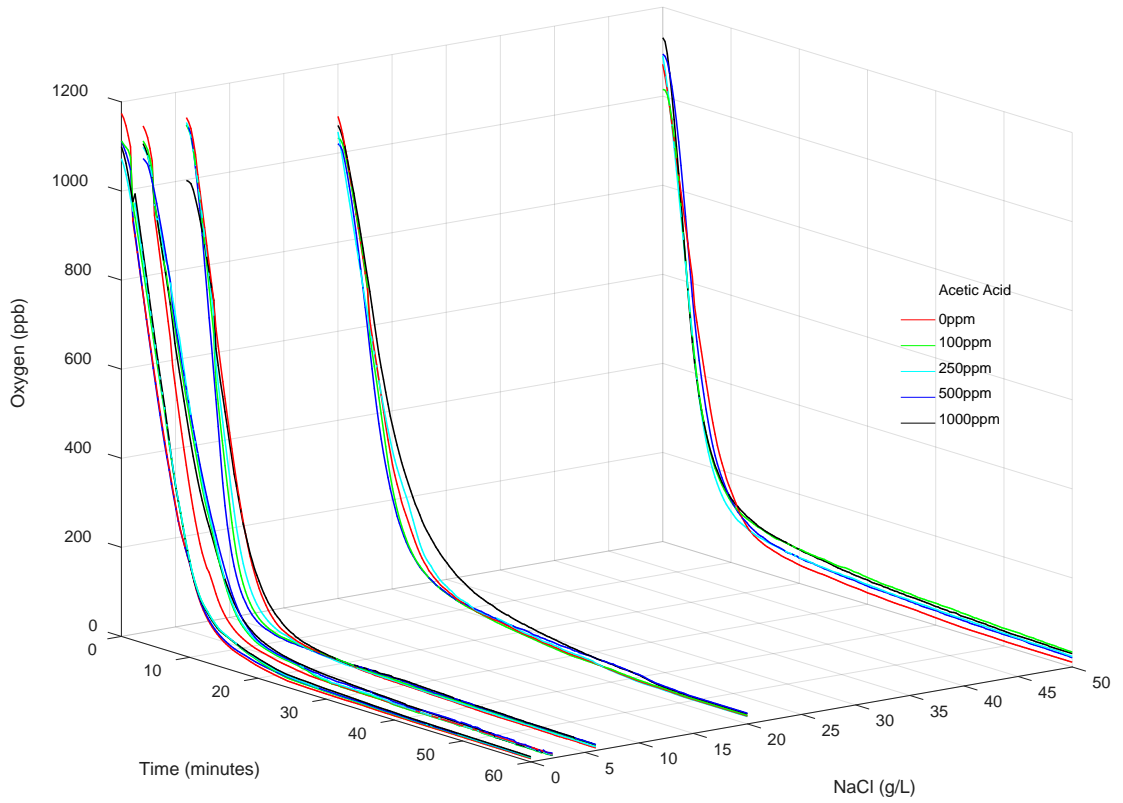


Figure E-5. Effect of salt content (NaCl) on oxygen removal performance at varying acetic acid concentration (pH 11)

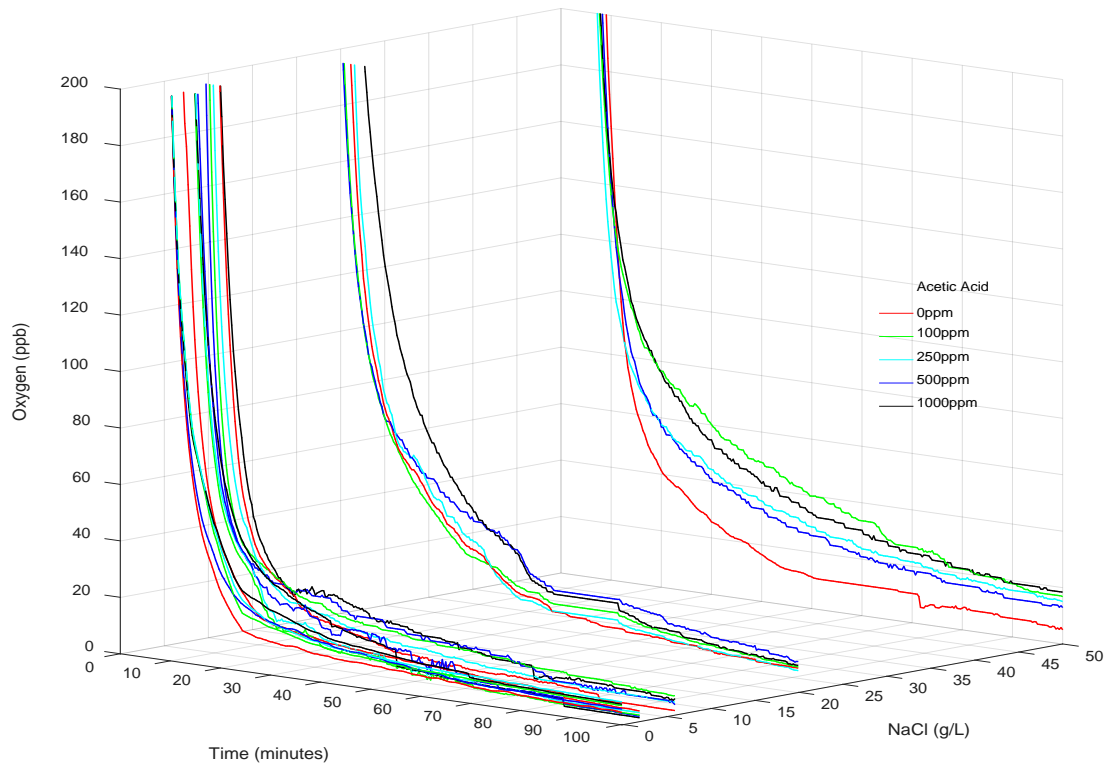


Figure E-6. Effect of salt content (NaCl) on oxygen removal performance at varying acetic acid concentration (<200 ppb oxygen region) (pH 11)

At an initial lean MEG pH of 9-10, the presence of NaCl appeared to have a noticeable impact on oxygen scavenger performance, as illustrated by Figure E-7, although, no direct reaction of sodium or chloride with the oxygen scavenger or catalyst should occur, a reduction in performance was nevertheless observed. It was further observed that with increasing sodium chloride concentration the final lean MEG pH produced following oxygen scavenger dosage was greater than corresponding low NaCl concentrations at equal acetic acid content (refer to Table E-2). At the initial solution pH of 9, the majority of acetic acid is present as acetate, where following dosage of the acidic oxygen scavenger a conversion of acetate back to acetic acid occurs. The presence of NaCl had essentially resulted in a lower conversion of acetate back to acetic acid. The resultant greater concentration of acetate was again found to be the primary factor reducing oxygen scavenger performance.

Table E-2. Effect of NaCl on final lean MEG pH

Initial pH	Acetic Acid (ppm)	NaCl (g/L)	Final pH after OS Dosage
9	0	0	5.65
		1	5.76
		2	5.90
		4	6.23
		6	6.37
		0	5.88
	100	1	5.95
		2	6.02
		4	6.52
		6	6.68
		0	6.10
		1	6.40
	250	2	6.53
		4	6.95
		6	7.20

5.0 Identification of Optimal Operating Window for Oxygen Removal at Varying Salt and Organic Acid Concentrations

The development of a defined operating window allows field operators to be certain that suitable operating conditions are maintained to ensure sufficient oxygen removal is achieved to prevent corrosion. The experimental matrix defined by Table E-1 was used to identify suitable initial lean MEG pH conditions for known organic acid and salt concentrations. Figure E-8, illustrates the effect of initial pH, acetic acid content and salinity in the form of NaCl on the performance of the sulphite oxygen scavenger at initial pHs of 10 to 12. The time taken to reach below 20 ppb oxygen concentration was used to quantify the effect of the three parameters. It is clear that the performance of sulphite oxygen scavenger suffered greatly when transitioning

between a pH of 10.5 to 10, in particular, during cases where 500 ppm and greater acetic acid were present. The worst performance of oxygen scavenger at pH 10 was found to occur when acetic acid was matched with low salt concentrations. In contrast, at pH 10.5 and greater, the presence of acetic acid had minimal impact on oxygen scavenger's performance.

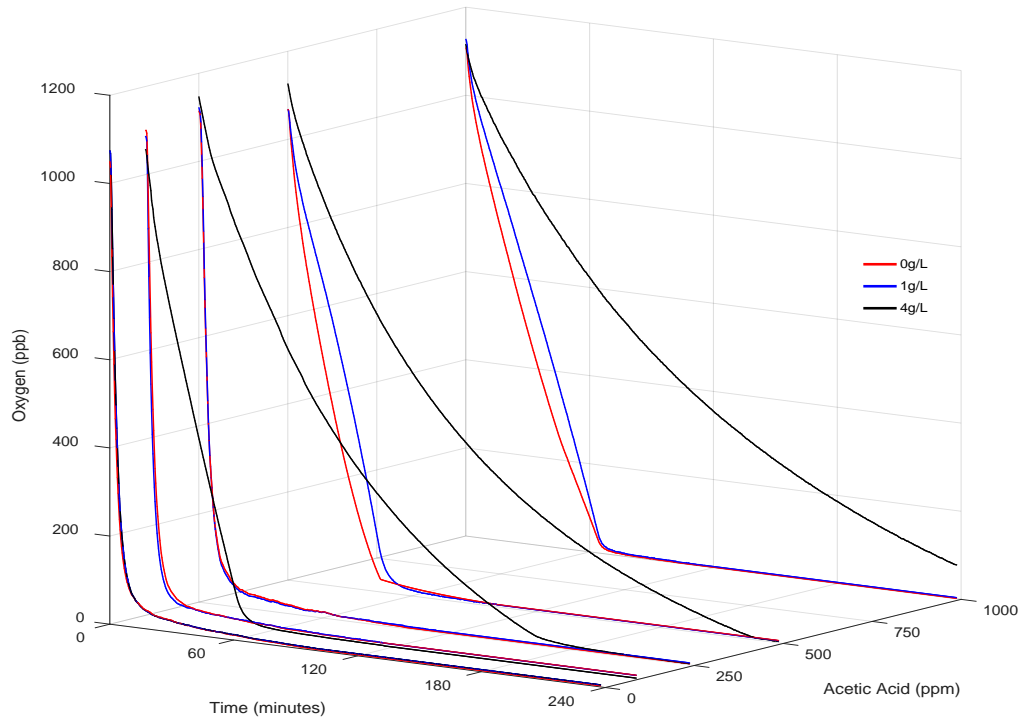


Figure E-7. Effect of acetic acid and NaCl on oxygen removal rate at pH 9 (0, 1 and 4 g/L NaCl)

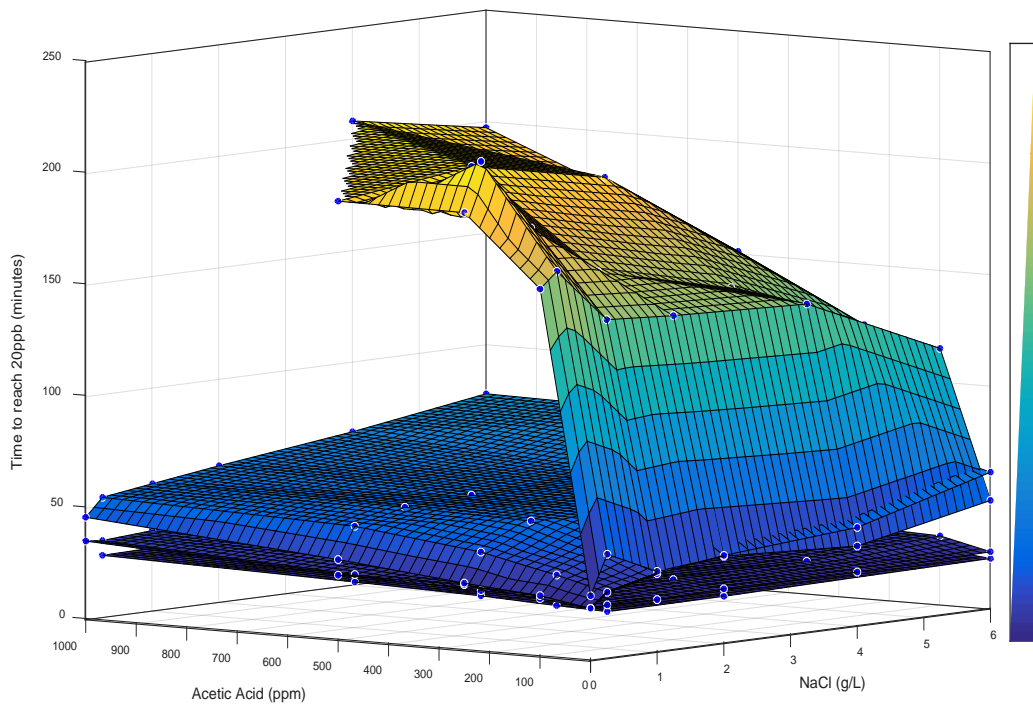


Figure E-8. Effect of pH, salinity (NaCl) and acetic acid on oxygen scavenger performance

The increase in oxygen scavenger performance at and above a pH of 10.5 can be attributed to the presence of excess hydroxide alkalinity. The presence of hydroxide alkalinity effectively provides a buffer against the pH change induced by the acidic metabisulphite allowing a greater conversion of bisulphite to sulphite and a final pH where greater oxygen removal can be achieved. The impact of acetic acid appears to be a function of both total concentrations and the relative speciation of the organic acid to its conjugate base. This effect was most pronounced in lean MEG solutions between pH 7-9.5 where the acetic acid present was fully dissociated to acetate resulting in significant reduction in oxygen scavenger performance. Figure E-9 illustrates the speciation of acetic acid – acetate with respect to pH overlapped with final lean MEG pHs where reduced oxygen scavenger performance was observed experimentally.

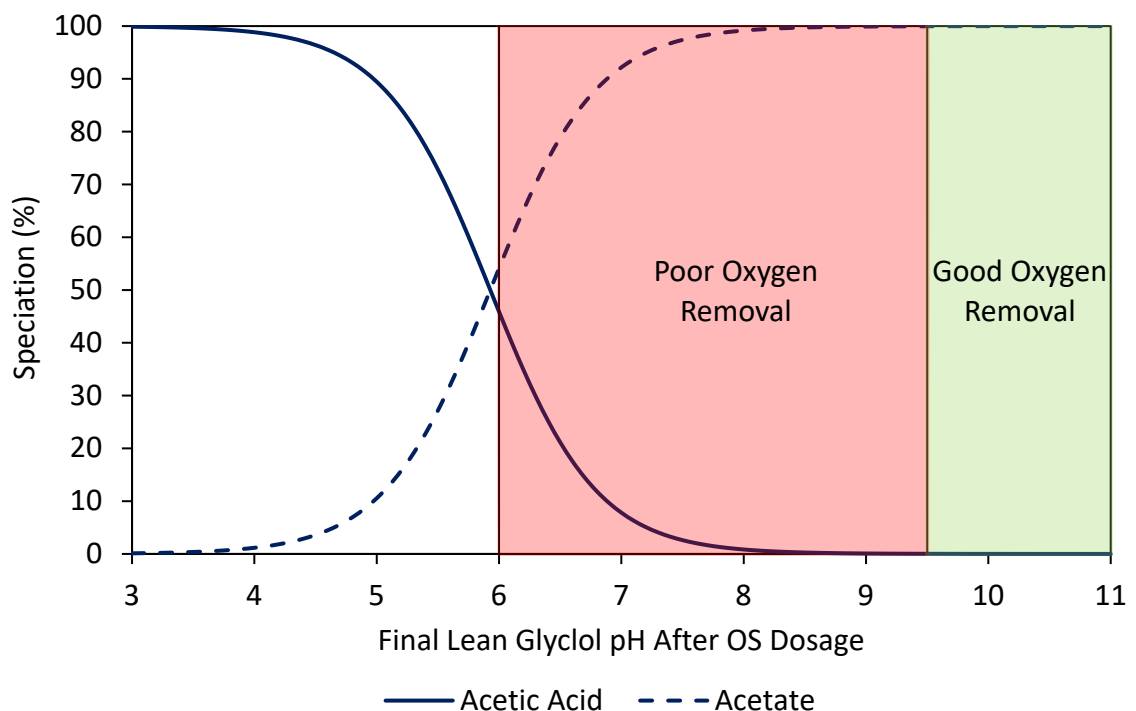


Figure E-9. Speciation of acetic acid in 85% MEG Solution^[199] and effect on oxygen scavenger performance

An interesting increase in oxygen scavenger performance was observed during pH 9-10 experiments within lean MEG solutions containing 0-1 g/L NaCl and 100-250 ppm acetic acid. Due to the dissociation behaviour of acetic acid (refer to Figure E-9), the reduction in pH by caused by the metabisulphite effectively caused the acetate to transition back to acetic acid. This was most prominent for cases where the final lean MEG pH after oxygen scavenger addition reached below 6.5. Within these experiments, a significantly greater oxygen removal rate was achieved in comparison to corresponding pH 9 tests conducted at higher acetic acid concentrations (final pH 7-8), refer to Figure E-2. The resulting low pH was found to be less detrimental to oxygen scavenger performance than the presence of acetate, further

emphasizing the significant effect of acetate on the performance of the sulphite oxygen scavenger.

6.0 Effect of Sulphite Oxygen Scavenger on Lean MEG pH

Due to the acidic nature of the bisulphite molecules formed by the dissociation of metabisulphite in water, a reduction in solution pH is expected upon injection (Equation (8-3)). Figure E-10 illustrates the change in pH caused by the metabisulphite within lean MEG at varying initial pHs, acetic acid and NaCl concentrations. The greatest drop in lean MEG pH occurred within solutions with low organic acid and salt content at pHs 9-10 due to the low buffer capacity of the solution. The resulting pH reduction ($pH_{final} < 7$) occurring under such conditions may pose an acidic corrosion risk and should be avoided. As the organic acid content increases, a greater buffer capacity to oppose the pH change is produced (between $pH_{initial} \approx 6-8.5$, Figure E-9) however this should not be relied upon to ensure a safe final lean MEG pH is maintained. Lean MEG solutions initially above a pH of 10 had sufficient hydroxide alkalinity to oppose the pH change induced by the oxygen scavenger at the dosed concentration (500 ppm), resulting in a final lean glycol pH within the optimal pH range indicated by Figure E-9.

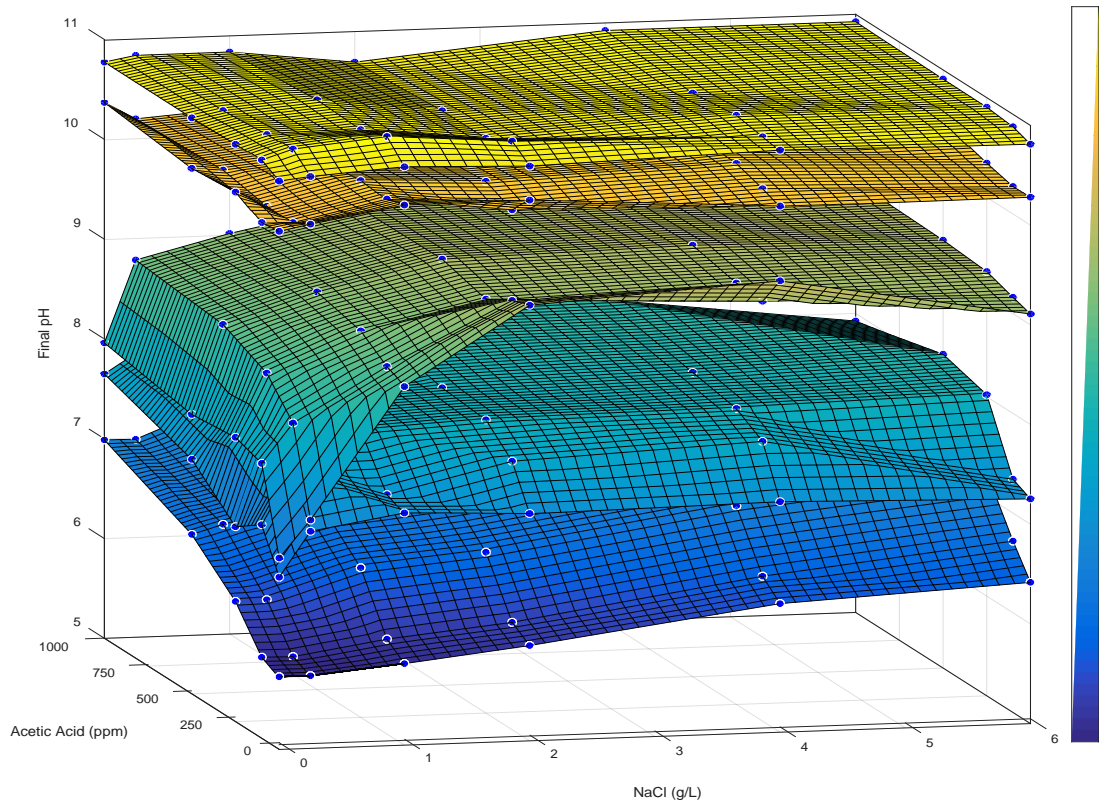


Figure E-10. Effect of oxygen scavenger on lean MEG pH

7.0 Conclusion

Due to the limited prior industrial use of sulphite oxygen scavengers within lean MEG solutions, the impact of various contaminants found within closed loop MEG systems are poorly understood. The effect of pH and two of the primary contaminants found during continuous MEG recycling, mineral salts and salts of organic acids, have hence been investigated to optimise oxygen scavenger performance within lean MEG. The experiments performed clearly demonstrate that significant reduction in sulphite oxygen scavenger performance can be expected within systems containing organic acids at pHs where the conjugate base is formed.

A significant reduction in oxygen scavenger performance can be expected at lean MEG pHs of 10 and below due to the presence of organic acids. It is therefore recommended that the lean MEG be maintained at a pH above 10.5 prior to oxygen scavenger dosage to ensure that sufficient hydroxide alkalinity is present to ensure a) full transition of bisulphite to sulphite and b) to avoid the negative impact of acetate and other organic acid conjugate bases. Table E-3 summarizes the recommended operating pH ranges based on known organic acid and salinities to achieve 20 ppb oxygen content within suitable time frames. Operating conditions highlighted in red are inadvisable either due to low final MEG pH posing a corrosion risk or sufficient oxygen removal occurring in greater than three hours or not at all. Conditions marked as orange successfully reached the target 20 ppb oxygen content, however, unexpected shifts in either organic acid or salt content may result in either a detrimental reduction in oxygen scavenger performance or an undesirably low final lean MEG pH and should be avoided. It should also be noted that operation of lean glycol systems above pH 11 may pose a significant scaling risk upon the sudden onset of formation water and should be considered during selection of suitable operating pH for oxygen scavenger usage.

Table E-3. Operating envelope for use of sulphite oxygen scavenger in lean MEG solutions

		Acetic Acid (mg/L)				
		0	100	250	500	1000
pH	9	pH (NaCl all)	pH (NaCl all)	pH (NaCl all)	pH (NaCl 0-2g/L)	pH (NaCl 0-0.25g/L)
					O ₂ (NaCl 4-6 g/L)	O ₂ (NaCl 4-6 g/L)
	9.5	pH (NaCl 0-0.25g/L)	O ₂ (NaCl all)	O ₂ (NaCl all)	O ₂ (NaCl all)	O ₂ (NaCl all)
	10	pH (NaCl 0g/L)	O ₂ (NaCl 0-0.25g/L)	O ₂ (NaCl 0-1g/L)	O ₂ (NaCl 0-4g/L)	O ₂ (NaCl all)
		pH (NaCl 0.25g/L)				
		O ₂ (NaCl 0.25-6g/L)	O ₂ (NaCl 1-6g/L)	O ₂ (NaCl 4-6g/L)		
	10.5					
	11	Up to 50g/L NaCl*	Up to 50g/L NaCl*	Up to 50g/L NaCl*	Up to 50g/L NaCl*	Up to 50g/L NaCl*
	12					
	O ₂ : >180 minutes pH _{final} : <7		O ₂ : 180-120 minutes pH _{final} : 7-8		O ₂ : <120 minutes	

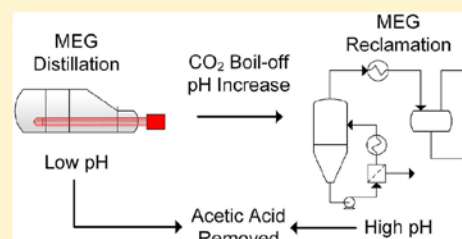
*maximum NaCl concentration tested

Removal of Organic Acids during Monoethylene Glycol Distillation and Reclamation To Minimize Long-Term Accumulation

Adam Soames,*[✉] Ahmed Barifcani, and Rolf Gubner

WA School of Mines: Minerals, Energy and Chemical Engineering, Curtin University, Kent Street, 6102 Perth, WA, Australia

ABSTRACT: Monoethylene glycol (MEG) is often used in offshore multiphase hydrocarbon transportation pipelines to prevent the formation of natural gas hydrates. Post hydrate inhibition, MEG is separated alongside the water phase and regenerated through a series of chemical and physical processes to remove excess water and process contaminants including mineral salts, production chemicals, and organic acids. The level of organic acids within closed-loop MEG systems is often controlled via vacuum reclamation systems through the formation of nonvolatile salt products allowing their separation from the evaporated MEG/water phase. However, if a reclamation system is unavailable, or operated at low pH, organic acids will ultimately accumulate within the MEG loop. Likewise, removal of organic acids may be achieved during the distillation process by vaporization of the acids in their undissociated volatile form. Within both processes, the removal efficiency of an organic acid is ultimately dictated by the acid's speciation behavior and system pH. The purpose of this study was to measure the removal efficiency of acetic acid during the regeneration and reclamation processes to identify key pH levels to minimize the long-term accumulation of acetic acid. Two equations have been proposed to estimate the removal efficiency of acetic acid during distillation and reclamation individually with an average error compared to reported experimental data of 0.38% and 2.6%, respectively. Combining the two proposed equations, the plant-wide removal of acetic acid can be predicted for a known rich glycol pH and pH rise across the regeneration system allowing practical application to industrial MEG regeneration systems.



1. INTRODUCTION

Monoethylene glycol (MEG) has found widespread use as a thermodynamic hydrate inhibitor to prevent the formation of natural gas hydrates within offshore multiphase hydrocarbon transportation pipelines.^{1–6} In order to minimize the operational costs associated with MEG injection, post hydrate inhibition, the excess MEG is separated alongside the water phase to be regenerated and recycled for further use.^{1–3,7,8} The MEG regeneration process entails a series of chemical and physical steps to remove a wide range of contaminants including excess water, mineral salts, and process chemicals.^{2,5,9,10} To produce a final lean MEG product suitable for reinjection at the wellhead, excess water is separated from rich MEG by distillation to regain a MEG concentration typically between 80 and 90% by weight.^{1,2,5,11,12} To achieve the desired lean MEG concentration, the MEG regeneration unit (MRU) is typically operated between 120 and 140 °C at atmospheric pressure.^{1,13,14}

Alongside other contaminants, organic acids such as acetic, propanoic, butanoic, and formic may be present within the regeneration system originating from the condensed water phase or following formation water breakthrough.^{2,5,15} Furthermore, the thermal degradation of MEG at high temperature in the presence of oxygen may also lead to the formation of organic acids including glycolic, acetic, and formic acid.^{7,15–17} The presence of organic acids within industrial

MEG regeneration systems can pose several operational issues including contributing to corrosion of downstream process equipment and pipe systems.² Organic acids have been found to increase the rate of corrosion of carbon and mild steel piping in natural gas and oil field systems.^{18–21} In combination with carbon dioxide, acetic acid may also exacerbate the rate of Top-of-the-Line-Corrosion (TLC).^{15,21–26} Additionally, organic acids will directly reduce the pH of the liquid phase increasing the solubility of protective iron carbonate films, reducing corrosion protection, and may also be directly reduced on the surface of metals enhancing the anodic reaction of the metal.^{21,27,28}

To minimize corrosion within natural gas pipelines, two primary corrosion inhibition strategies can be utilized including pH stabilization and injection of film forming corrosion inhibitors (FFCI).^{2,3,5,9,19} The basis of pH stabilization entails artificially increasing system pH to reduce the availability of hydrogen ions for the cathodic corrosion reaction, while also promoting the formation of a protective FeCO₃ film on the surface of the pipeline. The pH within pipelines is typically increased through addition of hydroxides,

Received: February 6, 2019

Revised: April 2, 2019

Accepted: April 2, 2019

Published: April 2, 2019



Operation of a MEG pilot regeneration system for organic acid and alkalinity removal during MDEA to FFCI switchover



Adam Soames^{a,*}, Edith Odeigah^a, Ammar Al Helal^a, Sami Zaboona^a, Stefan Iglauer^b, Ahmed Barifcani^a, Rolf Gubner^a

^a WA School of Mines: Minerals, Energy and Chemical Engineering, Curtin University, Perth W.A., Australia

^b Petroleum Engineering Department, Edith Cowan University, Perth W.A., Australia

ARTICLE INFO

Keywords:

Mono-ethylene glycol
Distillation
Corrosion
MDEA
Organic acids
Film forming corrosion inhibitors

ABSTRACT

The switch over from pH stabilisation using MDEA to film forming corrosion inhibitors (FFCI) may be beneficial following formation water breakthrough during hydrocarbon transportation and processing to prevent scaling at elevated pH and to extend the operational lifespan of a field. Where formation water is present, organic acids including acetic can be expected within MEG regeneration systems and can impose a corrosion risk together with carbon dioxide. A case study was performed to evaluate the potential of simultaneous removal of organic acids and MDEA/alkalinity during the switch over from pH stabilisation to film forming corrosion inhibitors (FFCI). Experimental testing was conducted using a MEG pilot regeneration plant operated by the Curtin Corrosion Engineering Industry Centre. Sufficient removal of organic acids was achieved to prevent accumulation within the MEG regeneration loop and subsequent corrosion issues through distillation by lowering the pH of the rich glycol feed to six to promote removal of organic acids with the water distillate. Simultaneously, removal of MDEA and reduction of lean glycol alkalinity was achieved through the reclamation system to facilitate FFCI switchover more rapidly than a comparative industrial operational methodology.

1. Introduction

The formation of natural gas hydrates in hydrocarbon transportation pipelines represents a major flow assurance concern with major implications upon safe and economical process operation. The inhibition of hydrate formation is of critical importance in maintaining process flow and the prevention of damage to process equipment and piping. The annual cost associated with preventing hydrate formation has been estimated to be greater than \$500 million through inhibition by methanol injection alone (Daraboina et al., 2013). In many recent oil and gas developments, Mono-Ethylene Glycol (MEG) has seen increasing popularity replacing methanol as the thermodynamic hydrate inhibitor of choice (Haghighi et al., 2009; Pojtanabuntoeng et al., 2017; Zaboona et al., 2017). The preference for MEG over methanol stems from its low volatility, toxicity and flammability, favourable thermodynamic behaviour and simple and proven technology requirements (Bikkina et al., 2012; Haque, 2012).

Post hydrate inhibition, the recovery and reuse of MEG is essential due to the significant volume required to provide effective hydrate control, its high cost and its effects on downstream processes (Haghighi et al., 2009; Pojtanabuntoeng et al., 2017; AlHarooni et al., 2015).

Following the three-phase separation from gaseous and liquid hydrocarbons, MEG is removed in combination with water and must be regenerated before it is recycled back to the wellhead for reinjection. The regeneration of MEG is typically performed by distillation to remove surplus water in order to regain a glycol purity between 80 and 90% by weight (Latta et al., 2013; Carroll, 2003).

Alongside hydrate inhibition, the prevention of corrosion in piping and processing systems is a critical aspect of hydrocarbon flow assurance. The majority of natural gas pipelines are manufactured from carbon steel and are susceptible to 'sweet' corrosion due to the presence of carbon dioxide and free water during transport and processing (Pojtanabuntoeng et al., 2017; Papavinasam et al., 2007; Nam et al., 2014). The annual global cost associated with corrosion has been estimated by Koch et al. (Koch et al., 2017) at roughly US \$2.5 trillion with up to 60% of corrosion experienced in the oil and gas industry resulting from CO₂ based corrosion (López et al., 2003). To combat corrosion in hydrocarbon pipelines two methods of corrosion control can be applied including the injection of film forming corrosion inhibitors (FFCI) and/or pH stabilisers (Pojtanabuntoeng et al., 2017; Latta et al., 2013; Dong et al., 2008). The presence of MEG itself has also been shown to impede CO₂ corrosion of carbon steels (Pojtanabuntoeng et al., 2017;

* Corresponding author.

E-mail address: Adam.Soames@postgrad.curtin.edu.au (A. Soames).

<https://doi.org/10.1016/j.petrol.2018.05.047>

Received 3 February 2018; Received in revised form 1 May 2018; Accepted 16 May 2018

Available online 18 May 2018

0920-4105/ © 2018 Elsevier B.V. All rights reserved.

Corrosion of Carbon Steel during High Temperature Regeneration of Monoethylene Glycol in the Presence of Methyldiethanolamine

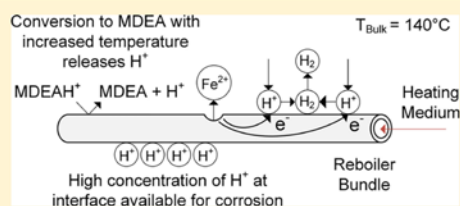
Adam Soames,^{*,†,‡,§} Mobin Salasi,^{‡,§} Ahmed Barifcani,[†] and Rolf Gubner[†]

[†]WA School of Mines: Minerals, Energy and Chemical Engineering, Curtin University, Kent Street 6102, Bentley WA, Australia

[‡]Curtin Corrosion Centre, WASM-MECE, Curtin University, 5 De Laeter Way 6102, Bentley WA, Australia

[§]School of Civil and Mechanical Engineering, Curtin University, Kent Street 6102, Bentley WA, Australia

ABSTRACT: The use of methyldiethanolamine (MDEA) as a pH stabilizer in natural gas pipelines utilizing monoethylene glycol (MEG) injection is an attractive option in systems with high carbon dioxide (CO₂) partial pressures. However, the presence of MDEA within MEG loops may pose a corrosion risk to carbon steel systems operating at high temperatures including the primary MEG regeneration unit due to the effect of temperature on MDEA dissociation behavior. Carbon steel corrosion rates were measured within CO₂-free lean glycol solutions containing 500 mM MDEA from pH_{25 °C} = 6–11 at 30, 80, 140, and 180 °C. Heating of the lean MEG solution, analogous to the regeneration process, facilitated corrosion through the deprotonation of MDEA's conjugate acid, MDEAH⁺, leading to an increase in hydrogen ions available for cathodic reduction. The effect of temperature on MDEA dissociation behavior led to carbon steel corrosion rates in excess of 1 mm/year for systems operating below pH_{25 °C} = 9 and ≥ 140 °C.



1. INTRODUCTION

The formation of gas hydrates pose a major risk to the continuous and safe operation of wet gas/condensate pipelines. Gas hydrates form when water molecules surround gas molecules, such as methane, creating a solid material at the low temperatures and high pressures typically encountered in offshore hydrocarbon production flow lines.^{1,2} Under favorable formation conditions, hydrate blockages can occur rapidly, with hydrate plugs potentially taking days or weeks to remove while significantly impacting production capabilities and representing a major safety risk for the asset. The injection of monoethylene glycol (MEG) is one of the preferred methods of preventing the formation of gas hydrates either during well restart and well testing operations, or in some instances, continuously during gas production.^{1,3–6} MEG as a thermodynamic hydrate inhibitor (THI) achieves hydrate inhibition through shifting of the hydrate formation temperature below the pipeline operational temperature.^{3,5,7–10}

In comparison to traditional THIs such as methanol, MEG can be effectively regenerated and reused over multiple regeneration cycles to significantly reduce long-term operational costs.^{1,3,5,7,11} The regeneration of MEG involves a series of chemical and physical processes to remove excess water, production chemicals, and contaminants including salts and organic acids.^{5,6,9,12,13} The primary MEG regeneration process involves the distillation of “rich MEG”, typically between 30 and 60% wt. MEG, to achieve a final “lean MEG” product above 80% wt.^{3,5,9,14} To achieve sufficient MEG purity to facilitate reinjection, the MEG regeneration unit (MRU) is

typically operated between 120 and 140 °C at atmospheric pressure.^{3,15,16}

Alongside hydrate inhibition, mitigating corrosion is also an important aspect in maintaining continued flow assurance during hydrocarbon transportation and processing. Due to the widespread use of low corrosion resistant carbon steel for pipeline construction because of its low cost relative to corrosion resistance alloys, the need for effective corrosion mitigation strategies is essential.^{7,17} The prevention of corrosion within carbon steel pipelines where CO₂ represents the primary corrosion risk^{5,18–20} is often achieved via one of two methods including pH stabilization or the injection of film forming corrosion inhibitors (FFCIs).^{5,7–9,21} Corrosion prevention via pH stabilization is achieved through the injection of basic chemicals including hydroxides, carbonates, or amines to artificially increase the pipelines liquid phase pH.^{3,6,7,20} Corrosion inhibition is achieved through a reduction in the availability of hydrogen ions (the primary corrosive species in CO₂ corrosion^{7,22,23}) for the cathodic corrosion reaction while simultaneously promoting the formation of a protective iron carbonate film on the internal surface of the pipeline.^{7,21,24} However, the use of pH stabilization is limited to systems where formation water breakthrough and the risk of scaling at high pH has not yet occurred.^{9,20,21} Under such circumstances, FFCIs are instead used due to the limited

Received: April 30, 2019

Revised: June 28, 2019

Accepted: July 19, 2019

Published: July 19, 2019



Contents lists available at ScienceDirect

Journal of Petroleum Science and Engineering

journal homepage: www.elsevier.com/locate/petrol

Effect of wettability on particle settlement behavior within Mono-Ethylene Glycol regeneration pre-treatment systems

Adam Soames^{a,*}, Sarmad Al-Ansari^{b,c}, Stefan Iglauer^b, Ahmed Barifcani^a, Rolf Gubner^a^a WA School of Mines: Minerals, Energy and Chemical Engineering, Curtin University, Perth, WA, Australia^b Petroleum Engineering Department, Edith Cowan University, Perth, WA, Australia^c Department of Chemical Engineering, College of Engineering, University of Baghdad, Iraq

ARTICLE INFO

Keywords:

Mono ethylene glycol
MEG
Particle settlement
Wettability

ABSTRACT

This study was undertaken to diagnose routine settling problems within a third-party oil and gas companies' Mono-Ethylene Glycol (MEG) regeneration system. Two primary issues were identified including; a) low particle size ($< 40 \mu\text{m}$) resulting in poor settlement within high viscosity MEG solution and b) exposure to hydrocarbon condensate causing modification of particle surface properties through oil-wetting of the particle surface. Analysis of oil-wetted quartz and iron carbonate (FeCO_3) settlement behavior found a greater tendency to remain suspended in the solution and be removed in the rich MEG effluent stream or to strongly float and accumulate at the liquid-vapor interface in comparison to naturally water-wetted particles.

As such, exposure of particles including quartz and FeCO_3 to the condensate phase within natural gas transportation pipelines may ultimately cause poor settlement of suspended particles downstream within MEG regeneration systems, leading to increase filtration requirements. The effect of oil-wetting on particle settlement was successfully managed through application of a cationic surfactants, including cetrimonium bromide (CTAB), to transition the initially oil-wetted surface to water-wetted. Cationic surfactants were found to be most suitable due to the negative surface charge of mineral particles at pH levels typical of MEG regeneration system pre-treatment systems ($\text{pH} > 8$).

1. Introduction

Mono-Ethylene Glycol (MEG) is widely used as a thermodynamic hydrate inhibitor to prevent the formation of gas hydrates within natural gas transportation pipelines (Brustad et al., 2005; Haghghi et al., 2009; Latta et al., 2013; Pojtanabuntoeng et al., 2017; Soames et al., 2018a, 2018b, 2018c; Zaboon et al., 2017). Due to the large dosage requirement to ensure sufficient hydrate control and cost of inhibitor dosage, the regeneration and reuse of MEG is essential to minimize operational costs (AlHarooni et al., 2015; Bikkina et al., 2012; Haghghi et al., 2009; Pojtanabuntoeng et al., 2017; Zaboon et al., 2017). The industrial regeneration of MEG entails a variety of chemical and physical processes to remove contaminants such as process chemicals, mineral salts and organic acids as well as the reconcentration of the MEG by removal of excess water (Bikkina et al., 2012; Latta et al., 2013; Soames et al., 2018c; Zaboon et al., 2017). In particular, following the breakthrough of formation water, the removal of divalent cations included calcium and magnesium is important to prevent the formation of scale within downstream equipment operating at high temperature

including the regeneration column (Al Helal et al., 2019; Babu et al., 2015; Baraka-Lokmane et al., 2013; Brustad et al., 2005; Pojtanabuntoeng et al., 2017; Sykes and Gunn, 2016).

If a slip-stream reclamation system is utilized for salt control, the removal of divalent cations including calcium, iron and magnesium is typically performed during pre-treatment (Fig. 1) (Lehmann et al., 2014; Soames et al., 2018c) by reaction within carbonate or hydroxide to form divalent salts that subsequently precipitate out under moderate to high temperatures ($> 80^\circ\text{C}$) (Al Helal et al., 2018; AlHarooni et al., 2017; Baraka-Lokmane et al., 2013; Kim et al., 2017; Latta et al., 2016). The precipitated solids can then be removed within downstream filtration systems (Latta et al., 2016). Likewise, the removal of pipeline corrosion products such as iron carbonate (FeCO_3) as well as other solid particles present with the reservoir fluids including sand may be required (Latta et al., 2016). Downstream of the pre-treatment system, the treated rich glycol is subsequently stored within the rich glycol tank of which may act as a settlement tank for particles not removed by initial filtration. If considerable levels of solid particulates are present or poor settlement occurs within the rich glycol tank, excessive

* Corresponding author.

E-mail address: Adam.Soames@postgrad.curtin.edu.au (A. Soames).<https://doi.org/10.1016/j.petrol.2019.04.108>

Received 12 November 2018; Received in revised form 30 April 2019; Accepted 30 April 2019

Available online 05 May 2019

0920-4105/© 2019 Elsevier B.V. All rights reserved.

Acid Dissociation Constant (pK_a) of Common Monoethylene Glycol (MEG) Regeneration Organic Acids and Methyldiethanolamine at Varying MEG Concentration, Temperature, and Ionic Strength

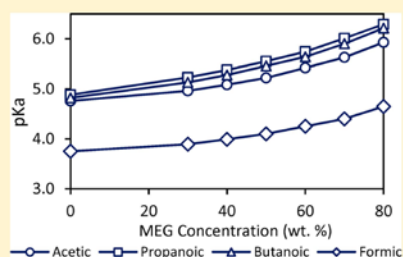
Adam Soames,^{*,†} Stefan Iglauer,[‡] Ahmed Barifcani,[†] and Rolf Gubner[†]

[†]WA School of Mines: Minerals, Energy and Chemical Engineering, Curtin University, Bentley, 6102 W.A. Australia

[‡]Petroleum Engineering Department, Edith Cowan University, Joondalup, 6027 W.A. Australia

Supporting Information

ABSTRACT: The acid dissociation constants (pK_a) of four organic acids (formic, acetic, propanoic, and butanoic) commonly found in monoethylene glycol (MEG) regeneration systems and methyldiethanolamine (MDEA) were measured via potentiometric titration. Dissociation constants were measured within varying concentration of MEG solution (0, 30, 40, 50, 60, 70, and 80 wt %) and at varying temperature (25, 30, 40, 50, 60, 70, and 80 °C). Thermodynamic properties of the dissociation process including Gibbs free energy (ΔG° kJ mol⁻¹), standard enthalpy (ΔH° kJ mol⁻¹), and entropy (ΔS° kJ mol⁻¹ K⁻¹) were calculated at 25 °C using the van't Hoff equation. Comparison of the reported experimental pK_a values and calculated thermodynamic properties in aqueous solution to the literature demonstrated good agreement. Two models have been proposed to calculate the pK_a of acetic acid and MDEA within MEG solutions of varying concentration, temperature, and ionic strength. The proposed models have an average error of 0.413% and 0.265% for acetic acid and MDEA, respectively.



INTRODUCTION

The presence of organic acids within MEG regeneration systems poses a potential corrosion risk to natural gas transportation pipelines.^{1–4} Organic acids such as acetic, propanoic, and butanoic typically enter into the MEG regeneration loop via the condensed water phase where free organic acids are present within the reservoir.⁵ Alternatively, following the breakthrough of formation water, organic acids may also be introduced alongside mineral salt ions.^{5,6} The thermal degradation of MEG at high temperature in the presence of oxygen may also lead to the formation of organic acids including glycolic, acetic, and formic acids.^{5,7–10}

The introduction of organic acids into natural gas transportation pipelines will ultimately reduce the pH of the liquid phase and hence pose a corrosion risk through increased solubility of the protective iron carbonate film.^{11–14} Furthermore, organic acids such as acetic acid have been demonstrated to increase the rate of top of the line corrosion (TLC) in the presence of carbon dioxide.^{5,15–20} As such, while operating under pH stabilization corrosion control it is important to ensure sufficient alkalinity is present to neutralize incoming organic acids.

Corrosion prevention through pH stabilization can be achieved through the addition of hydroxide or carbonate salts or amine-based compounds including MDEA.^{17,21} The application of MDEA within closed-loop MEG systems for pH stabilization is advantageous due to its thermal stability,

allowing multiple regeneration cycles before degradation occurs and its ability to be recovered during reclamation at high pH.^{22,23} However, upon the onset of formation water, the risk of scaling within subsea and MEG regeneration systems is present at high pH. As such, if scaling cannot be alternatively managed through scale inhibitors it may be beneficial to transition from pH stabilization using MDEA to more scaling friendly film forming corrosion inhibitors.^{6,24}

The removal of MDEA from the MEG regeneration loop can be accomplished alongside monovalent cations including sodium via vacuum reclamation.^{6,25} Removal of MDEA during the reclamation process involves first neutralizing the MDEA to facilitate reaction with anionic species including chlorides, sulfates, sulfides, and organic acid ions to form heat-stable salts in a similar manner to industrial CO₂ capture systems using amines.^{25–29} Upon the evaporation of lean MEG under vacuum, the heat-stable MDEA salts will remain, hence facilitating their removal. Likewise, removal of organic acids via the vacuum reclamation system may also be achieved in a similar manner to prevent their accumulation within the loop. As such, the acid dissociation behavior of a chemical is an important factor dictating the efficiency of its removal during reclamation.

Received: March 20, 2018

Accepted: June 13, 2018

Published: June 25, 2018

Experimental Vapor–Liquid Equilibrium Data for Binary Mixtures of Methyl-diethanolamine in Water and Ethylene Glycol under Vacuum

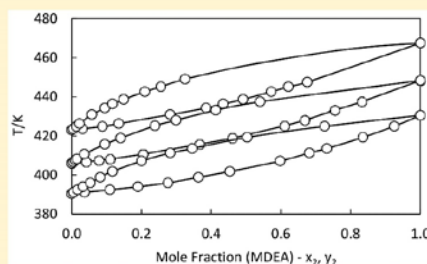
Adam Soames,^{*,†} Ammar Al Helal,[†] Stefan Iglauer,[‡] Ahmed Barifcani,[†] and Rolf Gubner[†]

[†]WA School of Mines: Minerals, Energy and Chemical Engineering, Curtin University, Bentley Western Australia 6102, Australia

[‡]Petroleum Engineering Department, Edith Cowan University, Joondalup Western Australia 6027, Australia

Supporting Information

ABSTRACT: Methyl-diethanolamine (MDEA) is a widely used chemical in the natural gas processing industry as a solvent for CO₂ and H₂S capture and as a basic compound for pH stabilization corrosion control. During pH stabilization corrosion control, the removal of MDEA during the (mono)ethylene glycol (MEG) regeneration process may occur under vacuum conditions during reclamation in which the removal of salt cations is performed. Isobaric vapor–liquid equilibrium data for the binary MEG–MDEA system is presented at (20, 10 and 5) kPa and water–MDEA system at (40, 20, 10) kPa to simulate its behavior during MEG reclamation under vacuum. Vapor and liquid equilibrium concentrations of MDEA were measured using a combination of ion chromatography and refractive index. The generated experimental VLE data were correlated to the UNIQUAC, NRTL, and Wilson activity coefficient models, and the respective binary parameters were regressed.



INTRODUCTION

Ethylene glycol (EG) and *N*-methyl-diethanolamine (MDEA) are common chemicals used in the natural gas processing industry. The injection of EG is performed to prevent the formation of natural gas hydrates within transportation pipelines.^{1–3} Whereas MDEA and other alkanolamines are typically used as chemical absorbents for the removal of carbon dioxide and hydrogen sulfide during natural gas processing.^{4,5} Furthermore, the application of MDEA within natural gas transportation extends to its use as a basic compound suitable for pH stabilization corrosion control.^{2,6}

pH stabilization corrosion control is performed to promote the formation of an iron carbonate protective film by artificially increasing the system pH.^{2,6–8} MDEA as a pH stabilizer may be preferable to salt based (hydroxide or carbonate) chemicals because of its ability to be recovered during vacuum reclamation minimizing operational losses and dosing requirements.^{2,9} Moreover, the thermal stability of MDEA is advantageous during industrial EG regeneration where exposure to high temperature (120–140 °C)³ is required allowing multiple regeneration cycles before thermal degradation occurs.^{10,11}

Vacuum reclamation is often performed to prevent the accumulation of salts within the EG regeneration loop.^{12–14} The vacuum reclamation process entails the vaporization of EG to remove nonvolatile salt compounds. Vacuum reclamation of EG is typically performed at low pressure (≈ 100 mbar^{12,15,16}) to minimize the required operational temperature (120–150 °C^{13,16}). Low temperature vaporization of EG is desired to prevent its degradation.^{14,15} However, the vacuum reclamation process may

inadvertently lead to MDEA losses due to its higher boiling point in comparison to EG. Therefore, ensuring the vaporization of MDEA alongside EG is an important aspect of EG regeneration during pH stabilization to minimize MDEA losses.

Alternatively, the removal of MDEA within EG regeneration systems operating under pH stabilization control is essential following formation water breakthrough.^{14,15} The combined presence of MDEA (high pH) and divalent cations including calcium, magnesium, and barium presents a scaling risk within both transportation lines and equipment operating at high temperature (heat exchangers, EG regeneration system).^{14,17} MDEA will react in the presence of CO₂ to form bicarbonate^{2,14,17} facilitating the formation of scaling products including CaCO₃. pH stabilization chemicals such as MDEA must therefore be removed to facilitate switch over to more scaling friendly film forming corrosion inhibitors (FFCIs). The removal of MDEA can be achieved via vacuum reclamation systems alongside mineral salts.¹⁴

Therefore, knowledge of the vapor–liquid equilibrium (VLE) of MDEA with respect to EG at low pressure is essential for the design of separation equipment. Current literature for MDEA VLE data in EG and water solutions is limited at the low-pressure conditions necessary for EG vacuum reclamation. This work outlines the VLE of MDEA with respect to water and EG under low pressure conditions (40–10 kPa) and (20–5 kPa), respectively. However, the operating conditions of reclamation

Received: January 16, 2018

Accepted: March 21, 2018

Published: March 28, 2018

Appendix G: Written Statements from Co-authors of the Publications

To Whom It May Concern

I, Adam Soames, contributed by conducting the experimental research, analysis of results and preparation of the manuscript entitled "**Removal of Organic Acids during Mono-Ethylene Glycol Distillation and Reclamation to Minimize Long-Term Accumulation**".

 Date: 24/04/2019
Signature of Candidate

I, as a Co-Author, endorse that this level of contribution by the candidate indicated above is correct and give permission for the full use of the manuscript in the candidates thesis.

Ahmed Barifcani
Full Name of Co-Author 1


Signature of Co-Author 1

Date: 24-04-2019


Rolf Gubner
Full Name of Co-Author 2


Signature of Co-Author 2

Date: 16-05-2019

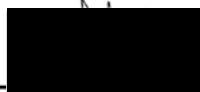
To Whom It May Concern

I, Adam Soames, contributed by conducting the experimental research, analysis of results and preparation of the manuscript entitled "**Operation of a MEG Pilot Regeneration System for Organic Acid and Alkalinity Removal during MDEA to FFCI Switchover**".

 Date: 24/04/2019
Signature of Candidate

I, as a Co-Author, endorse that this level of contribution by the candidate indicated above is correct and give permission for the full use of the manuscript in the candidates thesis.

Edith Odeigah
Full Name of Co-Author 1

 Date: 7/8/19
Signature of Co-Author 1

Ammar Al Helal
Full Name of Co-Author 2

 Date: 24/4/2019
Signature of Co-Author 2

Sami Zaboob
Full Name of Co-Author 3

 Date: 24/4/2019
Signature of Co-Author 3

Stefan Iglauer
Full Name of Co-Author 4

 Date: 23/5/2019
Signature of Co-Author 4

Ahmed Barifcani
Full Name of Co-Author 5


 Date: 24-04-2019
Signature of Co-Author 5

Rolf Gubner
Full Name of Co-Author 6

 Date: 16-05-2019
Signature of Co-Author 6

To Whom It May Concern

I, Adam Soames, contributed by conducting the experimental research, analysis of results and preparation of the manuscript entitled "**Corrosion of Carbon Steel during High Temperature Regeneration of Mono-Ethylene Glycol in the Presence of Methyldiethanolamine**".

 Date: 24/04/2019
Signature of Candidate

I, as a Co-Author, endorse that this level of contribution by the candidate indicated above is correct and give permission for the full use of the manuscript in the candidates thesis.

Mobin Salasi
Full Name of Co-Author 1


Signature of Co-Author 1


Date: 02-05-19

Ahmed Barifcani
Full Name of Co-Author 2


Signature of Co-Author 2

Date: 24-04-

Rolf Gubner
Full Name of Co-Author 3


Signature of Co-Author 3

Date: 16-05-201

To Whom It May Concern

I, Adam Soames, contributed by conducting the experimental research, analysis of results and preparation of the manuscript entitled "**Effect of Wettability on Particle Settlement Behaviour within Mono-Ethylene Glycol Regeneration Pre-Treatment Systems**".

 Date: 24/04/2019
Signature of Candidate

I, as a Co-Author, endorse that this level of contribution by the candidate indicated above is correct and give permission for the full use of the manuscript in the candidates thesis.

Sarmad Al-Anssari  Date: 21/05/2019
Full Name of Co-Author 1 Signature of Co-Author 1

Stefan Iglauer  Date: 23/05/2019
Full Name of Co-Author 2 Signature of Co-Author 2

Ahmed Barifcani  Date: 24-04-2019
Full Name of Co-Author 3 Signature of Co-Author 3

Rolf Gubner  Date: 16-05-2015
Full Name of Co-Author 4 Signature of Co-Author 4

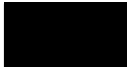
To Whom It May Concern

I, Adam Soames, contributed by conducting the experimental research, analysis of results and preparation of the manuscript entitled "**Acid Dissociation Constant (pKa) of Common MEG Regeneration Organic Acids and Methyldiethanolamine at Varying MEG Concentration, Temperature and Ionic Strength**".


 Date: 24/04/2019
Signature of Candidate

I, as a Co-Author, endorse that this level of contribution by the candidate indicated above is correct and give permission for the full use of the manuscript in the candidates thesis.


Stefan Iglauer
Full Name of Co-Author 1

 Date: 28/05/2019
Signature of Co-Author 1

Ahmed Barifcani
Full Name of Co-Author 2


 Date: 24-04-2019
Signature of Co-Author 2

Rolf Gubner
Full Name of Co-Author 3

 Date: 16-05-2019
Signature of Co-Author 3


To Whom It May Concern

I, Adam Soames, contributed by conducting the experimental research, analysis of results and preparation of the manuscript entitled "**Experimental Vapor-Liquid Equilibrium Data for Binary Mixtures of Methyldiethanolamine in Water and Ethylene Glycol under Vacuum**".


 Date: 24/04/2019
Signature of Candidate

I, as a Co-Author, endorse that this level of contribution by the candidate indicated above is correct and give permission for the full use of the manuscript in the candidates thesis.

Ammar Al Helal  Date: 24/4/19
Full Name of Co-Author 1 Signature of Co-Author 1

Stefan Iglauer  Date: 23/5/2019
Full Name of Co-Author 2 Signature of Co-Author 2

Ahmed Barifcani  Date: 24-04-2019
Full Name of Co-Author 3 Signature of Co-Author 3

Rolf Gubner  Date: 16-05-2015
Full Name of Co-Author 4 Signature of Co-Author 4

To Whom It May Concern

I, Adam Soames, contributed by conducting the experimental research, analysis of results and preparation of the manuscript entitled **“Effect of Organic Acids upon Sulphite Oxygen Scavenger Performance within Mono-Ethylene Glycol Injection Systems”**.


Date: 24/04/2019
Signature of Candidate

I, as a Co-Author, endorse that this level of contribution by the candidate indicated above is correct and give permission for the full use of the manuscript in the candidates thesis.

Mark Charlesworth
Full Name of Co-Author 1


Signature of Co-Author 1

Date: 27/5/19.

Jon Even Vale
Full Name of Co-Author 2


Signature of Co-Author 2

Date: 27/5/19

Rolf Gubner
Full Name of Co-Author 3


Signature of Co-Author 3

Date: 24/04/2019

Appendix H: Copyright Statements

The following section provides the copyright statements provided by the American Chemical Society – ACS (Chapters 4, 6, 9 and 10) and Elsevier (Chapters 5 and 8) for the chapters that form this thesis. Permission to use the conference paper in Appendix E is also provided by the conference organiser.

4/29/2019

Rightslink® by Copyright Clearance Center



RightsLink®

Home

Create Account

Help



Title: Removal of Organic Acids during Monoethylene Glycol Distillation and Reclamation To Minimize Long-Term Accumulation
Author: Adam Soames, Ahmed Barifcani, Rolf Gubner
Publication: Industrial & Engineering Chemistry Research
Publisher: American Chemical Society
Date: Apr 1, 2019
Copyright © 2019, American Chemical Society

LOGIN

If you're a **copyright.com** user, you can login to RightsLink using your copyright.com credentials. Already a **RightsLink** user or want to [learn more?](#)

PERMISSION/LICENSE IS GRANTED FOR YOUR ORDER AT NO CHARGE

This type of permission/license, instead of the standard Terms & Conditions, is sent to you because no fee is being charged for your order. Please note the following:

- Permission is granted for your request in both print and electronic formats, and translations.
- If figures and/or tables were requested, they may be adapted or used in part.
- Please print this page for your records and send a copy of it to your publisher/graduate school.
- Appropriate credit for the requested material should be given as follows: "Reprinted (adapted) with permission from (COMPLETE REFERENCE CITATION). Copyright (YEAR) American Chemical Society." Insert appropriate information in place of the capitalized words.
- One-time permission is granted only for the use specified in your request. No additional uses are granted (such as derivative works or other editions). For any other uses, please submit a new request.

BACK

CLOSE WINDOW

Copyright © 2019 Copyright Clearance Center, Inc. All Rights Reserved. [Privacy statement](#). [Terms and Conditions](#). Comments? We would like to hear from you. E-mail us at customercare@copyright.com

4/29/2019

Rightslink® by Copyright Clearance Center



RightsLink®

Home

Create Account

Help



Title: Operation of a MEG pilot regeneration system for organic acid and alkalinity removal during MDEA to FFCl switchover

Author: Adam Soames, Edith Odeigah, Ammar Al Helal, Sami Zaboon, Stefan Iglauer, Ahmed Barifcani, Rolf Gubner

Publication: Journal of Petroleum Science and Engineering

Publisher: Elsevier

Date: October 2018

© 2018 Elsevier B.V. All rights reserved.

LOGIN

If you're a **copyright.com** user, you can login to RightsLink using your copyright.com credentials. Already a **RightsLink** user or want to [learn more?](#)

Please note that, as the author of this Elsevier article, you retain the right to include it in a thesis or dissertation, provided it is not published commercially. Permission is not required, but please ensure that you reference the journal as the original source. For more information on this and on your other retained rights, please visit: <https://www.elsevier.com/about/our-business/policies/copyright#Author-rights>

BACK

CLOSE WINDOW

Copyright © 2019 Copyright Clearance Center, Inc. All Rights Reserved. [Privacy statement](#). [Terms and Conditions](#). Comments? We would like to hear from you. E-mail us at customer@copyright.com

<https://s100.copyright.com/AppDispatchServlet>

1/1

7/23/2019

Rightslink® by Copyright Clearance Center



RightsLink®

Home

Create Account

Help

ACS Publications
Most Trusted. Most Cited. Most Read.

Title: Corrosion of Carbon Steel during High Temperature Regeneration of Monoethylene Glycol in the Presence of Methyl-diethanolamine

Author: Adam Soames, Mobin Salasi, Ahmed Barifcani, et al

Publication: Industrial & Engineering Chemistry Research

Publisher: American Chemical Society

Date: Jul 1, 2019

Copyright © 2019, American Chemical Society

LOGIN

If you're a **copyright.com** user, you can login to RightsLink using your copyright.com credentials. Already a **RightsLink** user or want to [learn more?](#)

PERMISSION/LICENSE IS GRANTED FOR YOUR ORDER AT NO CHARGE

This type of permission/license, instead of the standard Terms & Conditions, is sent to you because no fee is being charged for your order. Please note the following:

- Permission is granted for your request in both print and electronic formats, and translations.
- If figures and/or tables were requested, they may be adapted or used in part.
- Please print this page for your records and send a copy of it to your publisher/graduate school.
- Appropriate credit for the requested material should be given as follows: "Reprinted (adapted) with permission from (COMPLETE REFERENCE CITATION). Copyright (YEAR) American Chemical Society." Insert appropriate information in place of the capitalized words.
- One-time permission is granted only for the use specified in your request. No additional uses are granted (such as derivative works or other editions). For any other uses, please submit a new request.

BACK

CLOSE WINDOW

Copyright © 2019 [Copyright Clearance Center, Inc.](#) All Rights Reserved. [Privacy statement](#). [Terms and Conditions](#). Comments? We would like to hear from you. E-mail us at customercare@copyright.com

<https://s100.copyright.com/AppDispatchServlet>

1/1

5/14/2019

Rightslink® by Copyright Clearance Center

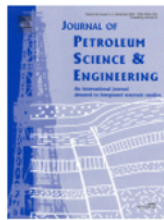


RightsLink®

Home

Create Account

Help



Title: Effect of wettability on particle settlement behavior within Mono-Ethylene Glycol regeneration pre-treatment systems

Author: Adam Soames, Sarmad Al-Anssari, Stefan Iglauer, Ahmed Barifcani, Rolf Gubner

Publication: Journal of Petroleum Science and Engineering

Publisher: Elsevier

Date: August 2019

© 2019 Elsevier B.V. All rights reserved.

LOGIN

If you're a **copyright.com** user, you can login to RightsLink using your copyright.com credentials.

Already a **RightsLink** user or want to [learn more?](#)

Please note that, as the author of this Elsevier article, you retain the right to include it in a thesis or dissertation, provided it is not published commercially. Permission is not required, but please ensure that you reference the journal as the original source. For more information on this and on your other retained rights, please visit: <https://www.elsevier.com/about/our-business/policies/copyright#Author-rights>

BACK

CLOSE WINDOW

Copyright © 2019 [Copyright Clearance Center, Inc.](#) All Rights Reserved. [Privacy statement](#). [Terms and Conditions](#). Comments? We would like to hear from you. E-mail us at customercare@copyright.com

4/29/2019

Rightslink® by Copyright Clearance Center



RightsLink®

Home

Create Account

Help

ACS Publications
Title: Most Trusted. Most Cited. Most Read.

Acid Dissociation Constant (pKa) of Common Monoethylene Glycol (MEG) Regeneration Organic Acids and Methyldiethanolamine at Varying MEG Concentration, Temperature, and Ionic Strength

Author: Adam Soames, Stefan Iglauer, Ahmed Barifcani, et al

Publication: Journal of Chemical and Engineering Data

Publisher: American Chemical Society

Date: Aug 1, 2018

Copyright © 2018, American Chemical Society

LOGIN

If you're a **copyright.com** user, you can login to RightsLink using your **copyright.com** credentials. Already a **RightsLink** user or want to [learn more?](#)

PERMISSION/LICENSE IS GRANTED FOR YOUR ORDER AT NO CHARGE

This type of permission/license, instead of the standard Terms & Conditions, is sent to you because no fee is being charged for your order. Please note the following:

- Permission is granted for your request in both print and electronic formats, and translations.
- If figures and/or tables were requested, they may be adapted or used in part.
- Please print this page for your records and send a copy of it to your publisher/graduate school.
- Appropriate credit for the requested material should be given as follows: "Reprinted (adapted) with permission from (COMPLETE REFERENCE CITATION). Copyright (YEAR) American Chemical Society." Insert appropriate information in place of the capitalized words.
- One-time permission is granted only for the use specified in your request. No additional uses are granted (such as derivative works or other editions). For any other uses, please submit a new request.

BACK

CLOSE WINDOW

Copyright © 2019 Copyright Clearance Center, Inc. All Rights Reserved. [Privacy statement](#). [Terms and Conditions](#). Comments? We would like to hear from you. E-mail us at customercare@copyright.com

4/29/2019

Rightslink® by Copyright Clearance Center



RightsLink®

Home

Create Account

Help

ACS Publications
Most Trusted. Most Cited. Most Read.

Title: Experimental Vapor-Liquid Equilibrium Data for Binary Mixtures of Methyl-diethanolamine in Water and Ethylene Glycol under Vacuum

Author: Adam Soames, Ammar Al Helal, Stefan Iglauer, et al

Publication: Journal of Chemical and Engineering Data

Publisher: American Chemical Society

Date: May 1, 2018

Copyright © 2018, American Chemical Society

LOGIN

If you're a **copyright.com** user, you can login to RightsLink using your copyright.com credentials. Already a **RightsLink** user or want to [learn more?](#)

PERMISSION/LICENSE IS GRANTED FOR YOUR ORDER AT NO CHARGE

This type of permission/license, instead of the standard Terms & Conditions, is sent to you because no fee is being charged for your order. Please note the following:

- Permission is granted for your request in both print and electronic formats, and translations.
- If figures and/or tables were requested, they may be adapted or used in part.
- Please print this page for your records and send a copy of it to your publisher/graduate school.
- Appropriate credit for the requested material should be given as follows: "Reprinted (adapted) with permission from (COMPLETE REFERENCE CITATION). Copyright (YEAR) American Chemical Society." Insert appropriate information in place of the capitalized words.
- One-time permission is granted only for the use specified in your request. No additional uses are granted (such as derivative works or other editions). For any other uses, please submit a new request.

BACK

CLOSE WINDOW

Copyright © 2019 Copyright Clearance Center, Inc. All Rights Reserved. [Privacy statement](#). [Terms and Conditions](#). Comments? We would like to hear from you. E-mail us at customer-care@copyright.com

From: [Lise Olaussen](#)
To: [Adam Soames](#)
Subject: SV: Permission to use conference paper - PhD Thesis
Date: Thursday, 23 May 2019 8:50:24 PM

You have hereby our permission

Yours sincerely
Lise Olaussen, Advisor Oil & Gas
[Tekna](#)

+47 22947500
+47 93259551
[Dronning Mauds gt 15, 0250 Oslo](#)
[P.O.Box 2312 Sollli, 0201 Oslo](#)

Tekna kjemper for deg og faget du brenner for

Fra: Adam Soames <adam.soames@postgrad.curtin.edu.au>
Sendt: torsdag 23. mai 2019 02:11
Til: Lise Olaussen <lise.olaussen@tekna.no>
Emne: Permission to use conference paper - PhD Thesis

Hi Lise,

I would like to receive your / Tekna's permission to use a conference paper I submitted to the 30th Oil field chemistry symposium – March 13-15th within my PhD thesis. As part of my PhD thesis it will also be uploaded electronically into my universities library/website.

The conference paper was entitled:

"Effect of Organic Acids upon Sulfite Oxygen Scavenger Performance within Mono-Ethylene Glycol Injection Systems".

Thanks,

Adam Soames.